Transcriptional responses to ionising radiation for biological dosimetry purposes

A thesis submitted for the degree of Doctor of Philosophy

by

Sylwia Kabacik

Department of Life Sciences

Brunel University

March 2015

Abstract

Exposures to ionising radiation resulting from natural sources or medical diagnostics are generally very low. In contrast, exposures to therapeutic radiation, although, they are often partial exposures, represent much higher doses. Similar levels of exposure may also occur as a consequence of a radiological accident, where it would be necessary to quickly separate individuals requiring urgent medical attention from the “worried-well”.

The well-established biodosimetry techniques based on cytogenetics, particularly scoring dicentric chromosomes, are accurate and sensitive, yet, they are unsuitable for mass screening due to limited capacity and the time required for providing dose estimates. Measuring gene expression changes following radiation exposure was suggested over a decade ago to be an alternative method for dose estimation, as it is a quick, sensitive and suitable technique for high throughput application. The qPCR protocol was extensively optimised for increased reproducibility and sensitivity in order to be suitable for biodosimetry purposes. Radiation-responsive transcripts were identified and characterised in terms of temporal- and dose-responses. Finally, candidate transcripts were validated in human blood irradiated *ex vivo* and *in vivo* in blood samples obtained from cancer patients undergoing radiotherapy treatment.

The data generated here serve as a proof of principle that qPCR-based gene expression assays can be used for radiation biodosimetry purposes to aid classical cytogenetics tools in an event of mass causality.

Declaration of originality

I declare that work presented in this thesis is my own; work done in collaboration or by others has been appropriately acknowledged in the materials and methods section and results chapters.

The majority of the work presented here has been published in peer reviewed journals.

Table of Contents

List of figures

List of tables

Abbreviations

4PCR – RNAqueous®-4PCR RNA extraction kit
ALL – acute lymphoblastoid leukaemia
AML – acute myeloid leukaemia
APAF1 – apoptotic peptidase activating factor 1
AT – Ataxia-Telangiectasia
ATM – Ataxia-Telangiectasia mutated
ATR – ATM and RAD3 related
BAX – BCL2-associated X protein
BBC3 – BCL2 binding component 3, also known as PUMA
BBQ1, 2, 3 – Black Hole Quencher 1, 2, 3
CBMN – cytokinesis-blocked micronucleus
CCNB1/CCNB2 – cyclins B1 and B2
CCND1 – cyclin D1
CCNG1 – cyclin G1
CDC25C – cell division cycle 25C
CDK1 – cyclin-dependent kinase 1
CDKN1A – cyclin-dependant kinase inhibitor 1A, also known as p21
CDKN2B-AS1 – CDKN2B antisense RNA 1, also known as ANRIL
cDNA – complementary cDNA
CHEK2 – checkpoint kinase 2
COV – coefficient of variation
CT – computed tomography
Ct – cycle treshold
DDB2 – DNA binding protein 2, 48kDa
ddPCR – digital droplet PCR
DDQ1 – Deep Dark Quencher 1
DDR – DNA damage response
DICER1 – dicer1, ribonuclease type III
DMSO – dimethyl sulfoxide
DNA - deoxyribonucleic acid
DNA-PK – DNA-dependent protein kinase
dNTP – deoxynucleotide triphosphate
DROSHA – drosha, ribonuclease type III
DSB – double strand break
EDTA – ethylenediaminetetraacetic acid
ENCODE – Encyclopedia of DNA Elements
ERIC – E2F1-regulated lncRNA XLOC 006942
FAM – 3’ 6-carboxyfluorescein
FAS-AS1 – FAS antisense RNA 1
FBS – foetal bovine serum
FDRX – ferredoxin reductase
FISH – fluorescent in-situ hybridisation
FOS – FBJ murine osteosarcoma viral oncogene homolog
GADD45A – growth arrest and DNA-damage-inducible alpha
GAS5 – growth arrest-specific 5 (non-protein coding)
gDNA – genomic DNA

GLM – General Linear Model
GOI – gene of interest
GR10 – growth medium 10
Gy – gray
H19 – H19, imprinted maternally expressedtranscript (non-protein coding)
HBSS – Hank's Balanced Salt Solution
HEX – 6-hexachlorofluorescein
Hprt – hypoxanthine guanine phosphoribosyl transferase (mouse)
HPRT1 – hypoxanthine phosphoribosyltransferase 1 (human)
HR – homologous recombination
IL2 – interleukin 2
IR – Ionising radiation
JADRR – JADE1 adjacent regulatory RNA
JUN – jun proto-oncogene
KRAS – Kirsten rat sarcoma viral oncogene homolog
KSRP – KH-type splicing regulatory protein
LCGM – lymphoblastoid cells growing medium
LDA – low density arrays
LET – linear energy transfer
linkRNA-RoR – long intergenic non-protein coding RNA, regulator of reprogramming
lncRNA – long non-coding RNA
MDM2 – Mdm2 TP53 binding protein homolog (mouse)
MIQE – minimum information for publication of quantitative real-time PCR experiments
miRNA – micro RNA
miRNeasy – miRNeasy mini kit
mirVana – mirVana™ miRNA Isolation Kit
MRE11 – meiotic recombination 11
MRN – Mre11-Rad50-Nbs1 complex
mRNA – messenger RNA
MYC – v-myc avian myelocytomatosis viral oncogene homolog
NAMA – non-protein coding RNA, associated with MAP kinase pathway and growth arrest
NATO – North Atlantic Treaty Organization
NER – nucleotide excision repair
NHEJ – non-homologous end joining
NTC – no template control
PANDAR – promoter of CDKN1A antisense DNA damage activated RNA
PBL – peripheral blood lymphocytes
PBS – phosphate buffered saline
PCC –premature chromatin concentration
PCNA – proliferating cell nuclear antigen
PCR – polymerase chain reaction
PHA – phytohaemagglutinin
PHPT1 – phosphohistidine phosphatase 1
PMAIP1 – phorbol-12-myristate-13-acetate-induced protein 1, also known as NOXA
pre-miRNA – precursor miRNA
pri-miRNA – primary miRNA transcript
qPCR – quantitative polymerase chain reaction

RBE – relative biological effectiveness
RG – reference gene
RIN^{e} – RNA integrity number equivalent
RISC – RNA-induced silencing complex
RNA – ribonucleic acid
RNA-Seq – deep sequencing of RNA
RNU6-1 – RNA, U6 small nuclear 1
RPA – replication protein A
rpm – rotor per minute
RPMI 1640 – Roswell Park Memorial Institute 1640 medium
RT – reverse transcription
SAM – significance analysis of microarrays
SD – standard deviation
SDS – sodium dodecyl sulphate
SI – International System of Units
SIPS – stress induced premature senescence
SNP – single nucleotide polymorphism
snRNA – small nuclear RNA
SOX2-OT – SOX2 overlapping transcript (non-protein coding)
SR10 – stimulating growth medium 10
SSB – single strand break
SSC – saline sodium citrate buffer
Sv – Sievert
TBE – Tris-Borate-EDTA buffer
TNF – tumor necrosis factor
TP53 – tumor protein TP53
TP53TG1 – TP53 target 1 (non-protein coding)
Trp53cor1 – tumor protein p53 pathway corepressor 1
TUG1 – taurine up-regulated 1 (non-protein coding)
UCA1 – urothelial cancer associated 1 (non-protein coding)
UNSCEAR – United Nations Scientific Committee on the Effects of Atomic Radiation
UTR – untranslated region
Xist – X inactive specific transcript (non-protein coding)

Acknowledgments

I would like to thank my supervisors: Dr Christophe Badie (Public Health England) and Dr Predrag Slijepcevic (Brunel University) for their support and advice during my PhD.

Furthermore, I would like to thank Dr Kai Rothkamm for putting my attention into numerous issues in radiation biodosimetry field and Dr Liz Ainsbury for help with statistical analysis. Special tanks go to Dr Simon Bouffler for his incredible support during my course and valuable comments on my thesis.

I would also like to express my gratitude to Public Health England for giving me the opportunity to do a PhD in a part-time basis and providing me with the financial support during the course.

I am extremely grateful to current and former members of my group at Public Health England, especially to Ms Claudine Raffy, who taught me the qPCR technique and helped me with the initial experiments and Ms Grainne Manning who also contributed to the results presented here.

I would also like to thank our collaborators who contributed to this project, especially Dr Ales Tichy for providing us with radiotherapy patients samples, Prof Michael Abend for inviting us to participate in the NATO exercise, Dr Alan Mackay for microarray experiments and data analysis and Dr Francois Pallier for TaqMan assays designs.

Finally, I would like to thank my husband and my friends for their support during my PhD.

Chapter 1. Introduction

1.1. Ionising radiation

Ionising radiation (IR) is a type of high energy radiation which is capable of ionising other particles, i.e. removing one or more electron from an atom. The quantity of absorbed radiation is expressed in the International System of Units (SI) by the unit called the gray (Gy) which corresponds to absorption of 1 J of energy per 1 kg of tissue. IR can be particulate in nature (such as α-particles, high energy electrons, protons, neutrons and heavy ions) or electromagnetic (X-rays and γ-rays). X-rays and γ-rays both have similar characteristic and physical properties but they differ in the process by which they are formed, i.e. X-rays are produced when electrons are accelerated using special device and stopped abruptly, that causes part of the electron's kinetic energy to be released in a form of X-rays, whereas γ-rays are produced naturally by radioactive isotopes like Cobalt-60 (IAEA, 2010, Hall and Giaccia, 2011).

All types of charged particulate radiation cause direct ionisation of molecules by physical interaction with the material through which they traverse and they directly produce chemical change and consequently the biological effect. Conversely, the mechanism of ionisation for electromagnetic radiation and neutrons is indirect – when they are absorbed, part of their energy is used to produce fast moving charged particles which are then capable of producing damage to target molecules. The different mechanisms of ionisation translate into different biological effectiveness – a dose of 1 Gy of α-particles causes more complex biological damage than the same dose of X-ray. This is a consequence of the linear energy transfer (LET) of the radiation which is the amount of energy deposited per unit distance along the track path in the traversed material. Charged particles deposit more energy per unit length along the track than X-rays or γ-rays, and therefore they have higher LET and cause larger

biological effects. Relative biological effectiveness (RBE) is used to compare biological effects caused by different types of radiation and it is expressed as ratio of a dose of a reference γ-ray radiation and a dose of a test radiation which is required to produce the same particular biological effect (for example kill 50 % of cells). The equivalent dose measured in the SI unit, Sievert (Sv) is used to compare doses of different types of radiation weighted for biological effectiveness and it is expressed by absorbed dose multiplied by radiation weighting factor. For X-rays and γ-rays 1 Gy is equal to 1 Sv, comparing to 2 Sv for protons and 20 Sv for α-particles. The effective dose is also expressed in Sv and it reflects the health risks from non-homogenous IR exposures. Each tissue has individual sensitivity to radiation and based on that organs have been assigned to three weighting factors. Effective dose is expressed as a sum of organ doses corrected for organ weighting factors and it bears the same health risks as if the same dose was delivered homogenously to the total body (ICRP, 2007, UNSCEAR, 2008, IAEA, 2010, Hall and Giaccia, 2011) .

The sources of exposure to ionising radiation can be natural (natural earth crust background radiation, radon gas), medical (computed tomography (CT) scans, radiotherapy), occupational (nuclear plant workers, aircraft crew), accidental (nuclear incidents) or malicious acts (acts of terrorism) (IAEA, 2010) (**Figure 1**). The exposure from natural sources is unavoidable, the United Nations Scientific Committee on the Effects of Atomic Radiation (UNSCEAR) estimates that the worldwide average annual effective dose of natural radiation to the population is 2.4 mSv (UNSCEAR, 2008). The range of effective doses used in clinical diagnostic radiography is between 0.01 and 100 mSv depending on the procedure (Mettler et al., 2008, Brenner, 2014). Nuclear accidents may lead to higher exposures, for example in Chernobyl accident, 134

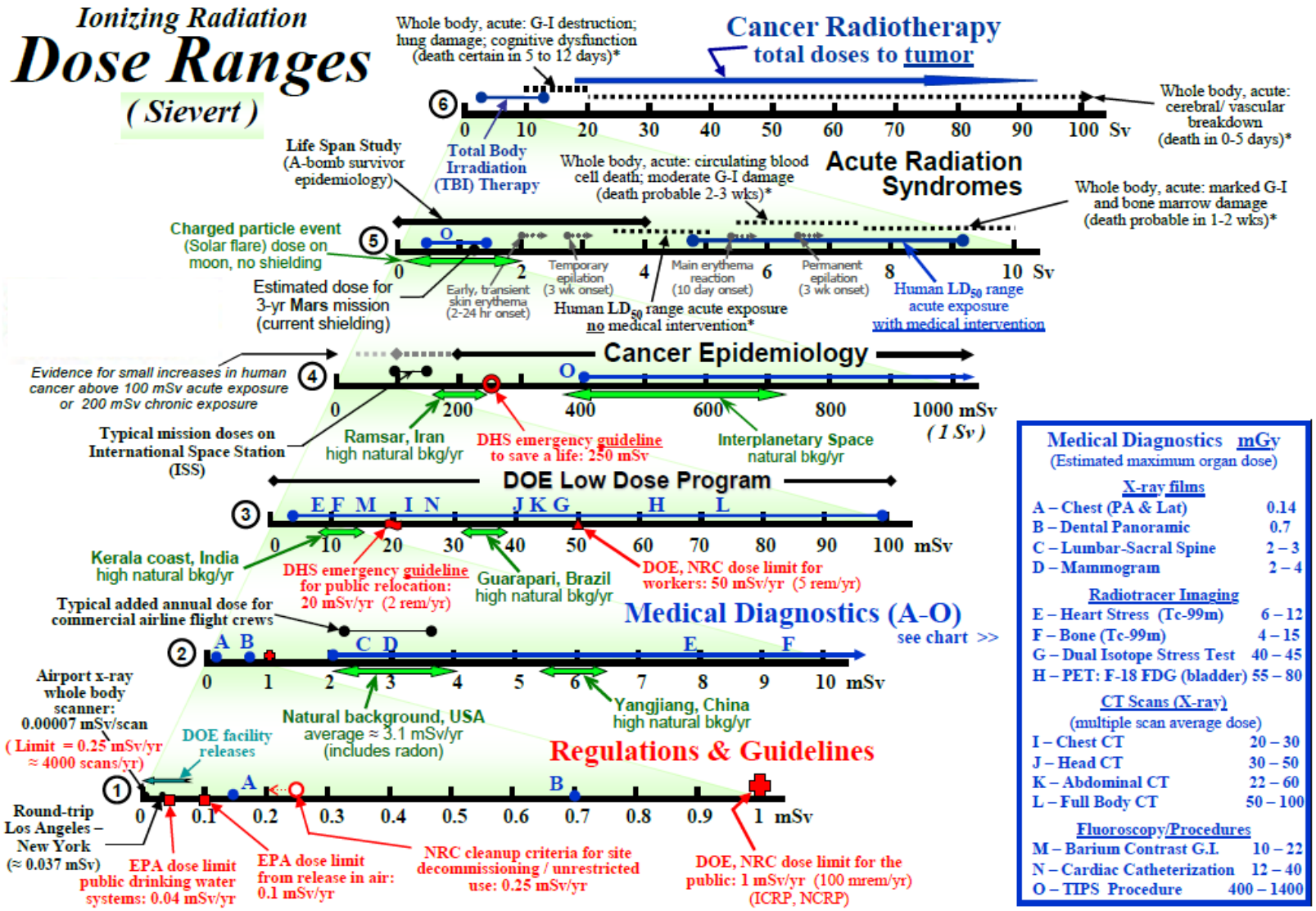

Medical Diagnostics mGy
(Estimated maximum organ dose)

X-ray films	
A – Chest (PA & Lat)	0.14
B – Dental Panoramic	0.7
C – Lumbar-Sacral Spine	2 – 3
D – Mammogram	2 – 4
Radiotracer Imaging	
E – Heart Stress (Tc-99m)	6 – 12
F – Bone (Tc-99m)	4 – 15
G – Dual Isotope Stress Test	40 – 45
H – PET: F-18 FDG (bladder)	55 – 80
CT Scans (X-ray) (multiple scan average dose)	
I – Chest CT	20 – 30
J – Head CT	30 – 50
K – Abdominal CT	22 – 60
L – Full Body CT	50 – 100
Fluoroscopy/Procedures	
M – Barium Contrast G.I.	10 – 22
N – Cardiac Catheterization	12 – 40
O – TIPS Procedure	400 – 1400

Figure 1. Sources and dose ranges of IR exposure

Graph presents "orders of magnitude" dose ranges delivered by natural sources, diagnostic and therapeutic medicine and occupational exposures. Doses of IR are expressed as equivalent dose except for medical diagnostics which are presented as maximum organ doses (adapted from lowdose.energy.gov).

DHS – Department of Homeland Security; DOE – U.S. Department of Energy; EPA – Environmental Protection Agency; G-I – gastrointestinal; LD50 – Lethal Dose to 50% (whole body dose that results in lethality to 50% of exposed individuals in 30-60 days); NRC – Nuclear Regulatory Commission; TIPS – Transjugular Intrahepatic Porto-systemic Shunt;

*Note: Whole body acute prognoses assume no medical intervention

rescuers were exposed to doses between 0.8 and 16 Gy and suffered from acute radiation syndrome; 28 of those exposed to doses above 2.2Gy died from radiation sickness within 2 months from exposure (UNSCEAR, 2008). However, in the Fukushima incident, despite being the second largest nuclear accident after Chernobyl, which resulted in major release of radioactive material into the environment, doses received by general public were low or very low with no deaths or radiation sickness cases reported and no excess of cancer risk is expected (UNSCEAR, 2013).

1.2. Effects of IR exposure on living organisms

Biological effects of exposure to IR can be broken down into two categories – deterministic effects, where the severity of reaction increases with the dose of radiation above certain threshold and below this threshold no reaction is observed (e.g radiation syndrome), and stochastic effects, where the probability of reaction increases linearly with the dose with no threshold (e.g. cancer risk) (IAEA, 2010).

Each tissue has a different tolerance to IR exposure; usually the highly proliferating tissues like bone marrow or small intestine are the most radiosensitive, whereas slowly proliferating tissues like kidneys or liver are considered to be more radioresistant and they can tolerate higher doses of radiation (Hall and Giaccia, 2011). There is also considerable inter-individual variation in sensitivity to IR and existence of hereditable radiosensitivity disorders caused by mutations in genes involved in sensing or repair of DNA damage like Ataxia-Telangiectasia (AT) (Savitsky et al., 1995), Nijmegen breakage syndrome (Varon et al., 1998, Carney et al., 1998), or Lig4 syndrome (O'Driscoll et al., 2001) suggests that this variation has significant genetic component (Barnett et al., 2009).

In cancer patients undergoing radiotherapy the treatment plan is designed to spare healthy tissue by targeting and fractionation of radiation, however patients still often suffer from normal tissue reactions. Normal tissue reaction is caused by radiation-induced cell killing that impairs tissue functionality and it can manifest as acute or late response (IAEA, 2010). Acute tissue reactions are usually observed within weeks following IR exposure and occur mainly in renewing tissues; depending on the irradiated tissue it can present itself as erythema and/or ulceration in skin or vomiting following abdomen irradiation. Late tissue reactions occur more than three months following IR exposure and they are the limiting factor for total dose delivered during the course of radiotherapy. The nature of late response depends on the irradiated tissue but usually it is manifested as weakened organ function caused by tissue fibrosis (IAEA, 2010, Hall and Giaccia, 2011).

In humans, exposure to a total body dose lower than 2 Gy will generally not produce any acute reaction whereas doses higher than 2 Gy will have early clinical manifestations (IAEA, 2010). Above a dose of 2 Gy, nausea and early vomiting is observed. For doses between 2 and 8 Gy individuals will suffer from haematopoietic syndrome caused by depletion of blood cell populations. Doses between 5 and 15 Gy will cause gastrointestinal syndrome, which is caused by damage of the mucosal lining of the intestine. Doses higher than 20 Gy result in a rapid death due to the neurological and vascular failure. The lethal total body dose for human is estimated between 4 and 7 Gy depending on the level of supportive care (IAEA, 2010) (**Figure 1**).

Long term effects of exposure to IR are both cancer and non-cancer. The life span study of a cohort of atomic bomb survivors from Hiroshima and Nagasaki provides the most comprehensive data regarding long term effects of radiation

exposure. There is a clear dose-dependent excess in cancer risk for atomic bomb survivors, the risk depends on sex and age at the exposure, moreover the excess risk for solid tumours seems to follow a linear non-threshold model. There is some nonlinearity in dose response for non-cancer effects including heart, respiratory and bladder diseases, where no effect could be seen for doses below 0.5 Gy (Preston et al., 2003). It is known that IR causes mutations and the hereditary effects of IR exposure are of great concern. Although no hereditary effects of IR exposure were described in the human population so far, mouse experiments clearly show that such effects exist (Dubrova et al., 2000, Barber et al., 2002, Barber et al., 2006) and based on animal data the absolute risk of hereditary effects in humans is estimated to be between 0.3 % to 0.5 % per Gy (UNSCEAR, 2013).

1.3. DNA damage

Any biological effect of IR exposure is primarily caused by damage to deoxyribonucleic acid (DNA) within the cell. The IR can damage the DNA molecule directly as generally happens for high LET radiations, or the damage can be a result of water radiolysis caused by low LET radiation, which in turn produces large amounts of free radicals capable of damaging DNA (Hall and Giaccia, 2011).

The IR exposure causes a wide spectrum of DNA lesions including base damage, single and double strand breaks and protein-DNA crosslinks. It is estimated that a dose of 1 – 2 Gy would induce more than a thousand base lesions, around a thousand single strand breaks (SSB) and about forty double strand breaks (DSB) in the DNA of mammalian cell (IAEA, 2010). Base damage and SSBs do not usually cause cell killing as they are easily repaired by various mechanisms using the opposite strand as a template, on the contrary, DSBs are the most toxic lesions caused by IR exposure, as

they are complex to repair and can potentially lead to loss of genetic information, chromosome breakage and rearrangements potentially leading to carcinogenesis or cell killing (Caldecott, 2001, Jackson and Bartek, 2009).

Eukaryotic cells have evolved two major DSB repair mechanisms: non-homologous end joining (NHEJ) and homologous recombination (HR) repair (extensively reviewed in (Shibata and Jeggo, 2014). NHEJ simply ligates two ends of broken DNA without requiring any sequence homology and therefore it is considered as an error-prone pathway, whereas HR uses an identical DNA molecule (usually sister chromatid in mammals) as a template to repair DNA damage therefore it is considered to be an error-free mechanism (Kakarougkas and Jeggo, 2014). In mammalian cells, NHEJ is the first choice DSB repair pathway and it is active through the whole cell cycle, while the HR requirement for a homologous DNA molecule restricts it to the late S/G2 phase (Mladenov and Iliakis, 2011). The complexity of DSB and its position in the chromatin are two major factors determining repair pathway utilised – complex DSB caused by high LET radiation or DSB localised in heterochromatin are repaired by HR, whereas repair of simple DSB is executed by NHEJ (Shibata et al., 2011, Yajima et al., 2013).

Unrepaired or misrepaired DSBs can lead to chromosome or chromatid aberrations depending on phase of cell cycle when the IR exposure took place. The aberrations induced by IR exposure include dicentric chromosomes, rings, anaphase bridges, translocations and deletions. Induction of dicentrics by IR is dose dependant and scoring dicentric chromosomes in stimulated human T-lymphocytes is currently a “gold standard” for biological dosimetry following IR exposure (IAEA, 2011).

1.4. Signalling cascade following IR exposure

Cells have developed a surveillance machinery called DNA damage response (DDR) which coordinates DNA repair process with all cellular activities. At the heart of the DDR are two signalling phosphoinositide 3-kinase related protein kinases: Ataxia-Telangiectasia mutated (ATM) and ATM and RAD3 related (ATR) which sense the damage and transmit a signal to effector proteins (Ciccia and Elledge, 2010). Although ATM and ATR have overlapping sets of substrates – large-scale proteomic analysis has shown that over 700 proteins are phosphorylated in response to DNA damage on ATM and ATR recognised sites – traditionally it is believed that they respond to different insults: ATM is activated by DSBs whereas ATR responds to replication protein A (RPA) coated single DNA strands caused by replicative stress and other forms of DNA damage (Matsuoka et al., 2007). However, there have been several reports showing that IR exposure can also activate ATR in an ATM, meiotic recombination 11 (Mre11) and cell cycle dependant manner (Jazayeri et al., 2006, Myers and Cortez, 2006). Moreover, Tomimatsu *et al* showed that in ATM-deficient cells, ATR is activated following IR exposure in an exonuclease 1 dependant manner and it is able to induce the G2/M cell cycle checkpoint in those cells (Tomimatsu et al., 2009).

Upon IR exposure ATM protein undergoes a rapid autophosphorylation at serine 1981 causing inactive ATM dimers to dissociate to active monomers and this event initiates the signalling cascade. The precise nature of the signal that ATM protein responds to is still unclear but the change in chromatin conformation following DSB has been suggested (Bakkenist and Kastan, 2003). The DSBs are sensed by Mre11-Rad50-Nbs1 (MRN) complex which further activates ATM and recruits it to the DSB site (Uziel et al., 2003). The fully active ATM phosphorylates a range of substrates involved

in signal transduction, DNA repair and cell cycle control including histone H2AX which takes part in DNA damage signal propagation and recruitment of DNA repair components to the damage site (Burma et al., 2001), checkpoint kinase 2 (CHEK2), the main kinase which amplifies the ATM signal (Matsuoka et al., 2000), tumor protein TP53 (TP53) the tumour suppressor gene which then determines the fate of damaged cell (Banin et al., 1998) (Canman et al., 1998), and Mdm2 TP53 binding protein homolog (mouse) (MDM2), the main negative TP53 protein regulator (Maya et al., 2001) (**Figure 2**).

ATM dependant phosphorylation of CHEK2 and MDM2 proteins, as well as TP53 protein leads to TP53 stabilisation and activation which is a key point in the cellular response to IR (Hirao et al., 2000). TP53 is a transcriptional factor which has an important role in many cellular processes, but it has been intensively studied due to its role as a tumour suppressor (Riley et al., 2008). In unstressed cells, TP53 protein is inactive; this is mainly due to MDM2 – an ubiquitin ligase which binds to TP53 blocking its activity and promoting its degradation. After a stress signal, MDM2 protein polyubiquitinylates itself which leads to its degradation and consequently to an increased TP53 stability (Haupt et al., 1997, Kubbutat et al., 1997).

TP53 responds to a broad range of stress signals including DNA damage, oncogene activation, hypoxia, telomere erosion or nutrient deprivation and coordinates response to these factors with cellular metabolism (Vousden and Lane, 2007). Stress mediators like ATM or ATR kinases activate TP53 by protein phosphorylation (Banin et al., 1998, Canman et al., 1998, Lakin et al., 1999, Tibbetts et al., 1999). In response to DNA damage, TP53 activates and represses a number of genes involved in cell-cycle arrest, DNA repair, stress induced premature senescence

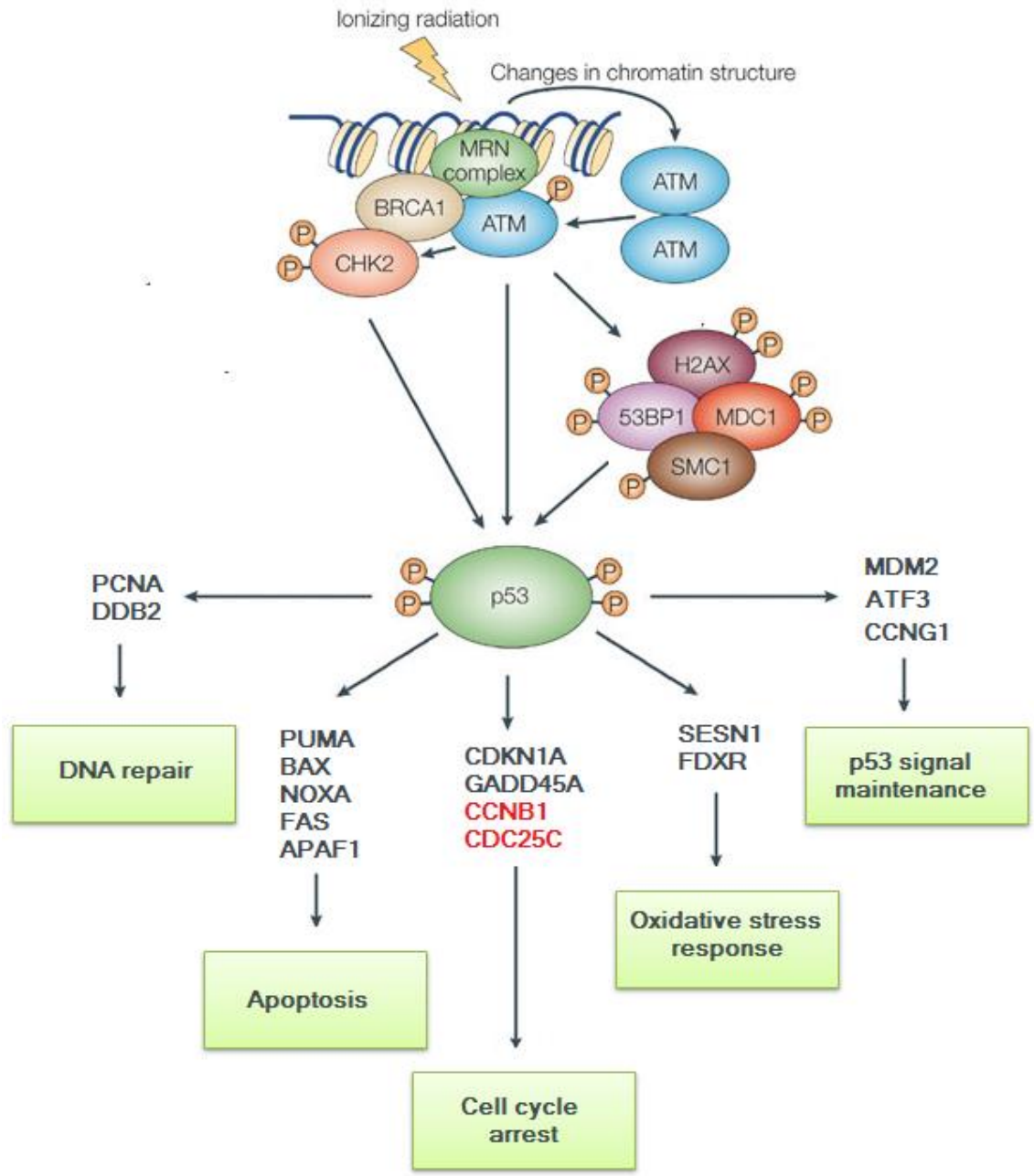

Figure 2. Signalling cascade following IR exposure.

Upon IR exposure ATM protein undergoes a rapid autophosphorylation causing inactive ATM dimers to dissociate to active monomers. The DSBs are sensed by MRN complex which further activates ATM and recruits it to the DSB site. The fully active ATM phosphorylates a range of substrates involved in signal transduction including CHEK2, γH2AX and TP53. TP53 transcriptionally activates a number of genes involved in cellular response to IR. Genes in red are down-regulated by TP53 following IR exposure. Adapted from (Sengupta and Harris, 2005).

(SIPS) and apoptosis (Rashi-Elkeles et al., 2011) (**Figure 2**).

TP53 executes G1/S cell cycle arrest mainly due to transcriptional activation of cyclin-dependant kinase inhibitor 1A (*CDKN1A* also known as p21) which is a potent proliferation and apoptosis inhibitor. CDKN1A binds and inhibits CyclinE/Cdk2 and CyclinD/Cdk4/6 complexes critical for entry into S phase of the cell cycle, causing G1/S phase cell cycle arrest, giving the cell time to repair the damage; however, if damage is extensive, CDKN1A induces SIPS (Wiebusch and Hagemeier, 2010). Senescence is defined as a permanent and irreversible arrest of cell proliferation and senescent cells show changes in gene expression, metabolism and morphology and are resistant to growth factors and apoptosis (Collado et al., 2007).

TP53 also plays a role in inducing the G2/M checkpoint upon DNA damage by inducing *CDKN1*A and growth arrest and DNA-damage-inducible alpha (*GADD45A*) (Wang et al., 1999). It also down-regulates cell division cycle 25C (CDC25C) phosphatase responsible for activating CyclinB/Cdk1 complex and thus preventing entry into mitosis (St Clair et al., 2004) and additionally it transcriptionally inhibits cyclins B1 and B2 (*CCNB1* and *CCNB2*) (Innocente et al., 1999, Krause et al., 2000).

In response to DNA damage TP53 up-regulates a number of DNA repair genes including damage-specific DNA binding protein 2, 48kDa (*DDB2*) involved in nucleotide excision repair (NER) (Hwang et al., 1999) and proliferating cell nuclear antigen (*PCNA*) (Xu and Morris, 1999). Moreover, following DSB induction, TP53 transcriptionally down-regulates RAD51 recombinase, a crucial protein for HR repair and in result favouring NHEJ repair (Arias-Lopez et al., 2006).

If the damage is beyond repair, TP53 can induce apoptosis. Apoptosis is a form of programmed cell death carried out in an organised manner which has a crucial role in mammalian development and homeostasis and it is characterised by fragmentation of the nuclear DNA and cellular membrane, formation of apoptotic bodies (Degterev and Yuan, 2008) and exposition of phosphatidylserine on surface of the cells (Fadok et al., 1992). The property of Annexin V preferentially binding to negatively charged phospholipids like phosphatidylserine has been used to develop an assay widely used for early detection of apoptotic cells (Koopman et al., 1994). In response to DNA damage TP53 activates a number of pro-apoptotic genes including BCL2 binding component 3 (*BBC3* also known as *PUMA*) (Yu et al., 2001, Nakano and Vousden, 2001), BCL2-associated X protein (*BAX*) (Miyashita and Reed, 1995), phorbol-12-myristate-13-acetate-induced protein 1 (*PMAIP1* also known as *NOXA*) (Oda et al., 2000) and apoptotic peptidase activating factor 1 (*APAF1*) (Moroni et al., 2001). Transcriptional activation of *BBC3* accounts for majority of TP53 pro-apoptotic capacity following DNA damage, as lymphocytes and thymocytes obtained from *Bbc3* deficient mice were highly resistant to IR induced apoptosis (Villunger et al., 2003). BBC3 protein inhibits anti-apoptotic genes and activates those which are pro-apoptotic. This event activates the mitochondrial apoptotic pathway involving mitochondrial outer membrane permeabilization, release of cytochrome c, and activation of caspases (Yu and Zhang, 2008).

Different cell types have different sensitivity to IR-induced apoptosis e.g. $CD8^+$ T-lymphocytes are more sensitive than $CD4^+$ (Schmitz et al., 2007, Finnon et al., 2012), whereas fibroblasts do not undergo apoptosis even after high doses of IR (i.e. 10 Gy

and above); instead they undergo TP53-dependant permanent cell cycle arrest (Tsuboi et al., 2007).

1.5. Ataxia-Telangiectasia

In humans, mutations in *ATM* gene cause the autosomal recessive neurodegenerative disorder, Ataxia-Telangiectasia (AT) (Savitsky et al., 1995). Characteristic symptoms of AT are cerebral ataxia, oculocutaneous telangiectasia, immunodeficiency, predisposition for cancer, mainly of lymphoid origin and severe radiosensitivity (Lavin, 2008). The majority of the mutations in the ATM gene are unique, so far over 400 different mutations have been reported and they usually lead to production of a truncated protein or no protein product at all (Campbell et al., 2003). However, leaky splice mutations or missense mutations usually give milder phenotype with later onset, slower progression and extended lifespan when comparing to classical AT, due to presence of residual ATM kinase activity (Saviozzi et al., 2002).

It is estimated that between 0.5 and 1 % of population caries a mutation in ATM gene (Swift et al., 1991). The majority of AT carriers show no clinical symptoms because truncated proteins are highly unstable and only wild type proteins are present in the cell, however they have higher risk of developing breast cancer than general population (Renwick et al., 2006), higher risk of dying from ischemic heart disease and they seem to die earlier than non-carriers (Su and Swift, 2000). Moreover, heterozygosity in the *ATM* gene accelerates chronic lymphocytic leukaemia progression due to loss of the remaining *ATM* allele (Skowronska et al., 2012).

Cells derived from AT patients display a characteristic phenotype, including hypersensitivity to ionising radiation, chromosomal instability (Taylor et al., 1975) and

are defective in cell cycle checkpoint induction following DNA damage (Kastan et al., 1992). Unstimulated lymphocytes from AT patients show poor induction of apoptosis by IR exposure compared to cells obtained from healthy donors, whereas lymphocytes from obligate AT carriers show intermediate level of radiation-induced apoptosis (Duchaud et al., 1996, Barber et al., 2000). In contrast, mitogen-stimulated lymphocytes obtained from AT-carriers show higher level of apoptosis following IR exposure (Finnon et al., 2008).

Following IR exposure, TP53 is also activated in ATM deficient cells although in delayed manner (Canman et al., 1994) suggesting that other kinases can activate DDR in response to DSBs with slower kinetics (Tibbetts et al., 1999).

1.6. Gene expression changes following IR exposure

The first reported mammalian IR induced protein coding gene – tumor necrosis factor (*TNF*) was identified in the late eighties (Hallahan et al., 1989). In the early nineties several other IR-responsive genes were identified by northern blotting including β-actin, interleukin 1 (Woloschak et al., 1990), FBJ murine osteosarcoma viral oncogene homolog (*FOS*) (Munson and Woloschak, 1990), jun proto-oncogene (*JUN*) (Sherman et al., 1990), *GADD45A* (Papathanasiou et al., 1991), *CDKN1A* (Di Leonardo et al., 1994), *BAX* (Zhan et al., 1994), *MDM2* (Chen et al., 1994) and cyclin G1 (*CCNG1*) (Okamoto and Beach, 1994). With the development of microarray technology, allowing the screening of hundreds of genes simultaneously (Schena et al., 1995), it became clear that many more genes are modulated in response to IR (Amundson et al., 1999a, Amundson et al., 2000, Park et al., 2002, Jen and Cheung, 2005, Zschenker et al., 2006, Gruel et al., 2006, Landmark et al., 2007, Turtoi et al., 2008) mostly in TP53 dependant manner for high doses of radiation (Rashi-Elkeles et al., 2011).

Experiments with mouse knockouts revealed that the transcriptional response to IR exposure depends in part on *TP53* and *ATM* status, where the expression of both proteins' downstream targets following irradiation is significantly reduced when compared to wild type (Bouvard et al., 2000, Kabacik et al., 2011b). Gene expression of IR responsive genes is also tissue dependent (Bouvard et al., 2000, Fei et al., 2002, Burns and El-Deiry, 2003) and cell population dependent (Mori et al., 2005, Gruel et al., 2008, Kabacik et al., 2011a, Riecke et al., 2012). Moreover, it has been reported that developmental stage influences transcription of TP53-dependent radiation-responsive genes (Gottlieb et al., 1997, Komarova et al., 1997).

The level of expression of a specific radiation-responsive gene is dose-dependent and dose-response curves have been obtained for many genes (Amundson et al., 2000, Gruel et al., 2006, Manning et al., 2013). Gene expression modulation was detected after exposure to very low doses e.g. $CD4^+$ T-lymphocytes irradiated *ex-vivo* with a dose of 50 mGy of γ-ray show changes in expression of a number of genes (Gruel et al., 2008) and linear dose-responses for several genes have been obtained down to 5 mGy X-ray in human blood irradiated *ex-vivo* (Manning et al., 2013) and in human $CD4^+$ T-lymphocytes (Nosel et al., 2013). Exposure to low doses of radiation seems to activate different genes than exposure to higher doses in normal human epidermal keratinocytes (Franco et al., 2005), normal human fibroblasts (Ding et al., 2005) and human skin exposed *ex-vivo* (Albrecht et al., 2012), hinting that IR can act differently depending on dose range. Recently, experiments on mice exposed chronically to a dose of 0.05 mGy/day over a period of 401 days receiving a total dose of 20 mGy which is an annual limit for radiation workers, showed modulation of expression of three genes involved in circadian rhythm, protein glycosylation and

ubiquitin cycle (Uehara et al., 2010) showing that cells can detect even extremely low doses of radiation. Also gene expression changes were detected in people occupationally exposed to cumulative IR doses lower than 40 mSv (Morandi et al., 2009, Fachin et al., 2009).

The long term effects of exposure to low doses are a matter of great concern with increased use of diagnostic techniques in medicine. A typical organ dose for CT scan, positron emission tomography or fluoroscopy procedure is between 5 and 100 mGy (Brenner, 2014) and there is still controversy over the cancer risk following low dose exposure as epidemiological data provide measurements only down to around 100 mGy (extensively reviewed in (Mullenders et al., 2009) and (Dauer et al., 2010)). However, recently, a retrospective study by Pearce *et al* showed that children exposed to CT scans carry a small increase in cumulative risk of leukaemia and brain tumours (Pearce et al., 2012) and 12% excess relative risk of childhood leukaemia per mSv of cumulative red bone marrow dose from gamma radiation of natural origin was reported (Kendall et al., 2013). Also, a significant dose response relationship between increase in childhood cancer risk and a number of CT scans was described (Mathews et al., 2013).

Expression of radiation-responsive genes also varies with time and for many genes time-course curves have been produced from exposed human peripheral blood lymphocytes (PBLs) (Amundson et al., 2000), lymphoblastoid cell lines (Jen and Cheung, 2003), human normal epidermal keratinocytes (Franco et al., 2005), and the human myeloid leukaemia cell line ML-1 (Amundson et al., 1999b). Exposure to IR induces different temporal profiles which are gene dependent and genes involved in one pathway tend to show similar temporal profiles (Jen and Cheung, 2003). The

modification of gene expression following IR exposure can be long-lasting; an up-regulation of *Cdkn1a* gene persisted for at least two months in the liver of mice exposed to IR (Pawlik et al., 2009) and modification of gene expression can be detected 7, 17 and 55 days post irradiation in cultured human T-lymphocytes (Falt et al., 2003).

Certain genes show different transcriptional response to IR depending on dose rate (Amundson SA, 2003) and respond differently to high- and low-LET radiation (Woloschak and Chang-Liu, 1990, Turtoi et al., 2008, Turtoi et al., 2010). Moreover, gene expression signatures after IR exposure are specific and can be distinguished from different types of genotoxic stress (Park et al., 2002, Amundson et al., 2005, Meadows et al., 2008) .

Unfortunately, gene expression is also prone to confounding factors, some IR-responsive genes were altered in smokers versus non-smokers (Paul and Amundson, 2011), also LPS-induced inflammation can confound the expression of IR-responsive genes in mice (Tucker et al., 2012) and human (Budworth et al., 2012). It has been also reported that transcriptional response to IR exposure varies greatly among individuals (Kabacik et al., 2011a, Kabacik et al., 2011b, Manning et al., 2013) showing the complexity of gene expression regulation after irradiation.

1.7. microRNA biogenesis and function

MicroRNAs (miRNAs) are class of small non-coding RNA which post-transcriptionally regulate gene expression (Filipowicz et al., 2008). They were discovered over twenty years ago in *C. elegans* (Lee et al., 1993, Wightman et al., 1993) and subsequently in almost all eukaryotic organisms including unicellular algae (Zhao et al., 2007) and even in some DNA viruses (Pfeffer et al., 2004) and retroviruses

(Klase et al., 2007). miRNAs are single stranded, 18-22 nucleotide long RNAs encoded by genomic DNA as an independent, very often polycistronic transcript which is usually transcribed by polymerase II, capped and polyadenylated (Lee et al., 2004). miRNAs can be also located in the introns and co-expressed with the host gene (Ruby et al., 2007). The intergenic transcripts coding for miRNAs, called pri-miRNA, are processed by nuclear complex containing ribonuclease type III enzyme – DROSHA, which cuts the pri-miRNA transcript to produce approximately 70 nucleotide long double stranded hairpins (pre-miRNAs) (Denli et al., 2004, Gregory et al., 2004). Some intronic miRNAs can bypass DROSHA cleavage and are processed by alternative pathway utilising the spliceosome which creates pre-miRNAs without DROSHA involvement (Ruby et al., 2007). The pre-miRNAs are transported from the nucleus to the cytoplasm by exportin 5 protein in a sequence independent manner (Lund et al., 2004) and in the cytoplasm the pre-miRNAs are further processed by another ribonuclease type III – DICER1, which creates about 18-22 nucleotide long duplexes containing mature miRNAs (Hutvagner et al., 2001). Mature miRNAs are then loaded into the RNA-induced silencing complex (RISC), where they posttranscriptionally regulate gene expression (Filipowicz et al., 2008). The 5’ and 3’ mature miRNAs derived from DICER1 cleavage have different thermodynamic properties and although one strand is usually preferentially loaded into RISC complex, both of the strands can be used for regulation of gene expression (Okamura K, 2008) (**Figure 3**).

miRNAs act mainly as negative regulators of gene expression, however, in specific circumstances they can activate translation as well (Vasudevan et al., 2007, Henke et al., 2008). Target recognition occurs by partial miRNA binding to the 3’ untranslated region (UTR) in the target mRNA and seven nucleotides at 5’ end of the

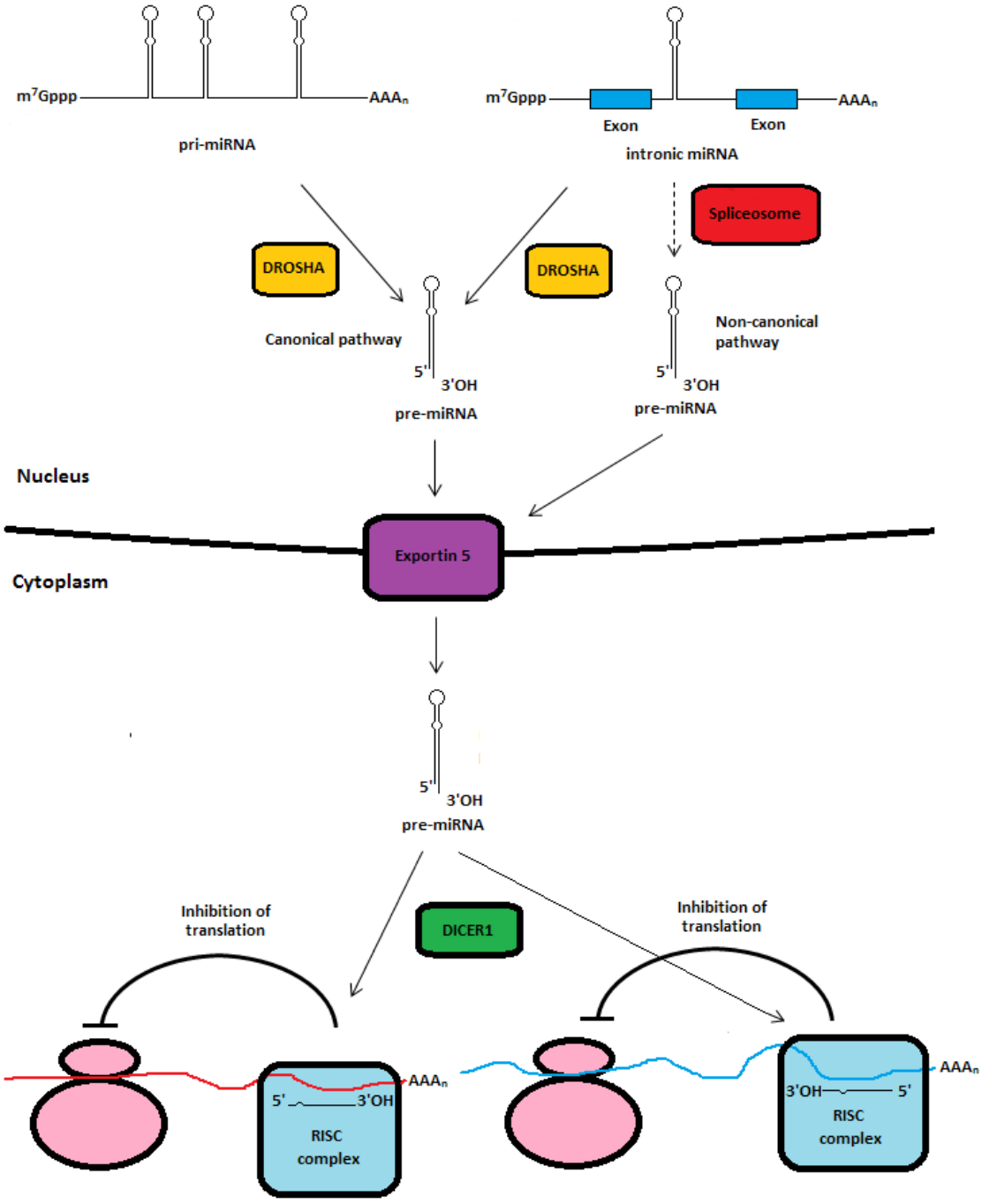

Figure 3. miRNA biogenesis.

The independent miRNA transcripts (pri-miRNAs) and miRNAs located in introns are processed by DROSHA ribonuclease to produce hairpin structure called pre-miRNA. Some miRNAs located in introns are processed by non-canonical pathway involving spliceosome to produce pre-miRNA. Pre-miRNAs are exported from the nucleus by exportin 5, where they are further processed by DICER 1 complex to produce mature miRNAs, which are subsequently loaded into RISC complex, where they regulate gene expression. Adapted from (O'Carroll and Schaefer, 2013)

miRNA (numbers 2-8), called the seed region, provide most specificity for target recognition (Filipowicz et al., 2008). Due to the short length of the seed sequence, one miRNA can target many mRNAs and one mRNA can be targeted by many different miRNAs (Chi et al., 2009). The mechanism of miRNA mediated repression is still debatable but inhibition of initiation of translation seems to be a critical event (Mathonnet et al., 2007, Meijer et al., 2013).

1.8. Effects of IR exposure on miRNA expression

Since their discovery, miRNAs have been implicated virtually in every process investigated in the cell (Filipowicz et al., 2008). Widespread reduction of microRNA gene expression has been reported in cancer (Lu et al., 2005). A number of miRNAs which target DDR components have been identified: *miR-100*, *miR-101* and *miR-421* down-regulate *ATM* expression (Ng et al., 2010, Yan et al., 2010, Hu et al., 2010a), *miR-125b* and *miR-504* directly regulate *TP53* expression (Le et al., 2009, Hu et al., 2010b) and *miR-605* and *miR-661* target *MDM2* gene (Xiao et al., 2011, Hoffman et al., 2014). Moreover, following DNA damage, TP53 increases rate of pri-miRNA processing of several growth suppressing miRNAs via interaction with DROSHA (Suzuki et al., 2009). Additionally, upon DSB induction, ATM directly activates KH-type splicing regulatory protein (KSRP) which interacts with DROSHA and DICER1 complexes regulating biogenesis of subset of miRNA and increases global miRNA processing (Zhang et al., 2011). miRNAs seem to be essential for cellular response to IR, as global miRNA reduction achieved by down-regulation of DICER, reduces cell survival following radiation mediated by impaired cell cycle checkpoint activation and increased apoptosis (Kraemer et al., 2011).

The pioneering work of Marsit *et al* showed that γ-ray exposure, in contrast to folate deprivation and arsenite exposure, did not induce significant alteration in global miRNA expression measured by microarray method in a human lymphoblastoid cell line (Marsit et al., 2006). In 2007, He *et al* reported that miRNAs belonging to *miR-34* family were induced in a TP53-dependent manner by IR in a variety of mouse tissues (He et al., 2007). This publication sparked the search for other IR-responsive miRNAs. Experiments on human primary foreskin fibroblasts revealed a very modest response of 29 miRNAs to X-ray exposure although they seemed to be dose- and time-point specific (Maes et al., 2008). Shin *et al* investigated miRNA responses to IR in human colon carcinoma cell lines differing with wild-type or knockout *TP53* gene and concluded that majority of observed miRNA differences were due to TP53 status rather than IR exposure, with only one miRNA (*miR-548c*) classified as radiation-responsive (Shin et al., 2009). The same group investigated miRNA expression after IR exposure in a human B lymphoblastic cell line utilising the same experimental approach and they found 87 miRNAs the expression of which was significantly different in irradiated cells (Cha et al., 2009). Interestingly, *miR-548c* was not reported, although some of the TP53 status responsive miRNAs from the human colon carcinoma cell line seemed to be radiation responsive in this cell line. Simone *et al* investigated miRNA expression following treatment with hydrogen peroxide, etoposide and γ-ray in normal human fibroblasts, they reported 17 IR-responsive miRNAs, and interestingly all of these miRNAs were responsive to hydrogen peroxide and/or etoposide as well, suggesting that they play a role in general stress response (Simone et al., 2009). Only ten miRNAs showed small changes in expression after IR exposure in human endothelial cells, six of them: *let-7g*, *miR-16*, *miR-18a*, *miR-20a*, *miR-21* and *miR-29c* were identified in at least one of the previous studies (Wagner-Ecker et al., 2010).

The experiments of Chaudhry *et al* with human cell lines differing in the TP53 and DNA-dependent protein kinase (DNA-PK) status seem to confirm that miRNA response to IR is specific to dose of radiation, time-point and genetic background (Chaudhry et al., 2010a, Chaudhry et al., 2010b). Moreover, the miRNA response to IR exposure depends on cell or tissue type (**Table 1**) and gender (Ilnytskyy et al., 2008, Koturbash et al., 2008, Koturbash et al., 2011). The miRNA response to IR can be long lasting as Shi *et al* reported increasing expression of *miR-21* in brain of irradiated mice up to a year post exposure (Shi et al., 2012).

Very importantly Jacob *et al* showed that *miR-150* exhibits dose- and time-dependent expression in serum of mice exposed to whole body doses of γ-ray which makes this miRNA particularly promising candidate for radiation biodosimetry (Jacob et al., 2013).

1.9. Long non-coding RNAs

The definition of long non-coding RNA (lncRNA) is very broad and unspecific: every RNA molecule longer than 200 nucleotides which is not ribosomal RNA or transfer RNA and lacks significant protein coding potential is defined as lncRNA (Mercer and Mattick, 2013). The first lncRNA – the H19, imprinted maternally expressed transcript (non-protein coding) (*H19)* was discovered in early nineties (Brannan et al., 1990) and discovery of the X inactive specific transcript (non-protein coding) (*Xist*) lncRNA followed the next year (Brockdorff et al., 1991); however, at the time it was believed that the majority of genes code for proteins, therefore these molecules were treated as curiosities for almost a decade. This view changed with the initial papers published by FANTOM consortium (Kawai et al., 2001, Okazaki et al., 2002) when for the first time it became clear that lncRNAs are much more common

Table 1. miRNAs showing altered expression following IR exposure in different cell lines adapted from (Metheetrairut and Slack, 2013)

Increase	Decrease
let-7a M059K – human glioblstoma cell line (Chaudhry et al., 2010b)	**let-7a** IM9 human lymphoblast line (Cha et al., 2009), normal human fibroblasts (Simone et al., 2009) and A549 lung cancer cell line (Weidhaas et al., 2007)
let-7b M059K – human glioblstoma cell line (Chaudhry et al., 2010b)	**let-7b** normal human fibroblasts (Simone et al., 2009) and A549 lung cancer cell line (Weidhaas et al., 2007)
let-7c normal human thyroid cells (Nikiforova et al., 2011) and M059K – human glioblstoma cell line (Chaudhry et al., 2010b)	**let-7c** IM9 human lymphoblast line (Cha et al., 2009) and A549 lung cancer cell line (Weidhaas et al., 2007)
let-7d normal human thyroid cells (Nikiforova et al., 2011), normal human fibroblasts (Simone et al., 2009) and M059K – human glioblstoma cell line (Chaudhry et al., 2010b)	**let-7d** AG1522 normal human skin fibroblasts (Chaudhry et al., 2012), and A549 lung cancer cell line (Weidhaas et al., 2007)
let-7e AG1522 normal human skin fibroblasts (Chaudhry et al., 2012), normal human fibroblasts (Simone et al., 2009) and M059K – human glioblstoma cell line (Chaudhry et al., 2010b)	**let-7e** , IM9 human lymphoblast line (Cha et al., 2009), human peripheral blood lymphocytes (Girardi et al., 2012) and A549 lung cancer cell line (Weidhaas et al., 2007)
let-7f b M059K – human glioblstoma cell line (Chaudhry et al., 2010b) and blood (Templin et al., 2011b)	**let-7f** IM9 human lymphoblast line (Cha et al., 2009), normal human thyroid cells (Nikiforova et al., 2011) and A549 lung cancer cell line (Weidhaas et al., 2007)
let-7g normal human thyroid cells (Nikiforova et al., 2011), normal human fibroblasts (Simone et al., 2009), M059K – human glioblstoma cell line (Chaudhry et al., 2010b), blood (Templin et al., 2011b), U87MG human malignant glioma cell line (Chen et al., 2010) and human dermal microvascular endothelial cells (Wagner-Ecker et al., 2010)	**let-7g** TPC-1 papillary thyroid carcinoma (Abou-El-Ardat et al., 2012)
let-7i AG1522 normal human skin fibroblasts (Chaudhry et al., 2012), normal human fibroblasts (Simone et al., 2009) and M059K – human glioblstoma cell line (Chaudhry et al., 2010b)	**let-7i** A549 lung cancer cell line (Weidhaas et al., 2007)
	miR-10a TPC-1 papillary thyroid carcinoma (Abou-El-Ardat et al., 2012) and human peripheral blood lymphocytes (Girardi et al., 2012)
miR-15a AG1522 normal human skin fibroblasts (Chaudhry et al., 2012), M059K – human glioblstoma cell line (Chaudhry et al., 2010b), A549 lung cancer cell line (Weidhaas et al., 2007)	
miR-16 human peripheral blood lymphocytes (Girardi et al., 2012), M059K – human glioblstoma cell line (Chaudhry et al., 2010b), blood (Templin et al., 2011b), human dermal microvascular endothelial cells (Wagner-Ecker et al., 2010) and A549 lung cancer cell line (Weidhaas et al., 2007)	**miR-16** IM9 human lymphoblast line (Cha et al., 2009)
miR-17-3p TPC-1 papillary thyroid carcinoma (Abou-El-Ardat et al., 2012), AG1522 normal human skin fibroblasts (Chaudhry et al., 2012), M059K – human glioblstoma cell line (Chaudhry et al., 2010b) and blood (Templin et al., 2011b)	**miR-17** human peripheral blood lymphocytes (Girardi et al., 2012)
miR-17-5p TPC-1 papillary thyroid carcinoma (Abou-El-Ardat et al., 2012), AG1522 normal human skin fibroblasts (Chaudhry et al., 2012), M059K – human glioblstoma cell line (Chaudhry et al., 2010b), blood (Templin et al., 2011b), A549 lung cancer cell line (Weidhaas et al., 2007) and HUVEC human umbilical vein endothelial cells (Vincenti et al., 2011)	**miR-17-5p** IM9 human lymphoblast line (Cha et al., 2009)

	miR-18a human dermal microvascular endothelial cells (Wagner-Ecker et al., 2010) and normal human fibroblasts (Maes et al., 2008)
miR-19a M059K – human glioblstoma cell line (Chaudhry et al., 2010b), blood (Templin et al., 2011b), A549 lung cancer cell line (Weidhaas et al., 2007) and HUVEC human umbilical vein endothelial cells (Vincenti et al., 2011)	
miR-19b AG1522 normal human skin fibroblasts (Chaudhry et al., 2012), M059K – human glioblstoma cell line (Chaudhry et al., 2010b), A549 lung cancer cell line (Weidhaas et al., 2007) and HUVEC human umbilical vein endothelial cells (Vincenti et al., 2011)	**miR-19b** human peripheral blood lymphocytes (Girardi et al., 2012) and IM9 human lymphoblast line (Cha et al., 2009)
miR-20a blood (Templin et al., 2011b),(Wagner-Ecker et al., 2010) and HUVEC human umbilical vein endothelial cells (Vincenti et al., 2011)	**miR-20a** IM9 human lymphoblast line (Cha et al., 2009)
miR-20b blood (Templin et al., 2011b) and A549 lung cancer cell line (Weidhaas et al., 2007)	
miR-21 AG1522 normal human skin fibroblasts (Chaudhry et al., 2012), normal human fibroblasts (Simone et al., 2009), M059K – human glioblstoma cell line (Chaudhry et al., 2010b), blood (Templin et al., 2011b), human dermal microvascular endothelial cells (Wagner-Ecker et al., 2010), (Mueller et al., 2013), HUVEC human umbilical vein endothelial cells (Vincenti et al., 2011)	**miR-21** IM9 human lymphoblast line (Cha et al., 2009)
miR-22 U87MG human malignant glioma cell line (Chen et al., 2010), A549 lung cancer cell line (Weidhaas et al., 2007) and LNCaP human prostate cancer cell lines (Li et al., 2011)	
miR-24 blood (Templin et al., 2011b), A549 lung cancer cell line (Weidhaas et al., 2007) and LNCaP human prostate cancer cell lines (Li et al., 2011)	**miR-24** normal human fibroblasts (Simone et al., 2009) and IM9 human lymphoblast line (Cha et al., 2009)
miR-26b normal human fibroblasts (Simone et al., 2009) and blood (Templin et al., 2011b)	
miR-27a blood (Templin et al., 2011b) and A549 lung cancer cell line (Weidhaas et al., 2007)	
miR-27b TPC-1 papillary thyroid carcinoma (Abou-El-Ardat et al., 2012), A549 lung cancer cell line (Weidhaas et al., 2007) and HUVEC human umbilical vein endothelial cells (Vincenti et al., 2011)	
miR-29a blood (Templin et al., 2011b) and HUVEC human umbilical vein endothelial cells (Vincenti et al., 2011)	
miR-29c blood (Templin et al., 2011b), human dermal microvascular endothelial cells (Wagner-Ecker et al., 2010), IM9 human lymphoblast line (Cha et al., 2009) and HUVEC human umbilical vein endothelial cells (Vincenti et al., 2011)	
miR-30a-5p A549 lung cancer cell line (Weidhaas et al., 2007) and LNCaP human prostate cancer cell lines (Li et al., 2011)	
miR-34a human peripheral blood lymphocytes (Girardi et al., 2012), A549 human non-small cell lung cancer cells (Shin et al., 2009), IM9 human lymphoblast line (Cha et al., 2009) and normal human thyroid cells (Nikiforova et al., 2011)	
miR-34b* human peripheral blood lymphocytes (Girardi et al., 2012), normal human thyroid cells (Nikiforova et al., 2011) and A549 human non-small cell lung cancer cells (Shin et al., 2009)	
miR-34c LNCaP and C4-2 human prostate cancer cell lines (Josson et al., 2008)	

miR-99a A549 lung cancer cell line (Weidhaas et al., 2007) and MCF7 breast cancer cell line (Mueller et al., 2013)	**miR-99a** human peripheral blood lymphocytes (Girardi et al., 2012)
miR-100 MCF7 breast cancer cell line (Mueller et al., 2013)	**miR-100** human peripheral blood lymphocytes (Girardi et al., 2012), normal human fibroblasts (Simone et al., 2009) and LNCaP and C4-2 human prostate cancer cell lines (Josson et al., 2008)
miR-106a blood (Templin et al., 2011b) and A549 lung cancer cell line (Weidhaas et al., 2007)	**miR-106a** TPC-1 papillary thyroid carcinoma (Abou-El-Ardat et al., 2012), IM9 human lymphoblast line (Cha et al., 2009) and A549 human non-small cell lung cancer cells (Shin et al., 2009)
	miR-106b LNCaP human prostate cancer cell lines (Li et al., 2011) and IM9 human lymphoblast line (Cha et al., 2009)
	miR-107 U87MG human malignant glioma cell line (Chen et al., 2010), IM9 human lymphoblast line (Cha et al., 2009) and LNCaP and C4-2 human prostate cancer cell lines (Josson et al., 2008)
	miR-125a human dermal microvascular endothelial cells (Wagner-Ecker et al., 2010) and A549 lung cancer cell line (Weidhaas et al., 2007)
miR-126 blood (Templin et al., 2011b) and HUVEC human umbilical vein endothelial cells (Vincenti et al., 2011)	
	miR-133b LNCaP and C4-2 human prostate cancer cell lines (Josson et al., 2008)
miR-142-3p AG1522 normal human skin fibroblasts (Chaudhry et al., 2012) and M059K – human glioblstoma cell line (Chaudhry et al., 2010b)	**miR-142-3p** IM9 human lymphoblast line (Cha et al., 2009)
miR-142-5p AG1522 normal human skin fibroblasts (Chaudhry et al., 2012), M059K – human glioblstoma cell line (Chaudhry et al., 2010b) and blood (Templin et al., 2011b)	**miR-142-5p** IM9 human lymphoblast line (Cha et al., 2009)
miR-143 AG1522 normal human skin fibroblasts (Chaudhry et al., 2012), M059K – human glioblstoma cell line (Chaudhry et al., 2010b)	**miR-143** blood (Templin et al., 2011b) and LNCaP and C4-2 human prostate cancer cell lines (Josson et al., 2008)
miR-145 AG1522 normal human skin fibroblasts (Chaudhry et al., 2012), human peripheral blood lymphocytes (Girardi et al., 2012) and blood (Templin et al., 2011b)	**miR-145** LNCaP and C4-2 human prostate cancer cell lines (Josson et al., 2008)
miR-148a blood (Templin et al., 2011b) and A549 lung cancer cell line (Weidhaas et al., 2007)	
	miR-152 TPC-1 papillary thyroid carcinoma (Abou-El-Ardat et al., 2012) and human peripheral blood lymphocytes (Girardi et al., 2012)
miR-155 M059K – human glioblstoma cell line (Chaudhry et al., 2010b)	**miR-155** AG1522 normal human skin fibroblasts (Chaudhry et al., 2012), A549 lung cancer cell line (Weidhaas et al., 2007) and IM9 human lymphoblast line (Cha et al., 2009)
	miR-181a human peripheral blood lymphocytes (Girardi et al., 2012) and U87MG human malignant glioma cell line (Chen et al., 2010)
miR-188-5p human peripheral blood lymphocytes (Girardi et al., 2012) and normal human thyroid cells (Nikiforova et al., 2011)	**miR-188-5p** normal human fibroblasts (Maes et al., 2008)
	miR-196a human peripheral blood lymphocytes (Girardi et al., 2012) and LNCaP and C4-2 human prostate cancer cell lines (Josson et al., 2008)
miR-191 U87MG human malignant glioma cell line (Chen et al., 2010) and LNCaP human prostate cancer cell lines (Li et al., 2011)	
miR-221 human peripheral blood lymphocytes (Girardi et al., 2012), blood (Templin et al., 2011b), A549 lung cancer cell line (Weidhaas et al., 2007) and HUVEC	

human umbilical vein endothelial cells (Vincenti et al., 2011)	
miR-222 blood (Templin et al., 2011b) and HUVEC human umbilical vein endothelial cells (Vincenti et al., 2011)	**miR-222** normal human fibroblasts (Simone et al., 2009)
miR-365 normal human thyroid cells (Nikiforova et al., 2011) and A549 lung cancer cell line (Weidhaas et al., 2007)	
miR-379 U87MG human malignant glioma cell line (Chen et al., 2010) and LNCaP and C4-2 human prostate cancer cell lines (Josson et al., 2008)	
	miR-521 U87MG human malignant glioma cell line (Chen et al., 2010) and LNCaP and C4-2 human prostate cancer cell lines (Josson et al., 2008)
miR-601 human peripheral blood lymphocytes (Girardi et al., 2012) and U87MG human malignant glioma cell line (Chen et al., 2010)	
miR-663 human peripheral blood lymphocytes (Girardi et al., 2012), IM9 human lymphoblast line (Cha et al., 2009) and normal human fibroblasts (Simone et al., 2009)	**miR-663** normal human fibroblasts (Maes et al., 2008)

and transcription is much more pervasive than previously thought. The same group reported that for many protein coding genes antisense RNAs are transcribed from the opposite strand which can regulate their transcription (Katayama et al., 2005) and that the majority of the mammalian genome is transcribed (Carninci et al., 2005). Instantly, questions about the nature of this transcription followed. The overwhelming majority of lncRNAs show no sequence conservation between species (Pang et al., 2006) and they are expressed at very low levels (Ravasi et al., 2006). These observations led some researchers to hypothesise that observed ubiquitous non-coding transcripts are non-functional and represent transcriptional noise (Struhl, 2007, Ebisuya et al., 2008). Nonetheless, lncRNAs show highly tissue-specific expression (Mercer et al., 2008) and precise functions for individual lncRNAs have been identified (Penny et al., 1996, Sleutels et al., 2002).

Guttman *et al* used chromatin structures associated with active polymerase II transcription to map unknown transcripts in the intergenic regions of the mouse genome and they discovered about 1600 new highly conserved lncRNAs and associated their likely functions with various cellular processes (Guttman et al., 2009). The completion of Encyclopedia of DNA Elements (ENCODE) project revealed that 75 % of the human genome is transcribed in some cell types and at some point in development and that majority of non-coding transcripts show nuclear localisation (Djebali et al., 2012). The number of non-coding RNAs, in contrast to protein coding sequences, does correlate with the complexity of multicellular organisms and it has been proposed that RNA played a central role in evolution of eukaryotic organisms (Taft et al., 2007).

lncRNAs exhibit various mechanisms of action. They can act as RNA decoys for miRNAs (Poliseno et al., 2010, Cesana et al., 2011) or repressive proteins (Zhao et al., 2008, Klattenhoff et al., 2013), scaffold for protein complexes (Sharma et al., 2011, Yoon et al., 2013), co-activators (Hube et al., 2011) or co-repressors (Rinn et al., 2007) (**Figure 4**). Although the function of the overwhelming majority of lncRNAs is still unknown, those characterised seem to play very diverse roles in genomic imprinting (Sleutels et al., 2002), chromosome X dosage compensation (Penny et al., 1996), growth arrest (Mourtada-Maarabouni et al., 2008), control of pluripotency and differentiation (Guttman et al., 2011), apoptosis (Yan et al., 2005), gene expression (Zhou et al., 2007) and DNA methylation (Imamura et al., 2004) just to name a few.

1.10. DNA damage responsive lncRNAs

The lncRNA concept is relatively new in radiation biology and only a handful of IR-responsive lncRNAs has been identified so far. Majority of experiments have been performed using radiomimetic drugs which induce DSBs like doxorubicin, bleomycin or etoposide. The first lncRNA showing modification of expression upon induction of DSBs was TP53 target 1 (non-protein coding) (*TP53TG1*) (Takei et al., 1998). The *TP53TG1* transcript did not possess significant protein coding potential and was up-regulated in normal human fibroblasts in TP53 dependent manner upon ultraviolet light exposure or bleomycin treatment. Huarte *et al* identified another direct TP53 target lncRNA – tumor protein p53 pathway corepressor 1 (*Trp53cor1*) which was induced upon doxorubicin treatment in a range of mouse cell lines and human fibroblasts and acted as a repressor in TP53 pathway (Huarte et al., 2010).

Several other lncRNAs have been found to be up-regulated following doxorubicin treatment in various cell lines, for example the non-protein coding RNA,

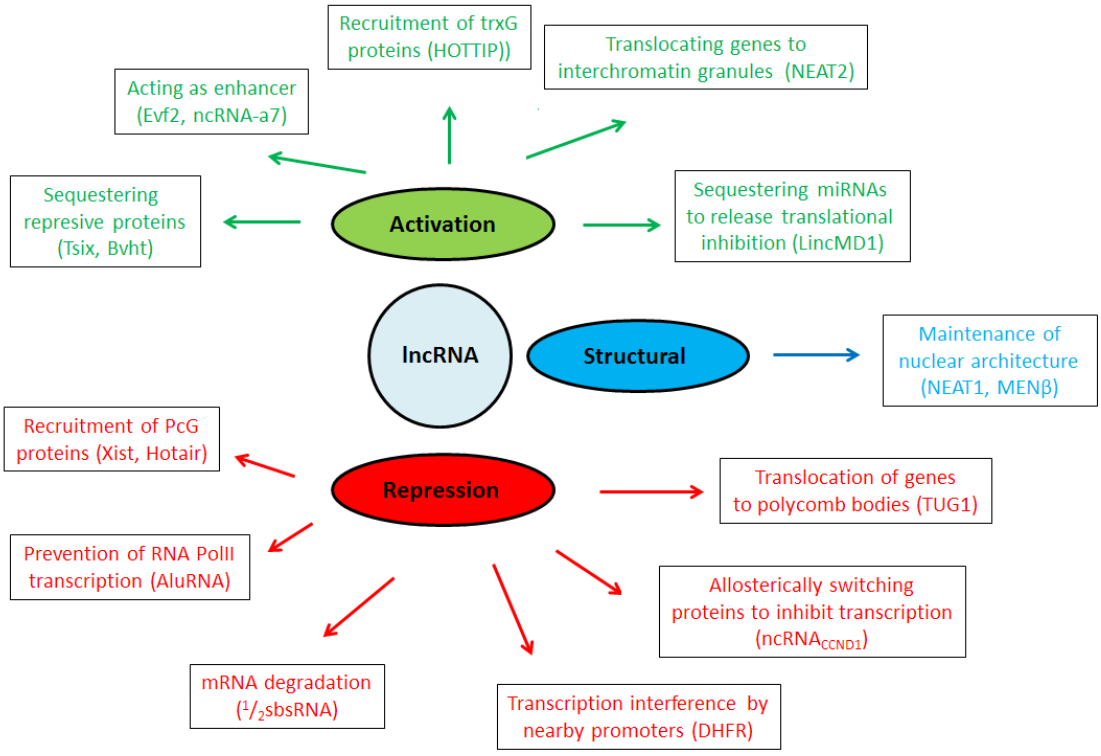

Figure 4. Mechanisms of action for lncRNAs.

lncRNAs can be divided in three functional categories, activators, repressors and structural. Copied from (Krishnan and Mishra, 2014).

associated with MAP kinase pathway and growth arrest (*NAMA*) in human papillary thyroid cancer and colon cancer cell lines (Yoon et al., 2007), the promoter of CDKN1A antisense DNA damage activated RNA (*PANDAR*) induced in normal human fibroblasts which negatively regulates apoptosis in TP53-dependent manner (Hung et al., 2011), the long intergenic non-protein coding RNA, regulator of reprogramming (*linkRNA-RoR*) induced in a TP53-dependent manner in several human cancer cell lines, involved in controlling TP53 level after DNA damage (Zhang et al., 2013), the urothelial cancer associated 1 (non-protein coding) lncRNA (*UCA1*) up-regulated by in TP53-independent manner in human breast cancer cell line (Huang et al., 2014). Also E2F1-regulated lncRNA XLOC 006942 (*ERIC*) was found to be up-regulated after etoposide treatment in a human osteosarcoma cell line (Feldstein et al., 2013).

Wan *et al* screened a human lymphoblastoid cell line for lncRNAs showing modification of expression following treatment with a radiomimetic drug (Wan et al., 2013b). The authors reported significant ATM-dependent up-regulation of the CDKN2B antisense RNA 1 (*CDKN2B-AS1* also known as *ANRIL*) following DNA damage, also down-regulation of *H19* and modest up-regulation of taurine up-regulated 1 (non-protein coding) (*TUG1*) and lncRNA transcribed from the promoter region encoding cyclin D1 (*lncRNA-CCND1*) was reported (Wan et al., 2013b). The same group identified a novel JADE1 adjacent regulatory RNA (*JADRR*) lncRNA which is induced following DNA damage in an ATM-dependent manner (Wan et al., 2013a).

Mizutani *et al* identified 25 novel genotoxic stress-inducible nuclear lncRNAs and six of them showed modulation of expression following doxorubicin treatment in HeLa cells, however they have not been annotated yet and their function is unknown (Mizutani et al., 2012).

The first reported lncRNA induced by IR-exposure was *lncRNA-CCND1*, it forms a ribonucleoprotein complex and represses *CCND1* transcription following DNA damage (Wang et al., 2008). Chaudhry *et al* investigated the temporal response of five lncRNAs, for which TaqMan assays were commercially available, following exposure to 2 Gy of X-ray, in human lymphoblastoid cell lines, however only SOX2 overlapping transcript (non-protein coding) (*SOX2-OT*) shown modification of expression more than 2 fold (Chaudhry, 2013).

Özgür *et al* investigated expression of ten well characterised lncRNAs playing roles in the TP53 pathway or DNA damage following γ-radiation exposure or bleomycin treatment in human cervical and breast cancer cell lines (Ozgur et al., 2013). They observed cell line dependent differences in expression of investigated lncRNAs and differences in transcriptional response to bleomycin and IR, although it should be noted that doses of bleomycin used induced much higher apoptotic response than IR indicating that doses of the drug and radiation were not equivalent. Nonetheless, three lncRNAs – *CDKN2B-AS1*, *lncRNA-CCND1* and growth arrest-specific 5 (non-protein coding) (*GAS5*) were significantly up-regulated by IR exposure at least in one cell line. Interestingly, contrary to the previous report (Hung et al., 2011), *PANDAR* was not responsive to bleomycin or IR treatment in neither of the cell lines, what can indicate tissue specific transcriptional response to DNA damaging agents (Ozgur et al., 2013).

1.11. Biomarkers of radiation exposure

According to the National Institute of Health, a biomarker is “a characteristic that is objectively measured and evaluated as an indicator of normal biological processes, pathogenic processes, or pharmacologic responses to a therapeutic intervention” (Biomarkers Definitions Working, 2001). A biomarker of radiation

exposure should allow exposed individuals to be distinguished from non-exposed ones and ideally should be able to provide an estimated absorbed dose. Cytogenetic biomarkers used in radiation biology take advantage of the fact that IR induces wide range of chromosomal aberrations in peripheral blood lymphocytes (PBL) like dicentric chromosomes, rings and translocations (IAEA, 2011).

Dicentric aberrations result from erroneous joining of DSBs from two different chromosomes and give rise to a chromosome with two centromeres and an acentric fragment which can be visualised in metaphases (IAEA, 2011). Dicentric aberrations arise almost exclusively due to IR exposure, have very low spontaneous occurrence and show linear-quadratic dose-response up to around 5 Gy what makes them a good biomarker for IR exposure (Romm et al., 2009). The lower limit of detection for dicentric assay is around 0.1 Gy of whole body exposure and it is possible to estimate a dose for partial exposure based on the dicentric distribution in scored methaphases (IAEA, 2011). All these features make dicentric assay the “gold standard” for radiation biodosimetry, however the biggest disadvantages of this method are low throughput and requirement for highly trained staff for scoring dicentric chromosomes (Wojcik et al., 2010). The necessity of culturing PBLs for 48 h before the assay can be performed implies that the sample preparation takes at least 51 h; additionally, the subsequent analysis takes between 5 and 25 h per sample for 500 scored metaphases depending on level of automation (Romm et al., 2009).

The cytokinesis-blocked micronucleus (CBMN) assay has been also used for radiation biodosimetry. Micronuclei are acentric chromosome fragments or whole chromosomes which have been left in the cytoplasm after mitosis and are visible in the cell as spherical small object (IAEA, 2011). Formation of micronuclei is not specific to

radiation, however IR-induced micronuclei consist mostly of acentric chromosome fragments therefore by using centromere specific probe in the CBMN assay and scoring only acentric micronuclei the lower limit of detection of around 0.1 Gy can be obtained (Vral et al., 1997). The CBMN assay is easy to perform and does not need highly trained personnel, however due to the requirement of three day culture of PBLs it takes longer than dicentric assay to obtain dose estimates and it does not allow estimating the partial body exposure (Fenech, 1993).

Another cytogenetic-based method for dose assessment is the premature chromatin concentration (PCC) assay, where the chromosomal aberrations are visualised in prematurely condensed interphase chromatin by using either chemical reagents or fusion with mitotic cells (IAEA, 2011). Although the dose estimations can be obtained much quicker with the fusion-based method, the technical difficulties make it a less common choice whereas for chemical-induction of PCC, PBLs have to be stimulated beforehand (Hatzi et al., 2006). In the PCC assay cells do not have to enter mitosis, therefore the most damaged cells are not lost from the population and this assay enables estimation of much higher doses than dicentric or CBMN assays; it is also suitable for partial body exposure (Lindholm et al., 2010)

The dicentric chromosomes and rings are unstable aberrations which are not passed to the daughter cell after division and disappear within around three years which is the average lifespan of the lymphocytes (IAEA, 2011). Alternatively, stable translocations which are exchanges between fragments of two or more chromosomes are passed to the next generation of cells and can be detected years after exposure by using fluorescent in-situ hybridisation (FISH) assay (Tawn and Whitehouse, 2003). In the FISH assay some or all of the chromosomes are painted in different colours using

fluorescent probes making any exchanges easily visible. There are many confounding factors such as age or smoking (Sigurdson et al., 2008), therefore the lower limit of detection is around 0.5 Gy. Additionally, this technique is also labour intense and needs at least five days to provide the dose estimates and for those reasons FISH assay is mainly used for occupational or historical dosimetry (Edwards et al., 2005)

Another developing non-cytogenetic based assay for radiation biodosimetry is the γ-H2AX assay. It takes advantage of the fact that histone H2AX is rapidly phosphorylated in response to DSBs formation and this phosphorylation can be detected by using specific antibodies and fluorescent microscopy (Burma et al., 2001). The γ-H2AX assay is the most sensitive technique described so far, capable of detecting 1 mGy exposure when the pre-exposed levels of foci are known (Rothkamm and Lobrich, 2003), therefore it is mostly applicable for dosimetry of planned exposures in medical diagnostic (Rothkamm et al., 2007) and therapy (Sak et al., 2007). The phosphorylation of γ-H2AX peaks at 1 h post exposure and then rapidly declines to the baseline limiting the use of this assay for triage purpose (Rothkamm and Horn, 2009).

Using gene expression signatures for radiation dosimetry was suggested for the first time by Amundson *et al* (Amundson et al., 2000) and since then this possibility has been under intense investigation. Although studies investigating gene expression changes following IR have been conducted using different cell types or tissues and involved broad dose range and time-points, several genes have been found constantly up-regulated in human blood like *CDKN1A*, phosphohistidine phosphatase 1 (*PHPT1*), *GADD45A*, *DDB2*, *CCNG1* or ferredoxin reductase (*FDRX*) (Amundson et al., 2000, Paul and Amundson, 2008, Kabacik et al., 2011a, Manning et al., 2013) and these radiation-responsive genes are candidate IR biomarkers.

Gene expression assays are quick to perform – a dose estimate can be provided within 8 h of receiving the samples, although there are large differences between laboratories both in time of reporting and precision of dose estimates (Badie et al., 2013). A recent comparison of established and developing assays for radiation biodosimetry indicated that under optimal conditions gene expression assay outperformed the γ-H2AX assay and was as accurate as the CBMN assay in dose estimation although still about 2.5 times less precise than the dicentric assay (Rothkamm et al., 2013). However, when doses were grouped into binary categories relevant from a medical point of view, gene expression assay performed almost as well as the dicentric assay but produced the dose estimates around 8 times quicker (Rothkamm et al., 2013) revealing its potential in triage scenario.

1.12. Using gene expression profiles as a biomarker of IR exposure

The possibility of using gene expression biomarkers for dose estimation has been intensively investigated over the recent decade. Most of the studies utilise whole blood (Amundson SA, 2004, Paul and Amundson, 2008, Manning et al., 2013) or PBLs (Dressman et al., 2007, Kabacik et al., 2011a) as blood is relatively easily accessible tissue in case of mass causality scenario.

Microarray technology enables the measurement of the expression level of thousands of genes simultaneously and many research groups have employed this method to find dose- and time-specific gene signatures and use them for dose estimation. Gruel *et al* used gene signatures specific to different doses of γ-radiation ranging from 20 mGy to 5 Gy and correctly estimated dose of IR received by the test mice with 83 to 100 % accuracy depending on the dose (Gruel et al., 2006). Another group using their gene signatures distinguished with 100 % efficiency control mice

from mice irradiated with 0.5 Gy and they correctly estimated doses of radiation within medically relevant dose ranges (Dressman et al., 2007, Meadows et al., 2008). Moreover, they were also able to distinguish with 94 % efficiency non-exposed human from patients undergoing total body radiotherapy using human specific gene expression signatures (Dressman et al., 2007). The same group reported gene signatures allowing prediction of radiation status of part body exposed mice with 79 – 100 % accuracy although they could not distinguish between doses of 0.5, 2 and 10 Gy X-ray (Meadows et al., 2010). Importantly, the gene signatures used for dose estimation in total body irradiation completely failed to predict radiation status in partially exposed mice (Meadows et al., 2010).

Gene signatures have also been described in human. Paul *et al* developed a 74 gene signature in human blood exposed to IR *ex vivo* which enabled estimation of the doses of 0.5, 2, 5 and 8 Gy of γ-ray with high accuracy between 6 and 48 h post exposure *ex vivo* (Paul and Amundson, 2008, Paul et al., 2013) and they used this signature to estimate the total body doses in radiotherapy patients with 98 % accuracy (Paul et al., 2011). Moreover, Knops *et al* used a 9-gene signature from PBLs exposed *ex-vivo* to estimate with 86.7 % accuracy a dose of 20 mGy and with 100 % accuracy dose of 100 mGy in blood irradiated *ex-vivo* (Knops et al., 2012).

miRNA signatures were also tested for potential use in radiation biodosimetry. Templin *et al* developed miRNA signatures in mice which distinguished between different types of radiation with 81 % accuracy and allowed dose estimation with 88 – 100 % accuracy depending on type of radiation (Templin et al., 2011a, Templin et al., 2012). The same group reported miRNA signatures in human which allowed total body

doses of 1.25 Gy of X-ray to be distinguished with 100 % accuracy in eight radiotherapy patients (Templin et al., 2011b).

Gene expression signatures obtained by microarray experiments hold great potential in radiation dosimetry, however, they usually consists of dozens of genes per dose/time-point with very little overlap (Dressman et al., 2007, Meadows et al., 2010). Moreover, the microarray technique is time consuming, quite expensive and data analysis is complicated which would be a disadvantage in triage scenario, therefore, some groups focused their interest on a gene or genes which show clear dose responses to IR and could be analysed by the quicker quantitative polymerase chain reaction (qPCR) technique and doses estimated using linear regression analysis.

Dose-responses for IR-responsive genes expressed in human blood exposed *ex-vivo* are best fitted with the linear quadratic model (Paul and Amundson, 2008, Manning et al., 2013), therefore if a calibration curve is present, a linear regression analysis can be employed to estimate the dose of radiation received by the unknown samples. Manning *et al* used a combination of two genes (*FDXR* and *DDB2*) in a high dose range (0.1 – 4 Gy) to produce a mean dose estimate of 0.7 Gy and 1.4 Gy for 'unknown' blood samples irradiated with respectively 1 Gy and 2 Gy of X-ray and a combination of three genes (*FDXR*, *DDB2* and *CCNG1*) for the low dose range (5 mGy – 100 mGy) to produce a mean dose estimate of 98 mGy for 100 mGy exposure (Manning et al., 2013). Another group used sets of three and four genes to accurately predict doses ranging from 0.5 to 6 Gy of γ-irradiated human blood samples up to two days post irradiation (Tucker et al., 2014) and up to seven days post irradiation in mice exposed to the same doses of γ-ray *in vivo* (Tucker et al., 2013). Filiano *et al* used expression of two genes *CDKN1A* and *CCNG1* and linear regression analysis to estimate

the dose of radiation in mice exposed to IR *in vivo* and the average predicted doses for the 0, 1, 2, 4, 6, and 8 Gy treatment groups were 0.0 (± 0.2), 1.6 (± 1.0), 2.9 (± 1.4), 5.1 (± 2.0), 5.3 (± 0.7), and 10.5 (± 5.6) Gy, respectively (Filiano et al., 2011). **Table 2** contains compiled dose responses in human samples published for biodosimetry purposes.

Recently, a portable device was developed enabling measurement of gene expression changes in small volumes of blood and this device was capable of distinguishing irradiated samples from non-irradiated and would be suitable for triage scenarios (Brengues et al., 2010).

1.13. Common methods for measuring gene expression

qPCR is the "gold standard" technique for measuring and quantifying expression of genes (Derveaux et al., 2010). In this method RNA is reverse transcribed to complementary DNA (cDNA), then amplified using specific primers and a fluorescent reporter such as an intercalating dye or a specific probe, which allow real time detection of the amplified product (Bustin, 2004) (**Figure 5**). This technique is quick, straightforward, relatively inexpensive and when properly optimised and performed is sensitive enough to detect minute quantities of the template (Nolan et al., 2006). However, despite its simplicity, there are many factors which can influence qPCR results like assay design (Bustin, 2004, Derveaux et al., 2010), RNA quality (Perez-Novo et al., 2005, Fleige et al., 2006, Vermeulen et al., 2011), RT reaction (Stahlberg et al., 2004, Nolan et al., 2006), operator's experience (Bustin, 2002), normalisation approach (Perez-Novo et al., 2005, Smits et al., 2009, Hruz et al., 2011) and data analysis (Bustin, 2004, Fleige et al., 2006). All these issues have to be addressed in order to obtain reliable, sensitive and meaningful data. In response to a lack of consensus on how

Table 2. Dose responses in human samples published for biodosimetry purposes

Gene	Time post exposure	Doses and type of IR	Sample	Publication
DDB2 CDKN1A XPC	4, 24, 48 and 72 h	0, 0.2, 0.5, 1 and 2 Gy γ-rays	peripheral blood lymphocytes	(Amundson et al., 2000)
CDKN1A CXCL10 DDB2 FCGR1A	6, 12, 18, 24, 30, 36 h	0 and 1.5 Gy X-ray fractionated every 6 h up to 9 Gy	peripheral blood of patients undergoing total body irradiations	(Amundson et al., 2004)
FDXR CDKN1A PHPT1 BBC3 SESN1	6 and 24 h	0, 0.5, 2, 5 and 8 Gy γ-rays	peripheral blood	(Paul and Amundson, 2008)
RPL19 RPS6 ATP5E COX8A NDUFA4 RPL21	3 h	0, 0.05 and 0.5 Gy γ-rays	CD4+ T-lymphocytes	(Gruel et al., 2008)
DDB CDKN1A APOBEC3H	6 h	0, 0.1, 0.5, and 2 Gy γ-rays	peripheral blood	(Paul and Amundson, 2011)
FDXR PFKFB3	24 and 48h	0, 0.02 and 0.1 γ-rays	peripheral blood lymphocytes	(Knops et al., 2012)
FDXR PHPT1 DDB2 GADD45A CCNG1 CDKN1A BBC3 MDM2 SESN1 TIGAR FAS PCNA MYC	2 and 24 h	0, 0.005, 0.01, 0.02, 0.05, 0.075, 0.1, 0.5, 1, 2 and 4 Gy X-ray	peripheral blood	(Manning et al., 2013)
MDM2 XPC FDXR ND2 MEX3D ANKRD33 TFAM	2.5, 5, 7.5 and 10 h	0, 5, 10, 25, 50, 100 and 500 mGy γ-rays	CD4+ T-lymphocytes	(Nosel et al., 2013)
CDKN1A DDB2 PCNA PHPT1 GNLY GZMA NKG7	48 h	0, 0.5, 2, 5 and 8 Gy γ-rays	peripheral blood	(Paul et al., 2013)
ASTN2 CDKN1A GDF15 ATM	12, 24 and 48 h	0, 0.5, 1, 1.5, 2, 2.5, 3, 4, 6, 8 and 10 Gy γ-rays	peripheral blood	(Tucker et al., 2014)

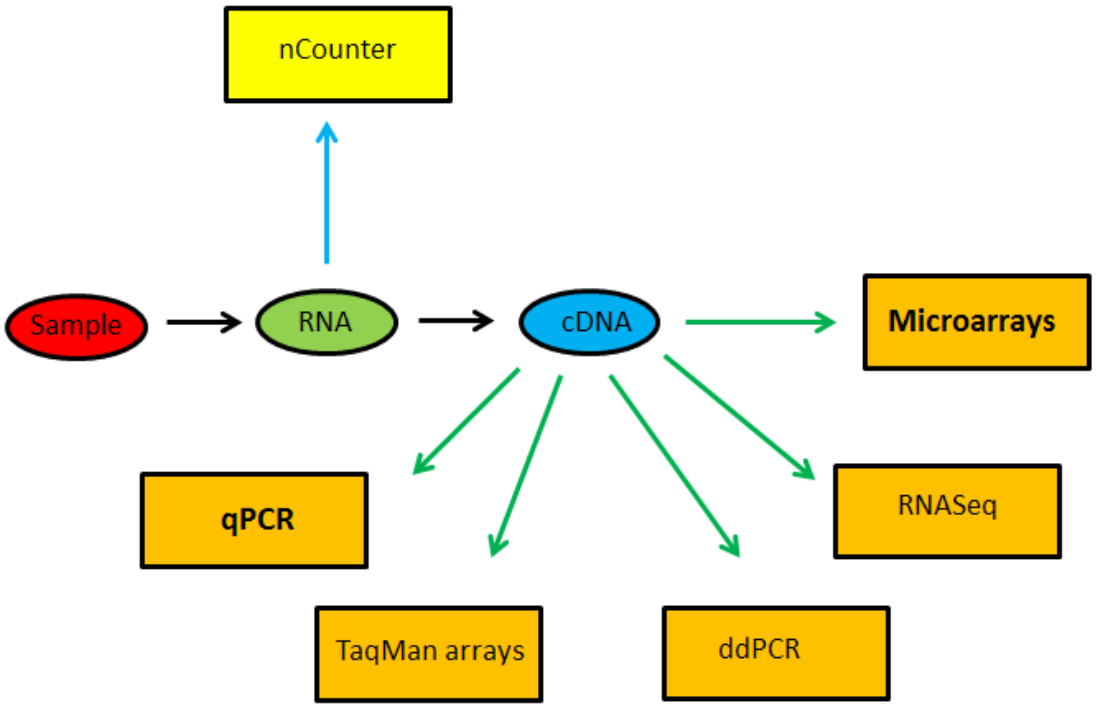

Figure 5. Common methods used for measuring changes in gene expression.

The first step in measuring gene expression is RNA extraction form the samples, next the RNA is reverse transcribed to cDNA which is then used in the downstream assays. Microarrays experiments utilise arrays with thousands of gene specific probes are immobilised on a solid surface. The fluorescently labelled cDNA is hybridised to the arrays and then detected with a laser scanner. PCR based methods amplify cDNA using specific primers and a fluorescent reporter such as an intercalating dye or a specific probe, which allow real time detection of the amplified product. In qPCR up to several genes can be measured in many samples whereas TaqMan low density arrays contain all the reagents necessary to perform a qPCR experiment aliquoted in the plate or card based system which allowing the expression of up to 360 genes to be assessed in one sample. Digital droplet PCR takes advantage of the fact that when aqueous solutionis mixed with oil, an emulsion is created. The PCR reaction is partitioned into tiny droplets containing on average 0 to 1 template molecule before amplification, then thermo cycled and positive droplets are scored with laser scanner. Deep sequencing of RNA allows sequencing of the whole transcriptome. The RNA is fragmented, reverse transcribed and ligated to adaptors with known sequence which allow PCR-based amplification and then sequenced. The short sequenced fragments are then mapped to the reference genome and the number of fragments mapped to a particular transcript reflects its expression level. The NanoString nCounter gene expression system utilises probes labelled with unique barcodes which are hybridised directly to RNA thus bypassing the need for any enzymatic reaction. The probe-target complexes are immobilised on cartridges, aligned and scored producing absolute copy number for tested gene. Highlighted in bold are techniques used in this thesis.

the qPCR experiments should be performed and analysed, a Minimum Information for Publication of Quantitative Real-Time PCR Experiments (MIQE) guidelines have been published to address these issues (Bustin et al., 2009).

Very recently a modified qPCR technique called digital droplet PCR (ddPCR) was developed. The PCR reaction is partitioned into tiny droplets containing on average 0 to 1 template molecule before amplification what enables absolute quantification of PCR product (Hindson et al., 2013) (**Figure 5**). This is especially useful in detecting rare events.

Although using TaqMan™ probes allow simultaneous expression measurement of up to six genes, generally the qPCR method is not suited for looking at expression of many genes. Recently, low density arrays (LDA) have been commercially introduced which contain all the reagents necessary to perform a qPCR experiment aliquoted in the plate or card based system allowing the expression of up to 360 genes to be assessed (Abruzzo et al., 2005) (**Figure 5**). The LDA have similar sensitivity and yield comparable results to conventional qPCR; however, the biggest drawback is that the assay design is very often confidential and controlling for PCR efficiency requires many samples what significantly increases the cost of the LDA assays (Goulter et al., 2006).

With the development of microarray technology (Schena et al., 1995), it became possible to look at gene expression on a global scale. In the microarray experiment thousands of gene specific probes are immobilised on a solid surface and fluorescently labelled cDNA are hybridised to these probes. Following several washes, transcripts complementary to the probes are retained on the array and can be detected with a laser scanner (Malone and Oliver, 2011) (**Figure 5**). As large differences between different microarray platforms were identified (Irizarry et al., 2005), a

standardization tool regarding data analysis, proper control and assay design has been published (Consortium et al., 2006), which significantly improved microarray experiments reproducibility.

Deep sequencing of RNA (RNA-Seq) is a relatively new technique enabling rapid sequencing of total transcriptome. The RNA is fragmented, reverse transcribed and ligated to adaptors with known sequence which allow PCR-based amplification and then sequenced. The short sequenced fragments are then mapped to the reference genome and the number of fragments mapped to a particular transcript reflects its expression level (Malone and Oliver, 2011) (**Figure 5**). This technique is more powerful in terms of detecting new transcripts, splicing isoforms and obtaining data from not yet annotated organisms, however it requires a dedicated bioinformatics staff to analyse the results (Malone and Oliver, 2011).

All the methods described above rely on enzymatic reaction (PCR amplification or reverse transcription) which is bound to introduce some bias. The NanoString nCounter gene expression system utilises probes labelled with unique barcodes which are hybridised directly to RNA thus bypassing the need for any enzymatic reaction (**Figure 5**). The technology enables to multiplex up to 800 targets in one reaction with sensitivity comparable to qPCR (Geiss et al., 2008, Manning et al., 2011).

1.14. Objectives of the project

The current, cytogenetics-based methods for dose estimation are not suitable for large scale radiological emergency, therefore a lot of effort has been put in finding new, accurate, sensitive, high-throughput assays for biological dosimetry purposes. Exposure to IR induces time- and dose-dependent changes in gene expression

(Amundson et al., 2000, Kabacik et al., 2011a, Manning et al., 2013) which can be accurately and quickly measured by qPCR.

The aim of this project was to investigate the possibility of using gene expression assay for radiation biodosimetry purposes. The work presented in this thesis includes:

1. Extensive optimisation of qPCR protocol
2. Identification of IR responsive genes suitable for biodosimetry purposes
3. Characterisation of temporal- and dose-responses of IR-responsive transcripts
4. Validation of the qPCR assay for dose estimation *in vitro* and *in vivo*

Chapter 2. Materials and methods

2.1. Common reagents and equipment

All microcentrifuge tubes and pipette tips were purchased from STARLAB (STARLAB UK Ltd., Milton Keynes, UK), 15 ml and 50 ml conical bottom tubes, tissue culture flasks and sterile pipettes were purchased from SARSTEDT (SARSTEDT Ltd. Leicester, UK). Tissue culture plates and cryovials were purchased from Nunc/Thermo Scientific (Thermo Scientific, Hemel Hempstead, UK). RNALater was purchased from Ambion/Life Technologies (Life Technologies Ltd., Paisley, UK, cat. AM7020). Fluorescent double-dye probes for qPCR were purchased from Eurogentec (Eurogentec Ltd., Southampton, UK), primers were purchased from Integrated DNA Technologies (Integrated DNA Technologies Ltd, Glasgow, UK). Microcentrifuge tubes were centrifuged in MicroStar 17R centrifuge (VWR International Ltd., Lutterworth, UK), conical bottom tubes in Sorvall Legend RT (Thermo Scientific).

2.2. Samples

2.2.1. Human blood

2.2.1.1. Fresh blood

For the blood collection tube comparison, two blood samples were collected from one healthy donor into lithium heparin or ethylenediaminetetraacetic acid (EDTA) blood collection tubes (BD Becton Dickinson, Oxford, UK, cat. 366643). 100 µl aliquots were sham irradiated or exposed to a dose of 4 Gy X-ray and collected 24 h post exposure.

For biomarkers identification 20 ml of peripheral blood samples were obtained anonymously from three healthy female working individuals (age range 37–53 years old) on three independent occasions with informed consent and ethical approval from

Berkshire Research Ethics Committee (reference number 09/HO505/87). Peripheral blood was collected via venipuncture into anticoagulant EDTA vacutainer tubes (Becton Dickinson) and kept on ice for a maximum of two hours until 30 minutes prior to irradiation. 5 ml of blood from each donor was aliquoted into two 5 ml cell culture tubes and placed at 37 °C 30 min prior irradiation. The rest of blood was used to set up T-lymphocyte cultures. Blood samples were sham irradiated or exposed to 2 or 4 Gy of X-ray and collected 2 or 24 h post exposure.

For assessment of inter-and intra-individual variability peripheral blood samples were obtained anonymously on three independent occasions from 32 healthy blood donors with informed consent and ethical approval from Berkshire Research Ethics Committee (reference number 09/HO505/87). Peripheral blood was collected via venipuncture into anticoagulant EDTA vacutainer tubes (Becton Dickinson) and kept on ice for a maximum of two hours until 30 minutes prior to irradiation. 500 µl of blood from each donor was aliquoted into two 2 ml screw-cap tubes and placed at 37 °C 30 min prior to irradiation. Samples were sham irradiated or exposed to a dose of 2 Gy X-ray and collected 2 h post irradiation.

2.2.1.2. Cultured blood

The sample preparation was performed in the laboratory of Prof. Michael Abend at Bundeswehr Institute of Radiobiology, (Munich, Germany). Briefly, 2-3 ml of whole blood from one healthy male individual (age 29) was collected into heparinized tubes (Becton Dickinson, cat. 367874) on two separate occasions. Blood was taken with informed consent and the approval of a local ethics committee. The blood was diluted 1:2 with Roswell Park Memorial Institute (RPMI) 1640 supplemented with 10 % foetal bovine serum (FBS) (all from GIBCO/Life Technologies Ltd., Paisley, UK, cat.

22409-015 and 10500-064 respectively) and incubated for 24 h at 37 °C before irradiation. One batch of blood was used to construct a calibration curve, the second batch represented “unknown” samples. Seven calibration curve samples were irradiated with a sham dose, 0.25 Gy, 0.5 Gy, 1 Gy, 2 Gy, 3 Gy and 4 Gy and collected 24 h post irradiation. Ten unknown samples were irradiated with doses ranging from 0 to 6.4 Gy and collected 24 h post irradiation.

2.2.1.3. Cancer patients

Blood collection from cancer patients was performed at University Hospital Hradec Kralove (Hradec Kralowe, Czech Republic) by Dr Ales Tichy. Peripheral blood samples were obtained anonymously from two cancer patients (two females, age 65-72) undergoing radiotherapy for endometrial cancer with informed consent and ethical approval from University Hospital Hradec Kralove Ethics Committee (Hradec Kralove, Czech Republic, reference number 201401-S15P). Neither of the patients had previous radiotherapy or chemotherapy treatment. 2.5 ml of peripheral blood was collected via venipuncture into PAXgene RNA blood tubes (Becton Dickinson, cat. 762165) before first dose of radiotherapy and 24 h after first 1.9 Gy fraction. After blood collection, the blood samples were mixed several times by inversion and incubated at room temperature for 2 h, then frozen at -20 °C and shipped to our lab on dry ice.

2.2.2. Mouse blood

For the RT validation experiments, blood from a C57Bl/6 mouse was collected by cardiac puncture into EDTA blood collection tubes (Becton Dickinson) and then 5 µl, 10 µl, 25 µl, 50 µl, 75 µl and 100 µl aliquots were transferred to 2 ml screw-cap tubes containing 0.5 ml of RNALater and stored at -80 °C until further analysis. The experiment was repeated twice.

2.2.3. Human stimulated T-lymphocytes

2.2.3.1. RNA extraction kit comparison

For the RNA extraction kit comparison, stimulated human T-lymphocytes obtained from healthy donor C2 were used. Cells were sham irradiated or exposed to a dose of 4 Gy X-ray (6 x 10^6 cells per dose) and collected 4 h post exposure.

2.2.3.2. Biomarkers identification

T-lymphocytes obtained from three blood donors described in **chapter 2.2.1.1** were used. Cells were sham irradiated or exposed to 2 or 4 Gy of X-ray and collected 2 or 24 h post exposure. Three independent repeats were performed.

2.2.3.3. Time course and dose-response experiments

For time course and dose response experiments, human stimulated T-lymphocytes from two healthy donors (C1 and C2, both females, age range 39-41) and one Ataxia – Telangiectasia patient (AT, a gift from Dr. Colin Arlett, University of Sussex, UK) were studied; 2 x 10^6 cells were used for each sample.

For time course experiments cells were sham irradiated or with a dose of 2 Gy X-ray and samples were collected at 15 min, 30 min, 1 h, 1.5 h, 2 h, 3 h, 4 h, 5 h, 6 h and 24 h post irradiation. The experiment was repeated three times, samples for the first repeat were cultured and prepared by Ms Claudine Raffy.

For high dose-response experiments cells were sham irradiated or exposed to a doses 0.1 Gy, 0.2 Gy, 0.3 Gy, 0.4 Gy, 0.5 Gy, 1 Gy, 2 Gy, 3 Gy, 4 Gy and 5 Gy of X-ray and collected at two different time-points – 2 h and 24 h. The experiment was repeated two times, samples for the first repeat were cultured and prepared by Ms Claudine Raffy.

For low dose-response experiments only T-lymphocytes obtained from donor C1 were used. Cells were sham irradiated or exposed to a doses 5 mGy, 10 mGy, 20 mGy, 30 mGy, 40 mGy, 50 mGy, 75 mGy and 100 mGy of X-ray and collected at two different time points – 2 h and 24 h. The experiment was repeated four times, samples for the first repeat at 2 h were cultured and prepared by Ms Claudine Raffy, two other repeats were performed by Ms Grainne Manning.

2.3. Cell counting and viability

For all cell counting and viability, the ADAM cell counter (Labtech International Ltd., Uckfield, UK) was used. Briefly, for every cell count, two 0.5 ml tubes were prepared. 20 µl of T solution was aliquoted into one and 20 µl of N solution into second tube. Cells for counting were disaggregated by vigorous shaking, then two 20 µl aliquots were taken and mixed in tubes containing proprietary N and T solutions (cat. ADR-1000) respectively and samples were incubated for 2 min at room temperature. After incubation samples were loaded into appropriate T and N positions in the cartridge and loaded into counter. The cell counter provides a value for total cell number (T), dead cell number (N) and percentage of viable cells.

2.4. Cell growth

2.4.1. Lymphoblastoid cell lines

A cryovial containing 3 x 10^6 cells was thawed at 37 °C in a water bath for around two minutes and then the cells were transferred with sterile pastette into a 15 ml conical bottom tube containing 10 ml of lymphoblastoid cell growth medium (LCGM) consisting of RPMI 1640 (Dutch modification) supplemented with 20 % heat inactivated FBS, 1 mM sodium pyruvate, 2 mM L-glutamine, 100 U/ml penicillin, 100 µg/ml streptomycin (all from Invitrogen/Life Technologies, cat. 11360-070, 25030-081

and 15140-122 respectively). Cells were mixed by inverting the tube and centrifuged for 5 min at 1200 rpm. The supernatant was aspirated, the cell pellet resuspended in 10 ml of LCGM and transferred into a vented 25 cm^2 culturing flask. Flasks were incubated at 37 °C with 5 % $C0_2$ in the upright position for 3 days. At this stage, cells were disaggregated and counted at daily intervals.

When cell numbers reached 0.8 x 10^6, 10 ml of fresh LCGM was added and the cells were transferred to 75 cm^2 flask. The cell number was maintained between 0.6 and 0.8 x 10^6 per ml by adding fresh medium.

2.4.2. Human T-lymphocytes

2.4.2.1. Feeder cell preparation

Lethally irradiated lymphoblastoid GM1899A cells were used as feeder cells for human T-lymphocytes. The culturing conditions for this lymphoblastoid cell line are described in the section **2.4.1**. The feeder cells were prepared as follows: when the culture reached at least 5 x 10^7 cells, the cells were transferred into one or two 50 ml conical bottom tubes (depending on the volume) and centrifuged at room temperature for 5 min at 1200 rpm. The supernatant was aspirated and cell pellets were resuspended in 5 ml of LCGM. The cells were lethally irradiated at room temperature with a dose of 40 Gy X-ray at dose rate 1.7 Gy per min. The lethally irradiated feeders were diluted with freeze mix consisting of 10 % dimethyl sulfoxide (DMSO, Sigma-Aldrich Company Ltd., Gillingham, UK, cat. 472301-100ML) and 90 % of FBS (Life Technologies) to 3 x 10^6 cells per ml. One ml aliquots of the cell suspension were transferred into cryovials and frozen at -80 °C in Mr. Frosty™ (Thermo Scientific, cat. 5100-0001) containers which allow cooling at rate of 1 °C per minute. The next day vials were transferred to the liquid nitrogen container for long term storage.

2.4.2.2. Preparation of human stimulated T-lymphocytes

The stimulated human T-lymphocytes were prepared as follows: 10 ml of blood from a donor was collected into BD Vacutainer® lithium heparin tubes (Becton Dickinson). For each donor 5 ml of Histopaque-1077 (Sigma-Aldrich, cat. 10771-100ML) pre-warmed to room temperature was aliquoted into four 15 ml conical bottom centrifuge tubes. 10 ml of blood was mixed with 10 ml of Hank's Balanced Salt Solution (HBSS, Life Technologies, cat. 14170088) pre-warmed to room temperature in a 50 ml conical bottom tube. 5 ml of diluted blood was layered slowly onto each of the four tubes containing Histopaque-1077 using a sterile pastette (Alpha Laboratories, Eastleigh, UK, cat. LW4005). Tubes were centrifuged at room temperature at 1600 rpm for 20 min. After phase separation the top serum layer was aspirated from each tube leaving around 0.5 cm of liquid above the buffy coat cell layer. The buffy coats from two tubes for each donor were collected using sterile pastette and transferred into one fresh 15 ml tube with 10 ml of HBSS and mixed by inverting. The tubes were centrifuged at room temperature at 1200 rpm for 5 min. The supernatant was aspirated and cell pellet was re-suspended in 5 ml of HBSS. Cell suspensions from two tubes for each donor were combined into one tube and centrifuged again at room temperature at 1200 rpm for 5 min. The supernatant was aspirated, cells were washed with 10 ml of HBSS and two 20 µl aliquots of cell suspension were taken for cell counting. The tube was centrifuged at room temperature at 1200 rpm for 5 min and the supernatant was aspirated. Next the cells were re-suspended at concentration 3 x 10^6 cells per ml in freeze mix and frozen at -80 °C, 1 ml per cryogenic vial in Mr. Frosty™ container (Thermo Scientific). The next day vials were transferred to liquid nitrogen container for long term storage.

2.4.2.3. Culturing conditions

A cryovial containing 3 x 10^6 cells was thawed at 37 °C in a water bath for around two minutes and then the cells were transferred with sterile pastette into 15 ml conical bottom tube containing 10 ml of stimulating growth medium (SR10) comprised of RPMI 1640 (Dutch modification) supplemented with 10 % heat inactivated FBS, 1 mM sodium pyruvate, 2 mM L-glutamine, 100 U/ml penicillin, 100 µg/ml streptomycin, 50 µM 2-mercaptoethanol (GIBCO/Life Technologies, cat. 21985-023), 250 IU/ml recombinant interleukin-2 (Novartis Pharmaceuticals UK Ltd., Camberley, UK, cat. PL-00101/0936) and 0.4 µg/ml phytohaemagglutinin (PHA; Remel Ltd., Lenexa, USA, cat. R30852801). Cells were mixed by inverting the tube and centrifuged at room temperature for 5 min at 1200 rpm. The supernatant was aspirated, cell pellet was re-suspended in 10 ml of SR10 and centrifuged at room temperature for 5 min at 1200 rpm. In the meantime a cryovial of feeder cells was thawed in the water bath at 37 °C for around two minutes. The supernatant from T-lymphocytes was aspirated and the cells were re-suspended in 10 ml of SR10. The feeder cells were transferred with sterile pastette into a 15 ml conical bottom tube containing T-lymphocytes, mixed by inverting the tube several times and centrifuged at room temperature for 5 min at 1200 rpm. The supernatant was aspirated and the cell pellet was re-suspended in 10 ml of SR10. The cell suspension was transferred into vented 25 cm^2 flask and incubated at 37 °C with 5 % $C0_2$ at an angle of about 10 ° from horizontal position. Cells were left undisturbed for 4 days and thereafter they were disaggregated and counted daily. When the cells reached a density of 0.8 x 10^5 cells per ml they were diluted 1:2 with growth medium (GR10) which comprised of SR10 without PHA.

2.5. Irradiations

2.5.1. Blood

2.5.1.1. Human blood

Fresh whole blood samples for biomarkers identification were irradiated at 2 or 4 Gy using a Siemens Stabilipan (Siemens AG, Munich, Germany) therapy X-ray set (output 14 mA, 250 kV peak, 1.2 mm Cu HVL, 0.7 Gy min71) at room temperature at the Medical Research Council, Harwell. Blood samples were maintained at 37 °C at least 30 min prior to irradiation and then until agreed time-point after irradiation. At 2 or 24 h time-point blood leukocytes were trapped on LeukoLOCK™ filters, washed twice with ice-cold PBS and submerged in RNA Later according to manufacturer's instructions (all from Ambion/Life Technologies, cat. AM1923). Leukocytes trapped on filters were kept at -80 °C until RNAs were extracted.

The irradiations of 32 healthy blood donors samples were performed at room temperature with an A.G.O. HS X-ray system. After irradiation samples were incubated at 37 °C for 2 or 4 h and then 1.3 ml of RNALater was added. Samples were mixed by inverting the tubes several times and stored at - 80 °C.

Cultured blood samples were irradiated at the Bundeswehr Institute of Radiobiology, (Munich, Bavaria, 80937, Germany). The samples were irradiated at 37 °C using single doses of X rays with mean photon energy of 100 keV (240 kVp; X-ray tube type MB 350/1 in Isovolt 320/10 protection box; Agfa NDT Pantak Seifert GmbH & Co.KG, Ahrensburg, Germany) filtered with 7.0 mm beryllium and 2.0 mm aluminum. The absorbed dose was measured using a duplex dosimeter (PTW, Freiburg, Germany). The dose-rate was approximately 1.0 Gy per min at 13 mA.

2.5.2. Cells

Stimulated T-lymphocytes were disaggregated and 2 x 10^6 cells were seeded at a density of 4 x 10^5 cells per ml in 25 cm^2 cell culture flasks containing the appropriate growing medium. Cells were irradiated at room temperature, using a Siemens Stabilipan [Siemens AG, Munich, Germany] therapy X-ray set (output 14 mA, 250 kV peak, 1.2 mm Cu HVL, 0.7 Gy min-1) at the Medical Research Council, Harwell or an A.G.O. HS X-ray system (Aldermaston, Reading, UK) (output 13 mA, 250 kV peak, 0.5 Gy/min for doses 0.1 – 5 Gy and 0.2 mA 4.9 mGy/min for doses up to 100 mGy) at Public Health England. Cell cultures were maintained at 37 °C after irradiation until the agreed time-point, and then cells were washed twice with ice-cold PBS (Sigma-Aldrich). For gene expression experiments cells were resuspended in 1 ml of RNALater and stored at - 80 °C.

2.5.3. Cancer patients

The two endometrium cancer patients were irradiated with a dose of 1.9 Gy of X-ray using Clinac 2100C Linear Accelerator (Varian Medical Systems International AG, Cham, Switzerland).

2.6. RNA extraction

2.6.1. Human blood

2.6.1.1. Human blood leukocytes trapped on LeukoLOCK™ filters

Human blood leukocytes stabilised on LeukoLOCK™ filters were extracted by using LeukoLOCK™ Total RNA Isolation System (Ambion/Life Technologies, cat. AM1923). The manufacturer's protocol with optional DNase I treatment was followed exactly, samples were eluted with 100 µl of preheated elution solution. After RNA

quantification and quality assessment samples were stored at – 80 °C.

2.6.1.2. Human blood samples stored in RNAlater

Human blood samples stabilised in RNALater were extracted by using RiboPure™-Blood RNA Isolation Kit (Ambion/Life Technologies, cat. AM1928). The manufacturer's protocol with optional DNase I treatment was followed exactly, samples were eluted with 50 µl of preheated elution solution. After RNA quantification and quality assessment samples were stored at – 80 °C.

2.6.1.3. Cultured human blood

RNA extraction from cultured human whole blood was done by using QIAamp RNA Blood Mini kit (Qiagen, cat. 52304) according to manufacturer's protocol: "Purification of Total Cellular RNA from Human Whole Blood". Red blood cell lysis and leukocyte lysis were performed in Prof. Michael Abend's lab (Bundeswehr Institute of Radiobiology, Germany). The cell lysates were frozen and shipped to Public Health England laboratories on dry ice. Before extraction frozen lysates were incubated at 37 °C in a block heater (Bibby Scientific Ltd., Stone, UK) until completely thawed and any salts dissolved. Then the manufacturer's protocol was followed exactly, samples were eluted in 50 µl of RNase free water.

DNA contamination was removed by using Ambion® DNA-free™ (Ambion/Life Technologies, cat. AM1906). Briefly, 5 µl of 10X DNase I Buffer and 1 µl of DNase I were added to each sample and mixed gently, then samples were incubated for 30 min at 37 ° C in a block heater. After incubation 5 µl of resuspended DNase Inactivation Reagent was added and mixed well. Samples were incubated at room temperature for 2 min with occasional flicking and centrifuged at 10 200 rpm for 1.5 min to pellet the beads. The supernatant was transferred into a fresh 0.5 ml tube and after quality control

frozen at – 80 °C.

2.6.1.4. Blood collected into PAXgene blood RNA tubes

Human blood samples collected into PAXgene blood RNA tubes were extracted by using PAXgene Blood miRNA Kit (Qiagen Ltd., Crawley, UK, cat. 763134). The manufacturer's protocol with DNase I treatment was followed exactly, samples were eluted with 100 µl of elution solution. After RNA quantification and quality assessment samples were stored at – 80 °C.

2.6.2. Human cell lines

2.6.2.1. mRNA and lncRNA analysis

RNA from human T-lymphocytes for mRNA and lncRNA analysis was extracted with RNAqueous®-4PCR kit (Ambion/Life Technologies, cat. AM1914).

Briefly, tubes containing cells in RNALater were thawed at room temperature and cell suspensions were transferred into 1.5 ml RNase free tubes. Cells were centrifuged for 5 min at 12000 rpm, then the supernatant was removed and 350 µl of Lysis Buffer provided with the kit was added. Cells were vortexed for around a minute until they were completely lysed, then 350 µl of 64 % ethanol was added and tube was mixed by inverting several times. From this step manufacturer's protocol with optional DNase I treatment was followed exactly, samples were eluted in 60 µl of elution solution heated to 80 °C. After RNA quantification and quality assessment samples were stored at - 80 °C.

2.6.2.2. miRNA analysis

RNA from human T-lymphocytes and mouse tissues for miRNA analysis was extracted by using miRNeasy Mini Kit (Qiagen, cat. 217004).

Briefly, cell samples in RNALater were thawed at room temperature. Cell suspensions were transferred into 1.5 ml tubes and centrifuged for 5 min at 14000 rpm, then all traces of RNALater were removed. 700 µl of QIAzol Lysis reagent was added to each tube and samples were vortexed until complete lysis. From this step manufacturer's protocol with on-column DNase I treatment was followed exactly, samples were eluted in 50 µl of RNase free water applied on the filter.

For the RNA extraction kit comparison, mirVana™ miRNA Isolation Kit (Ambion/Life Technologies, cat. AM1560) was used additionally with the manufacturer's protocol for extraction total RNA with DNase I treatment being followed exactly; samples were eluted in 50 µl.

2.7. RNA concentration and quality assessment

RNA concentrations were measured by using NanoDrop 1000 spectrophotometer (Thermo Scientific).

2.7.1. Agarose gel

The quality of all RNA samples except for those extracted with miRNeasy Mini kit was assessed using 1.3 % agarose gel. Briefly, 0.65 g of Certified Molecular Biology Grade Agarose (Bio-Rad Laboratories Ltd., Hemel Hempstead, UK, cat. 161-3101) was added to 50 ml of 1 x Tris-Borate-EDTA buffer (TBE, Sigma-Aldrich, cat. T4415-10L) and heated in a microwave until the agarose dissolved. The agarose was cooled down under running water and 5 µl of GelRed Nucleic Acid Gel Stain, 10,000X in water (Cambridge Bioscience Ltd., Cambridge, UK, cat. 41003) was added and mixed thoroughly. The gel was poured into electrophoresis tray (Bio-Rad) and left at room temperature for an hour to solidify. The solidified gel was placed in Mini-Sub® Cell GT electrophoresis system (Bio-Rad) containing 1 x TBE buffer.

3 µl of a sample and 1 µl of loading buffer consisting of 40 % sucrose and 0.25 % of bromophenol blue (both from Sigma-Aldrich, cat. S7903 and B0126 respectively) in water, were mixed on a piece of parafilm and loaded into a gel well. 0.3 ng of 1 Kb Plus DNA Ladder (Life Technologies, cat. 10787-018) in loading buffer was run with every gel. Samples were separated for 45 min at 80 V and visualised by using U:Genius3 gel documentation system (Syngene Europe, Cambridge, UK). Good quality RNA was characterised by absence of genomic DNA above the 12 kb band and sharp 28 S and 18 S ribosomal RNA bands, where the upper band was approximately twice as intense as the lower band in fluorescence.

2.7.2. 2200 TapeStation instrument

The quality of RNA samples extracted by using miRNeasy kit was assessed using 2200 TapeStation instrument (Agilent Technologies UK Ltd., Wokingham, UK) according to manufacturer's protocol. Briefly, R6K ScreenTape and Reagents (Agilent, cat. 5067-5576 and 5067-5577 respectively) were warmed to room temperature. 4 µl of R6K reagent and 1 µl of RNA sample were mixed in 8 well strips (ABgene/Thermo Scientific, cat. AB-0264). Strips were vortexed at 2500 rpm for 15 s in MixMate (Eppendorf UK Ltd., Stevenage, UK) and centrifuged at room temperature for one minute at 3000 rpm on SIGMA 2-16P Centrifuge (Sciquip Ltd. Newtown, UK). Next the samples were incubated for 3 min at 72 °C in a Thriller® thermoshaker-incubator (Peqlab Ltd., Sarisbury Green, UK) to denature RNA and then cooled down on ice for two minutes. The strip was centrifuged at room temperature for one minute at 3000 rpm on SIGMA 2-16P Centrifuge (Sciquip) and samples were loaded into TapeStation. The TapeStation analysis software produced RNA Integrity Number equivalent (RINe) number which indicated level of RNA integrity.

2.8. Microarray experiment

Microarray experiments and data analysis were performed by Dr Alan Mackay (Breakthrough Breast Cancer Research Centre, the Institute of Cancer Research, London, UK).

Briefly, 1 μg of total RNA was T7 amplified by in vitro transcription using the MessageAmp™ kit (Ambion/Life Technologies, cat. 4385821) according to manufacturer's instruction. 1 mg of amplified RNA was coupled to either Cy3 or Cy5 dye and hybridised to Breakthrough 20K cDNA microarrays in replicate dye swap hybridisations. Overnight hybridisation was performed at 42 °C in a hybridisation buffer (GE Healthcare, Amersham, UK, cat. RPN3006), then the arrays were washed at 65 °C in a wash buffer 1 comprised of 2 × SSC and 0.1 % SDS and wash buffer 2 comprised of 0.1 × SSC and 0.1 % SDS. After washing, the arrays were scanned on an Axon 4000B microarray scanner and GenePix 5.1 software (Axon Instruments/Molecular Devices Corporation Sunnyvcale, CA, USA) was used for TIFF images analysis.

Expression values from spots with extremely low intensities were converted to missing values and probes with missing values in more than 80% of hybridisations within each cell type were removed from subsequent analysis. The raw intensity values were converted to log2 ratios of sample to reference and log2 average spot intensity. Data from blood samples and lymphocyte samples were analysed separately. The dye biases were removed by using LOESS local regression function and then log2 ratios were subjected to quantile normalisation. The final data sets contained 10736 and 9698 probes for the analysis of lymphocytes and blood samples respectively. Significance analysis of microarrays (SAM) was used to identify differential gene

expression by comparing irradiated samples with respective controls in each tissue, at each time point with 5% false discovery rate used as a cut-off.

2.9. RT reaction

2.9.1. mRNA and lncRNA

Reverse transcription (RT) reactions for mRNA and lncRNA expression analysis were performed in iQ5 thermocyclers (Bio-Rad), using High Capacity cDNA Reverse Transcription Kit (Life Technologies, cat. 4368814) according to manufacturer's protocol with 700ng of total RNA in 50 µl reaction volume. "-RT" reactions were performed on representative samples to control for genomic DNA (gDNA) contamination by adding water instead of RT enzyme. The cycling conditions were 10 min at 25 °C, 2 h at 37 °C and 5 min at 85 °C. The cDNA samples were stored at – 20 °C.

2.9.2. miRNA

RT reactions for miRNA expression analysis were performed using qScript™ microRNA cDNA Synthesis Kit (Quanta BioSciences, Gaithersburg, USA, cat. 95107-025) according to manufacturer's protocol. Briefly, total RNA containing small RNA species was normalised to concentration 100 ng in 7 µl of RNase free water (Ambion/ Life Technoogies, cat. AM9937). Polyadenylation reactions were set up on ice as follows: 7 µl of normalised RNA was mixed in 0.2 ml tube stips (ABgene/Thermo Scientific) with 2 µl of Poly(A) Tailing Buffer and 1 µl of Poly(A) Polymerase. The reactions were gently vortexed, centrifuged briefly to collect all liquid on the bottom of the tube and placed in Veriti® 96-Well Thermal Cycler (Life Technologies). Cycling conditions were 20 min at 37 °C and 5 min at 70 °C. Samples were then briefly centrifuged and placed on ice.

The first strand cDNA synthesis reaction was performed as follows: 9 µl of cDNA Reaction Mix and 1 µl of qScript Reverse Transcriptase were added to Poly(A) Tailing Reactions from the step above. Samples were mixed by gentle vortexing, then briefly centrifuged to collect contents and incubated for 20 min at 42 °C followed by 5 min at 85 °C. Several controls were prepared: (1) "-RT" reactions to control for genomic DNA contamination and (2) "-poly(A)" reactions to control for non-specific binding of universal primers were performed on representative samples by adding water instead of enzyme. Prepared cDNA was diluted 50 x before performing qPCR analysis.

2.10. Quantitative Real-Time PCR (qPCR)

2.10.1. TaqMan assays design

For each assay a set of primers, a fluorescent probe and a set of covering primers spanning the amplification region were designed. All TaqMan assays for mRNA detection were designed and validated *in silico* by Dr François Paillier (bioMérieux Ltd, Rhône-Alpes, France). All lncRNA assays were designed by using PrimerQuest software (Integrated DNA Technologies, Leuven, Belgium).

2.10.2. Standard curve preparation

For each qPCR assay a set of covering primers flanking the amplicon was designed. The covering primers were used to obtain PCR products for standard curve preparation. Briefly, for each assay a 100 µl PCR reaction containing 10 µl of 10 x PCR Buffer, 2.5 units of Taq DNA Polymerase (both from Qiagen, cat. 201205), 200 µM of each dNTP (Invitrogen/Life Technologies, cat. 10297-018), covering primers at 300 nM each and 10 µl of representative cDNA was set up in 0.2 ml strip tubes (ABgene/Thermo Scientific). The cycling conditions were 3 min at 94 °C, then 35 cycles of 30 s at 94 °C, 30 s at 60 °C and 30 s at 72 °C and final extension for 10 min at 72 °C.

The resulting PCR product was loaded in 3 wells of a 1.3 % agarose gel and run for 45 min at 100 V. After electrophoresis the gel was placed on a UVT 400-M ultraviolet transilluminator (International Biotechnologies Inc., New Haven, Connecticut, US) to visualise the PCR product. The band of appropriate size was excised with sterile scalpel blade and placed in 1.5 ml tube and the PCR product was purified by using MinElute Gel Extraction Kit (Qiagen, cat. 28604). The manufacturer's protocol was followed exactly and samples were eluted with 15 µl of Elution Buffer. The DNA quantity was assessed using Nanodrop 1000 (Thermo Fisher) and molar mass of the PCR product was calculated using online software Mongo Oligo Mass Calculator v2.06 (http://mods.rna.albany.edu/masspec/Mongo-Oligo).

Approximate number of PCR product copies per µl was calculated by using following formula:

$$Copy\ number\ per\ \mu l = \frac{Concentration}{\frac{M}{N_A}}$$

where M is molar mass of PCR product and N_A is Avogadro's constant.

Standard curve stock was prepared by mixing 1.5625 x 10^9 molecules of each PCR product in 50 µl of TE buffer (Sigma, cat. 93283-100ML). The standard curve stock was diluted 1600 times by serial dilutions to obtain the first concentration used for standard curve. The standard curve was prepared by eight 5-fold dilutions and spanned concentrations from 25 to 9765625 copies of each PCR product per µl. To avoid repeated freeze-thaw cycles, 5 µl of each concentration was aliquoted into 12-wells strips (ABgene/Thermo Scientific) and stored at -20 °C.

2.10.3. TaqMan assay qPCR experiment

TaqMan assay qPCR experiments were performed using PerfeCTa® MultiPlex qPCR SuperMix (Quanta Biosciences, cat. 95063-200). Reactions were performed in 30 µl volumes on an iQ5 real time platform (Bio-Rad) or in 10 µl volumes in a Rotor-Gene Q (Qiagen). Reagent concentrations were as follows: 1 x PerfeCTa® MultiPlex qPCR SuperMix, 300 nM of each primer, 300 nM of each probe and 10 % of a template. All reactions were run in triplicate, standard curve reactions and no template control (NTC) were run in each plate. 3' 6-Carboxyfluorescein (FAM)/Black Hole Quencher 1 (BHQ1), 6-Hexachlorofluorescein (HEX)/BHQ1, Texas Red/BHQ2, CY5/BHQ3, ATTO390/Deep Dark Quencher 1 (DDQ1) and ATTO680/BHQ3 were used as fluorochrome/quencher pairs for the hydrolysis probes analysed in multiplexed reactions. Cycling parameters were 2 min at 95 °C, then 45 cycles of 10 s at 95 °C and 60 s at 60 °C.

Cycle threshold (Ct) is defined as cycle where amplification curve crosses predefined threshold and it is inversely proportional to starting template amount. Ct values were converted to copy numbers using standard curve and then normalised to hypoxanthine phosphoribosyltransferase 1 (*HPRT1*) reference gene for human samples or hypoxanthine guanine phosphoribosyl transferase (*Hprt*) for mouse samples. Relative gene expression levels after irradiation were obtained comparison with sham irradiated controls.

2.10.4. TaqMan assays validation protocol

Sequences of all designed assays were first checked by using the Ensembl database (http://www.ensembl.org/index.html) for transcript coverage and single nucleotide polymorphism (SNP) presence. The aim was to design an assay with

maximum alternative transcript coverage and no SNPs in the sequence as the SNP present in the primer or probe annealing site would significantly affect the oligonucleotide specificity and binding efficiency.

The specificity of the designed assay primers and covering primers was validated by a SYBR Green assay. Validation qPCR experiments were performed using an iQ5 thermocycler (Bio-Rad). 25 µl reactions were set up as follows: 12.5 µl of PerfeCTa® SYBR® Green SuperMix for iQ™ (Quanta Biosciences, cat. 95053-500), 300 nM concentrations of each forward and reverse primers and 1 µl of template were mixed in 0.2 ml strip tubes (ABgene/Thermo Scientific). All reactions were run in triplicate with a separate NTC reaction for every assay. The cycling conditions were 2 min at 95 °C then 45 cycles of 10 s at 95 °C and 60 s at 60 °C followed by melt curve. Data were collected and analysed by iQ5 Detection System software. Primers were considered as specific if only one peak was present on the melt curve graph and the PCR product was of expected size on an 1.3 % agarose gel.

The performance of the probes was assessed in TaqMan qPCR experiments with a standard curve. The assay was considered as validated only if PCR efficiency was between 93 and 105 % and R^2 value for the standard curve linear regression fit was greater than 0.998.

2.10.5. miRNA detection

miRNA expression analysis experiments were performed on Rotor-Gene Q (Qiagen). 10 µl qPCR reactions were set up as follows: 5 µl of PerfeCTa®SYBR®Green SuperMix, 10 µM concentration of each PerfeCTa microRNA Assay Primer and PerfeCTa Universal PCR Primer (all from Quanta Biosciences, cat. 95054-500) and 1 µl of miRNA cDNA were mixed. All reactions were run in triplicate and a NTC reaction was

run for each assay with a calibrator sample included in each plate. One cDNA sample was used as a calibrator for all runs in order to normalise for inter-run variation. The cycling conditions were 2 min at 95 °C then 45 cycles of 10 s at 95 °C and 30 s at 60 °C followed by a melt curve. Data was collected and analysed by Rotor-Gene Q analysis software.

The NormFinder algorithm (Andersen CL, 2004) was used to find the most stable control genes combination. Irradiated samples were normalised to the non-irradiated controls and presented as fold change in expression.

2.11. Statistical methods

The statistical analysis was performed in Minitab software (Minitab Ltd., Coventry, UK).

Anderson-Darling test was performed in Minitab in order to assess normality of the data. It generates probability plot and performs a hypothesis test whether or not the observations follow a normal distribution and provides associated p values (Minitab help).

General Linear Model (GLM) was used to perform univariate analysis of variance. It allows estimation of the relative statistical significance of each parameter, taking into account the errors associated with them (Minitab help).

Linear regression analysis was used for curve fitting and dose estimation. The best fit was determined by the highest R^2 value.

2.11.1. Uncertainty measurement

The measurement error was calculated as follows. Standard deviation (SD) of copy number was calculated from triplicate qPCR reactions for *HPRT1* and *FDXR* genes

in each sample. Next, for each sample the SDs for both genes were combined by taking the square root of the sum of SD squares, then, the error was normalised by dividing it by average of *HPRT1* copy number.

The intra-individual variation was calculated as follows. The mean and SD of endogenous level for *FDXR* gene from three independent experiments was calculated for each one of 32 healthy blood donors, then coefficient of variation (COV) was calculated by dividing SD by the mean. Finally, the intra-individual variation was calculated by averaging COV from control and irradiated samples.

In order to calculate the inter-individual variation the average and SD of 32 healthy blood donors in endogenous level for *FDXR* gene was calculated for each of three independent experiment. Then, COV was calculated by dividing SD by the mean. Finally, the inter-individual variation was calculated by averaging COV from three independent repeats for control and irradiated samples.

The uncertainty of dose estimation was calculated as follows. The measurement error and intra- or inter-individual variability were combined by calculations square root of the sum of squares and then outcome was multiplied by the dose estimation given by equation.

Chapter 3. Results

3.1. qPCR protocol optimisation

3.1.1. Introduction

qPCR is a 'gold standard' method for measuring gene expression. The principle of the technique is relatively simple, however, in order to obtain meaningful results many aspects of the workflow have to be tightly controlled, which is very often ignored (Derveaux et al., 2010). Many factors can influence the outcome of a qPCR experiment; for example: assay design, sample collection and stabilisation, RNA extraction method, RNA quality, cDNA synthesis strategy, cycling conditions or normalisation choice (extensively reviewed in (Bustin, 2004)). All these factors contribute to technical variation and may mask real biological responses or contribute to false positive results.

In response to a lack of consensus on how best to perform and interpret qPCR experiments, Bustin *et al* published in 2009 a set of MIQE guidance (Bustin et al., 2009). The paper stressed the need for standardisation and transparency of qPCR experiments. Being aware of this report, we performed extensive optimisation of our workflow as qPCR is the main technique used in this project.

In this chapter, we present results of optimisation of several aspects of the qPCR protocol: assay design and validation, sample collection, RNA extraction, cDNA synthesis and multiplexing.

3.1.2. Assay design validation protocol

Designing a robust and specific assay is the first and essential step to obtain meaningful and reliable qPCR results. In order to ensure a successful approach we have developed a design validation protocol involving several quality control steps. All mRNA assays were designed by Dr Francois Paillier (bioMérieux) using RT_qPCR_SLv8 software developed by Dr Paillier according to the protocol described in **Figure 6**. The

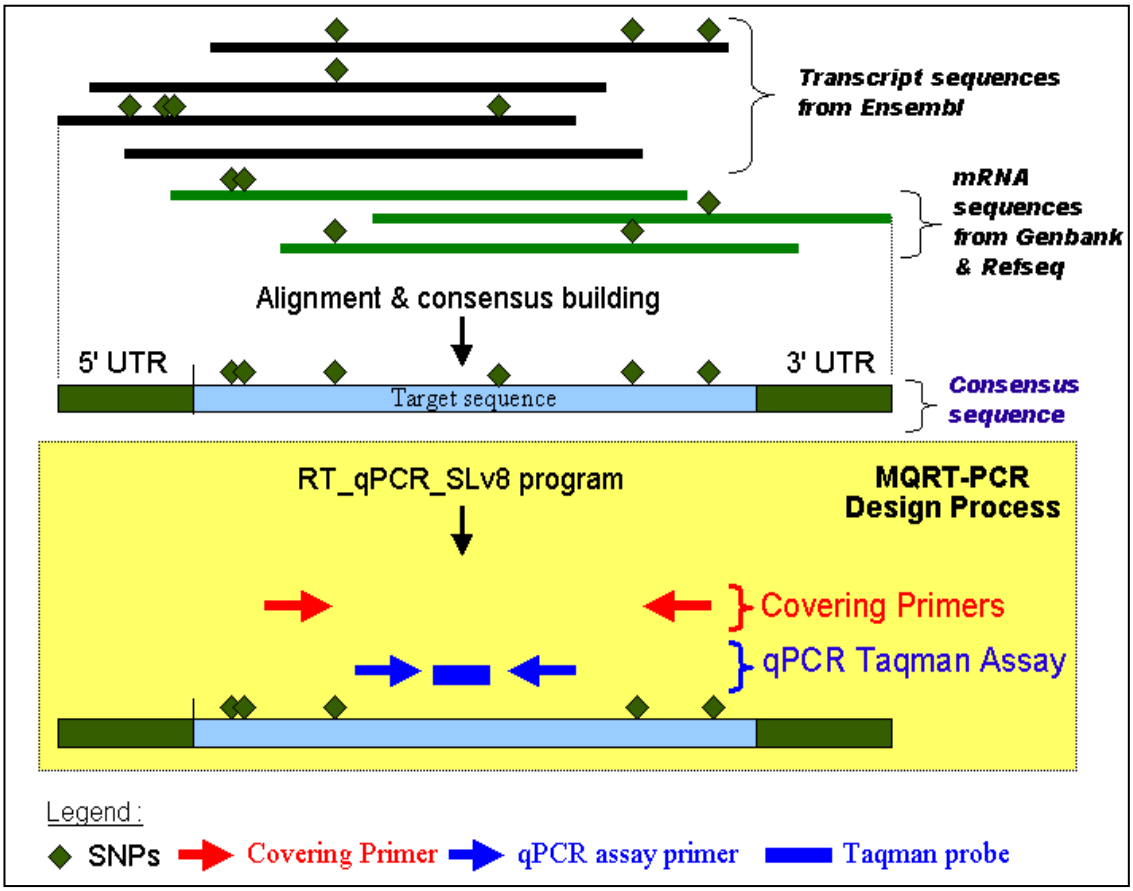

Figure 6. Individual design workflow using RT_qPCR_SLv8 software.

Entries corresponding to transcribed sequences from a single gene were downloaded from Ensembl and/or Refseq Genbank division automatically (both databases can provide non overlapping data). Conflict bases and/or SNPs were masked in each of the corresponding sequences (base replaced by a -N). The masked sequences populations were aligned (multiple alignment using ClustalX 2.0) and a consensus was built after 5' and 3' UTR masking using a dedicated script. The consensus sequence was used for the assay design (3 oligonucleotides in blue) and for the covering PCR primers (2 oligonucleotides in red) necessary to amplify the DNA fragment used for the standard curve (figure produced in collaboration with Dr Francois Pallier, bioMérieux, France).

lncRNA assays were designed by us using PrimerQuest software from Integrated DNA Technologies (https://eu.idtdna.com/PrimerQuest/Home/Index).

The oligonucleotide sequences of all designed assays were examined on the Ensembl (http://www.ensembl.org/index.html) database against transcript coverage and SNP presence. A SNP present in the primer or probe annealing site would change the oligonucleotide binding efficiency and negatively impact the assay performance. The ideal assay would target all alternatively spliced transcripts, have no SNPs in the primers and probe sequences and overlap two exons to avoid amplification of gDNA. Unfortunately, quite often there was no common sequence present in all the alternatively spliced transcripts, therefore it was not always possible to design an assay which would cover all of them; in this situation the assay was designed in a region present in most of the transcripts. The presence of one or more SNPs in the sequence of any oligonucleotides led to the exclusion of this particular assay from further investigation and a new assay was designed.

When an assay passed *in silico* quality control, the assay primers were synthesised and tested by qPCR as described in **chapter 2.10.4**. A specific primer set should produce a single, sharp peak on melt curve profile (**Figure 7B**) and single band of expected size on a 1.3 % agarose gel. Any primers producing multiple peaks on melt curve profile (**Figure 7A**) or multiple bands on a gel were discarded as nonspecific and new assay was designed.

When assay primers specificity was confirmed, the covering primers were synthesised and tested in the same way as above. If covering primers produced unspecific products, a new set of covering primers was designed. After passing quality

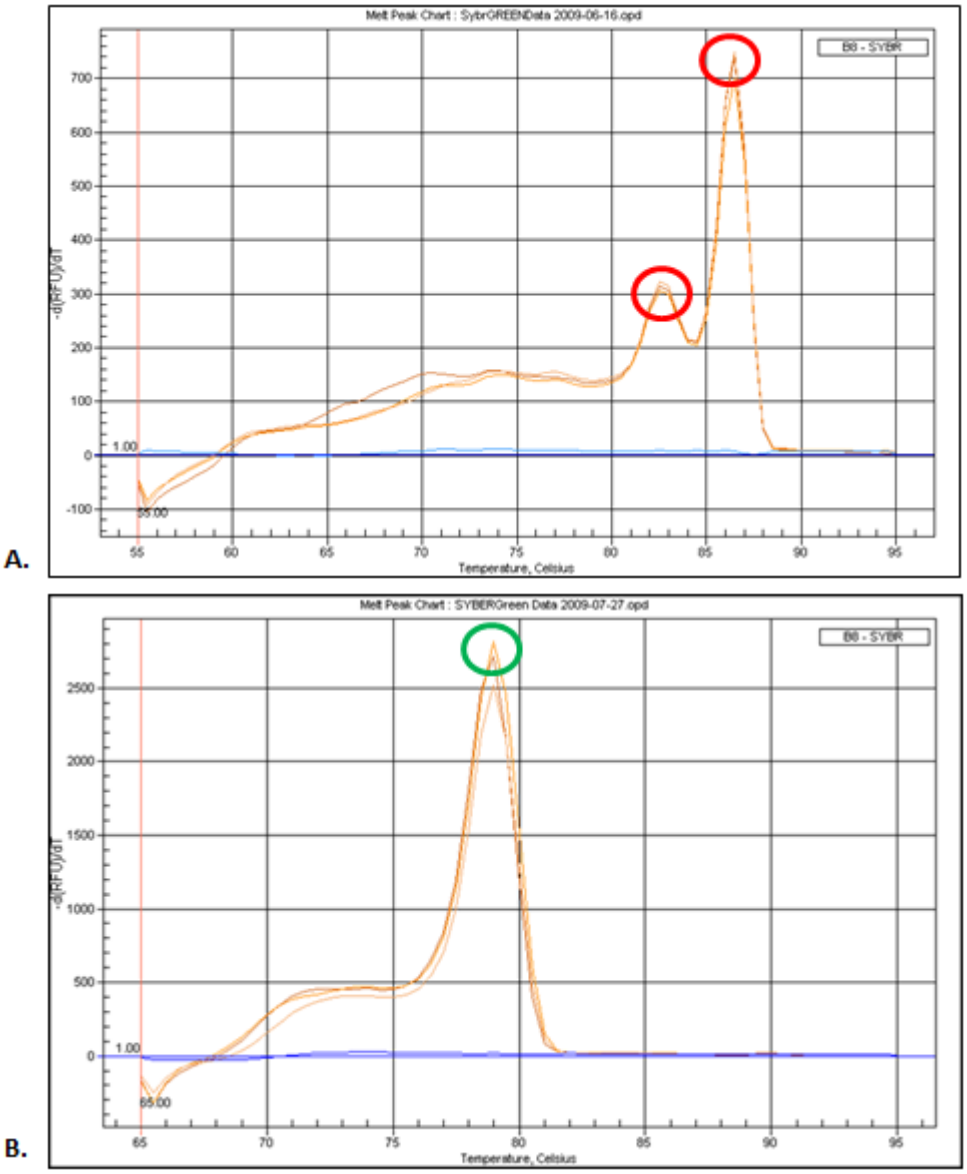

Figure 7. Melt curve analysis of gene specific primers product by SYBRGreen assay.

A. An example of unspecific primer set for the mouse gene *Cenpe* – two peaks (red circles) are visible confirming that there are two PCR products with melting temperature of respectively 83 °C and 86 °C. **B.** Re-designed primers for the mouse *Cenpe* gene – only one PCR product (green circle) is now present with a melting temperature of 79 °C.

control, a PCR template was prepared as described in **chapter 2.10.2** using covering primers. In order to test PCR template quality a SYBRGreen experiment was performed using assay primers and 1000 x diluted PCR template; amplification and melt curve shapes were assessed as described above.

When specificity of covering primers was confirmed, a double-dye, fluorescent probe was ordered. Probe performance was tested by running a TaqMan assay as described in **chapter 2.10.3** using a standard curve prepared as described in **chapter 2.10.2.** Design was considered as validated only if PCR efficiency in multiplex reaction was between 93 % and 105 % and linear regression analysis gave $R^2 > 0.998$ (**Figure 8**).

We performed a microarray experiment (described in the next chapter) and literature search in order to find radiation-responsive genes and we designed assays for 16 human and nine murine genes listed in **Table 3** and **Table 4** respectively. In total 27 assays were designed, including two assays for human (*HPRT1*) and mouse (*Hprt*) reference genes. Four sets of primers and probes for human and two for mouse had to be re-designed because they did not pass the quality control. Primer and probe sequences for each assay can be found in **Appendix A**.

3.1.3. Blood collection

A part of our project involved using blood samples which requires use of an anticoagulant like heparin or EDTA in collection tubes. We investigated if the choice of anticoagulant for blood sample collection influenced the gene expression results in our experimental system, as it has been previously reported that heparin is a potent PCR reaction inhibitor (Holodniy et al., 1991).

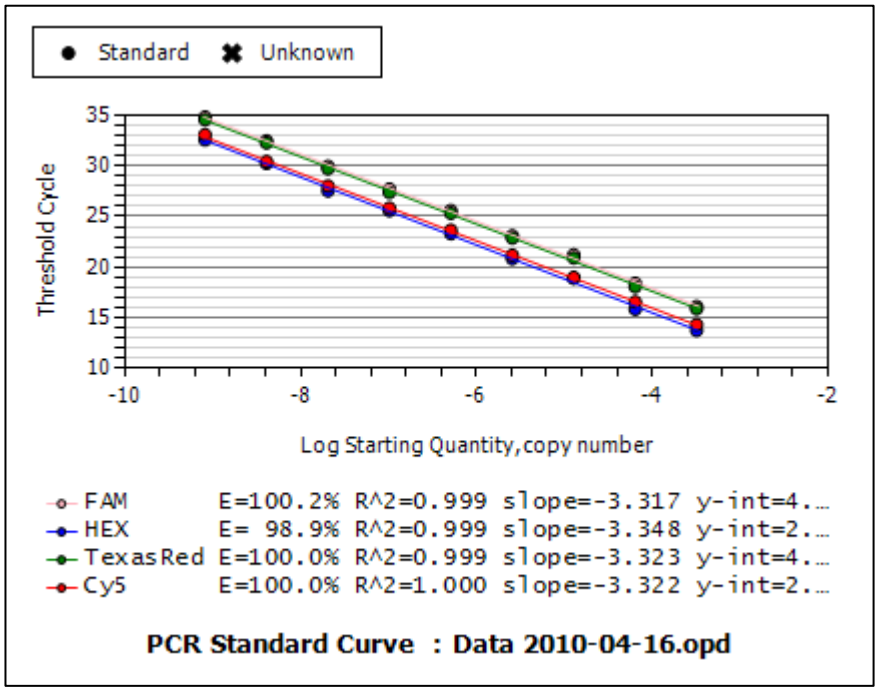

Figure 8. Four-colour multiplex TaqMan assay.

Serial dilution of PCR-amplified DNA fragments for the following four mouse genes: *Hprt*, *Phpt1*, *Fdxr* and *Cenpe*. They were co-amplified in order to check PCR efficiency of primers and probe sets, and multiplexing compatibility. All four designs passed the quality control.

Table 3. Human radiation responsive genes identified by microarray experiment and literature search for which qPCR assays were designed.

Gene name	Description
ATF3[M]	activating transcription factor 3
BBC3(PUMA)	BCL2 binding component 3 (Badie et al., 2008) up-regulated 2 h post 2 Gy X-ray exposure
CCNB1	cyclin B1 (Badie et al., 2008) down-regulated 2 h post 2 Gy X-ray exposure
CCNG1[M]	cyclin G1
CDKN1A(p21)[M]	cyclin-dependent kinase inhibitor 1A
DDB2	damage-specific DNA binding protein 2, 48kDa (Paul and Amundson, 2008) up-regulated 6 h and 24 h post exposure to 0.5, 2, 5 and 8 Gy of γ-ray
*FAS-AS1**	FAS antisense RNA 1 (Yan et al., 2005)
FDXR	ferredoxin reductase (Paul and Amundson, 2008) up-regulated 6 h and 24 h post exposure to 0.5, 2, 5 and 8 Gy of γ-ray
GADD45A[M]	growth arrest and DNA-damage-inducible, alpha
MDM2	Mdm2 TP53 binding protein homolog (mouse) (Paul and Amundson, 2008) up-regulated 6 h and 24 h post exposure to 0.5, 2, 5 and 8 Gy of γ-ray
*PANDAR**	promoter of CDKN1A antisense DNA damage activated RNA (Hung et al., 2011) up-regulated after doxorubicin treatment
PHPT1	phosphohistidine phosphatase 1 (Paul and Amundson, 2008) up-regulated 6 h and 24 h post exposure to 0.5, 2, 5 and 8 Gy of γ-ray
PLK3	polo-like kinase 3 (Paul and Amundson, 2008) up-regulated 6 h and 24 h post exposure to 0.5, 2, 5 and 8 Gy of γ-ray
PRC1[M]	protein regulator of cytokinesis 1
SESN1[M]	sestrin 1
*TP53TG1**	TTP53 target 1 (non-protein coding) (Takei et al., 1998) up-regulated after exposure to bleomycin

*long non coding RNA

[M] genes identified by microarray experiment

Table 4. Mouse radiation responsive genes identified by literature search.

Gene name	Description
Atf3	activating transcription factor 3
Bbc3(Puma)	BCL2 binding component 3
CcnB1	cyclin B1
Cdkn1a(p21)	cyclin-dependent kinase inhibitor 1A
Cenpe	centromere protein E
Fdxr	ferredoxin reductase
Phpt1	phosphohistidine phosphatase 1
Sesn1	sestrin 1
Sesn2	sestrin 2

Human blood samples were collected into either potassium-EDTA or lithium-heparin blood collection tubes (Becton-Dickinson). Two 100 µl aliquots were taken from each blood sample and irradiated with a sham dose or exposed to 4 Gy of X-ray. Blood samples were incubated at 37 °C for 24 h followed by RNA stabilisation by adding 1 ml of RNALater (Invitrogen) and then samples were frozen at – 80 °C. RNA was extracted as described in **chapter 2.6.1.2** and reverse transcribed as described in **chapter 2.9.1**. Expression of four genes: *HPRT1, CCNB1, BBC3* and *CDKN1A* was evaluated by qPCR as described in **chapter 2.10.3.** There was no difference in the yield or purity of RNA obtained from samples collected into two types of collection tubes (**Table 5**), however the Ct values for the samples collected into heparin tubes are at least 2 Cts higher than for samples collected into EDTA tubes, indicating that indeed significant inhibition takes place in samples collected into heparin tubes (**Table 6**).

3.1.4. RNA extraction optimisation

Historically in our lab, RNAqueous®-4PCR kit (4PCR, Ambion/Life Technologies) was used for RNA extractions. However, despite the fact that the kit allowed extraction of good quality RNA from broad range of samples, it did not quantitatively preserve small RNA species (notably those below 200 bp as stated in the RNAqueous®-4PCR kit manual). When we started working with miRNAs it was obvious that we had to find another kit for RNA extraction. We decided to test mirVana™ miRNA Isolation Kit (mirVana) from Ambion/Life Technologies and miRNeasy mini kit (miRNeasy) from Qiagen. Both kits allowed extraction of total RNA including small RNA species from broad ranges of samples.

In order to compare the kits, we performed a pilot experiment using two human T-lymphocyte samples (control and irradiated with 4 Gy X-ray, collected 4 h

Table 5. Nanodrop 1000 spectrophotometer readings on RNA samples collected into EDTA or heparin blood collection tubes.

	Sample ID	ng/uL	A260	260/280	260/230
EDTA	0Gy 24h	27.59	0.69	1.97	1.47
	4Gy 24h	31.38	0.785	1.93	1.36
Heparin	0Gy 24h	30.26	0.756	1.96	1.35
	4Gy 24h	30.88	0.772	1.91	1.35

Table 6. Ct values of samples collected into EDTA or heparin blood collection tubes.

		Ct mean			
	Sample	*HPRT1*	*CCNB1*	*BBC3*	*CDKN1A*
EDTA	0Gy 24h	27.54	28.08	24.18	25.53
	4Gy 24h	27.69	28.65	24.08	24.61
Heparin	0Gy 24h	30.13	30.57	28.89	27.47
	4Gy 24h	30.83	31.11	28.43	27.39
Ct difference	0Gy 24h	2.59	2.49	4.72	1.94
	4Gy 24h	3.14	2.46	4.35	2.79

post exposure) frozen in RNALater (Ambion/Life Technologies). Each sample contained 6 x 10^6 cells, samples were split into three aliqots containing equal numbers of cells and RNA was extracted with three different kits: 4PCR, mirVana and miRNeasy according to manufacturer's protocols and eluted in 50 µl of corresponding elution buffer.

RNA extracted with all three kits was of good quality as represented on an electrophoresis gel (**Figure 9**) with well-defined 28S and 18S ribosomal bands; all samples had RIN^e values above 9. Nanodrop 1000 spectrophotometer readings obtained from RNA samples are presented in **Table 7**. All three kits produced RNA free from protein contamination as indicated by A260/A280 ratios around 2, as well as free from organic contaminants, like phenol or ethanol, as indicated by ratio A260/A230 higher than 1.8 (except for sample mirVana 0 Gy 4 h). The mirVana kit gave the highest RNA yield, however the large band below 200 bp visible on the gel (lines 3 and 4 on **Figure 9**) contributed significantly to the total RNA concentration. Both Ambion's kits use DNase I digestion at the last step of RNA extraction protocol where DNA digestion fragments are still present in the eluted solution; Qiagen's kit uses on column digestion with subsequent washes to purify RNA from any DNA contamination. We assumed that the band below 100 bp consists of DNA digestion products and small RNA species.

Next, we wanted to check if there is any difference in qPCR results between samples extracted with three different kits. We prepared cDNA from mRNA as described in **chapter 2.9.1** using 700 ng of total RNA per 50 µl reaction and from miRNA as described in **chapter 2.9.2** using 200 ng of total RNA per 20 µl reaction. We measured the expression level of six genes by TaqMan assay qPCR as described in **chapter 2.10.3.** We observed quite large differences in Ct values between samples

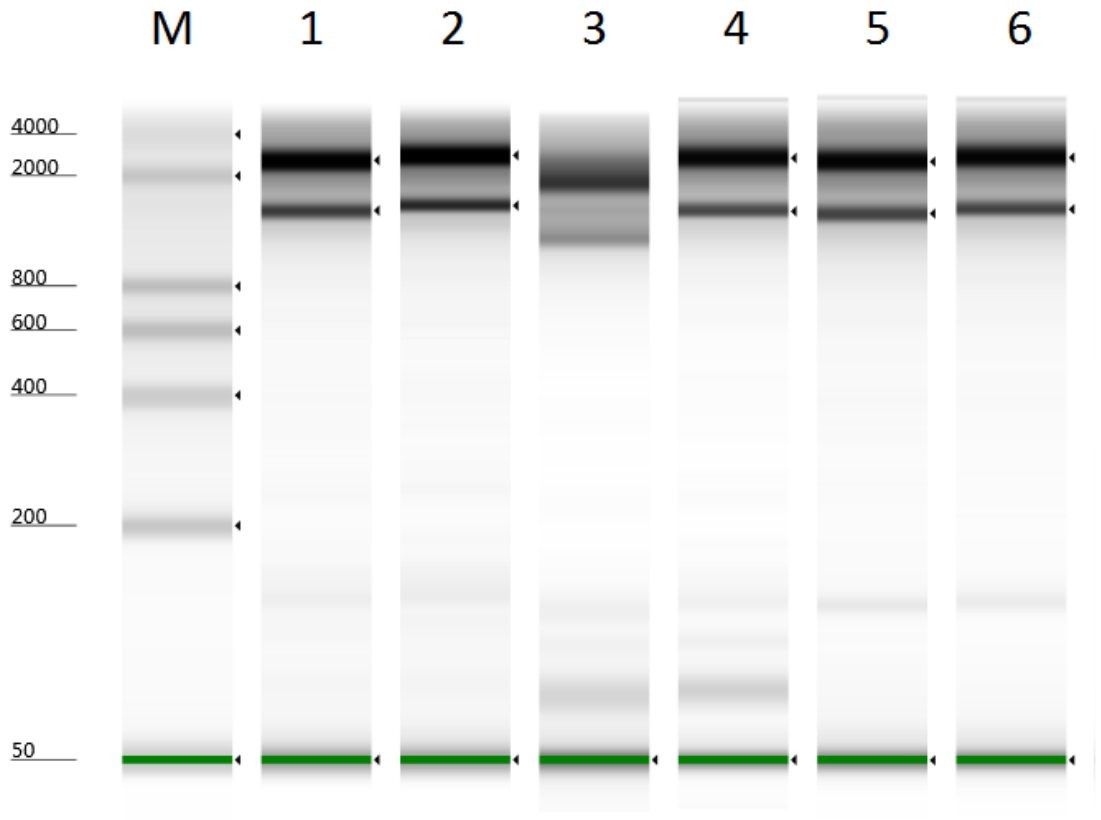

Figure 9. Gel electrophoresis produced by TapeStation 2200 instrument

Six RNA samples were analysed using TapeStation 2200, lines represent: **M** – RNA size marker (bp), **1** – 0 Gy 4 h miRNeasy kit, **2** – 4 Gy 4 h miRNeasy kit, **3** – 0 Gy 4 h miRVana kit, **4** – 4 Gy 4 h miRVana kit, **5** – 0 Gy 4 h 4PCR kit, **6** – 4 Gy 4 h 4PCR kit . The green band at 50 bp represents lower marker used by instrument for lines alignment.

Table 7. Nanodrop 1000 spectrophotometer readings on RNA samples extracted with three different kits.

	Sample ID	ng/ul	A260	A280	260/280	260/230
mirVana	0Gy 4h	153.52	3.838	1.973	1.94	1.47
	4Gy 4h	213.74	5.344	2.757	1.94	1.96
4PCR	0Gy 4h	85.02	2.126	1.069	1.99	1.94
	4Gy 4h	114.81	2.87	1.423	2.02	2.01
miRNeasy	0Gy 4h	50	1.25	0.592	2.11	1.85
	4Gy 4h	61.42	1.535	0.736	2.09	1.89

Table 8. mRNA Ct values obtained for samples extracted with three different RNA extraction kits

	Sample	Ct mean					
		HPRT	GADD45A	FDXR	DDB2	ATF3	SESN1
mirVana	0Gy 4h	22.77	24.05	21.80	21.01	25.61	23.73
	4Gy 4h	22.78	21.53	19.37	19.32	23.08	21.95
4PCR	0Gy 4h	21.85	23.93	21.65	20.23	24.85	23.35
	4Gy 4h	21.93	21.50	19.34	18.90	22.51	21.19
miRNeasy	0Gy 4h	21.10	22.84	21.27	19.76	24.11	22.09
	4Gy 4h	21.13	20.58	18.93	18.12	21.74	20.31

extracted with different kits (**Table 8**) despite using the same amount of RNA for cDNA synthesis, and the same amount of cDNA per qPCR reaction. The samples extracted with the miRNeasy kit gave lowest Cts, then samples extracted with 4PCR kit and samples extracted with mirVana gave the highest Ct values meaning that there were more mRNA templates per reaction in samples prepared with miRNeasy than in other kits. By contrast, there was no major difference in the fold change results between samples extracted with different kits (**Figure 10A**). The most probable explanation for this observation is that DNA degradation products seen in samples extracted with Ambion kits overestimated total RNA yield given by Nanodrop reading. However, there was still possibility that samples extracted with the mirVana kit contained more small RNA species than samples extracted with the miRNeasy kit and simply diluted the mRNA. To test this possibility we looked at expression of two miRNAs and one small nuclear RNA (snRNA) in the same samples.

The expression of these two miRNAs and one snRNA does not seem to be influenced by IR exposure in our system, we also could not see any obvious difference in the fold change after radiation exposure between samples extracted with different kits (**Figure 10B**). However, the samples extracted with miRNeasy again gave lowest Ct values for two out of three small RNA assays (**Table 9**). Our pilot experiment results suggest, that most of the small fragments on the gel are in fact DNA degradation products, because the mirVana kit does not seem to extract small RNA species more efficiently than the miRNeasy kit. As expected, samples extracted with 4PCR kit gave the highest Ct values, because kit is not optimised for extraction of small RNA species.

Finally, we looked at melt profiles to assess if we detected the correct products (**Figure 11**). RNA, U6 small nuclear 1 (*RNU6-1*) had the same melting temperature for

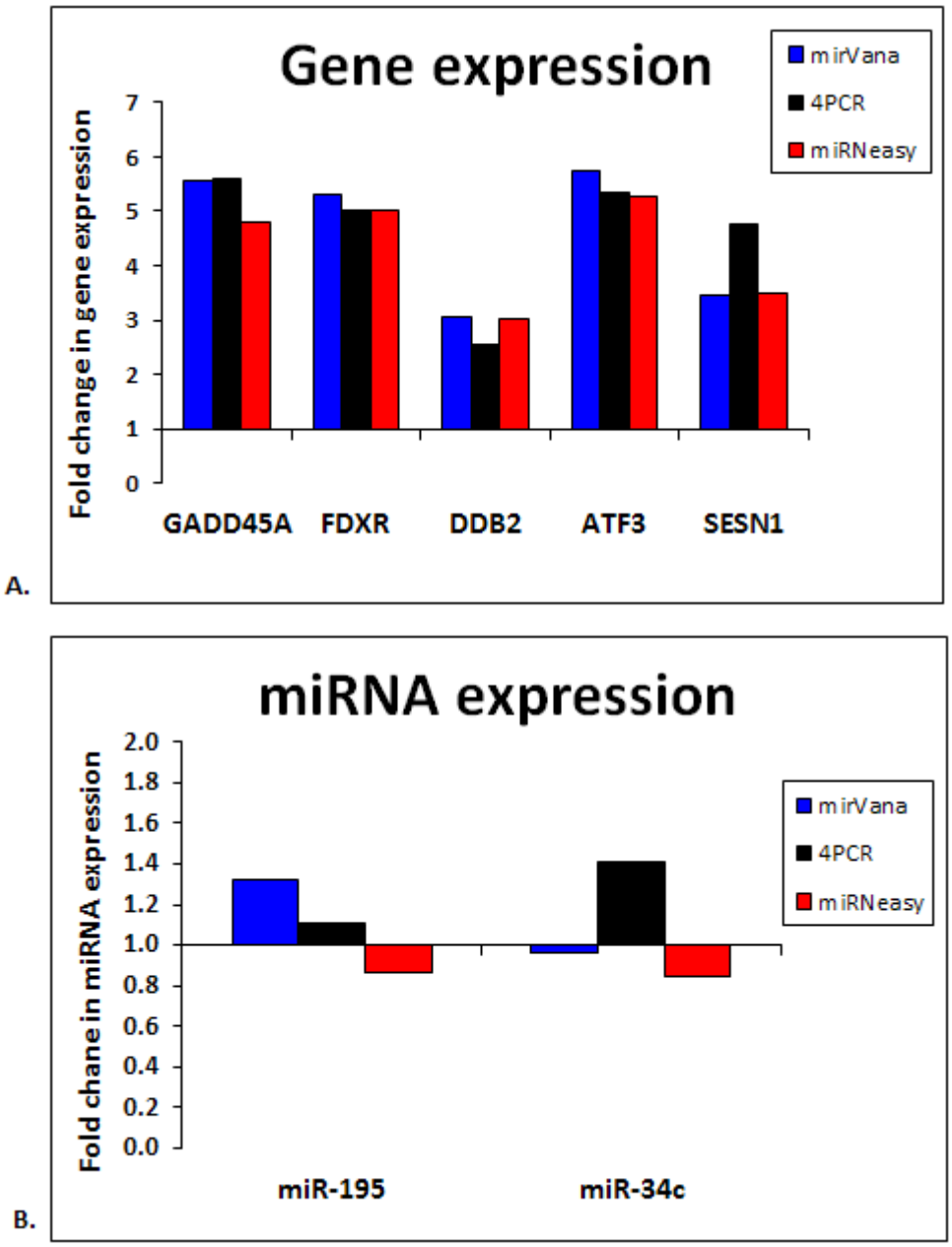

Figure 10. Gene and miRNA expression results from RNA samples extracted with three different kits.

A. Comparison of fold changes in expression of six genes analysed in 6-plex qPCR reaction between samples extracted with three different RNA extraction kits. All samples were normalised to *HPRT1* internal control and then irradiated samples were normalised to the controls. **B.** Comparison of fold changes in expression of two miRNAs analysed by SybrGREEN reaction between samples extracted with three different RNA extraction kits. All samples were normalised to *RNU6-1* internal control and then irradiated samples were normalised to the controls. Both graphs represent results of a single experiment

Table 9. miRNA Ct values obtained for samples extracted with three different RNA extraction kits

	Sample	Ct mean		
		RNU6-1	miR-195	miR-34c
mirVana	0Gy 4h	13.48	19.15	25.43
	4Gy 4h	13.42	18.69	25.43
4PCR	0Gy 4h	15.82	27.26	29.58
	4Gy 4h	16.10	27.39	29.36
miRNeasy	0Gy 4h	12.61	17.61	26.06
	4Gy 4h	12.24	17.46	25.93

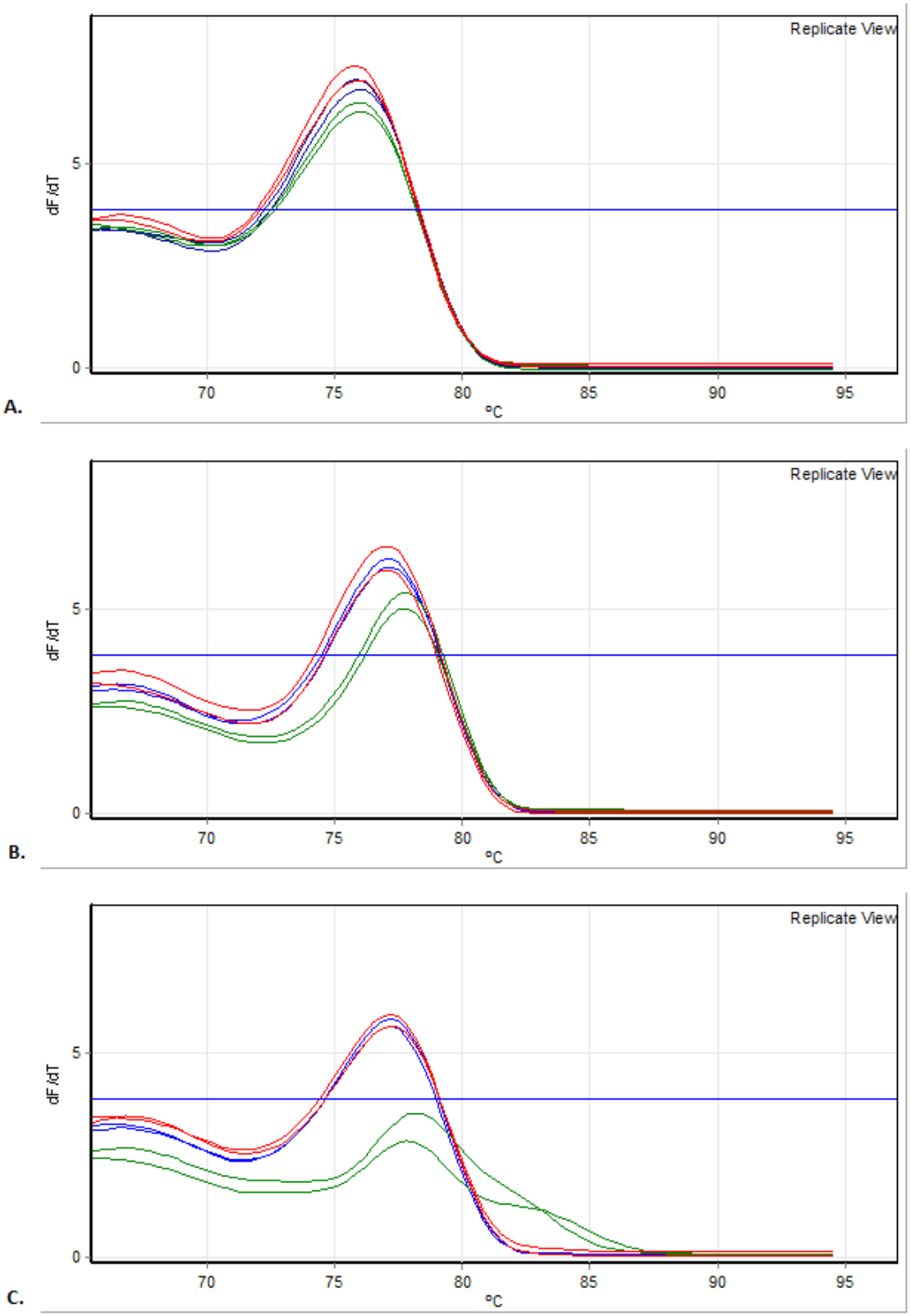

Figure 11. Melt profiles of samples extracted with three different kits

Melt profiles of samples extracted with miRNeasy (red), mirVana (blue) and 4PCR (green) kits were assessed by SYBRGreen for RNU6-1 (**A**), miR-195 (**B**) and miR-34c (**C**).

all samples, however samples extracted with the 4PCR kit have a one degree higher melting temperature for *miR-195* and produce multiple unspecific products for *miR-34c*. These differences in melt profiles are probably caused by the fact 4PCR kit is not suitable for extraction of short RNA species, however, human *RNU6-1* is 106 nucleotides long in contrast to miRNAs which are around 20 nucleotides and it may be just long enough for efficient extraction with the 4PCR kit.

3.1.5. RT reaction optimisation

The High Capacity cDNA Reverse Transcription Kit (Life Technologies) utilising random hexamers has been historically used in our lab. From the literature it is known that the RT step introduces the highest level of variability into qPCR experiments (Stahlberg et al., 2004). It has been also shown that using random hexamers results in different transcription efficiencies between targets and non-linear reverse transcription (Nolan et al., 2006). We, therefore, wanted to assess the performance of our cDNA synthesis kit.

In order to test the kit performance, different volumes of mouse blood from 5 µl up to 100 µl were prepared and RNA was extracted. The experiment was repeated twice and a linear correlation between blood volume used and amount of total RNA extracted was observed with a linear regression R^2 value of 0.9981 thus confirming that in the range we have tested, there is a linear relationship between the amount of blood used and the amount of extracted RNA (**Figure 12**).

Next, we investigated if the amount of total RNA used for reverse transcription reaction influences the performance of our RT kit. It has been previously reported that RT efficiency depends on total RNA concentration and is different for different genes (Stahlberg et al., 2004). In order to investigate this issue, an RT reaction was set up

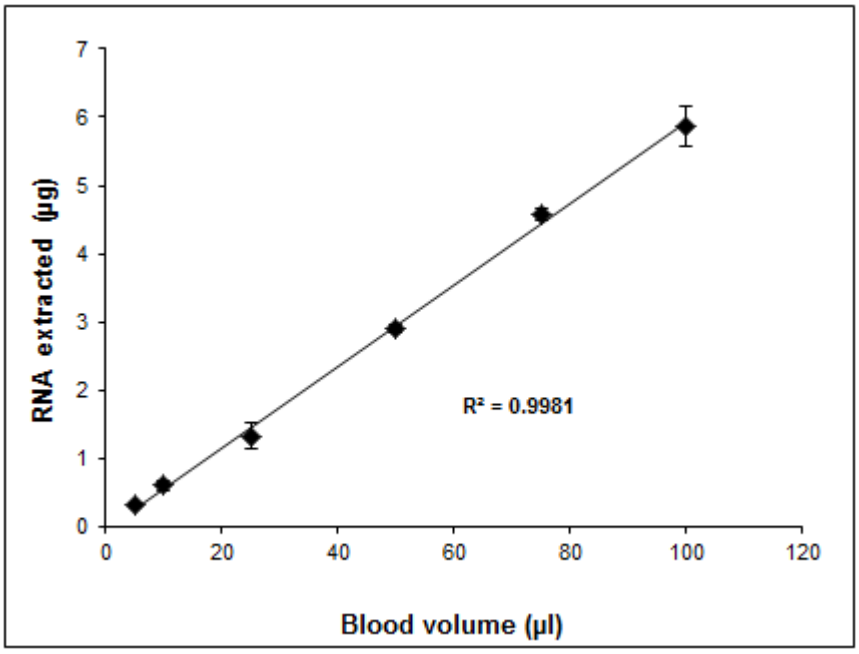

Figure 12. Correlation between volume of blood used and amount of total RNA extracted.

RNA was extracted from different volumes of mouse blood; error bars represent standard deviation between two independent experiments.

using equal volumes but different concentrations of total RNA extracted from aliquots of mouse blood. A qPCR reaction was performed and Ct values for seven mouse genes: *Hprt*, *Ccnb1*, *Bbc3, Cdkn1a, Sesn1, Sesn2* and *Atf3* were converted into mRNA copy numbers using a standard curve. The results of this experiment are presented in **Figure 13**. The reproducibility of RT reaction was good for all genes except for *Bbc3* and *Ccnb1*, as indicated by error bars representing SD. There was a linear dependence between the amount of RNA used in cDNA synthesis and the gene copy number measured by qPCR suggesting that the amount of total RNA used does not affect the RT reaction efficiency in the range tested (from 60 ng up to 1.2 µg of total RNA per reaction) for all seven genes. However, the linear regression R^2 value for *Bbc3* was slightly lower suggesting that there might be some other factors influencing the cDNA synthesis step for this particular gene.

It has been reported that using random hexamers can overestimate transcript copy number by up to 19 fold (Zhang and Byrne, 1999), and consequently we wanted to investigate if it was true for our RT kit. We assumed that when a transcript is reverse transcribed with 100 % efficiency, doubling of RNA input should result in doubling of transcript copy number measured by qPCR. Using the mouse blood samples from the previous experiment, we calculated theoretical mRNA copy numbers which should be measured if RT reaction efficiency was 100 %, by multiplying the gene copy number for the lowest RNA concentration by fold increase in RNA input. For example, if the measured mRNA copy number for gene X was 10 in the sample with the lowest RNA concentration and the next sample contained twice as much RNA as the first one, then if the RT reaction efficiency was 100 %, the measured copy number in the second sample should be 20. We have performed two independent repeats of this exercise for

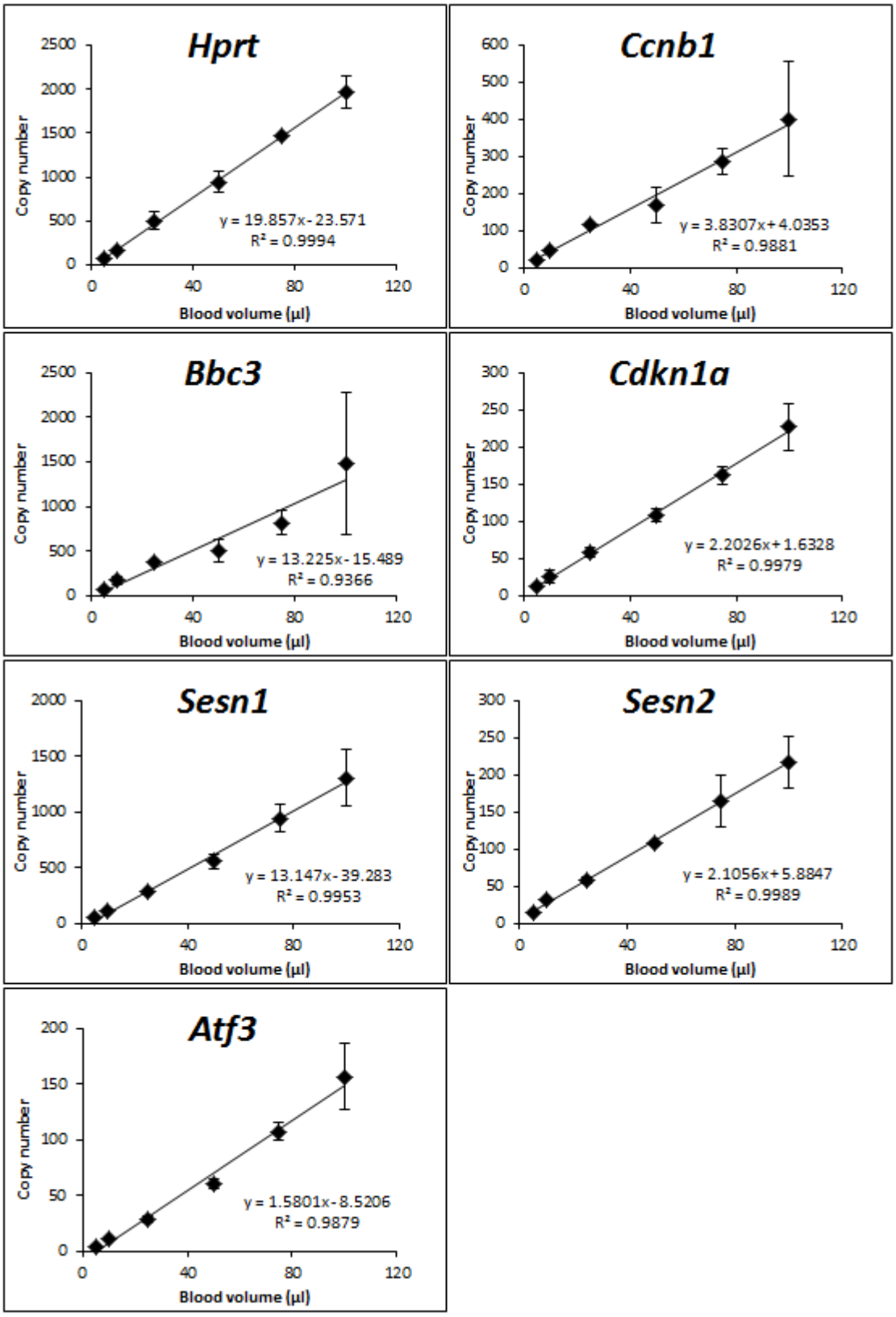

Figure 13. Correlation between volume of blood used and gene copy number for seven mouse genes.

RNA was extracted from different volumes of mouse blood and equal volumes of total RNA have been used for cDNA synthesis, prepared cDNA was used in 4-plex qPCR reactions; error bars represent standard deviations for two independent experiments.

all seven genes and our results show that the RT reaction efficiency indeed seems to be gene dependant confirming previous findings (Stahlberg et al., 2004) (**Figure 14**), however, we did not observe a massive overestimation of gene copy number reported by Zhang *et al*. Gene copy numbers for some genes (*Hprt, Sesn1* and *Atf3*) seem to be slightly overestimated (maximum of 1.8 fold for *Atf3* in the sample with the highest RNA concentration). Three genes (*Ccnb1, Bbc3* and *Cdkn1a*) were faithfully reverse transcribed whereas copy number of *Sesn2* transcript was slightly underestimated (1.3 fold for the sample with the highest RNA concentration).

3.1.1. 6-plex protocol development

A 4-plex qPCR protocol had been developed in our laboratory by Ms Claudine Raffy. More recently, a new qPCR platform become available – the Rotor-Gene Q 6-plex (Qiagen) – which replaced the four channel iQ5 system. The Rotor-Gene Q was capable of measuring fluorescence in six different channels in 10 µl reaction volumes. To take advantage of this extra capacity, other dyes compatible with the new system were required. The new machine had two extra channels: crimson (laser source 680 ±5 nm and detection at 710 high pass) and blue (laser source 365 nm ±20 and detection at 460 nm ±20).

We started our optimisation with crimson channel as there was already a report of successful 5-plex qPCR reaction with Quasar® 705 dye fluorescing in far red spectrum of visible light (Bio-Rad, private communication). We ordered four probes for the human *ATF3* gene with different dyes emitting fluorescence in crimson channel: Quasar® 705, AlexaFluor® 680, ATTO 680 and CY® 5.5. In order to test which dye performed the best, we set up four independent single-plex reactions with a standard curve in 30 µl reaction volumes.

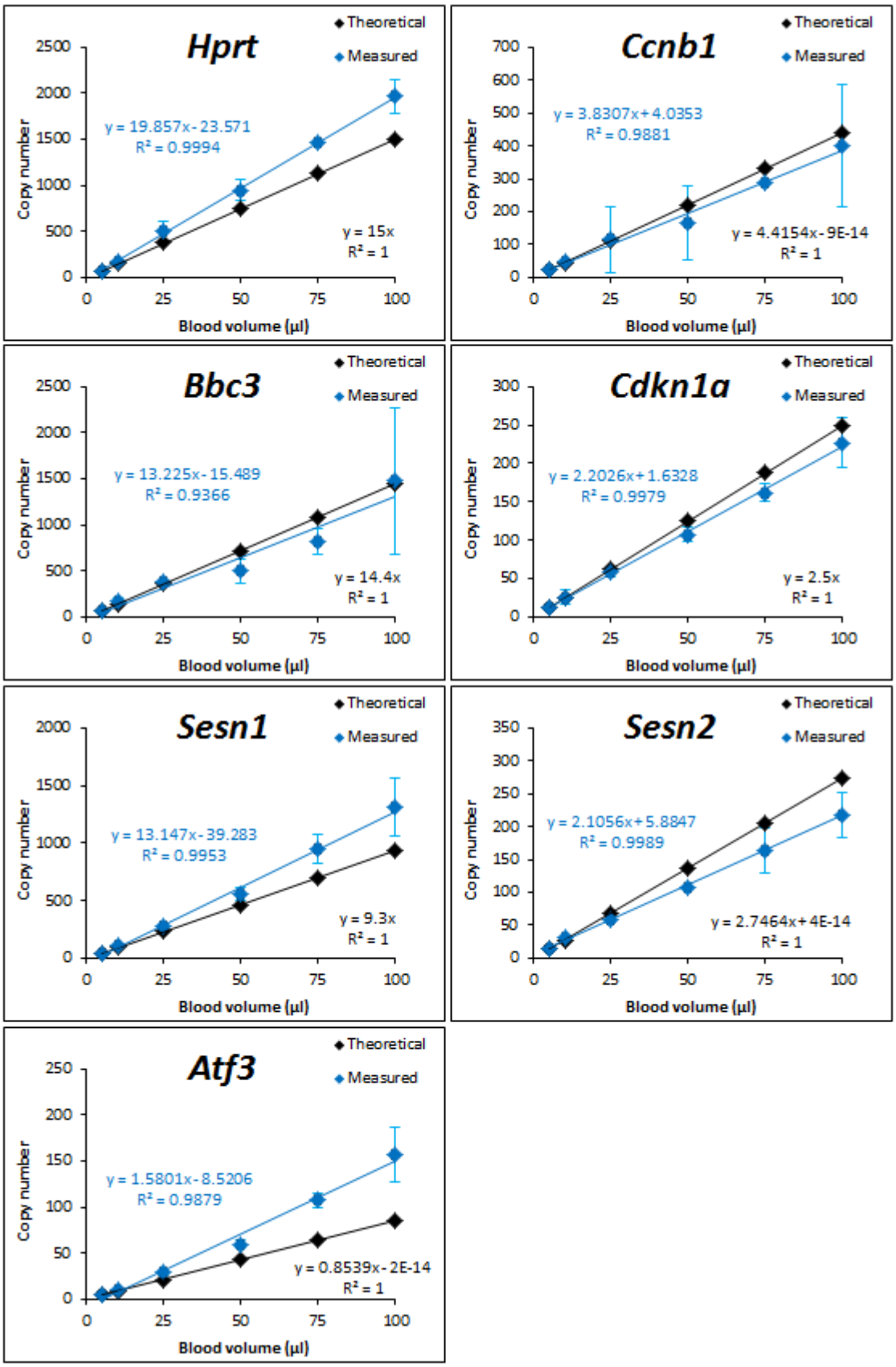

Figure 14. Comparison of theoretical and measured transcript copy number

Theoretical gene copy number (black diamonds) was calculated from RNA input and compared to measured gene copy number (blue diamonds); error bars represent standard deviations for two independent experiments.

First, we looked at raw fluorescence data (**Figure 15**) and it was clear that Alexa Fluor® 680 probe had very high background fluorescence and therefore was unsuitable for our multiplex setup. The other probes had acceptable background fluorescence level with CY® 5.5 labelled probe having the lowest but it also had the shortest exponential phase which is a disadvantage in qPCR experiments. Next, we looked at four probes PCR efficiency in single-plex reaction (**Figure 16**) and all four probes showed good PCR efficiencies and linear regression R^2 values except for the Quasar® 705 probe which showed a lower than acceptable R^2 value but this could have been caused by pipetting error. We excluded Alexa Fluor® 680 and CY® 5.5 labelled probes as unsuitable for multiplexing based on raw fluorescence data, and although Quasar® 705 had the longest exponential phase, it was significantly more expensive than ATTO 680 dye, therefore we decided to focus our interest on the ATTO 680.

Finally, we wanted to investigate ATTO 680 probe performance in 5-plex reaction. We set up 5-plex reaction with a standard curve in a 30 µl reaction volume. All five genes in 5-plex reaction showed PCR efficiency above 93 % and linear regression R^2 values above 0.999 (**Figure 17**) confirming that ATTO 680 probe is compatible with our multiplex setup.

We also wanted to investigate if we could reduce the reaction volume without compromising assay performance as this would lower the cost of running the qPCR assays. In order to test this possibility we performed 5-plex reaction with the same genes as above but in a 10 µl reaction volume where the concentrations of all reagents were kept the same. As illustrated in **Figure 18**, the PCR efficiencies for all five assays were between 93 and 104 % and the linear regression R^2 values were above 0.998, confirming that reducing reaction volume does not compromise assay performance.

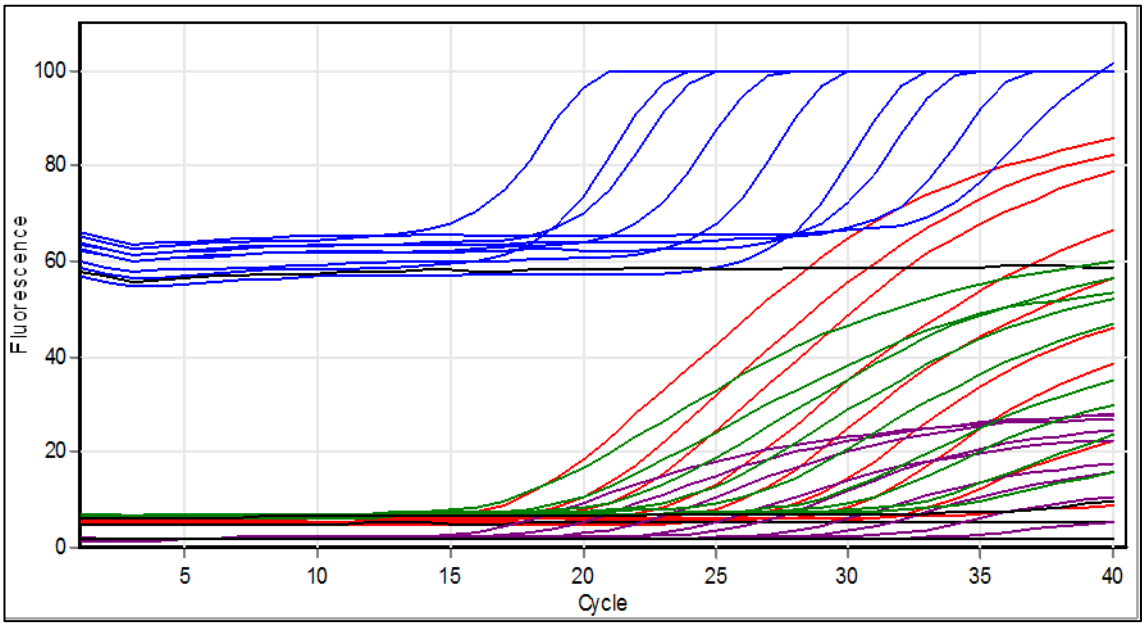

Figure 15. Raw fluorescence data for crimson channel.

Raw fluorescence data was collected for Quasar® 705 (red), Alexa Fluor® 680 (blue), ATTO 680 (green) and CY® 5.5 (purple) dyes.

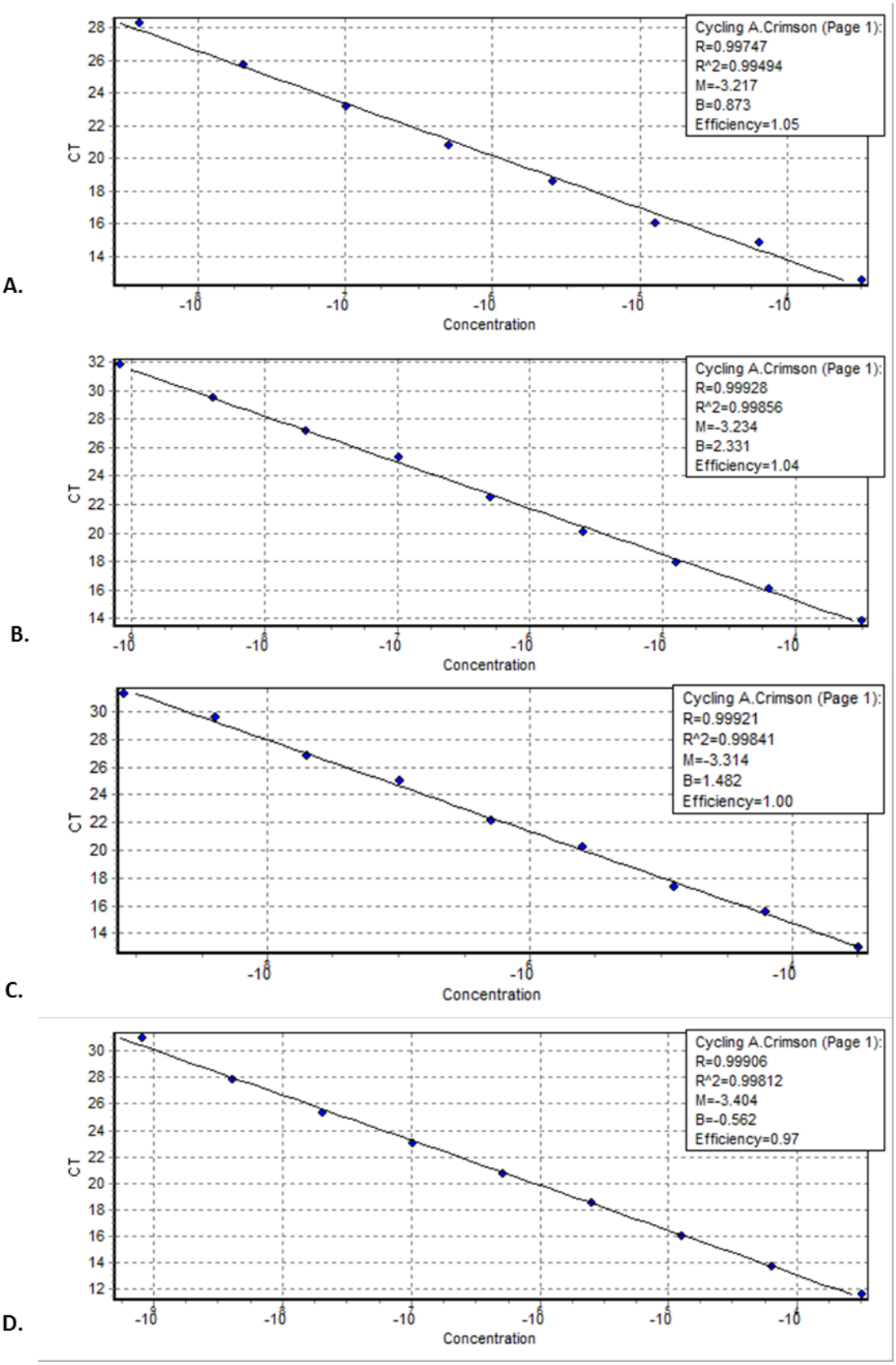

Figure 16. Standard curve in single-plex reaction.

Standard curves for *ATF3* gene with four different dyes: Quasar® 705 (**A**), Alexa Fluor® 680 (**B**), ATTO 680 (**C**) and CY® 5.5 (**D**) were run in single-plex reaction.

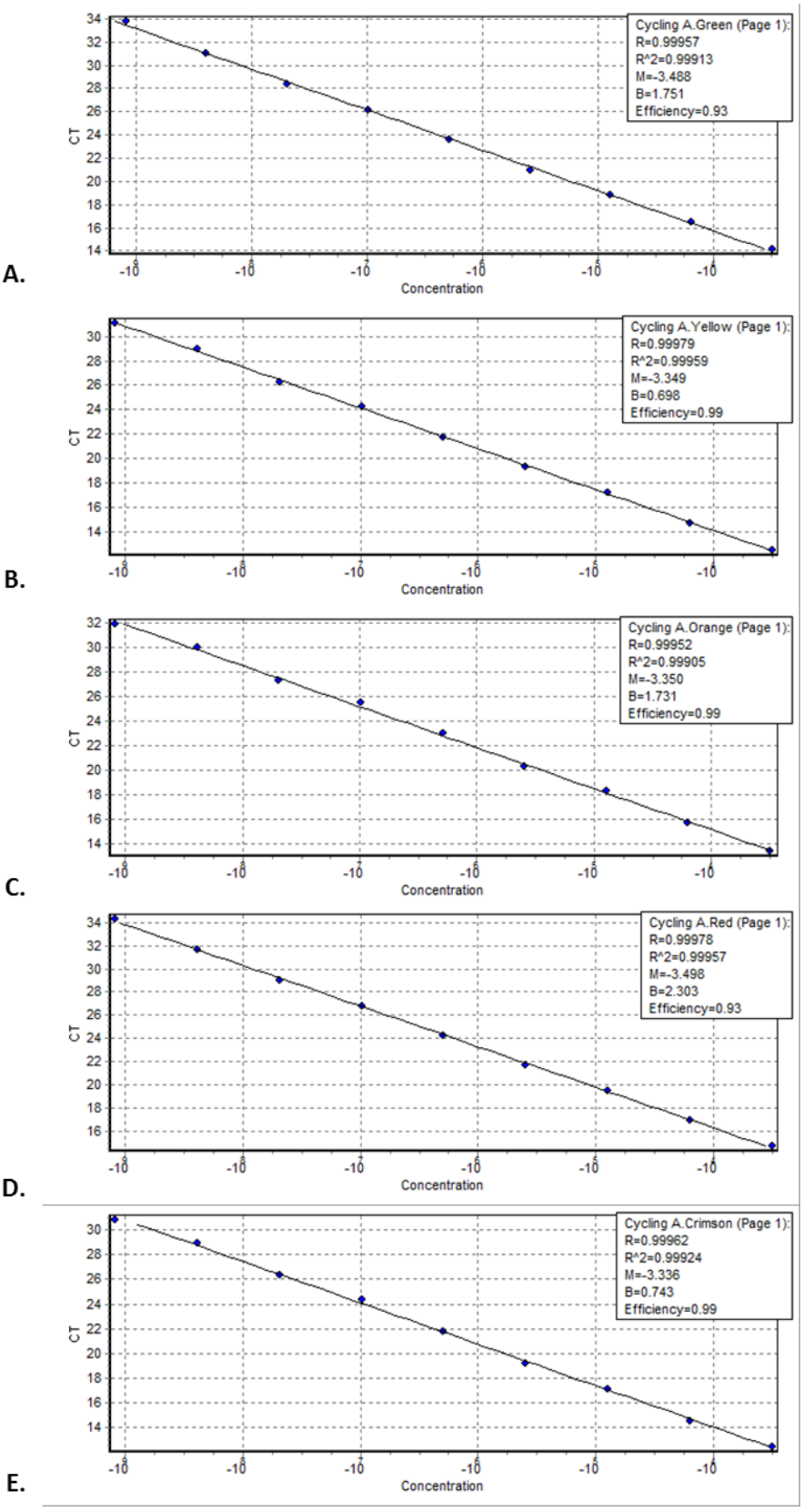

Figure 17. Standard curve in 5-plex 30 µl reaction with ATTO 680 probe.

Standard curve with five human genes: *HPRT1* (**A**), *GADD45A* (**B**), *FDXR* (**C**) *MDM2* (**D**) and *ATF3* (**E**) was run in 5-plex 30 µl reaction.

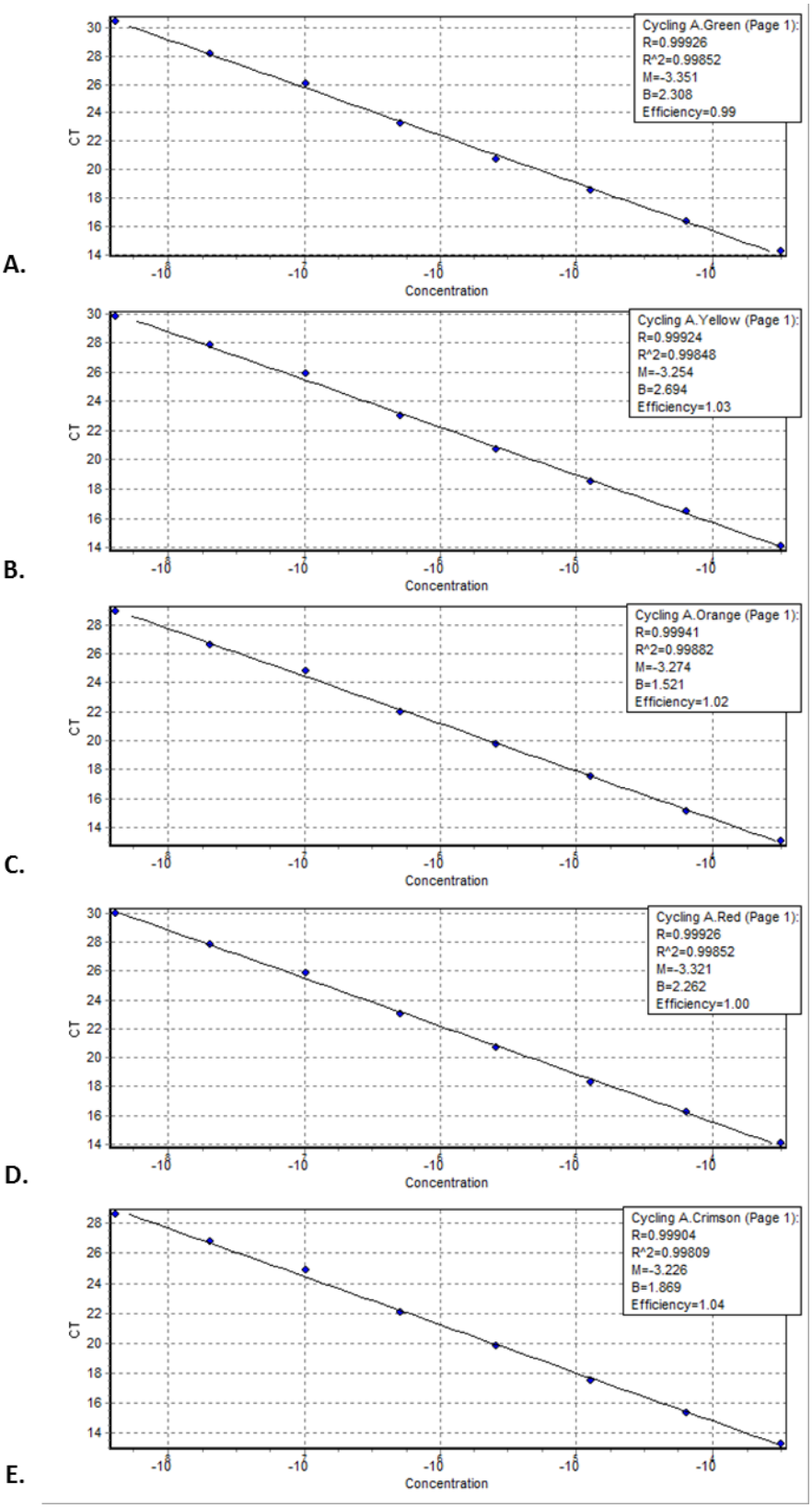

Figure 18. Standard curve in 5-plex 10 µl reaction with ATTO 680 probe.

Standard curve for five human genes: *HPRT1* (**A**), *GADD45A* (**B**), *FDXR* (**C**) *MDM2* (**D**) and *ATF3* (**E**) was run in 5-plex 10 µl reaction.

After the successful development of 5-plex qPCR assay, we proceeded to 6-plex assay optimisation. We identified four dyes compatible with the blue channel of theRotor-Gene Q: ATTO 390, ATTO 425, Marina Blue® and Alexa Fluor® 390. We ordered four probes for human *SESN1* gene labelled with these dyes and DDQ1 quencher.

First, we tested the probes on a standard curve in a single-plex reaction. As presented on the raw fluorescence plot (**Figure 19**) all four probes have very short exponential phase. ATTO425 showed the lowest background but also the shortest exponential phase; alternatively ATTO390 presented the best combination of background level and length of exponential phase. Then we looked at PCR efficiency of these probes (**Figure 20**) and all probes except for ATTO 425 showed good PCR efficiency, although linear regression R^2 values for Marina Blue and Alexa Fluor 390 were slightly lower than acceptable. Considering raw fluorescence data and probes performance we decided to focus on ATTO 390 dye in further optimisation.

To validate the two new dyes in 6-plex reaction, we prepared a standard curve consisting of eleven 5-fold dilutions containing from 1 up to 9765625 copies of each gene per 10 µl reaction, the standard curve was run in triplicate. All six genes presented very good PCR efficiency and high R^2 values in the 6-plex assay (**Figure 21**).

Finally, we wanted to be sure that the same gene run in 6-plex and single-plex reaction performs similarly. In order to do so, we assessed the expression of six genes in one sample run in quadruplicate and a standard curve, assayed both in 6-plex and single-plex reactions. The standard curve results are presented in **Figure 22**. Five out of six genes shown no differences between standard curves assayed in 6-plex or single-plex reaction, however *MDM2* gene detected in red channel demonstrated a shift in Ct

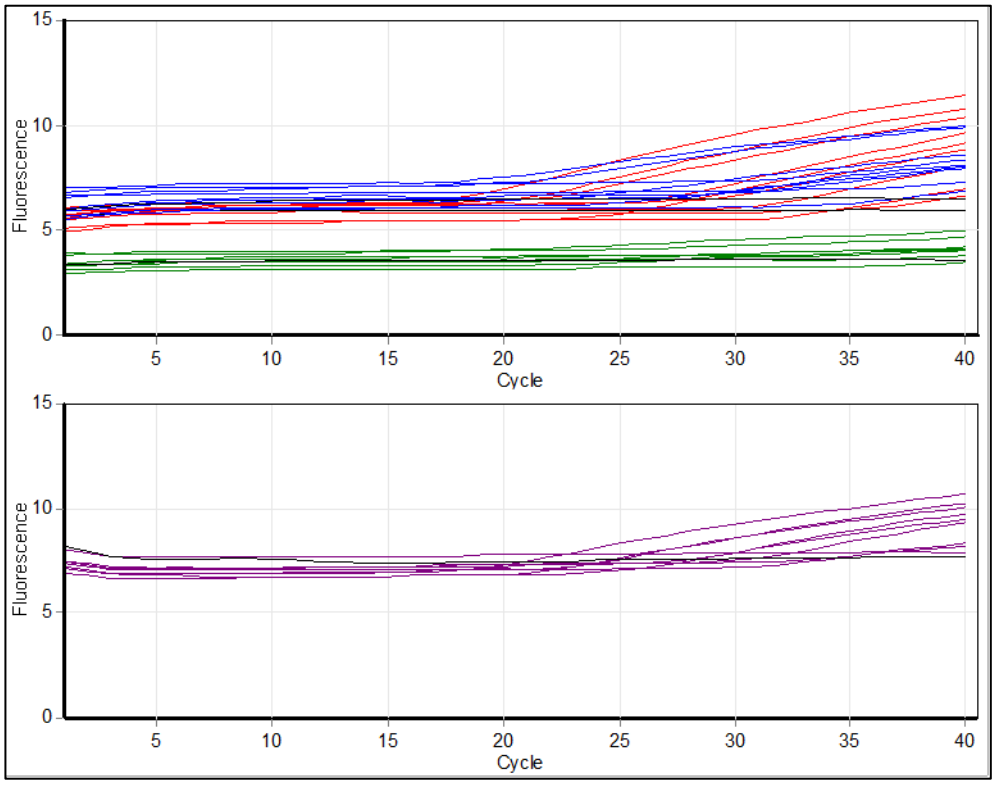

Figure 19. Raw fluorescence data for blue channel.

Raw fluorescence data was collected for *SESN1* probe with ATTO 390 (red), Marina Blue® (blue), ATTO 425 (green) and Alexa Fluor 390 (purple) dyes.

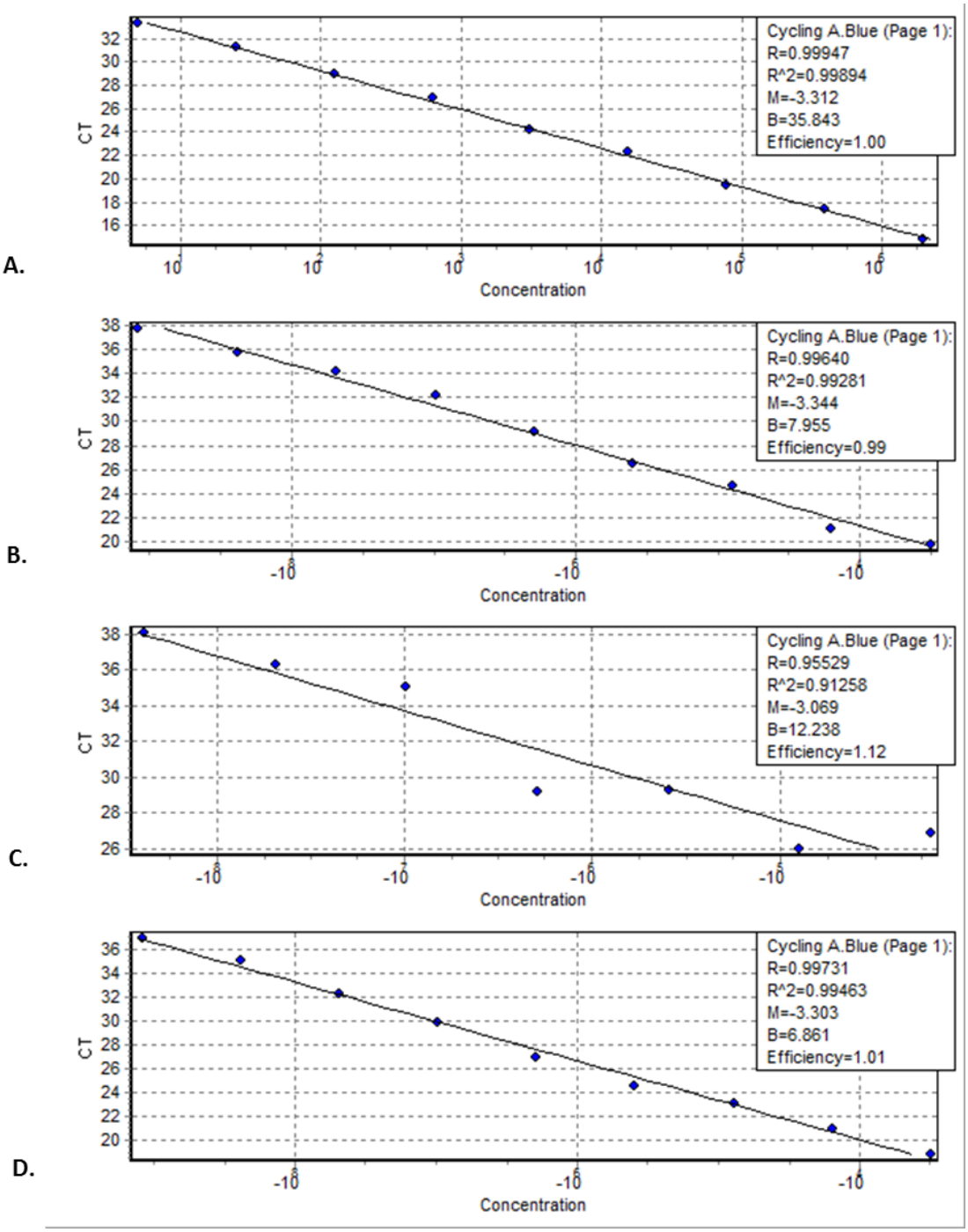

Figure 20. Standard curve in single-plex reaction.

Standard curve for *SESN1* gene with four different probes: ATTO 390 (**A**), Marina Blue (**B**), ATTO 425 (**C**) and Alexa Fluor 390 (**D**) were run in single-plex reaction.

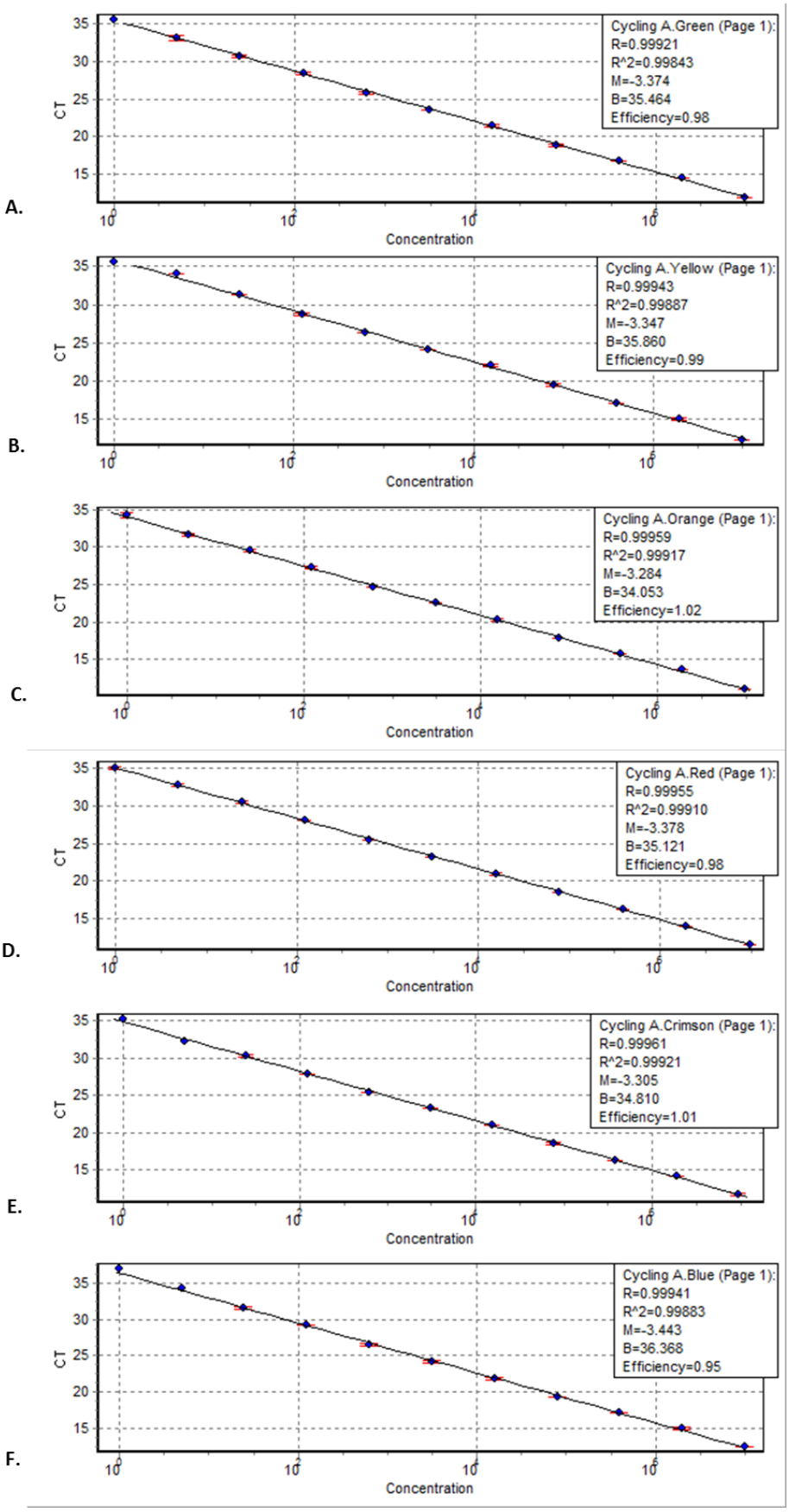

Figure 21. Standard curve in 6-plex reaction.

Standard curve for 6 genes: *HPRT1* (**A**), *GADD45A* (**B**), *FDXR* (**C**), *MDM2* (**D**), *ATF3* (**E**) and *SESN1* (**F**) was run in triplicates. Error bars represent standard deviation.

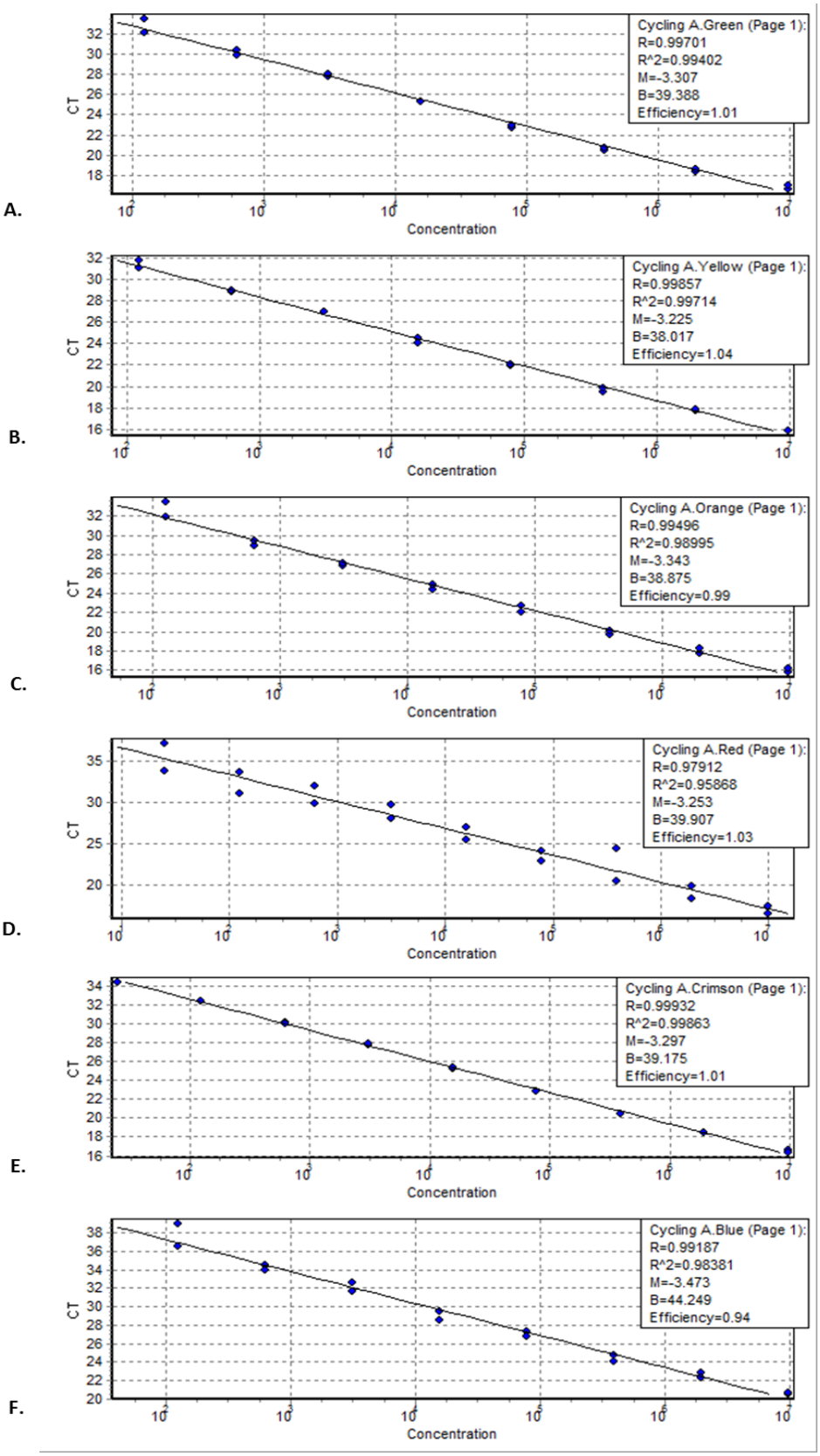

Figure 22. Comparison of 6-plex vs single-plex reaction.

Standard curve for 6 genes: *HPRT1* (**A**), *GADD45A* (**B**), *FDXR* (**C**), *MDM2* (**D**), *ATF3* (**E**) and *SESN11* (**F**) was run in 6-plex and single-plex reaction. On each graph there are points from 6-plex and single-plex reaction.

values. This is probably caused by Texas Red (orange) dye bleeding into red detection channel as shown on **Figure 23A**. We have also noticed that FAM (green dye) is bleeding slightly into yellow channel although it does not change the *GADD45A* gene Ct values (**Figure 23B**).

The Ct values for the test sample assessed in 6-plex and single-plex reaction are presented in **Table 10**. The Ct means for samples assayed in single-plex and 6-plex reactions are within 0.5 Ct from each other, which is perfectly acceptable threshold for technical replicates (Nolan et al., 2006); however samples run in 6-plex reactions have slightly lower replicate reproducibility as indicated by higher standard deviation.

3.1.2. Discussion

Quantitative PCR is considered to be the "gold standard" for accurate and sensitive measurement of gene expression. Nevertheless, because of its simplicity it is easy to forget that in order to obtain biologically meaningful and statistically significant results, strict quality control must be applied to all steps of the workflow (Derveaux et al., 2010). The major part of our project was investigation of gene expression changes by qPCR, therefore, in order to obtain sound data, it was decided to spend considerable time and effort to demonstrate that we controlled every step of the qPCR.

One of the first issues that must be addressed when setting up a new qPCR experiment is the quality of primers and probe design. This step is crucial as poor/unspecific primers or probe result in poor PCR efficiency and unreliable results (Bustin, 2004). We decided to use TaqMan probe based chemistry because of its specifity and because it allows multiplexing. High efficiency multiplexing is a real challenge and we needed to be sure that all designs were specific, showing high PCR

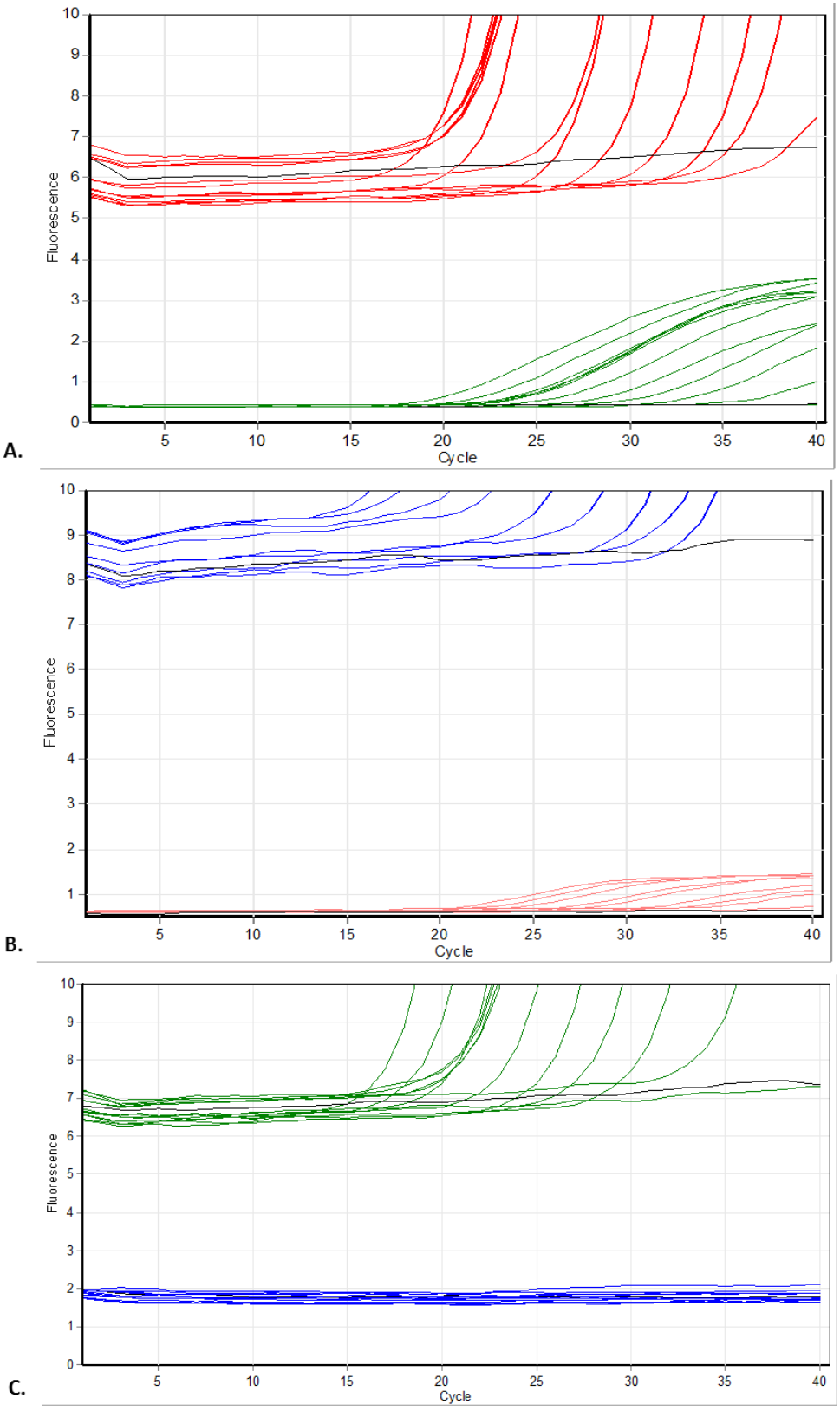

Figure 23. Raw fluorescence data for channels red (A), yellow (B) and orange (C).

High magnification of raw fluorescence plot. **A**. Texas Red® probe (green) bleeds through red channel and amplification can be detected in background level of CY5® probe (red). **B**. FAM probe (pink) bleeds through yellow channel and amplification can be detected in the background of HEX probe (blue).**C.** No amplification of HEX probe (blue) can be detected in the background level of Texas Red® probe (green)

Table 10. Comparison of Ct values between sample assayed in 6-plex and single-plex reaction.

	6-plex		Single-plex	
	Ct mean	SD	Ct mean	SD
HPRT1	20.45	0.17	20.38	0.14
GADD45A	20.38	0.18	20.64	0.08
FDXR	20.53	0.12	20.89	0.10
MDM2	18.83	0.24	19.24	0.09
ATF3	22.49	0.17	22.94	0.06
SESN11	23.64	0.07	23.81	0.19

efficiency and low background fluorescence. All designs were *in silico* and experimentally validated for specificity, SNPs presence, alternative transcript coverage and PCR efficiency. The obvious advantages of multiplex qPCR experiments are cost reduction, conservation of limited or precious samples and decreased technical variability due to the detection of reference gene and genes of interest in a single reaction.

A part of our project involved processing blood samples. Blood contains considerable amount of heme – a powerful inhibitor of PCR reaction (Akane et al., 1994) but also the sampling procedure can introduce additional inhibitors like heparin (Holodniy et al., 1991). Our data showed that heparin used as an anti-coagulant in blood sampling can somehow survive phenol-chloroform extraction and substantially inhibit qPCR reactions (**Table 6**). As a result of this pilot, we decided to use EDTA blood collection tubes for our experiments, except for the NATO exercise described further in **chapter 3.4**, where collaborative nature of the study required using heparin as an anticoagulant.

RNA extraction is another critical step in performing qPCR experiments as it is widely accepted that RNA quality is significantly negatively correlated with Ct values (Fleige et al., 2006) and reference genes vary in their sensitivity to degradation (Perez-Novo et al., 2005). We investigated the performance of three extraction kits and observed that although there was no difference in RNA quality or fold change gene expression results, the miRNeasy kit consistently produced lower Ct values for both mRNA and miRNA despite using the same amount of RNA for cDNA synthesis step. The most probable explanation for this phenomenon is dilution of transcripts with products of DNase treatment as the DNase treatment is performed at the end of the

extraction in the 4PCR and mirVana kits as opposite to the miRNeasy kit and we did not observe higher yields of small RNA species in samples produced by other kits (**Table 9**). Although, we did not observe any differences in fold change results between samples extracted with different kits, the lower Ct values produced by the miRNeasy kit are advantageous especially when investigating genes expressed at low level. As a result of this study we decided to use the miRNeasy kit for all future RNA extractions.

We also studied performance of our cDNA synthesis kit, as it is generally considered to be the most variable step in qPCR workflow (Stahlberg et al., 2004). Our kit utilises random hexamers as a priming strategy and it has been reported that using random hexamers is the least reliable method of priming RT reaction as it results in (i) overestimation of mRNA copies when compared to gene specific primers (Zhang and Byrne, 1999), (ii) gene-dependant transcription efficiencies and (iii) non-linear amplification of mRNA depending on RNA concentration (Nolan et al., 2006).

Our results show that in contrast to Nolan *et al* report (Nolan et al., 2006) the performance of our RT kit does not seem to be influenced by total RNA concentration in the range tested as our kit enables linear reverse transcription over a broad range of RNA input for all seven genes (**Figure 13**), however the linear regression R^2 value for *Bbc3* is slightly lower implying that other factors, such as complicated secondary RNA structure, may play a role as well.

Zhang *et al* reported that using random hexamers can overestimate transcript copy number by as much as 19 fold (Zhang and Byrne, 1999). In contrast to this report, we did not observe massive overestimation of gene copy number of seven tested genes (maximum of 1.8 fold in case of *Atf3* gene when using 1.2 µg of RNA per RT

reaction) (**Figure 14**); however, we cannot exclude the possibility that other genes are reverse transcribed more efficiently.

The efficiency of RT reactions seems to be gene dependant as previously reported (Stahlberg et al., 2004), with copy number for some transcripts being slightly overestimated, others underestimated or faithfully transcribed. One very important conclusion emerges from our results – the same amount of total RNA should always be used for cDNA synthesis, because different genes are reverse transcribed with different efficiencies and the gene of interest/reference gene ratio changes with different RNA concentrations. Overall, we concluded that our RT kit allows reproducible and relatively faithful cDNA synthesis as long as we use the same RNA concentration for all samples.

A strict quality control and robust assay design allowed us to multiplex six genes in 10 µl reaction without compromising assay performance (**Figure 21,Figure** 22 and **Table 10**) this is an achievement in itself as not many labs can accomplish such deep multiplexing. The only gene which showed discrepancy in Ct values between samples assayed in 6-plex and single-plex is *MDM2* (red channel). We believe this is caused by the TexasRed® probe signal bleeding into red channel (**Figure 23A**). The discrepancy is observed only in standard curve samples (**Figure 22D**) but not in the unknown sample (**Table 10**). The most probable explanation for this phenomenon is the fact that in the standard curve, the PCR products for all six genes are in equimolar concentration; therefore, the Texas Red® probe signal is stronger and bleeds into the red channel more significantly. In the unknown samples *FDXR* gene has lower expression than *MDM2*, consequently it affects the red channel to lesser extent. We concluded that as long the gene measured by the orange channel had lower

expression than the gene measured in red channel, the multiplexing does not affect relative gene expression results.

3.2. Identification of biomarkers for IR dose estimation

3.2.1. Introduction

The dicentric chromosome assay is considered to be the gold standard for biodosimetric estimation of IR exposures, however it is not well suited to cases requiring mass screening in a triage scenario due to limited capacity, as it is labour intense, time consuming and requires experienced staff for scoring (Wojcik et al., 2010). There is clearly a need for new, minimally invasive and rapid biodosimetry techniques.

It is well known that expression of a number of genes are modified after IR exposure, and depends on tissue type (Pawlik et al., 2009), dose of radiation and time between the exposure and analysis (Franco et al., 2005, Meadows et al., 2008, Manning et al., 2013), features that potentially make gene expression very useful for biodosimetry purposes. Gene expression assays are much quicker than dicentric chromosome assays, as they can provide dose estimation within 8 h following samples receipt as demonstrated in Badie *et al* (Badie et al., 2013) and it is suitable for high throughput application.

The aim of this project was to establish a panel of robust and highly responsive genes for biodosimetry purposes and to study inter- and intra-individual variation in transcriptional response to IR exposure. We were also interested in comparing gene expression signatures in blood and stimulated T-lymphocytes obtained from the same donor in order to assess the role of cell cycle in transcriptional response to IR exposure. The gene expression signatures in T-lymphocytes can be also informative in terms of individual sensitivity to IR, as we had demonstrated previously that aberrant transcriptional response of *CDKN1A* to IR was associated with abnormal normal tissue reaction to therapeutic radiation treatment for breast cancer (Badie C, 2008).

3.2.2. Identification of IR-responsive genes

In order to identify genes responsive to IR, we first performed a microarray experiment. To obtain information about the impact of the dose of radiation and time post-exposure on gene expression profiles, blood samples and corresponding stimulated T-lymphocytes obtained from three donors were irradiated with a sham dose or exposed to 2 or 4 Gy of X-ray and collected 2 h and 24 h following exposure. Total RNA was extracted and half was sent to Dr Alan Mackay (Breakthrough Breast Cancer Research Centre, the Institute of Cancer Research, London, UK) for microarray analysis, the other half was kept for later qPCR validation experiments. Three independent experiments were carried out and the results presented in this chapter have been already published (Kabacik et al., 2011a).

The microarray experiment identified genes, the expression of which was significantly modified by IR exposure in blood leukocytes and/or in stimulated T-lymphocytes. Altogether, 570 up-regulated and 31 down-regulated genes were detected in non-cycling blood leukocytes compared to 232 up-regulated and 1357 down-regulated genes in stimulated T-lymphocytes when using false discovery rate of < 5 % (**Table 11**). The heatmap representing the top twenty genes the expression of which is up- or down-regulated in response to IR in blood leukocytes and in stimulated T-lymphocytes is presented in **Figure 24.** The corresponding tables with the ranking of genes based on fold change in expression after radiation are shown in **Table 12A, B, C** and **D**. More genes were up-regulated in blood leukocytes than in T-lymphocytes following IR exposure, whereas many more down-regulated genes are observed in cycling lymphocytes, i.e. there were very few genes significantly down-regulated in blood at the 2 h time-point (**Table 11** and **Table 12D**). The stimulated T-lymphocytes,

Table 11. Radiation responsive genes in blood leukocytes and stimulated T-lymphocytes

	Blood				Lymphocytes			
	2h		24h		2h		24h	
	2Gy	4Gy	2Gy	4Gy	2Gy	4Gy	2Gy	4Gy
up	296	234	13	247	31	100	107	116
down	0	1	7	29	29	267	113	1109

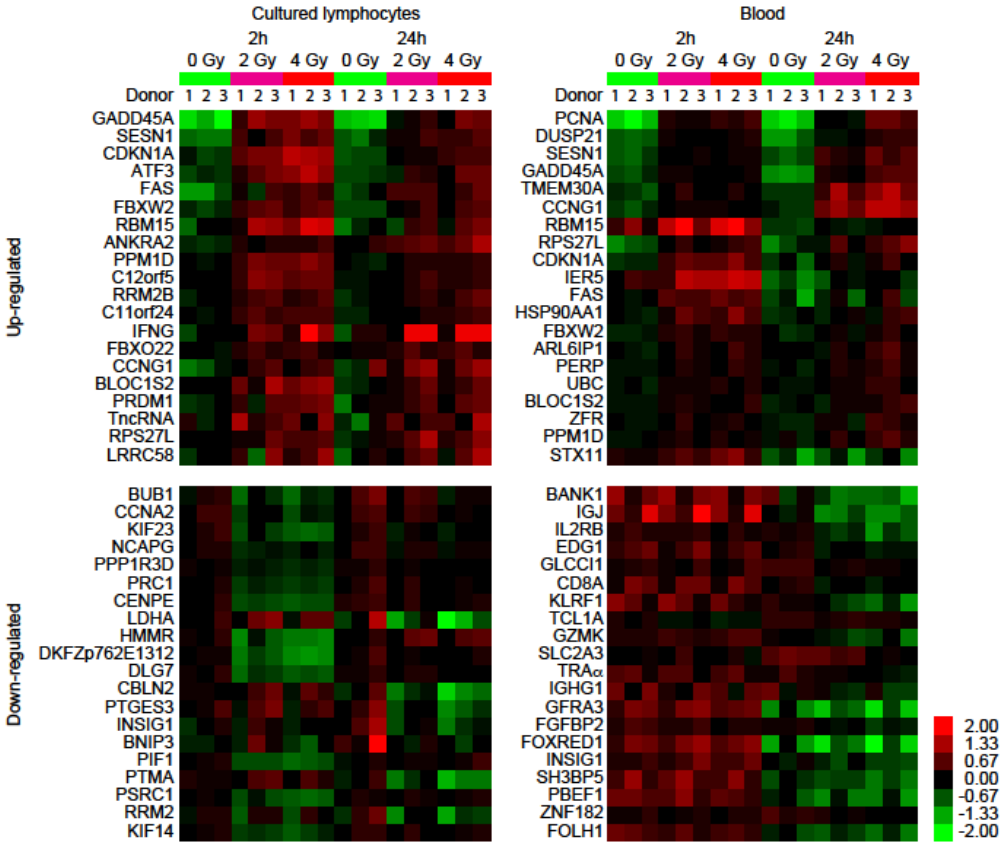

Figure 24. Heatmaps of microarray data.

Twenty of the most radiation responsive genes are shown in stimulated lymphocytes (left panels) and blood (right panels). A colour bar showing the level of expression is shown in the bottom right of the figure. Figure was prepared by Dr Alan Mackay.

Table 12A. Most significantly up-regulated genes in irradiated stimulated T-lymphocytes

Symbol	Description	Unigene entry	2h 2Gy	2h 4Gy	24h 2Gy	24h 4Gy
GADD45A	Growth arrest and DNA-damage-inducible, alpha	Hs.80409	1*	1	1	1
SESN1	Sestrin 1	Hs.591336	3	5	3	3
CDKN1A	Cyclin-dependent kinase inhibitor 1A (p21, Cip1)	Hs.370771	2	3	7	5
ATF3	Activating transcription factor 3	Hs.460	5	6	13	4
FAS	Fas (TNF receptor superfamily, member 6)	Hs.244139	6	8	4	11
FBXW2	F-box and WD repeat domain containing 2	Hs.494985	7	14	6	6
RBM15	RNA binding motif protein 15	Hs.435947	4	4	42	8
ANKRA2	Ankyrin repeat, family A (RFXANK-like), 2	Hs.239154	23	33	31	9
PPM1D	Protein phosphatase 1D magnesium-dependent, delta isoform	Hs.591184	11	20	60	35
C12orf5	Chromosome 12 open reading frame 5	Hs.504545	12	32	48	43
RRM2B	Ribonucleotide reductase M2 B (TTP53 inducible)	Hs.512592	22	54	45	16
C11orf24	Chromosome 11 open reading frame 24	Hs.303025	19	47	85	29
IFNG	Interferon, gamma	Hs.856	NS	9	2	2
FBXO22	F-box protein 22	Hs.591115	28	69	94	80
CCNG1	Cyclin G1	Hs.79101	10	23	10	NS
BLOC1S2	Biogenesis of lysosome-related organelles complex-1, subunit 2	Hs.576605	NS	15	12	18
PRDM1	PR domain containing 1, with ZNF domain	Hs.436023	NS	19	21	15
TncRNA	Trophoblast-derived noncoding RNA	Hs.523789	14	39	NS	7
RPS27L	Ribosomal protein S27-like	Hs.108957	NS	44	5	20
LRRC58	Leucine rich repeat containing 58	Hs.518084	NS	36	23	14

NS: Not Significant (false discovery rate higher than 5%)

* The numbers indicate the ranking of genes based on fold change (1 being the most responsive gene at a particular dose and time-point); prepared by Dr Alan Mackay.

Table 12B. Most significantly down-regulated genes in irradiated stimulated T-lymphocytes

Symbol	Description	Unigene entry	2h 2Gy	2h 4Gy	24h 2Gy	24h 4Gy
BUB1	BUB1 budding uninhibited by benzimidazoles 1 homolog (yeast)	Hs.469649	8*	19	NS	242
CCNA2	Cyclin A2	Hs.58974	22	22	NS	474
KIF23	Kinesin family member 23	Hs.270845	6	3	NS	686
NCAPG	Non-SMC condensin I complex, subunit G	Hs.567567	20	79	NS	720
PPP1R3D	Protein phosphatase 1, regulatory (inhibitor) subunit 3D	Hs.42215	26	34	NS	771
PRC1	Protein regulator of cytokinesis 1	Hs.567385	17	26	NS	826
CENPE	Centromere protein E, 312kDa	Hs.75573	5	11	NS	913
LDHA	Lactate dehydrogenase A	Hs.2795	NS	NS	1	1
HMMR	Hyaluronan-mediated motility receptor (RHAMM)	Hs.72550	1	2	NS	NS
DKFZp762E1312	Hypothetical protein DKFZp762E1312	Hs.532968	2	1	NS	NS
DLG7	Discs, large homolog 7 (Drosophila)	Hs.77695	3	5	NS	NS
CBLN2	Cerebellin 2 precursor	Hs.569851	NS	NS	8	2
PTGES3	Prostaglandin E synthase 3 (cytosolic)	Hs.50425	NS	NS	6	5
INSIG1	Insulin induced gene 1	Hs.520819	NS	NS	3	8
BNIP3	BCL2/adenovirus E1B 19kDa interacting protein 3	Hs.144873	NS	NS	2	9
PIF1	PIF1 5'-to-3' DNA helicase homolog (S. cerevisiae)	Hs.112160	4	7	NS	NS
PTMA	Prothymosin, alpha (gene sequence 28)	Hs.459927	NS	NS	13	4
PSRC1	Proline/serine-rich coiled-coil 1	Hs.405925	9	8	NS	NS
RRM2	Ribonucleotide reductase M2 polypeptide	Hs.226390	NS	NS	7	11
KIF14	Kinesin family member 14	Hs.3104	7	18	NS	NS

NS: Not Significant (false discovery rate higher than 5%)

*The numbers indicate the ranking of genes based on fold change (1 being the most responsive gene at a particular dose and time-point); prepared by Dr Alan Mackay.

Table 12C. Most significantly up-regulated genes in irradiated whole blood

Symbol	Description	Unigene entry	2h 2Gy	2h 4Gy	24h 2Gy	24h 4Gy
PCNA	Proliferating cell nuclear antigen	Hs.147433	1*	1	1	1
DUSP21	Dual specificity phosphatase 21	Hs.534478	5	6	11	7
SESN1	Sestrin 1	Hs.591336	6	5	22	11
GADD45A	Growth arrest and DNA-damage-inducible, alpha	Hs.80409	2	3	38	15
TMEM30A	Transmembrane protein 30A	Hs.108530	4	4	40	18
CCNG1	Cyclin G1	Hs.79101	3	2	62	26
RBM15	RNA binding motif protein 15	Hs.435947	108	13	13	10
RPS27L	Ribosomal protein S27-like	Hs.108957	7	NS	3	4
CDKN1A	Cyclin-dependent kinase inhibitor 1A (p21, Cip1)	Hs.370771	39	NS	6	3
IER5	Immediate early response 5	Hs.15725	50	NS	12	14
FAS	Fas (TNF receptor superfamily, member 6)	Hs.244139	32	NS	23	24
HSP90AA1	Heat shock protein 90kDa alpha (cytosolic), class A member 1	Hs.525600	73	NS	17	12
FBXW2	F-box and WD repeat domain containing 2	Hs.494985	90	NS	49	30
ARL6IP1	ADP-ribosylation factor-like 6 interacting protein 1	Hs.634882	104	NS	64	105
PERP	PERP, TTP53 apoptosis effector	Hs.520421	56	NS	105	119
UBC	Ubiquitin C	Hs.520348	86	NS	134	99
BLOC1S2	Biogenesis of lysosome-related organelles complex-1, subunit 2	Hs.576605	64	NS	169	90
ZFR	Zinc finger RNA binding protein	Hs.435231	40	NS	179	156
PPM1D	Protein phosphatase 1D magnesium-dependent, delta isoform	Hs.591184	48	NS	185	153
STX11	Syntaxin 11	Hs.118958	215	NS	72	150

NS: Not Significant (false discovery rate higher than 5%)

*The numbers indicate the ranking of genes based on fold change (1 being the most responsive gene at a particular dose and time-point); prepared by Dr Alan Mackay.

Table 12D. Most significantly down-regulated genes in irradiated whole blood

Symbol	Description	Unigene entry	2h 2Gy	2h 4Gy	24h 2Gy	24h 4Gy
BANK1	B-cell scaffold protein with ankyrin repeats 1	Hs.480400	NS	NS	1*	2
IGJ	Immunoglobulin J polypeptide	Hs.651109	NS	NS	2	4
IL2RB	Interleukin 2 receptor, beta	Hs.474787	NS	NS	3	3
EDG1	Endothelial differentiation, sphingolipid G-protein-coupled receptor, 1	Hs.154210	NS	NS	5	13
GLCCI1	Glucocorticoid induced transcript 1	Hs.131673	NS	NS	7	24
CD8A	CD8a molecule	Hs.85258	NS	NS	6	26
KLRF1	Killer cell lectin-like receptor subfamily F, member 1	Hs.183125	NS	NS	NS	1
TCL1A	T-cell leukemia/lymphoma 1A	Hs.2484	NS	1	NS	NS
GZMK	Granzyme K (granzyme 3; tryptase II)	Hs.277937	NS	NS	4	NS
SLC2A3	Solute carrier family 2, member 3	Hs.419240	NS	NS	NS	5
TRA@	T cell receptor alpha locus	Hs.74647	NS	NS	NS	6
IGHG1	Immunoglobulin heavy constant gamma 1 (G1m marker)	Hs.510635	NS	NS	NS	7
GFRA3	GDNF family receptor alpha 3	Hs.58042	NS	NS	NS	8
FGFBP2	Fibroblast growth factor binding protein 2	Hs.98785	NS	NS	NS	9
FOXRED1	FAD-dependent oxidoreductase domain containing 1	Hs.317190	NS	NS	NS	10
INSIG1	Insulin induced gene 1	Hs.520819	NS	NS	NS	11
SH3BP5	SH3-domain binding protein 5 (BTK-associated)	Hs.654642	NS	NS	NS	12
PBEF1	Pre-B-cell colony enhancing factor 1	Hs.489615	NS	NS	NS	14
ZNF182	Zinc finger protein 182	Hs.189690	NS	NS	NS	15
FOLH1	Folate hydrolase (prostate-specific membrane antigen) 1	Hs.654487	NS	NS	NS	16

NS: Not Significant (false discovery rate higher than 5%)

*The numbers indicate the ranking of genes based on fold change (1 being the most responsive gene at a particular dose and time-point); prepared by Dr Alan Mackay.

unlike the blood leukocytes, are actively cycling and dividing, and seven out of the twenty highest ranked down-regulated genes in T-lymphocytes after IR exposure have cell division associated functions (e.g. *BUB1, CCNA1, KIF23, NCAPG, PRC1, CENPE, KIF14,* **Table 12B**).

Among the IR-responsive genes identified by the microarray experiment, there are some in which the response is specific to blood leukocytes (e.g. *PCNA*, **Table 12C**) or T-lymphocytes (e.g *ATF3*, *PRC1* **Table 12A** and **B**), however ten genes are consistently up-regulated in at least one dose or time-point in blood and lymphocytes, in all donors and in three independent experiments: *GADD45A, CDKN1A, SESN1, CCNG1, FAS, FBXW2, RBM15, PPM1D, RPS27L* and *BLOC1S2* (**Table 12A** and **C**) suggesting that these genes play a role in general, cellular response to IR exposure. The highlighted genes play a role in cell cycle progression (*GADD45A, CDKN1A, CCNG1, PPM1D, RPS27L*), apoptosis (*FAS*), oxidative stress response (*SESN1*), proteolysis (*FBXW2*), proliferation (*BLOC1S2*) and regulation of haematopoiesis (*RBM15*).

There are genes which seem to be particularly good IR exposure biomarkers in stimulated T-lymphocytes (*ATF3*) or in blood (*PCNA*). *ATF3* is a stress response gene and a direct target of TP53, it plays a role in proliferation, oncogenesis, DNA damage response and apoptosis (Taketani et al., 2012). *PCNA* is involved in DNA replication, repair, chromosome segregation chromatin structure maintenance and cell cycle progression (Stoimenov and Helleday, 2009). Crucially for biological dosimetry purposes, both genes are significantly up-regulated in all donors at all doses and time-points (**Figure 24**).

3.2.3. Validation of IR-responsive genes identified by microarray by qPCR

We performed qPCR experiments on the same samples to validate microarray results for four genes (*GADD45A, CDKN1A, PRC1* and *SESN1*). All four genes were confirmed to be IR-responsive and displayed similar alteration in expression pattern following IR exposure when tested by both techniques (**Figure 25**). However, it should be mentioned that several promising genes identified in other studies like *BBC3*, *MDM2*, *DDB2* or *CCNB1* were not identified by the present microarray experiment. Nonetheless, we confirmed by qPCR that *BBC3* and *MDM2* genes were significantly up-regulated in blood and T-lymphocytes, for all donors used in this study and at all doses and time-points (**Figure 26A** and **B** respectively). Moreover, *BBC3* gene showed dose-dependent up-regulation in T-lymphocytes assessed 2 h post exposure. The probe for another candidate gene, *FDXR,* which was previously identified as radiation responsive (Paul and Amundson, 2008), was not present on the array and therefore could not be detected. The qPCR analysis revealed that this gene was highly up-regulated in a dose-dependent manner in blood at 24 h post exposure (**Figure 26C**), making it particularly promising for biodosimetry purposes.

Independently, we were also interested in the individual response to IR exposure. In order to investigate the significance of the differences in transcriptional response between the three donors we performed statistical analysis using the General Linear Model (GLM) as described in **chapter 2.11**. GLM analysis of variance allows estimation of the relative statistical significance of each parameter (in this case: sample type, donor, repeat, dose or time), taking into account the errors associated with them.

A. *GADD45A*

Cultured lymphocytes

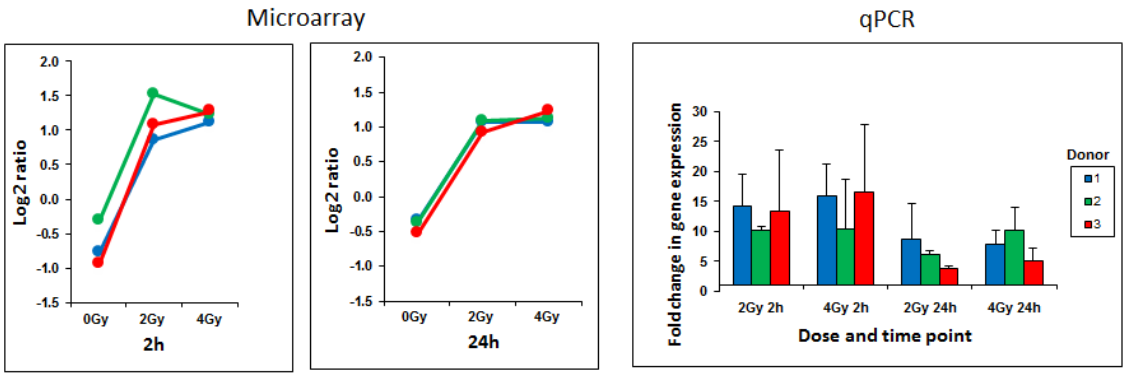

Blood

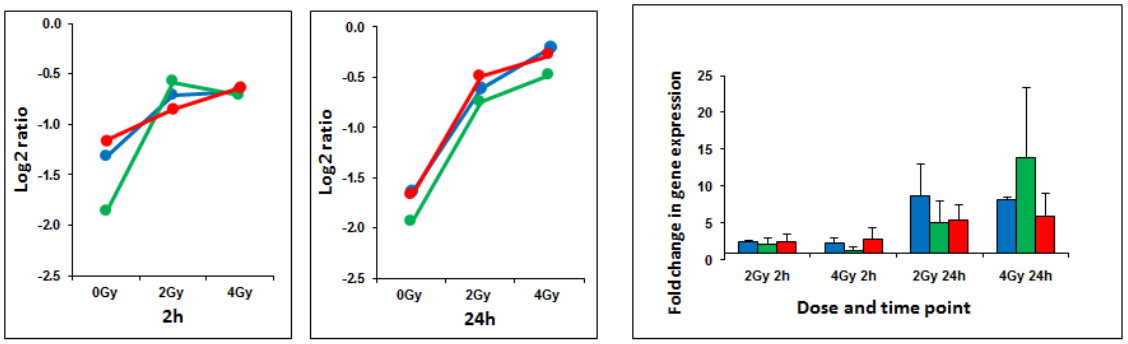

B. *CDKN1A*

Cultured lymphocytes

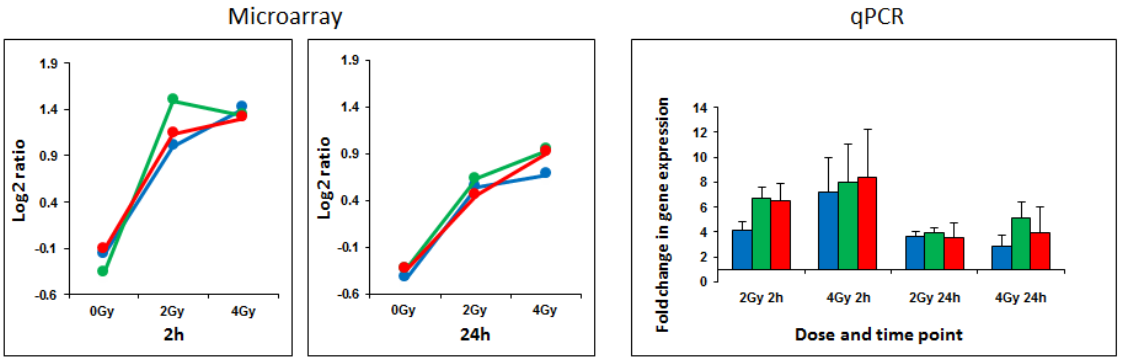

Blood

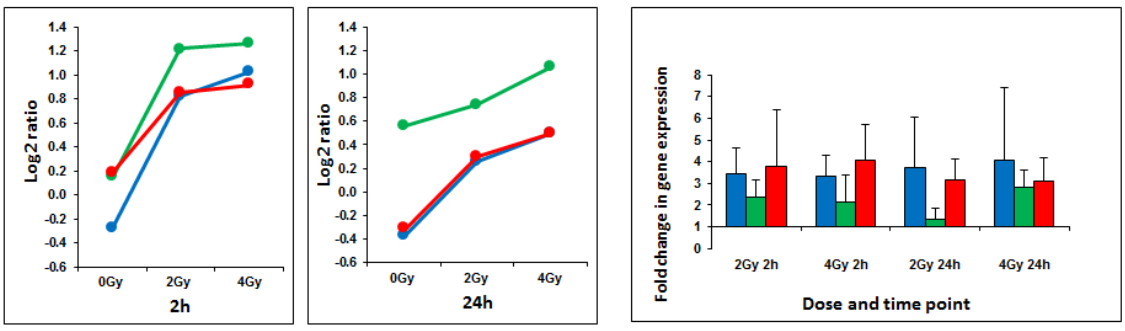

C. *PRC1*

Cultured lymphocytes

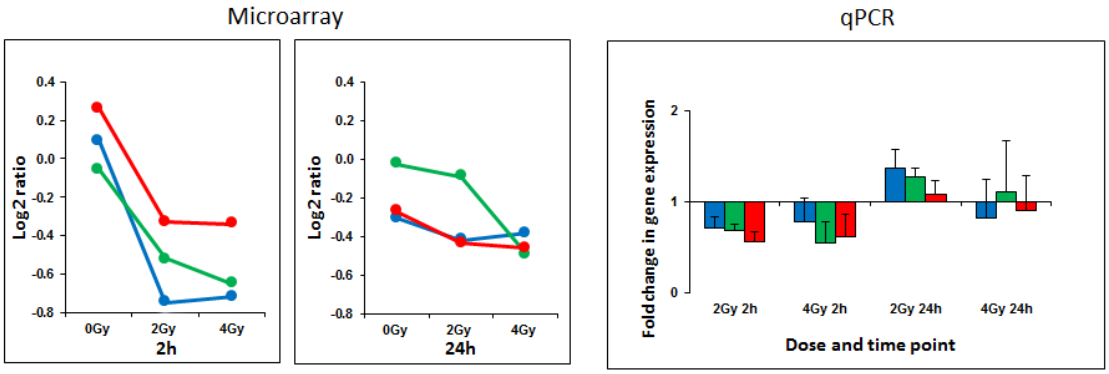

Blood

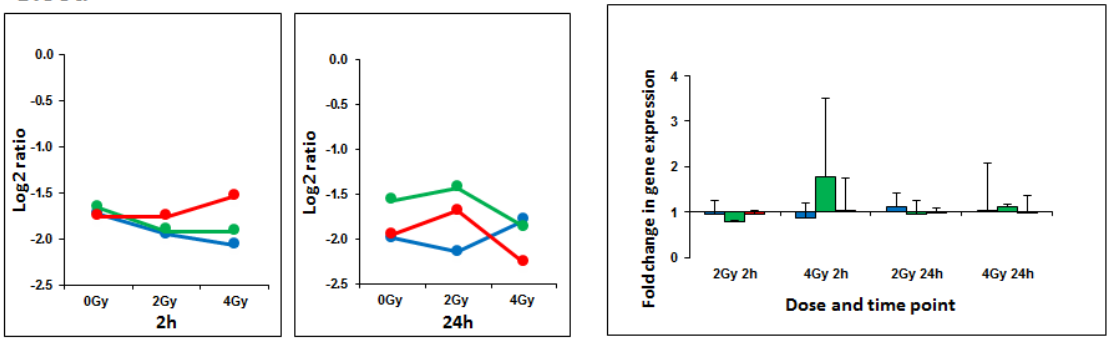

D. *SESN1*

Cultured lymphocytes

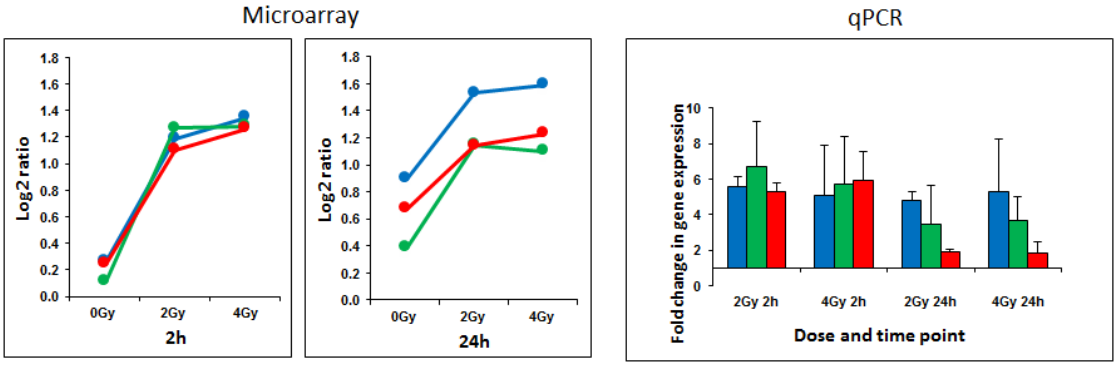

Blood

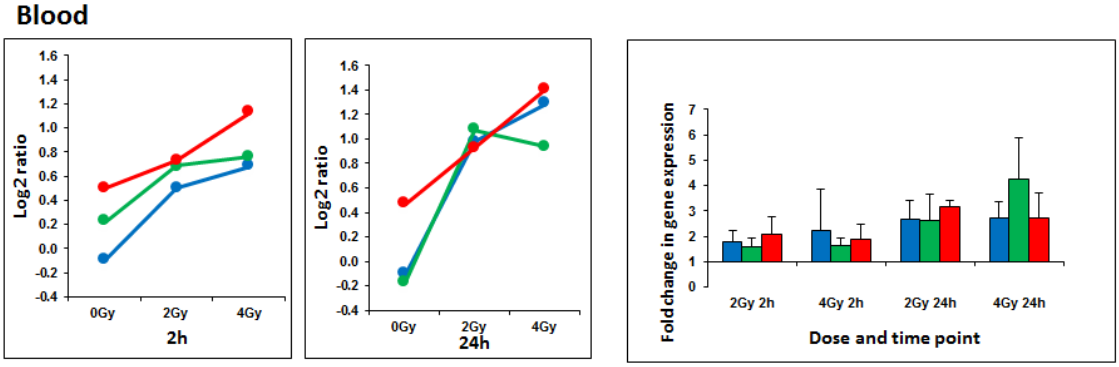

Figure 25. Validation of microarray data by qPCR for four selected genes.

Comparison of microarray (left panel) and qPCR (right panel) gene expression data in T-lymphocytes (top panel) and blood (bottom panel) for four genes: *GADD45A* (**A**), *CDKN1A* (**B**), *PRC1* (**C**) and *SESN1* (**D**) and three donors (1, 2 and 3). For microarray log2 ratios of each gene are plotted for each donor after 2 h and 24 h in response to either 2 Gy or 4 Gy of X-ray. Data are presented for one of the three replicate experiments. For qPCR the fold change relative to non-irradiated control and normalised to the *HPRT1* reference gene are presented. The mean of three independent experiments with triplicate reactions is presented. Data for donor 1 are presented in blue, in green for donor 2 and in red for donor 3. Error bars indicate the standard error of the mean for three independent experiments.

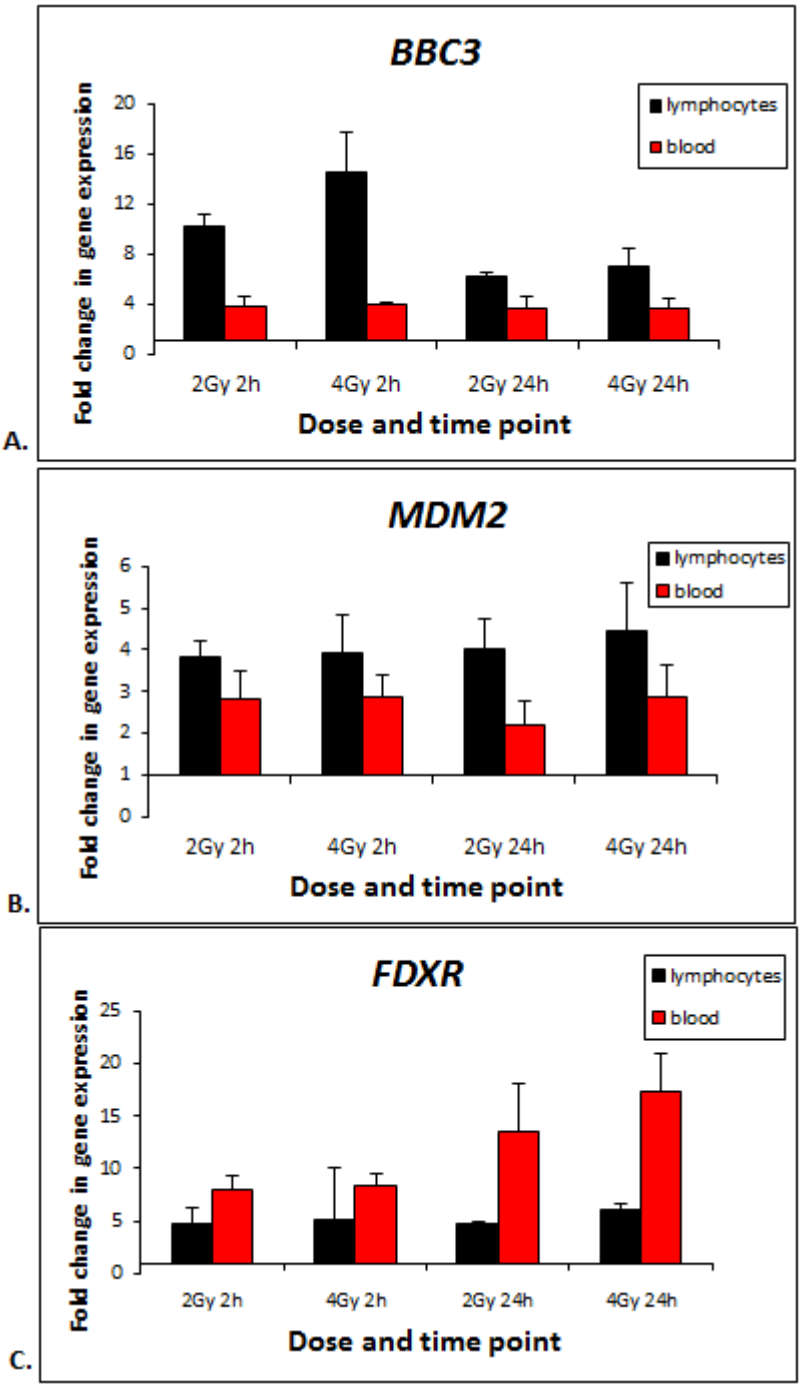

Figure 26. Up-regulation in stimulated lymphocytes and blood of three genes *BBC3* (A), *MDM2* (B) and *FDXR* (C) not identified by microarray.

Fold changes in expression assessed by qPCR compared to non-irradiated controls and normalised to the *HPRT1* reference gene of each gene are plotted for each donor after 2 h and 24 h in response to either 2 Gy or 4 Gy irradiations. The mean of three independent experiments with triplicate reactions are presented, error bars represent the standard error of the mean for three independent experiments

Gene expression data are not normally distributed (Bengtsson et al., 2005), (**Figure 27A**), therefore in order to obtain normally distributed data to perform GLM analysis we log-transformed the fold change values (**Figure 27B**). We used the log-transformed fold change values for nine genes the expression of which was measured by qPCR (*PLK3, PRC1, CDKN1A, GADD45A, SESN1, ATF3, PUMA, FDXR* and *MDM2*) for GLM analysis. The p-values associated with every parameter are presented in **Table 13**. The gene expression pattern was significantly different in blood and T-lymphocytes for all genes except for *PRC1* ($p<0.001$). The transcriptional response of five genes (*PCR1, CDKN1A, ATF3, BBC3* and *FDXR*) measured 2 h post irradiation was significantly different than when measured 24 h post exposure suggesting time-dependant expression changes after IR exposure. There were significant differences in *CDKN1A* expression between three independent experiments ($p=0.031$). Interestingly, only one gene – *FDXR* showed significant differences in expression post IR exposure between three donors ($p=0.007$) which might be due to genetic influence. We also observed a trend of donor dependence in gene expression response to IR – i.e. when a donor displayed the highest transcriptional response to IR in T-lymphocytes it usually also showed the highest response in blood (**Figure 28**), again suggesting the influence of genetic factors.

3.2.4. Discussion

RNA microarray experiments are very useful for identification of responsive transcripts and have been successfully used for the discovery of radiation exposure biomarkers (Amundson SA, 2004, Gruel et al., 2008, Meadows et al., 2008, Paul et al., 2011). Here, we used microarray profiling to identify genes, the expression of which is modified by IR in human blood leukocytes and stimulated T-lymphocytes. We found a

A.

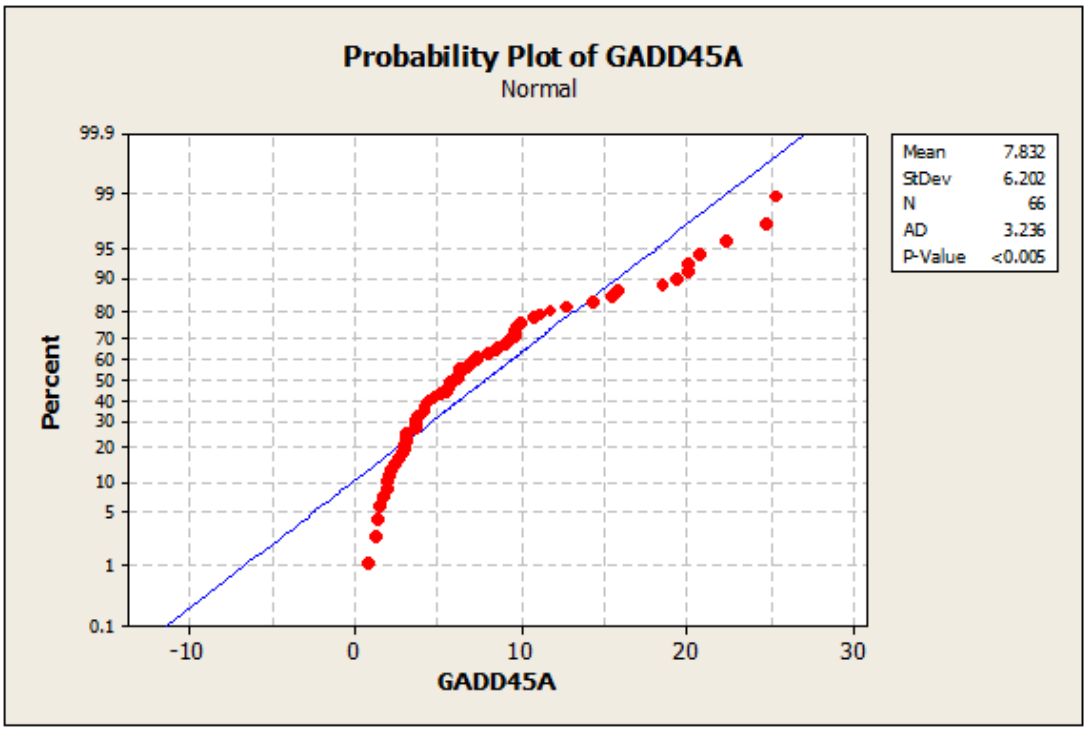

B.

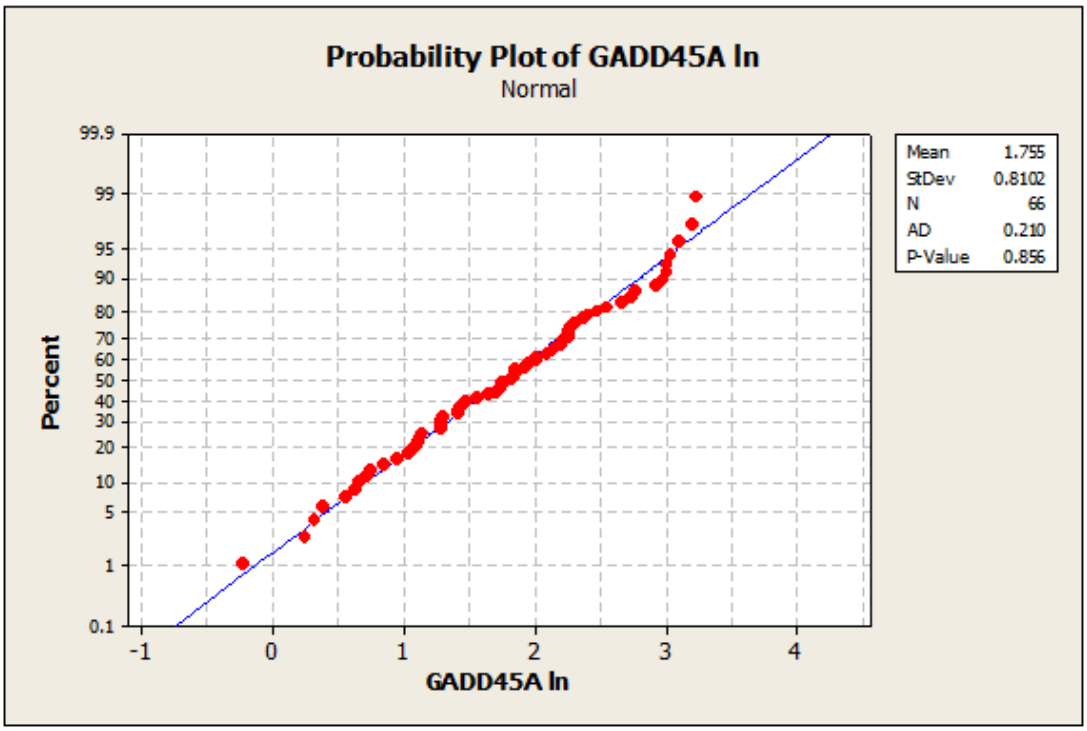

Figure 27. Normal probability plot for *GADD45A* gene.

Normal probability plot was created in Minitab, the software also performs Anderson-Darling normality test and provides associated p-value. **A.** Fold changes for *GADD45A* gene obtained in qPCR analysis were used, data shows significant deviation from normal distribution ($p<0.005$). **B.** Log-transformed fold change values for the same gene show normal distribution ($p=0.856$)

Table 13. p-values associated with GLM

	PLK3	***PRC1***	***CDKN1A***	***GADD45A***	***SESN1***	***ATF3***	***BBC3***	***FDXR***	***MDM2***
Sample type (blood, T-lymphocytes)	**<0.001**	0.157	**<0.001**	**<0.001**	**<0.001**	**<0.001**	**<0.001**	**<0.001**	**<0.001**
Experiment (1, 2, 3)	0.159	0.260	**0.031**	0.464	0.649	0.168	0.954	0.618	0.902
Donor (1, 2, 3)	0.399	0.691	0.407	0.362	0.347	0.470	0.113	**0.007**	0.265
Dose (2 Gy, 4 Gy)	0.499	0.303	0.456	0.476	0.983	0.069	0.170	0.101	0.445
Time (2 h, 24 h)	0.200	**0.024**	**0.003**	0.153	0.630	**<0.001**	**<0.001**	**0.001**	0.711

Significant differences are shown in bold

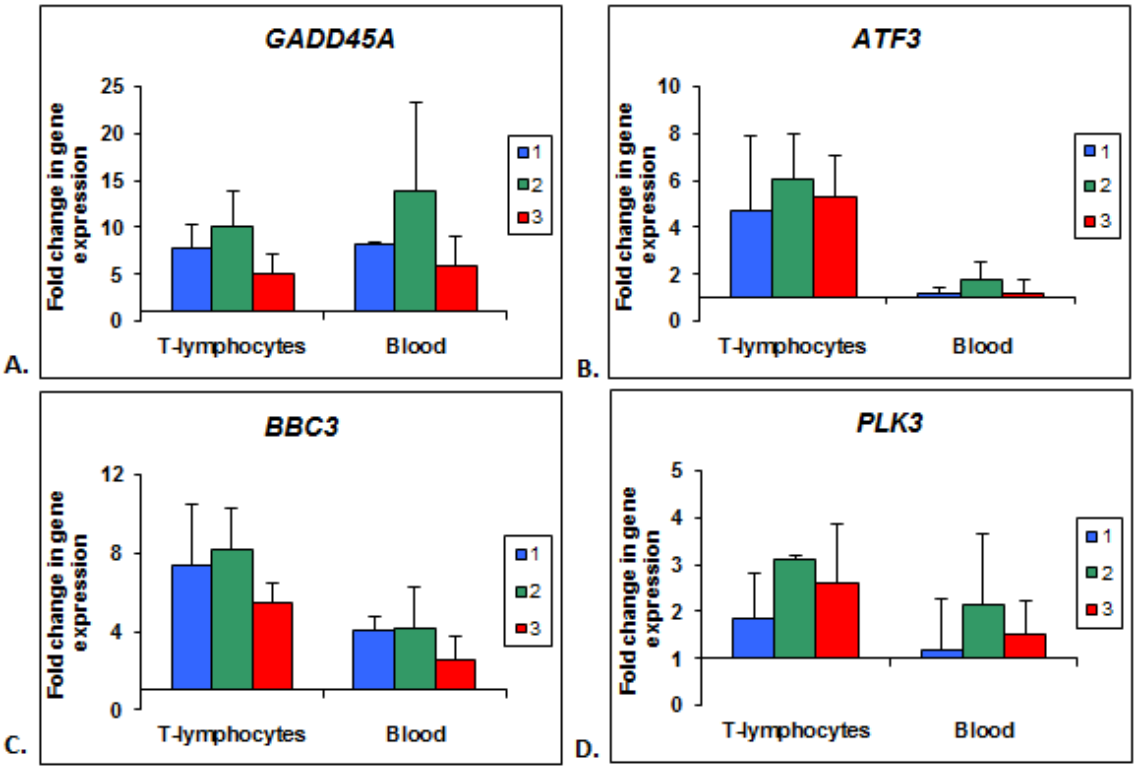

Figure 28. Individual transcriptional responses to radiation exposure.

Gene expression changes 24 h after 4 Gy of X-ray in three donors for four radiation responsive genes: *GADD45A* (**A**), *ATF3* (**B**), *BBC3* (**C**) and *PLK3* (**D**) were measured by qPCR; error bars indicate standard error of the mean for three independent experiments.

number of transcripts which expression was either up- or down-regulated in response to IR exposure *in vitro*. While some of the identified genes were specific to blood (*PCNA*) or T-lymphocytes (*ATF3*) (**Table 12**), ten genes (*GADD45A, CDKN1A, SESN1, CCNG1, FAS, FBXW2, RBM15, PPM1D, RPS27L* and *BLOC1S2*) were consistently up-regulated by at least one dose in blood and lymphocytes and in all donors, indicating that these genes may play a role in general response to IR (**Figure 24**).

Interestingly, several promising candidates identified by others, like *BBC3*, *DDB2*, *MDM2* or *CCNB1* were not detected by the microarray experiment, either because no significant difference was found or because they were not represented on the array (e.g. *FDXR*). Three such transcripts (*BBC3, MDM2* and *FDXR*) were confirmed by qPCR assays to be highly responsive to IR (**Figure 26**). Microarrays are a powerful technique to provide an overview of expression of thousands of transcripts at the same time, however, at least in our hands, it lacks the sensitivity of qPCR. Moreover, microarray results have been reported to be affected by the statistical methods used for analysis (Albanese et al., 2007); this would therefore influence the level of significance for the gene expression changes characterised as radiation responsive.

This is, to our knowledge, the first time that a comparison of the transcriptional response to IR in cell subpopulations obtained from the same donor has been made using resting blood leukocytes and stimulated cycling T-lymphocytes. Blood leukocytes are composed of different cell types such as lymphocytes, monocytes and neutrophils each of which have specific gene expression patterns and differ in response to IR exposure (Mori et al., 2005, Gruel et al., 2008). Undoubtedly, some of the genes differentially expressed between blood and lymphocytes can be attributed to the cell type specific response to IR; however, a large proportion of the twenty most down-

regulated genes in cycling T-lymphocytes are associated with cell division (*BUB1, CCNA1, KIF23, NCAPG, PRC1, CENPE, KIF14,* **Table 12B**) which is the main reason for the differences in the responsive genes observed between both cell populations. These genes are poor candidates for biodosimetry purposes as they are not responsive in blood; however, the down-regulation of these genes by IR exposure is still very interesting and can have important consequences. For example, Carter *et al* have reported gene expression profile signatures of chromosomal instability which predicts clinical outcome in multiple human cancers (Carter et al., 2006) and remarkably, eleven out of the 25 genes from their classifier are significantly down-regulated after IR-exposure in our stimulated T-lymphocyte samples. The modification of expression of these genes can therefore provide information which could not be obtained using blood as source of material.

Also, it is worth noting, that gene expression can also be useful for identification of individuals sensitive to IR or those predisposed to severe normal tissue reactions after radiotherapy. For example, we have reported that in breast cancer radiotherapy patients expression of *CDKN1A* in stimulated T-lymphocytes after IR exposure was significantly lower in patients with severe acute skin reactions than in patients with minimal skin reaction (Badie C, 2008). We have also shown that an individual with AT disorder, characterised by extreme sensitivity to IR exposure, has significantly lower post irradiation induction of direct TP53 target genes like *BBC3* (Kabacik et al., 2011b).

A good candidate gene for biodosimetry purposes should show relatively little intra- and inter-individual variation. We adopted GLM analysis to investigate this issue. The sample type (blood leucocytes or stimulated T-lymphocytes) most significantly

influenced gene expression results as eight out of nine investigated genes showed p-values of less than 0.001 (**Table 13**). Five genes (*PRC1, CDKN1A, ATF3, BBC3* and *FDXR*) showed significantly different transcriptional responses to IR exposure when assessed at the early time-point (2 h post irradiation) than when assessed at 24 h post exposure indicating that some genes may be better for dose assessment at early time-points whereas others may be more suitable for later dosimetry, what is in agreement with previous reports (Manning et al., 2013, Paul et al., 2013). We did not observe any significant differences between the two doses of radiation used which is surprising, however this can be at least partially explained by the shape of dose response curve in blood irradiated *ex-vivo*. We have shown previously that for the majority of the investigated genes, the dose-response in blood collected 24 h post exposure was best fitted by the quadratic function and reached a plateau around 2 Gy, making distinguishing between higher doses very difficult (Manning et al., 2013).

Only the *CDKN1A* gene showed significant differences in expression in three independent experiments suggesting high intra-individual variability, that suggest that *CDKN1A* transcriptional response to IR exposure may be influenced by other factors and makes it a poor candidate for biological dosimetry purposes. In contrast, the *FDXR* gene, showed significant differences in expression between three donors indicating high inter-individual variation, although taking into account the small number of individuals a bigger experiment is needed to confirm this finding. Overall, we have shown that gene expression responses to IR can be a valuable source of information for many aspects of radiation biology including individual radiosensitivity and biological dosimetry.

3.3. Investigation of transcriptome response to IR exposure

3.3.1. Introduction

There have been many attempts to use gene expression endpoints as biomarkers of IR exposure (Amundson SA, 2004, Gruel et al., 2006, Gruel et al., 2008, Templin et al., 2011a, Kabacik et al., 2011a, Manning et al., 2013) or sensitivity (Badie C, 2008, Kabacik et al., 2011b). Although gene expression assays offer significant advantages in terms of speed and throughput they have so far been less precise in dose estimation than classical cytogenetics assays (Badie et al., 2013, Rothkamm et al., 2013). In order to improve dose prediction accuracy it is essential to learn more about transcriptional changes occurring following radiation. The detailed temporal and dose response characteristics of candidate transcripts have to be known. As we have shown recently, for some genes, there is significant variability in the transcriptional response to IR within the healthy population (Manning et al., 2013). There are also individuals in the population who show abnormal radiosensitivity like Ataxia-Telangiectasia (AT) or Nijmegen breakage syndrome patients. AT is an autosomal, recessive disorder and while cases are very rare the estimated frequency of heterozygous carriers is around 0.5 % in the UK (Taylor and Byrd, 2005). It has been reported that AT heterozygous carriers have increased cancer risk and cellular experiments have revealed increased sensitivity to IR (Watts et al., 2002).

A growing body of evidence suggests that the majority of the mammalian genome is actively transcribed but only about 2% of the transcriptome encodes for proteins (Okazaki et al., 2002, Carninci et al., 2005, Djebali et al., 2012). The “dark matter” of the genome consists of non-coding RNAs. There are several groups of non-coding RNAs: well-known tRNAs and rRNAs, small nucleolar and nuclear RNAs implicated in various steps of RNA processing, miRNAs which are posttranscriptional

regulators of gene expression, piRNA involved in the epigenetic silencing of transposons in germ lines and finally a large group of long non-coding RNA (lncRNA) the function of which is just starting to be uncovered. Gene expression changes after exposure to IR are well documented (Kabacik et al., 2011a, Manning et al., 2013) and also numerous miRNAs the expression of which is altered following IR exposure have been reported (Templin et al., 2011a, Templin et al., 2012), (Sokolov et al., 2012). By contrast, there are only about two dozen lncRNAs for which it is reported that expression is modified after treatment with radiomimetic drugs. Examples of such responsive lncRNAs include *TP53TG1* (Takei et al., 1998), *Trp53cor1* (Huarte et al., 2010), *PANDAR* (Hung et al., 2011). So far only four IR-responsive lncRNAs have been reported: *lncRNA-CCND1* (Wang et al., 2008, Ozgur et al., 2013), *CDKN2B-AS1* (Ozgur et al., 2013), *GAS5* (Ozgur et al., 2013) and *SOX2-OT* (Chaudhry, 2013).

In this part of the project, we investigated temporal and dose-dependent changes in the expression of several radiation responsive protein coding genes identified in the previous chapter and by literature search. This was done in stimulated human T-lymphocytes derived from two healthy donors and one AT patient. We also studied the possibility of employing lncRNAs and miRNAs as biomarkers of IR exposure. The majority of the results presented in this chapter have been published (Kabacik et al., 2015).

3.3.2. Temporal transcriptome response to IR in human T-lymphocytes

The temporal, transcriptiome response to ionising radiation was assessed in stimulated T-lymphocytes obtained from two healthy donors (C1 and C2) and from one AT patient (AT). The cells were exposed to a sham dose or 2 Gy of X-ray and collected

at various time-points ranging from 15 min up to 24 h post exposure. From 13 assays designed for human protein coding genes (**Table 3**) we selected ten, which gave the greatest response to IR in the stimulated T-lymphocytes – *CDKN1A, SESN1, ATF3, MDM2, CCNB1, DDB2, FDXR, CCNG1, BBC3* and *GADD45A.* The results for mRNA expression are presented in **Figure 29**.

The majority of genes investigated responded rapidly with the peak of expression around 2-3 h post exposure (*CDKN1A, SESN1, ATF3, MDM2, BBC3* and *GADD45A*). Three genes: *DDB2*, *FDXR* and *CCNG1* responded with slower kinetics reaching the peak of expression between 5 and 24 h in the time range tested. Expression of *CCNB1* decreased rapidly following IR exposure but increased 24 h post irradiation. For all the genes studied here, AT lymphocytes showed a lower and delayed response to IR than healthy donors at the early time-points, however differences disappeared at the 24 h time-point.

We also investigated the lncRNA response to IR, however there was very limited literature published on lncRNA and IR; we therefore selected two lncRNAs the expression of which was reported to be altered by radiomimetic drugs treatment: T*P53TG1* (Takei et al., 1998) and *PANDAR* (Hung et al., 2011) as well as FAS antisense RNA 1 (*FAS-AS1*) which is transcribed in anti-sense orientation to FAS gene (Yan et al., 2005) - a well-known, IR-responsive transcript (Manning et al., 2013).

The lncRNA temporal response data is presented in **Figure 30**. While *PANDAR* showed no alteration of expression after IR exposure in the range of time points studied, *TP53TG1* demonstrated a radiation-responsive expression profile similar to *CCNG1* with a time dependant increase in expression, however, the up-regulation stayed relatively low (maximum of 1.5 times at 24 h). In contrast, *FAS-AS1* was

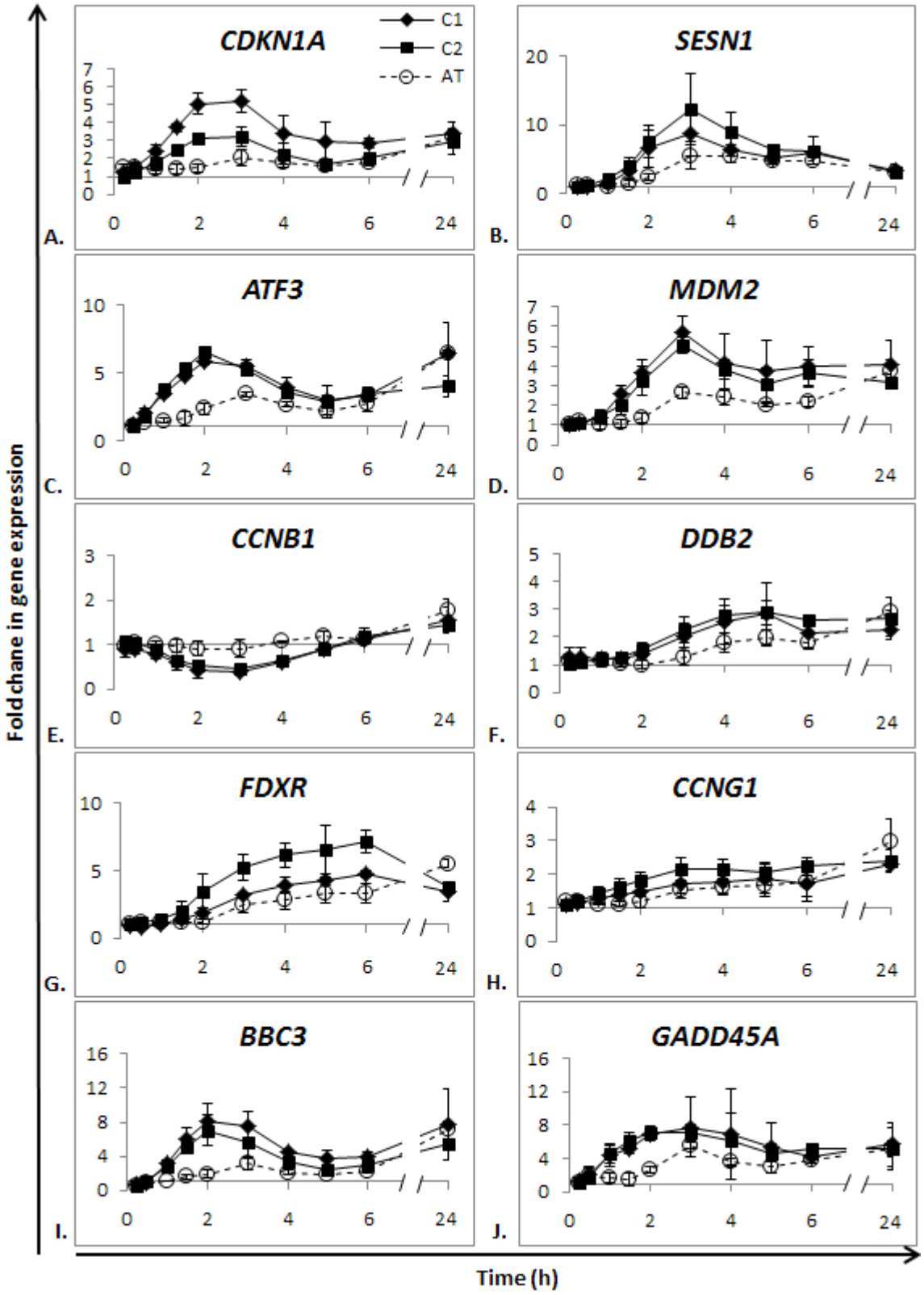

Figure 29. Temporal expression pattern of protein coding genes after exposure to IR

T-lymphocytes from two healthy donors (C1 – black diamonds and C2 – black squares) and one AT patient (AT – empty circles) were exposed to a sham dose or 2Gy of X-ray and collected at various time-points ranging from 15 min up to 24 h. The expression level of genes of interest *CDKN1A* (A), *SESN1* (B), *ATF3* (C), *MDM2* (D), *CCNB1* (E), *DDB2* (F), *FDXR* (G), *CCNG1* (H), *BBC3* (I) and *GADD45A* (J) was normalised to the *HPRT1* reference gene first, then the radiation-induced fold change in expression was calculated relative to non-irradiated control. Error bars represent ± one standard deviation from three independent experiments.

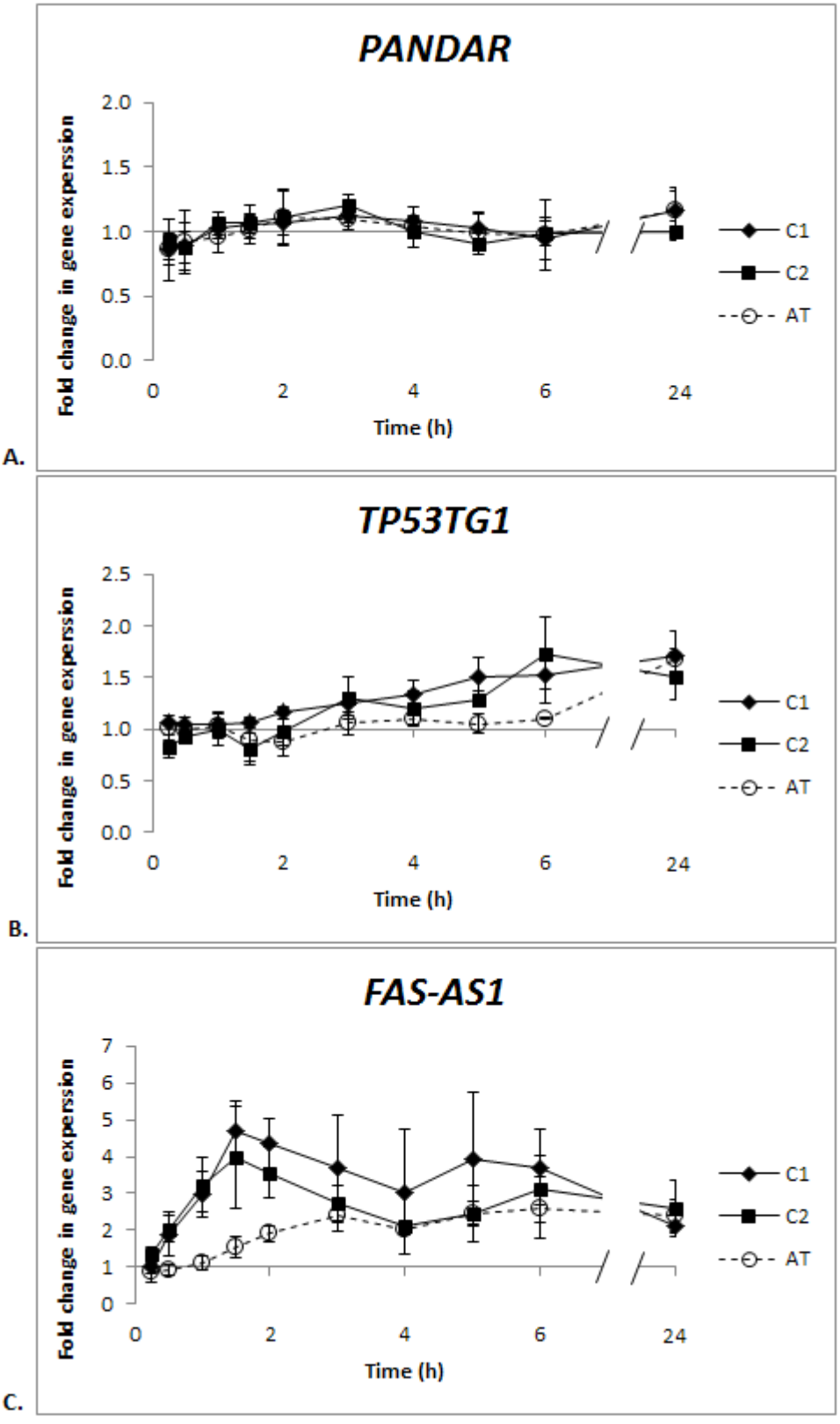

Figure 30. Temporal expression pattern of three lncRNAs after exposure to IR

T-lymphocytes from two healthy donors (C1 – black diamonds and C2 – black squares) and one AT patient (AT – empty circles) were exposed to a sham dose or 2Gy of X-ray and collected at various time-points ranging from 15 min up to 24 h. Expression levels of three lncRNAs: *PANDAR* (A), *TP53TG1* (B) and *FAS-AS1* (C) were normalised to the *HPRT1* reference gene first, then fold change was calculated relative to non-irradiated control. Error bars represent ± one standard deviation from three independent experiments.

up-regulated by up to 5 fold by IR and showed two peaks of expression: one early peak at 1.5 h and a later one around 6 h post exposure. Similarly to expression of protein coding genes, the *FAS-AS1* up-regulation in AT lymphocytes, was delayed compared to healthy controls, however the differences disappeared as early as 3 h following irradiation.

Next, we studied miRNA response to IR exposure. We investigated the expression of 19 miRNAs which had been highlighted in the literature as radiation responsive or were reported to be involved in the DDR network: *let-7a-5p, let-7b-5p, let-7g-5p, miR-15a-5p, miR-16-5p, miR-19b-3p, miR-21-5p, miR-27a-3p, miR-32-5p, miR-34a-5p, miR-106b-5p, miR-107, miR-125b-5p, miR-150-5p, miR-182-5p, miR-185-5p, miR-192-5p, miR-195-5p* and *miR-215-5p* (**Figure 31**). In our experimental setup, only *miR-34a-5p* and *miR-182-5p* showed a significant modification of expression after IR exposure (**Figure 32A** and **B** respectively). The up-regulation occurred at late time-points reaching a few fold at 24 h but no difference in response to IR between controls and AT lymphocytes could be detected. Interestingly, we noticed that the endogenous level of *let-7b-5p* in non-irradiated samples was very different for each donor (**Figure 33A**) with the AT lymphocytes showing the lowest *let-7b-5p* expression; differences between donors are highly significant as measured by two-tailed t-test (**Figure 33B**). *let-7b-5p* was the only miRNA in our panel which showed such differences in endogenous level.

3.3.3. Transcriptome dose-response to ionising radiation

The dose-response in three donors was investigated for three genes presenting different temporal profiles: *CDKN1A*, *FDXR* and *CCNB1*. The cells were exposed to a series of doses ranging from 0.1 Gy up to 5 Gy and collected 2 h and 24 h post

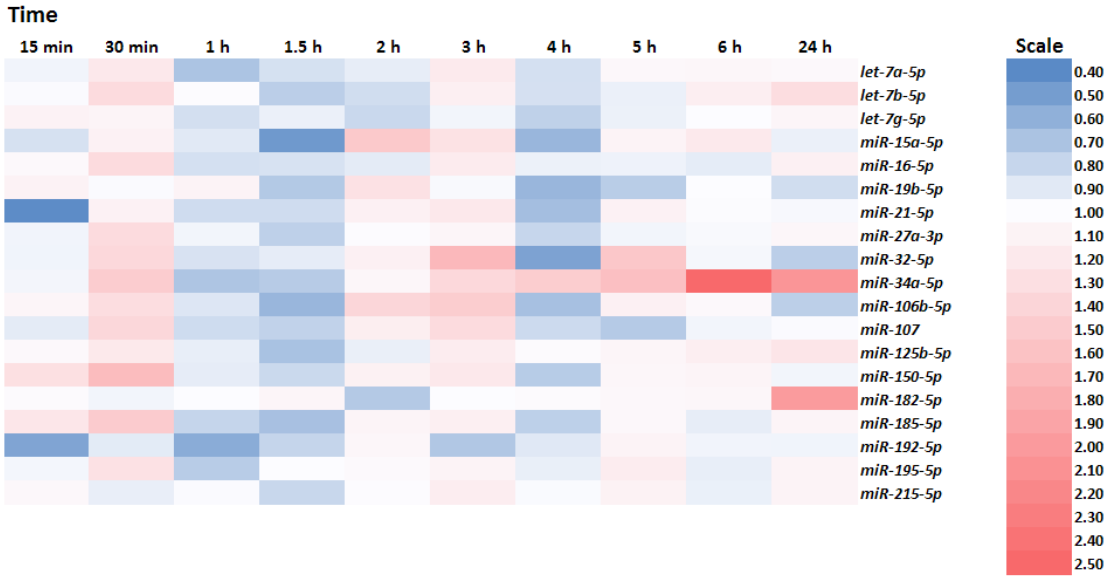

Figure 31. Temporal expression pattern of two miRNAs after exposure to IR in stimulated T-lymphocytes

Heatmap representing time course expression profiles from 19 miRNAs in averaged C1 and C2 samples after 2 Gy irradiation treatment *in vitro*: *let-7a-5p, let-7b-5p, let-7g-5p, miR-15a-5p, miR-16-5p, miR-19b-3p, miR-21-5p, miR-27a-3p, miR-32-5p, miR-34a-5p, miR-106b-5p, miR-107, miR-125b-5p, miR-150-5p, miR-182-5p, miR-185-5p, miR-192-5p, miR-195-5p* and *miR-215-5p*. Expression level of miRNAs was normalised to *SNORD44* and *SNORA73A* small RNA expression first, then fold change was calculated relative to non-irradiated control. The arbitrary scale is used to show up-regulated miRNAs (red) and down-regulated (blue) relative to untreated control.

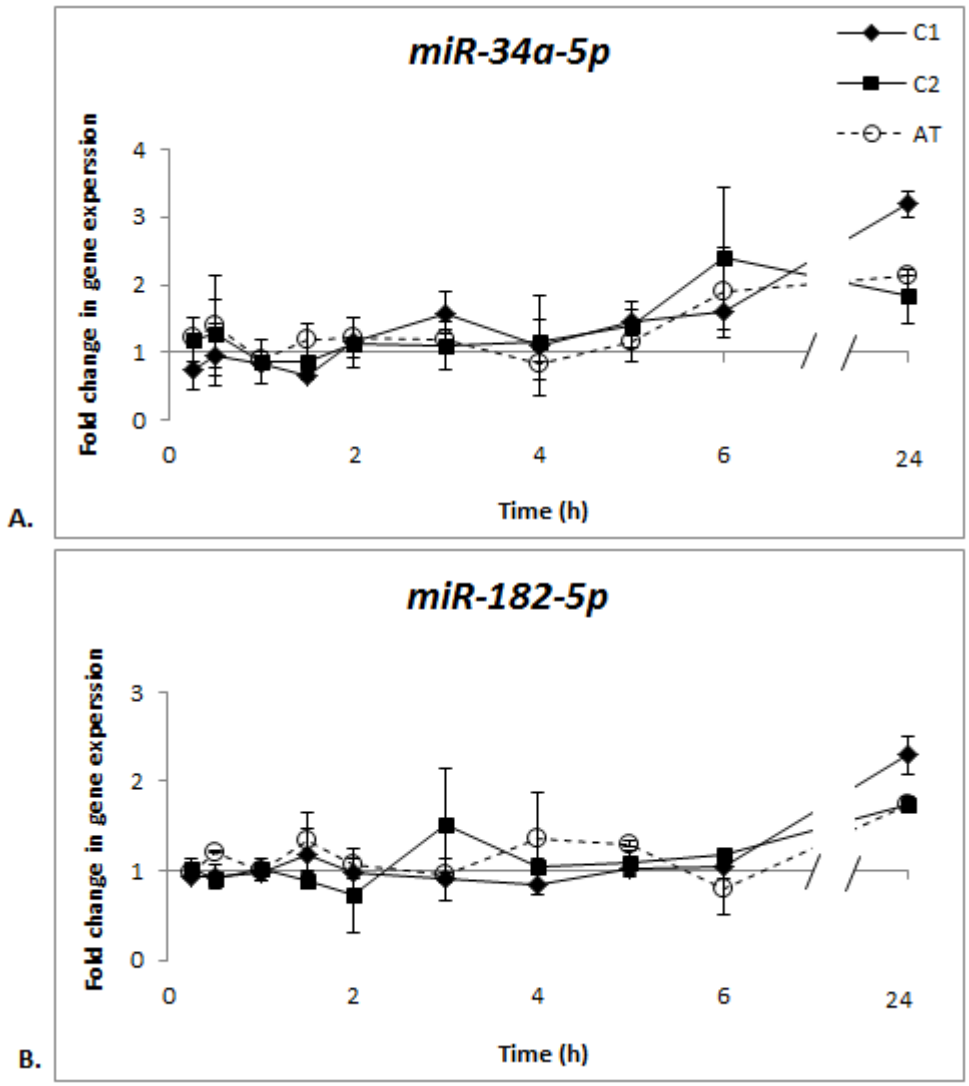

Figure 32. Temporal expression pattern of two IR-responsive miRNAs

Expression level of two miRNAs: *miR-34a-5p* (**A**) and *miR-182-5p* (**B**) was normalised to *SNORD44* and *SNORA73A* small RNA expression first, then the radiation-induced fold change in expression was calculated relative to non-irradiated control. Error bars represent ± one standard deviation from two independent experiments.

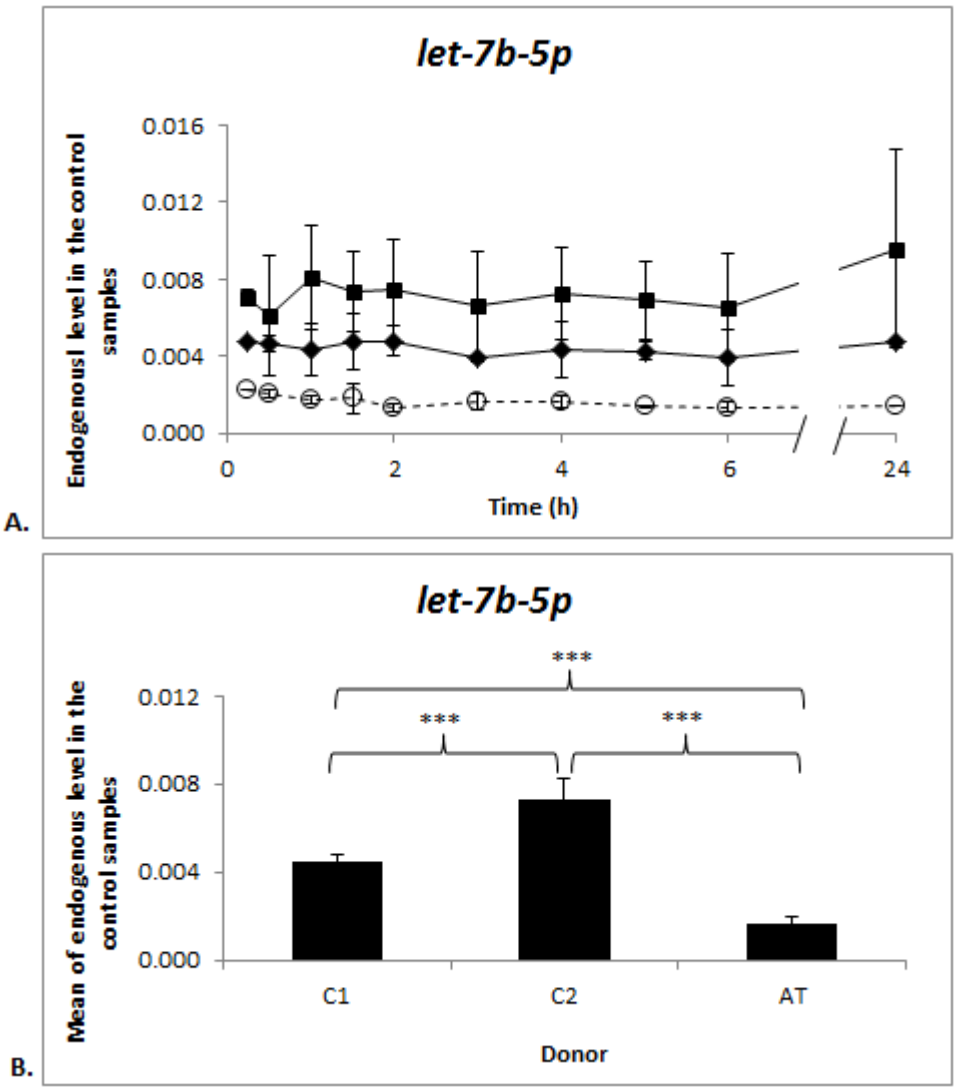

Figure 33. Endogenous level of *let-7b-5p* in the control samples.

A. Endogenous level of *let-7b-5p* in the non-irradiated samples normalised to *SNORD44* and *SNORA73A* small RNA expression; Error bars represent ± one standard deviation from two independent experiments. **B.** Mean of *let-7b-5p* expression level in the ten non-irradiated samples for three donors, error bars represent ± one standard deviation; three stars represent $p<0.001$ calculated by two-tailed t-test.

irradiation. The results of dose response experiment are presented in **Figure 34**. The shape of dose response curves was very different for samples collected at 2 h and 24 h. After 2 hours, the data points for C1 and C2 were best fitted by a logarithmic function with strong transcriptional response for low doses and up to 1 Gy then reaching a plateau phase at higher doses (2-5 Gy). The transcriptional response to IR was much weaker in AT than in C1 and C2 and interestingly, the data points for *CDKN1A* and *FDXR* were best fitted by the linear regression curve, not the logarithmic one as for C1 and C2. The dose response for *CCNB1* gene in the AT has similar shape as in controls, however, the magnification of the repression is much lower (**Figure 34E**).

The dose responses for *CDKN1A* and *FDXR* obtained for samples collected 24 h post irradiation was linear and AT could not be distinguished from C1 and C2 at this time-point (**Figure 34B** and **D** respectively). The data points for *CCNB1* gene better fit a quadratic function with a peak of up-regulation at approximately 3 Gy. Again, the AT patient responded in the same way as healthy donors at 24 h (**Figure 34F**).

We also investigated the dose response of two lncRNAs which showed modification of expression after IR exposure: *TP53TG1* and *FAS-AS1* (**Figure 35**). *TP53TG1* lncRNA, as expected from temporal response data, showed no response to IR at 2 h time-point (**Figure 35A**); on the contrary the dose dependent fold of change at 24 h time-point was linear and reached 3-fold after 5 Gy. Although expression in AT was slightly lower, no real differences between AT and controls could be seen (**Figure 35B**). The *FAS-AS1* transcript was radiation-responsive already at 2 hours post exposure and the data points for C1 and C2 were best fitted by power function whereas for AT it was obtained using the quadratic function. AT showed lower response than healthy donors which was especially evident at lower doses

A.

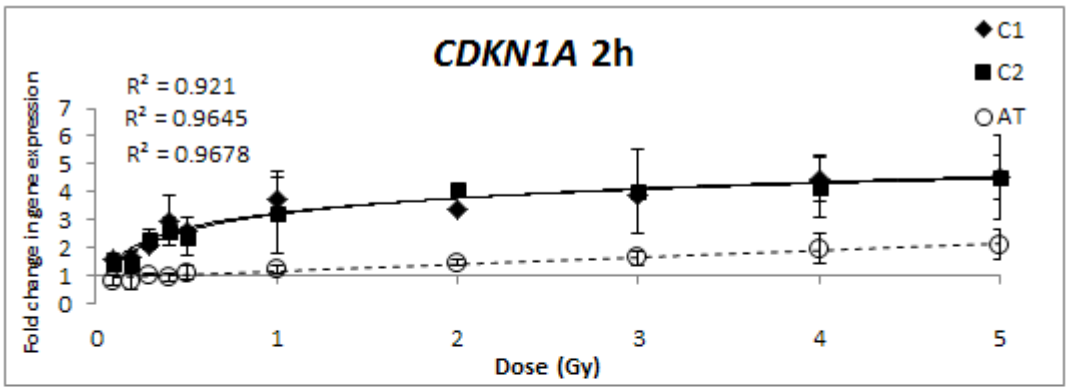
CDKN1A 2h
C1
C2
AT
R² = 0.921
R² = 0.9645
R² = 0.9678
Fold change in gene expression
Dose (Gy)

B.

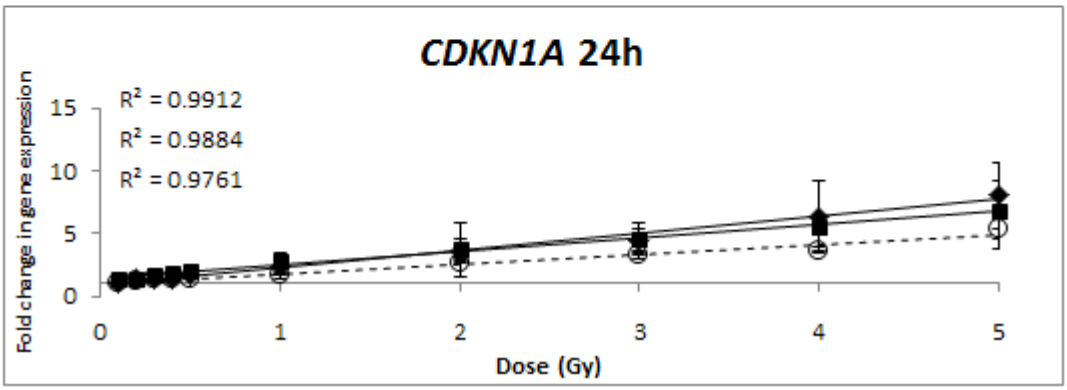
CDKN1A 24h
R² = 0.9912
R² = 0.9884
R² = 0.9761
Fold change in gene expression
Dose (Gy)

C.

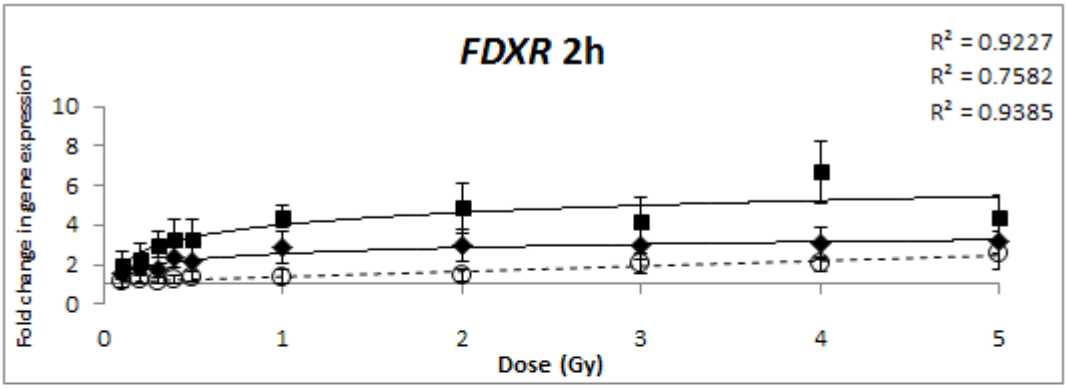
FDXR 2h
R² = 0.9227
R² = 0.7582
R² = 0.9385
Fold change in gene expression
Dose (Gy)

D.

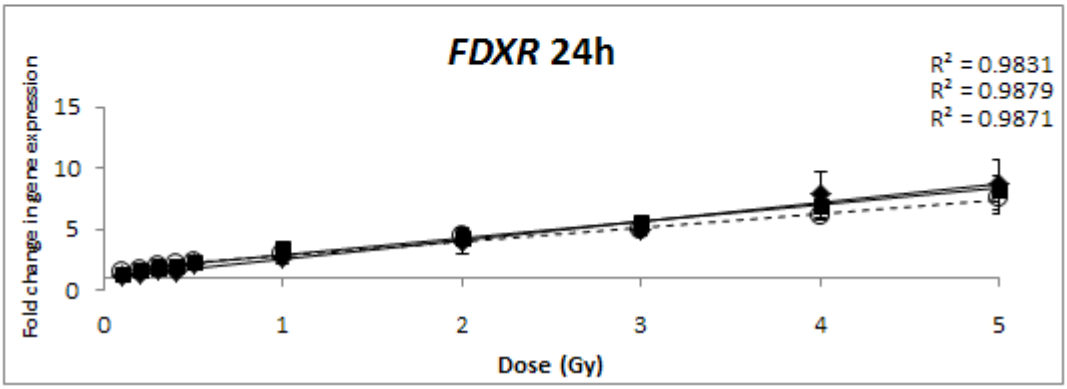
FDXR 24h
R² = 0.9831
R² = 0.9879
R² = 0.9871
Fold change in gene expression
Dose (Gy)

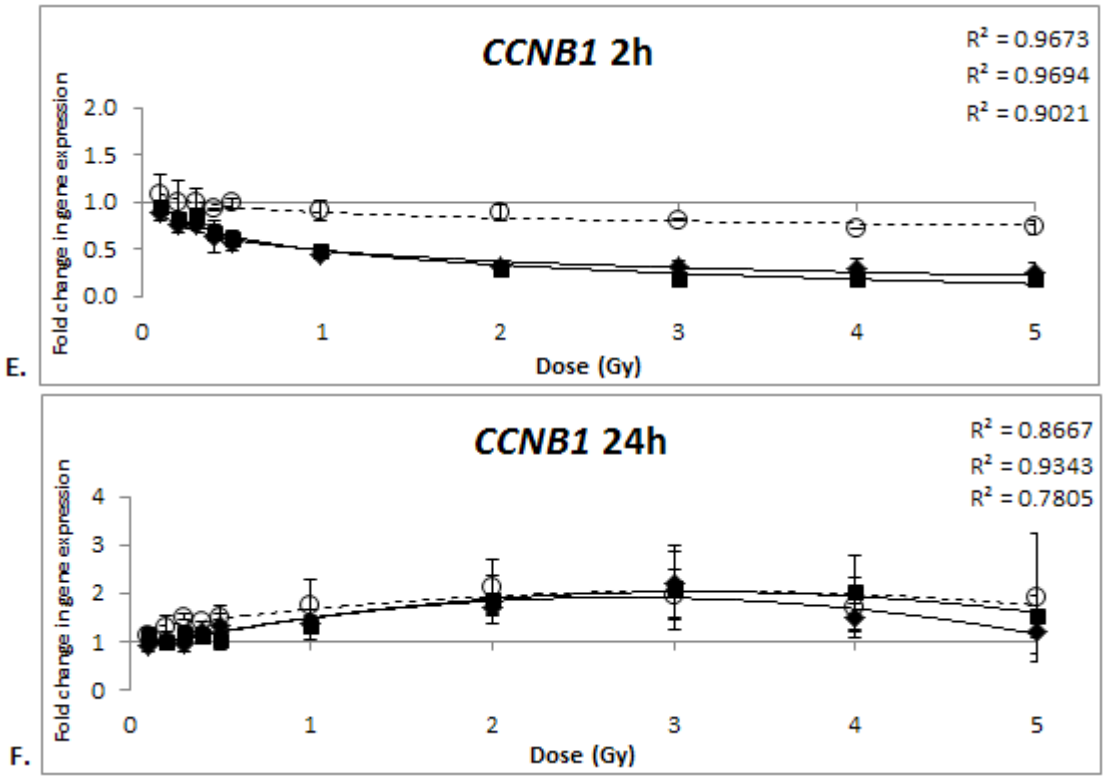

Figure 34. Dose response of three protein coding genes.

T-lymphocytes from two healthy donors (C1 – black diamonds and C2 – black squares) and one AT patient (AT – empty circles) were exposed to a series of X-ray doses ranging from 0.1 Gy up to 5 Gy. The expression levels of three genes *CDKN1A*, *FDXR*, *CCNB1* were analysed 2 h (**A**, **C** and **E** respectively) and 24 h (**B**, **D** and **F** respectively) post irradiation. Expression levels for three genes were normalised to the *HPRT1* reference gene first, then the radiation induced fold change in expression was calculated relative to non-irradiated control. R^2 values ale listed in the following order top –C1, middle – C2, bottom – AT. Error bars represent ± one standard deviation from two independent experiments.

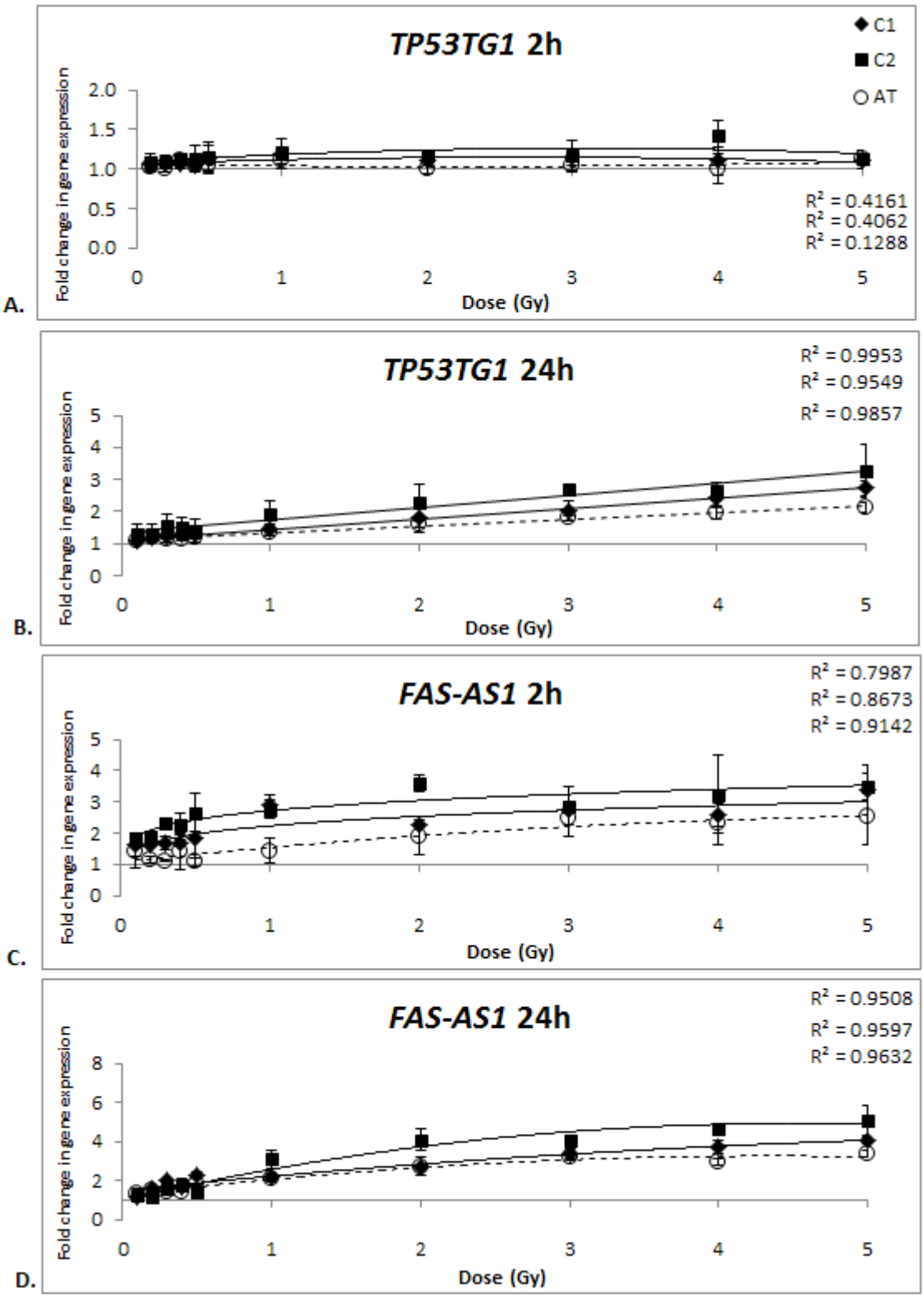

Figure 35. Dose responses of two lncRNAs

Expression level of two lncRNAs: *TP53TG1* and *FAS-AS1* after exposure to doses ranging from 0.1 to 5 Gy of X-ray were analysed 2 h (**A**, **C** respectively) and 24 h (**B**, **D** respectively) post irradiation. Copy numbers were normalised to the *HPRT1* reference gene first, then radiation-induced fold change in expression was calculated relative to non-irradiated control. R^2 values ale listed in the following order top –C1, middle – C2, bottom – AT. Error bars represent ± one standard deviation from two independent experiments.

(**Figure 35C**).At the 24 h time-point, similarly as for *CCNB1* gene, data-points for all donors seemed to fit the best quadratic function regression with the maximum of up-regulation for the highest dose tested (i.e. 5 Gy).

We then studied the dose responses for the two miRNAs which showed alteration in their expression following IR exposure: *miR-34a-5p* and *miR-182-5p;* however, as the up-regulation was minor after 2 Gy and observed only at a late time-point, with no differences between AT and controls, we limited the experiment to C1 and C2 at the 24 h post exposure (**Figure 36**). Five doses ranging from 1 up to 5 Gy were studied and results showed a dose-dependent up-regulation for both miRNAs with differences between C1 and C2 becoming apparent for the higher doses. This was already clear at 2 Gy for *miR-182-5p*. Interestingly, the higher up-regulation (approximately 3 fold for both miRNA) with C2 cells reached a plateau-phase around 5 Gy, while for C1, the up-regulation was at maximum around 3 Gy and then decreased in response to higher doses, hence showing clear differences in response between cells from different donors. Data were best fitted with the quadratic function linear regression

Additionally, we have investigated transcriptional response of ten protein coding genes and two lncRNAs to low doses of IR. T-lymphocytes from C1 were exposed to a series of doses ranging from 5 mGy up to 100 mGy and collected 2 h and 24 h post irradiation. From twelve transcripts tested, only 3 genes: *MDM2*, *CDKN1A* and *SESN1* showed linear response to IR exposure (**Figure 37**). Expression levels for samples collected 2 h post irradiation were higher than samples collected 24 h.

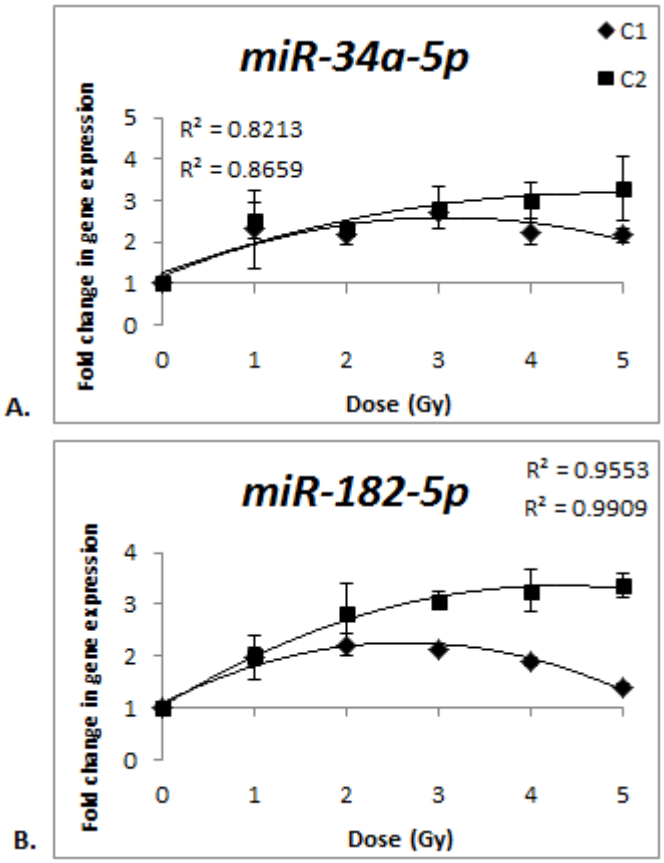

Figure 36. Dose response of two miRNAs

T-lymphocytes from two healthy donors (C1 – black diamonds and C2 – black squares) were exposed to five doses ranging from 1 Gy up to 5 Gy and collected 24 h post exposure. Expression levels of *miR-34a-5p* (**A**) and *miR-182-5p* (**B**) were normalised to *SNORD44* and *SNORA73A* small RNA expression first, then radiation-induced fold change in expression was calculated relative to non-irradiated control. R^2 values ale listed in the following order top – C1, bottom – C2. Error bars represent ± one standard deviation from two independent experiments.

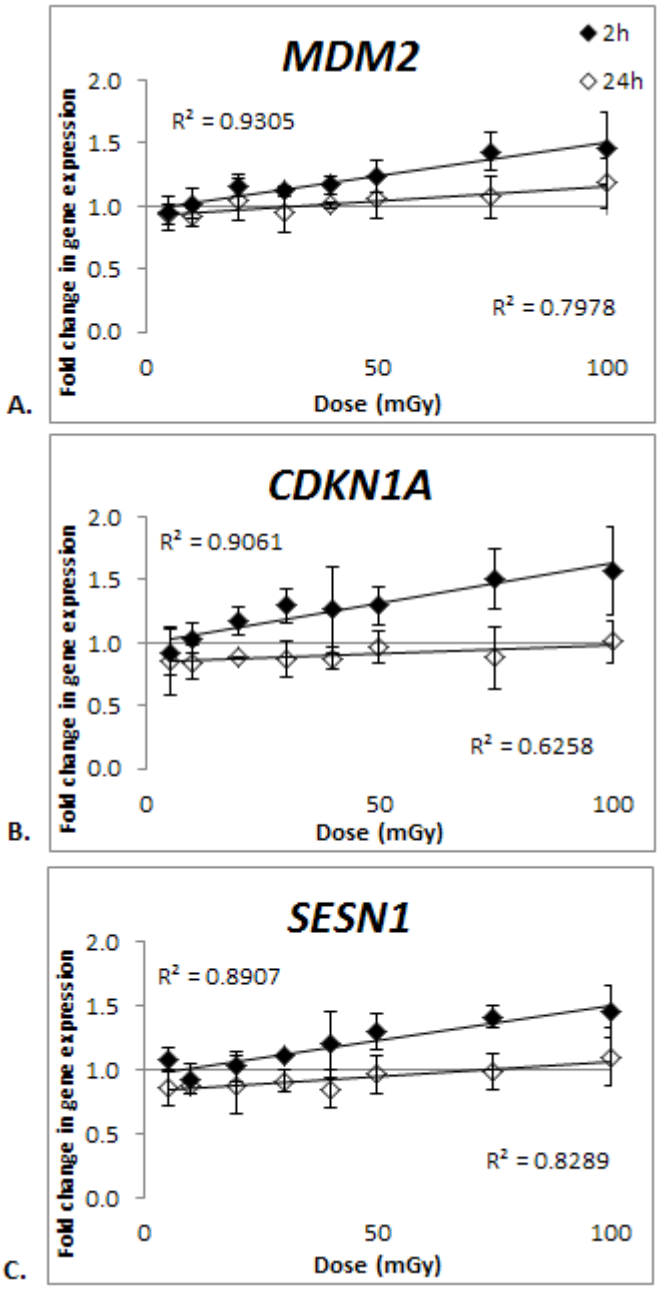

Figure 37. Low dose response of three protein coding genes.

T-lymphocytes from healthy donors C1 were exposed to a series of doses ranging from 5 mGy up to 100 mGy. Expression level of three genes *MDM2* (**A**), *CDKN1A* (**B**), and *SESN1* (**C**) was analysed 2 h (black diamonds) and 24 h (empty diamonds) post irradiation. Expression level for three genes was normalised to *HPRT1* reference gene first, then radiation-induced fold change in expression was calculated relative to non-irradiated control. R^2 values obtained from linear regression fits are listed in the following order top – 2 h, bottom – 24 h. Error bars represent ± one standard deviation from four independent experiments.

3.3.4. Discussion

Gene expression signatures have proved to be useful for estimating the dose of radiation *in vitro* (Badie et al., 2013) and *in vivo* (Paul et al., 2011). Despite the fact that gene expression dose estimation is still less accurate and precise than the "gold standard" dicentric assay, it holds great potential due to the speed and high capacity(Rothkamm et al., 2013). Better understanding the transcriptional response to IR is essential in order to identify specific and sensitive transcriptional biomarkers of IR exposure and improve the accuracy of gene expression based biodosimetry. Here, we investigated transcriptional temporal and dose-response of stimulated T-lymphocytes from two healthy donors and one A-T patient in order to better understand how cells respond to IR insult.

We have decided to use stimulated T-lymphocytes because obtaining blood samples, particularly from AT patients was impossible for us as the disease is very rare. By using stimulated T-lymphocytes we were able to culture the cells to obtain sufficient material for all our experiments. Due to the large number of cells from the same donors required for dose-responses as well as time course experiments, we believe the use of stimulated lymphocytes was the only realistic choice.

Moreover, in the previous chapter we have shown that, although there are differences between blood and simulated T-lymphocytes obtained from the same individual in terms of genes, the expression of which is modified in response to radiation, they mostly relate to cell cycle such as cyclins A and B, PRC1, BUB1, CDC25C, MAD2L1 or CENPE. On the contrary most genes up-regulated following IR exposure (e.g. SESN1, GADD45A, CCNG1, RBM15, CDKN1A, FAS, PPM1D, BLOC1S2) were up-regulated in all donors in both blood and T-lymphocytes indicating that those genes

represent universal response to IR (Kabacik et al., 2011a). Our previous results suggest that stimulated human T-lymphocytes can be used as a model for studying IR responsive genes for biodosimetry purposes.

In order to study the temporal response to IR, human T-lymphocytes were collected at various time-points ranging from 15 min to 24 h post exposure. The majority of protein coding genes responded to IR very rapidly, with detectable modulation of expression as early as 30 min post exposure for *GADD45A, CDKN1A* and *ATF3* genes (**Figure 29**). The rapidly responding genes play a role in cell cycle progression (*CDKN1A*, *CCNB1*, *CCNG1*, *GADD45A*, *SESN1*), apoptosis (*PUMA*, *FDXR*, *GADD45A*, *CDKN1A*), oxidative stress response (*SESN1*, *FDXR*) and TP53 stabilisation (*ATF3*, *MDM2*, *CCNG1*). It is not surprising that these genes are early responders, as many participate in processes essential for maintaining genome stability after DNA damage.

Recently, Melanson *et al* have reported that an overwhelming majority of transcripts involved in DDR and regulated by TP53 including *CDKN1A*, *SESN1*, *ATF3* and *MDM2* are unstable with a half-life shorter than 2h, and that their short half-life is due to presence of destabilising sequences in their 3' UTR (Melanson et al., 2011). The rapid turnover of TP53 regulated genes ensures plasticity of the DDR system and has one important implication for our results – the fluctuations in short lived mRNA level we observed in the time-course experiment, are caused by mRNA synthesis activity as the mRNA degradation rate seems to be fast and constant. This emphasises the importance of performing gene expression biodosimetry at a precise time-point post IR exposure, when the dose response shape for a particular transcript is known.

It is worth noting that Melanson et al placed *FDXR* mRNA in a stable transcript cluster with a half-life of 4-6 h, which explains the constant increase of the *FDXR* mRNA we observed – the mRNA is synthesised but not degraded rapidly. One could speculate that the *FDXR* transcript number should be less sensitive to variation with time after irradiation than the fast degraded genes.

We were also interested in transcriptional alterations in non-coding RNA expression caused by IR exposure. Non-coding RNAs significantly outnumber protein coding genes, their expression is very often tissue specific and they are just emerging as potential biomarkers (Sorensen et al., 2013, Pescador et al., 2013). We looked at the expression of three lncRNAs and 19 miRNAs selected from literature. One lncRNA – *PANDAR*, showed no changes in expression after IR exposure (**Figure 30A**) despite the fact that it has been previously reported as being up-regulated after DNA damage. Interestingly, recently Özgür *et al* reported no change in *PANDAR* expression in HeLa and MCF-7 cells following IR or bleomycin treatment (Ozgur et al., 2013). *PANDAR* is a direct TP53 target and in parallel with *CDKN1A* it promotes cell cycle arrest by repressing pro-apoptosis genes after DNA damage through the NF-YA transcription factor (Hung et al., 2011). The up-regulation of *PANDAR* following doxorubicin treatment was reported in human primary foreskin fibroblasts which enter cell cycle arrest after DNA damage but not apoptosis and *PANDAR* has been implicated in supporting this response. In contrast, DNA damage induces a strong apoptotic response in human T-lymphocytes, so it may be an evolutionary conserved, tissue specific pattern of expression.

The second lncRNA investigated – *TP53TG1* showed a slight up-regulation following IR exposure at the late time-point (**Figure 30A**) which is dose dependant at

24 h following irradiation (**Figure 35B**). *TP53TG1* is also a direct target of TP53 and it has been reported to be responsive to DNA damage in the human SW480 colon cancer cell line and normal human dermal fibroblasts (Takei et al., 1998); again the very modest response to IR in human T-lymphocytes can be attributed to tissue specific differences.

The third lncRNA investigated – *FAS-AS1* was rapidly up-regulated by IR exposure in T-lymphocytes derived from two healthy donors reaching first peak of expression 1.5 h and second between 5 and 6 h post exposure. *FAS-AS1* has been identified by Yan *et al* (Yan et al., 2005) as an antisense transcript of the *FAS* gene and the authors proposed that it might protect T-lymphocytes from FAS-mediated apoptosis. It is very interesting to see pro- and anti-apoptotic genes being up-regulated at the same time in a very similar manner. To our knowledge, this is the first report of *FAS-AS1* being up-regulated by IR, but we believe that there are other radiation-responsive lncRNAs awaiting discovery.

For both protein coding genes and responsive lncRNAs, AT lymphocytes consistently showed a lower and delayed response to IR than lymphocytes obtained from healthy donors at the early time-points; however, the difference disappeared at 24 h time-point. We observed that activation of ATM downstream targets has been delayed and impaired but not abrogated (**Figure 29** and**Figure** 34) and this observation is in agreement with previous reports e.g. (Canman et al., 1994), but it also suggests that in the absence of ATM, some other kinases can activate ATM downstream targets but they seem to be less efficient. Over 14 year ago, Tibbetts *et al* suggested that another kinase – ATR can be responsible for this action (Tibbetts et al., 1999) and

subsequent reports seem to support this hypothesis (Jazayeri et al., 2006, Myers and Cortez, 2006).

From the 19 radiation-responsive miRNAs identified from the literature only two demonstrated modulation of expression after IR exposure in our experimental setup: *miR-34a-5p* and *miR-182-5p*. The most probable explanation for this discrepancy is the fact that every study seems to employ a different experimental model and that there are considerable differences in miRNA expression between tissues and miRNA response to IR seems to be tissue dependent (**Table 1**). Moreover, the majority of the miRNA research is performed using microarrays, however, at least in our hands, it is not the most reliable technique for miRNA detection (own unpublished observation).

The IR-responsive *miR-34a-5p* is a direct target of TP53 and it exhibits strong pro-apoptotic and anti-proliferating properties (He et al., 2007). *miR-182-5p* is considered to have dual properties as an oncogene and tumour suppressor depending on the cellular context. It targets many genes positively regulating DDR but also cyclin-dependent kinase 6 (CDK6) which can phosphorylate retinoblastoma 1 protein and consequently promote cell cycle progression (Krishnan et al., 2013). Both miRNAs were up-regulated at the late time-point and we could not detect any differences between healthy controls and the AT. Interestingly, when we looked at miRNA level in the non-irradiated samples, we noticed that the endogenous level of *let-7b-5p* is significantly higher in healthy controls that in the AT. The *let-7* miRNA family is considered to act as tumour suppressors because they target genes positively regulating cell proliferation such as Kirsten rat sarcoma viral oncogene homolog (*KRAS*), cyclin D1 (*CCND1*), v-myc avian myelocytomatosis viral oncogene homolog (*MYC*) or *CDC25A*, their deletion is

associated with cancer and their overexpression inhibits cancer cell proliferation and sensitises them to radiation (Johnson et al., 2007). miRNAs belonging to let-7 family were reported to be down-regulated after IR exposure in primary fibroblasts and human colon cancer cell line HCT116 (Saleh et al., 2011). Mi *et al* showed that *let7b* expression is lower in acute lymphoblastic leukaemia (ALL) patients than in acute myeloid leukaemia (AML) and healthy controls (Mi et al., 2007). Interestingly, ALL is the most common cancer in AT patients and it is usually of T-cell origin in contrast to ALL in the general population (Reiman et al., 2011). Unfortunately, we have no information related to the AT patient from whom the lymphocytes were obtained and it is unknown if this person was diagnosed with ALL, therefore we could not conclude if lower *let-7b* level was an underlying cause of ALL or a marker of existing cancer, nonetheless, it seems to be an exciting possibility.

The transcriptional response of *CDKN1A* and *FDXR* to IR at the 2 h time-point in healthy donors reached a plateau at around 2 Gy. The AT showed a constant and linear up-regulation of the transcripts which was still lower than in controls even after a dose of 5 Gy (**Figure 34A** and **C**). However, at 24 h post exposure, the dose-response is linear and AT cannot be distinguished from healthy donors (**Figure 34B** and **D**). *CCNB1* expression in the C1/C2 controls is significantly repressed by doses as low as 0.4 Gy 2 h following exposure and the repression reaches a plateau around a dose of 3 Gy whereas the AT sample does not significantly repress *CCNB1* for exposures as high as 2 Gy (**Figure 34E**). At the 24 h time-point all donors present the same dose response shape which is best described by quadratic function, indicating that the higher the dose of radiation used, the longer time the cells require to recover and resume cell cycle (**Figure 34F**). CCNB1 is a main cyclin active during G2/M phase of the cell cycle

and together with cyclin-dependent kinase 1 (CDK1) form maturation-promoting factor which is necessary for entry into mitosis, therefore *CCNB1* expression is under tight control as entering mitosis with unrepaired DNA damage can have significant consequences for cells (Yu et al., 2002).

From the two lncRNAs for which the dose-response was assessed, only *TP53TG1* seems to be suitable for biodosimetry purposes as, although its expression was not modified by IR 2 h post irradiation, a linear dose-response to IR 24 h post exposure was seen for all three donor cells (**Figure 35**). *FAS-AS1* transcriptional up-regulation reached a plateau at around 1 Gy 2 h post irradiation, but after 24 h the dose-response was not linear but best described by quadratic function.

The dose response for the two IR-responsive miRNAs was also not linear but described by quadratic function, similar to the *CCNB1* gene (**Figure 36**). However, the overall miRNA expression pattern in blood is probably different. Recently there has been much interest in exosomes, which are nanosize vesicles secreted by all cells into extracellular space and body fluids. It is believed that exosomes serve as a form of communication between distant cells in the body and they can contain proteins, lipids, miRNAs and some regulatory mRNAs (reviewed in (Zhang and Grizzle, 2014). It is very likely that after *in vivo* irradiation the blood will contain other IR-responsive miRNAs secreted in a form of exosomes coming from different types of cells, and some of these miRNAs may be better suited for biodosimetry purposes. Very recently, Jacob and colleagues identified *miR-150* as a sensitive biomarker of *in vivo* exposure in mouse serum (Jacob et al., 2013).

Low doses of radiation are increasingly being used in diagnostics, however, there is still a lot of uncertainty regarding health effects of low dose exposure

(extensively reviewed in (Morgan and Bair, 2013)). We were interested in the transcriptional response of human T-lymphocytes to low doses of radiation. T-lymphocytes obtained from one healthy donor were exposed to a range of doses from 5 mGy to 100 mGy and the cells were collected 2 and 24 h following exposure. Three out of twelve tested transcripts (*MDM2*, *CDKN1A* and *SESN1*) showed linear response to IR at both time-points (**Figure 37**). Our data show that at the transcriptional level, cells can detect very low doses of radiation (20 mGy after 2 h for *CDKN1A*) and the three genes could be potentially used as biomarkers of low dose exposure.

In summary, our data indicates that gene expression profiles at early time-points can highlight individuals with AT deficiency and associated radiation sensitivity to IR. It would be very interesting to see gene expression profiles in T-lymphocytes obtained from AT carriers, as Watts et al showed that lymphoblastoid cells from AT carriers have an "expression phenotype" which was different than in lymphoblastoid cells obtained from healthy donors (Watts et al., 2002)we have previously demonstrated that monitoring expression of IR–responsive TP53 downstream targets can be used as a surrogate assay for assessing ATM/CHK2/TP53 pathway activity, in order to assess individual cancer risk when analysed at an early time point (i.e. 2 h) (Kabacik et al., 2011b). Our results also suggest that it is best to use 24 h time-point for biodosimetry purposes, as the dose responses tend to be linear and inter-individual differences in radiation sensitivity do not in general confound the response, since the expression profiles obtained from the AT patient characterised by extreme radiosesitivity cannot be distinguished from healthy donors.

3.4. Gene expression as a biomarker for radiation exposure

3.4.1. Introduction

Gene expression biomarkers of radiation exposure hold great potential in terms of speed and throughput in the case of a mass screening scenario but assays utilising gene expression are still less accurate than the "gold standard" dicentric chromosome assay. In 2011 North Atlantic Treaty Organization (NATO) ran a biodosimetry exercise organised by Prof Michael Abend from Bundeswehr Institute of Radiobiology, (Munich, Germany), which aimed to compare established (dicentric chromosome and CBMN) and emerging (γ-H2AX foci and gene expression) biodosimetry assays for radiation injury assessment in a triage scenario (Rothkamm et al., 2013, Badie et al., 2013). We were one of the eight laboratories which participated in a gene expression assay comparison. The results of our work are presented in this chapter.

It is vital to validate the potential gene expression biomarkers *in vivo*, however it is very difficult to obtain suitable samples. There are several publications investigating gene expression changes in humans undergoing radiotherapy (Amundson SA, 2004, Dressman et al., 2007, Meadows et al., 2008, Filiano et al., 2011), however, to our knowledge, there were only two reports published utilising gene expression changes to estimate the dose of radiation received by radiotherapy patients (Paul et al., 2011, Templin et al., 2011b). In both papers blood samples from patients undergoing total body irradiation before bone marrow transplant were used and all patients had previous radiotherapy and chemotherapy treatments which could potentially affect the transcriptional response to IR and confound the results. The results provided proof-of-principle that the dose can be predicted following *in vivo* exposure. However in the case of a mass casualty scenario, the majority of exposed

individuals would most likely be partially exposed and part body exposures present a particular challenge for all biodosimetry methods.

In this chapter we selected the most suitable gene for dose estimation and we validated it *in vitro* as well as *in vivo*, additionally we measured intra- and inter-individual variation in its expression before and after irradiation in blood samples obtained from 32 healthy donors. It should be noted that for *in vitro* dose estimation collaborative nature of this project required using slightly different protocol that the one described in **chapter 3.1**, namely, blood was collected into heparin tubes and RNA was extracted by using Qiamp RNA Blood Mini kit. Additionally, in order to save time expression of only two genes was measured by qPCR. Part of the work presented in this chapter has been already published (Badie et al., 2013).

3.4.2. Identification of the best gene for biodosimetry purposes

The blood collection, irradiation and preparation of white blood cell pellets were performed in Prof Michael Abend's laboratory as described in **chapters 2.2.1.2, 2.5.1.1** and **2.6.1.3.** In the first part of the NATO study the blood sample was taken from one individual and was irradiated with known doses of radiation which was sent to all participating laboratories in order to prepare a calibration curve. We selected eight genes (*GADD45A, CCNG1, BBC3, FDXR, CDKN1A, DDB2, PCNA* and *SESN1*) identified in **chapter 3.2** or in the literature (Manning et al., 2013), the expression of which was modified 24 h post IR exposure in blood. The expression of these genes was investigated for the samples used to prepare calibration curve provided by Prof Abend's laboratory (**Figure 38**).

The expression level among all eight genes was very diverse with 57 fold difference between the lowest expressed *FDXR* and the highest *CCNG1* (0.05 and 3.04

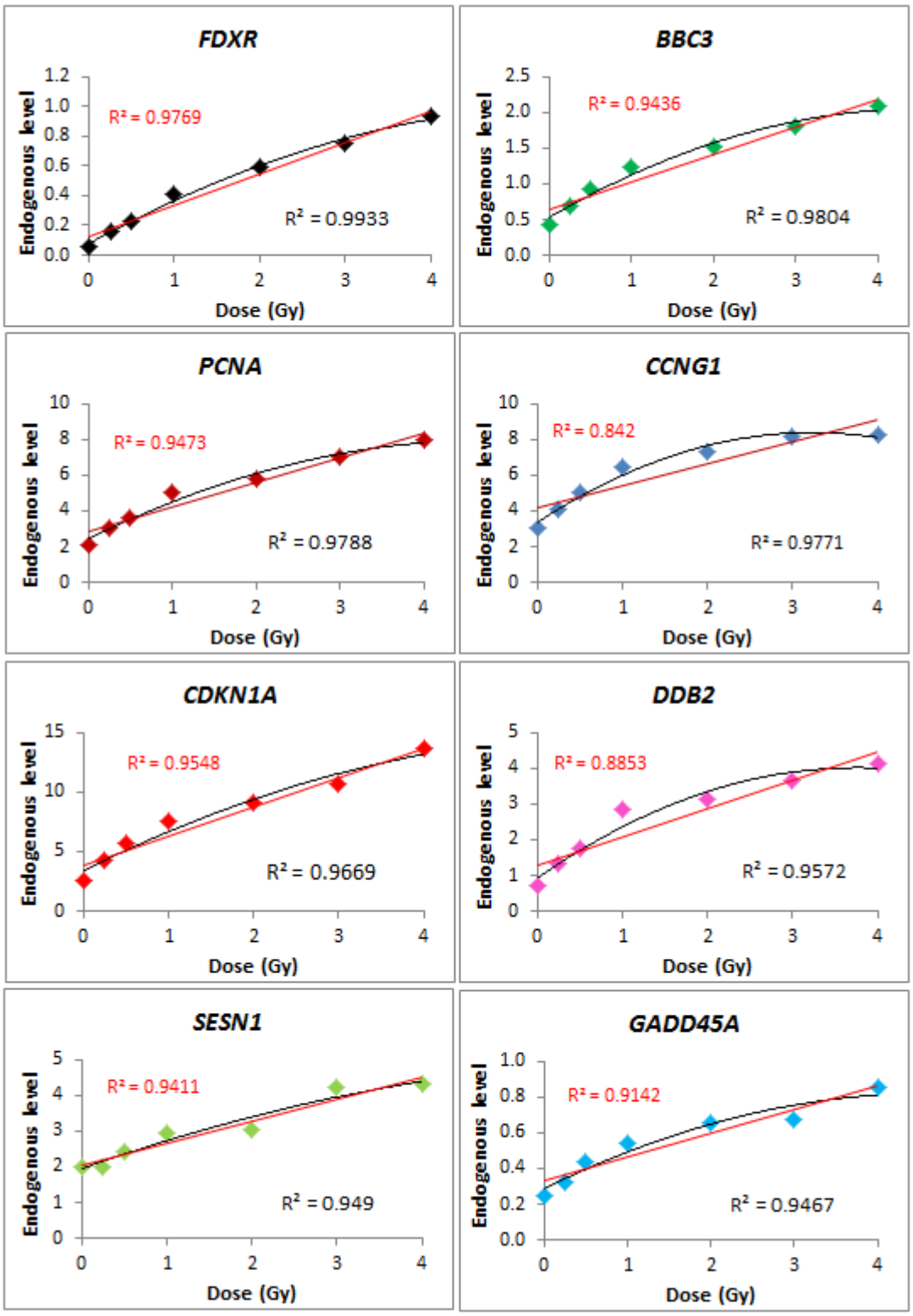

Figure 38. Blood calibration curve expression of eight radiation-responsive genes.

The expression of eight radiation-responsive genes was investigated in human blood samples irradiated *ex-vivo* with known doses of X-ray to produce a calibration curve. Endogenous levels for each gene were normalised to *HPRT1* expression; black lines represent quadratic polynomial regression fits, red lines represent linear regression fits with corresponding R^2 values.

relative to *HPRT1* in the control sample respectively). The dose response curve for all tested genes was best fitted by a quadratic function, the linear regression fit being the second best. Amongst tested genes, *FDXR* expression demonstrated the highest R^2 value of all eight genes (R^2=0.9933 with respect to the quadratic function fit), it also had the most linear response with R^2=0.9769 (**Figure 38**).

3.4.3. Assessment on inter- and intra-individual variability in transcriptional response to IR in blood samples

A good biomarker should ideally display low inter- and intra-individual variability to allow precise dose estimation in different exposed individuals. In order to assess these parameters for our candidate gene, we took blood samples from 32 healthy donors on three independent occasions. The blood samples were split in half and irradiated with either a sham dose or exposed to 2 Gy X-ray and collected 2 h post irradiation. We investigated the expression of *FDXR* and two other genes, *CCNG1* and *CDKN1A,* which have been reported previously as displaying respectively low and high inter-individual variability (Manning et al., 2013), in control and irradiated samples.

The intra-individual variation is presented as COV, (SD expressed as percentage of the mean) for three independent measurements for each donor (**Table 14**). In both, control and irradiated samples expression of the *CCNG1* gene showed the smallest variation between three independent repeats, *CDKN1A* the highest variation and *FDXR* variation was intermediate. Donors displaying lower variability in *CDKN1A* expression in control samples tend to show lower variability in irradiated samples (Pearson product moment correlation coefficient r= 0.441, p=0.011); this may indicate influence of genetic factors. The inter-individual variation in expression of *CCNG1*, *CDKN1A* and *FDXR* is presented in **Table 15**. Expression of *CCNG1* again showed the smallest

Table 14. Coefficient of variation in transcriptional response to IR exposure measured in three independent repeats

	Control			Irradiated		
Donor	***CCNG1***	***CDKN1A***	***FDXR***	***CCNG1***	***CDKN1A***	***FDXR***
H2	18	18	11	21	18	37
H7	7	17	24	15	5	28
H8	18	9	17	16	29	27
H9	12	25	34	7	14	5
H12	22	20	7	26	16	24
H14	22	6	22	17	13	25
H17	6	18	40	16	7	25
H19	26	12	35	21	15	23
H20	20	11	12	25	10	24
H29	26	16	25	28	10	20
H30	15	31	26	14	12	31
H31	30	19	16	15	26	31
H33	8	15	6	19	22	18
H34	6	34	14	26	20	36
H43	25	29	17	14	27	4
H48	10	35	11	13	33	29
H50	10	22	38	11	35	8
H53	12	28	28	13	23	12
H54	12	29	7	15	46	19
H56	25	15	6	7	49	3
H57	17	26	23	16	39	26
H58	7	13	23	11	45	24
H59	23	28	5	18	44	24
H60	6	66	21	19	55	33
H61	31	27	13	11	39	19
H62	28	42	10	10	36	39
H63	17	44	19	8	37	55
H64	29	7	6	17	47	13
H65	14	72	23	10	58	33
H66	27	20	31	21	24	30
H67	25	26	16	32	12	28
H68	10	40	8	26	8	25
Mean	17.64	25.61	18.54	16.83	27.35	24.31
SD	8.05	14.99	10.03	6.39	15.32	10.88

SD – standard deviation

Table 15. Inter-individual variation in transcriptional response to IR exposure represented and coefficient of variation measured in 32 healthy donors

	Control			Irradiated		
	Repeat 1	Repeat 2	Repeat 3	Repeat 1	Repeat 2	Repeat 3
CCNG1	16.71	19.11	15.39	15.09	16.96	17.97
CDKN1A	39.43	35.06	28.19	41.62	22.18	18.64
FDXR	15.51	23.29	23.89	29.82	32.02	37.79

differences between 32 donors both before and after IR exposure as represented by low coefficients of variation. The inter-individual variation in *CDKN1A* expression was very variable with coefficients of variation ranging from 18.64 to 41.62 in the irradiated samples, which can be at least partially explained by high intra-individual variation (**Table 14**). Expression of the *FDXR* gene showed quite low inter-individual variation in the control samples (COV between 15.51 and 23.89), however it was much higher in irradiated samples (COV between 29.82 and 37.79) suggesting that there was more variability in the response to IR exposure between the donors than intrinsic variation.

3.4.4. *In vitro* dose estimation

In the second part of the NATO study, a blood sample was taken from the same donor used for preparation of calibration curve, irradiated with ten unknown doses and sent out to participants. The aim of this exercise was to (i) assess accuracy of dose prediction by gene expression, (ii) measure inter-laboratory variation in dose estimation, (iii) assess the time necessary to provide dose estimation. In order to save time during the reaction setup and data acquisition we focused on the most promising gene, *FDXR*.

Unknown samples were received early morning and we performed RNA extraction, RT reaction and duplex qPCR with *HPRT1* and *FDXR* only as described in **chapters 2.6.1.3**, **2.9.1** and **2.10.3** respectively. The calibration curve samples were measured by qPCR together with unknown samples in order to avoid run-to-run variation. Each sample had prepared a "-RT" control which did not contain reverse transcriptase enzyme in order to control for gDNA contamination. Three samples showed minor gDNA contamination, however the signal for gDNA was detected above 35 Ct and at least 10 Cts away from the highest Ct in the samples, therefore it did not

influence the results. The whole procedure from receiving the samples until providing dose estimates took just below 8 h. We were the first, along with a group utilising non-enzymatic Chemical Ligation Dependent Probe Amplification methodology, to deliver the results amongst all participating laboratories (Table 1 extended in (Badie et al., 2013)). The time needed for reporting the results was comparable to that for the γ-H2AX assay, but 6.75 times quicker than dicentric chromosome assay and 12 times quicker than CBMN assay (Rothkamm et al., 2013).

The results for the unknown samples and calibration curve samples measured together are presented in **Figure 39**. It is clear that four unknown samples had a higher expression level of *FDXR* than the highest calibration sample. The standard curve obtained from calibration samples measured together with unknown samples was best fitted by linear quadratic function, the linear fit being the second best; the corresponding equations used for dose estimations are presented in **Figure 40.** It has to be noted that the quadratic function cannot provide a dose estimate for values higher than the maximum of the function (dotted line on **Figure 39**).

We noticed that the endogenous levels for calibration samples measured by qPCR the second time gave higher values than in the first measurement (**Figure 41A**); we believe the differences in the expression level are due to the use of a different batch of standard curve in two independent qPCR experiments. When a standard curve is prepared, a highly concentrated template for each gene is added, leading to variability in the amount of the added template due to unavoidable technical error. Thus, the ratio between gene of interest and reference gene is going to be different in each batch of the standard curve. That will influence the calculated endogenous levels for each gene. If we normalise *FDXR* endogenous levels obtained in two runs to the

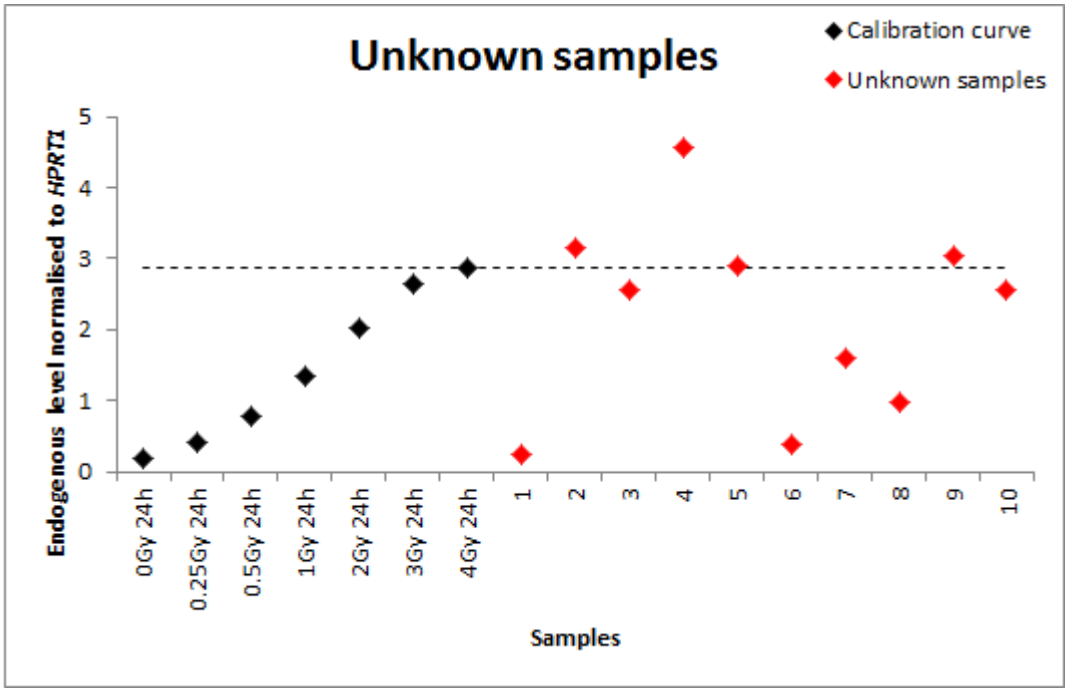

Figure 39. Endogenous expression level of *FDXR* obtained from blood calibration curve and unknown samples.

Endogenous expression levels of the *FDXR* gene are plotted for calibration curve samples (black) and unknown samples (red), the dotted line represents maximum value for calibration curve samples.

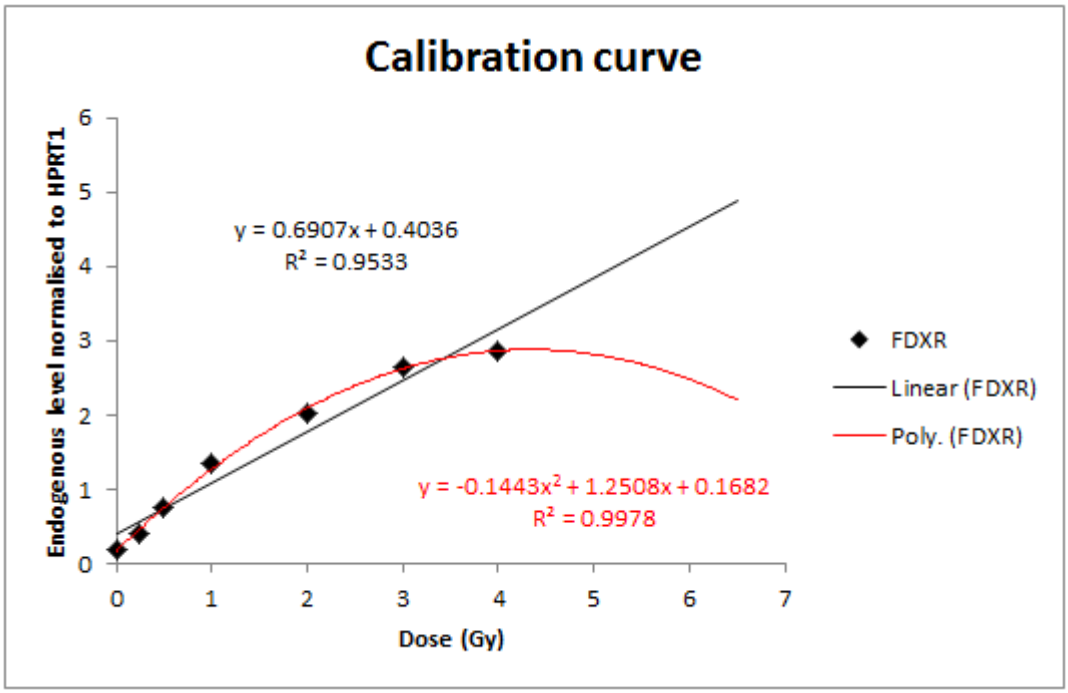

Figure 40. Endogenous level of *FDXR* obtained from blood calibration curve run together with unknown samples.

Two regression fits were employed in order to estimate the dose of unknown samples: polynomial (red line) and linear (black line). The trendlines were projected forward in order to estimate for doses higher than in calibration curves.

A.

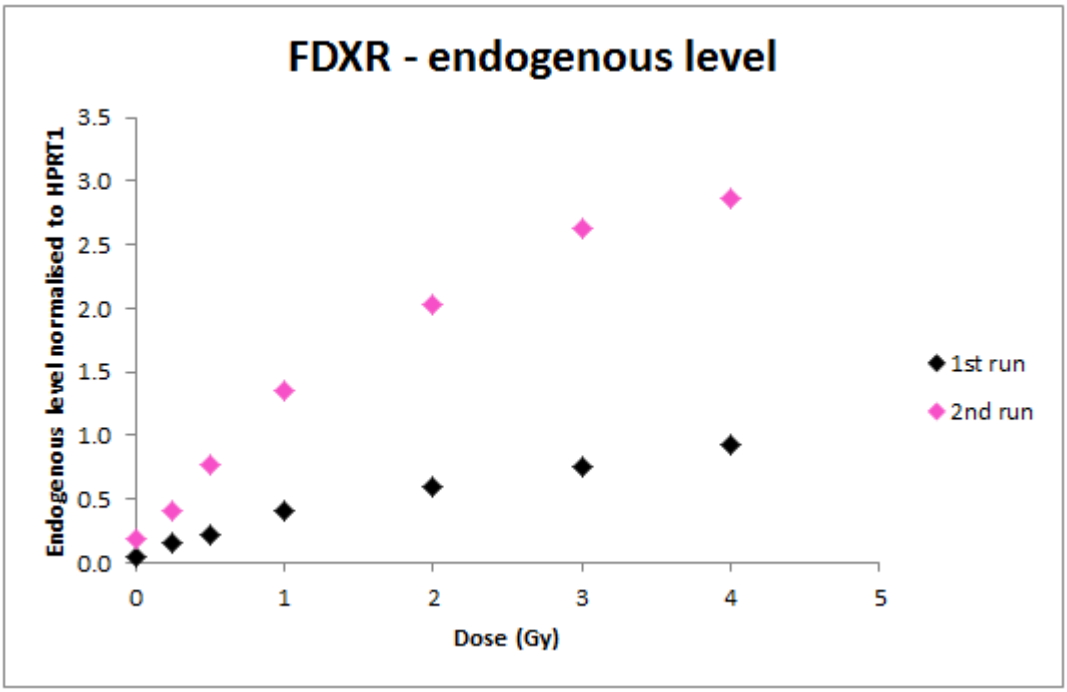

B.

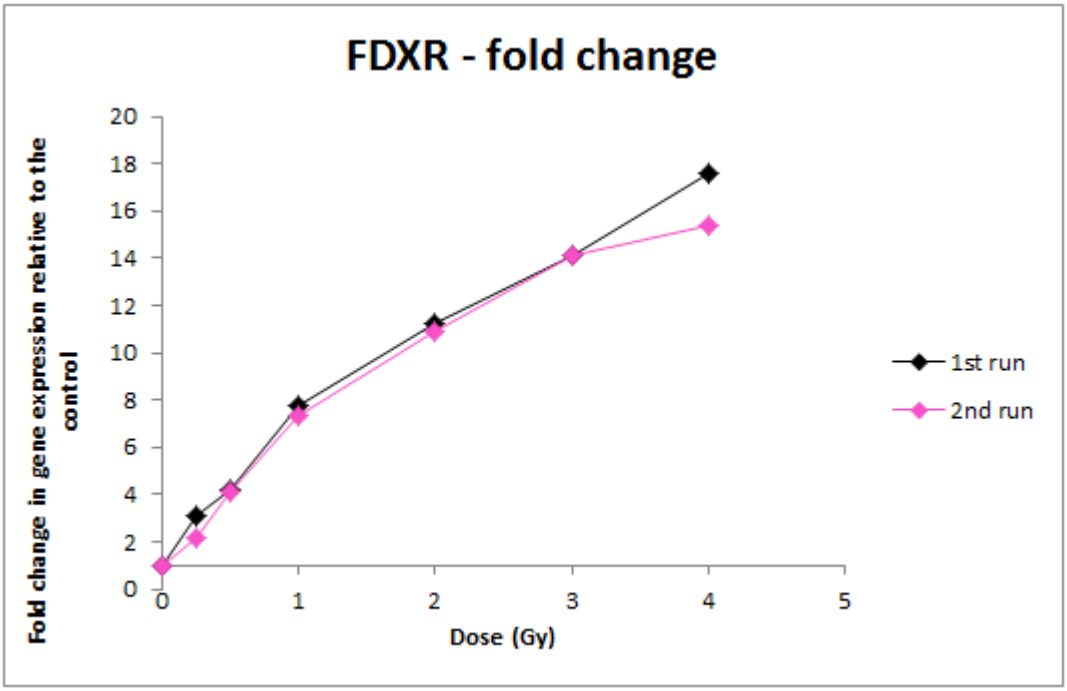

Figure 41. Comparison of *FDXR* expression measurement in two separate qPCR experiments in calibration curve samples.

A. Endogenous levels of *FDXR* in calibrator curve samples were measured in two qPCR experiments. The expression values for the second run (pink) are higher than for first run (black). **B.** Endogenous level values for two qPCR experiments were normalised to non-irradiated control.

non-irradiated control, the differences disappear (**Figure 41B**) supporting this theory. As the unknown samples and calibrator curve samples were measured in one qPCR experiment, using different batches of standard curve does not influence our results.

In order to estimate the doses of radiation the unknown samples were exposed to, we used both linear and quadratic equations obtained from fitting the calibrator samples (**Figure 40**). The dose estimates together with real doses to which the unknown samples were exposed to are presented in **Table 16**. As expected, the polynomial fit failed to estimate doses of radiation for four samples, which had measured *FDXR* endogenous levels higher than the maximum of the quadratic function. However, for the remaining six samples, the dose estimates were more accurate than provided by linear fit, with only one estimate being further than 0.5 Gy from the real dose. The dose estimates provided by the linear fit were slightly less accurate with 3 samples out of 10 outside of the 0.5 Gy threshold, however, in contrast to linear quadratic function, the linear fit provided dose estimation for all ten samples and seven out of ten acceptable dose estimates. The graphical representation of dose estimates is provided in the **Figure 42.**

Finally, we wanted to assess the uncertainty associated with our dose estimates. We calculated the measurement error as described in **chapter 2.11.1**, and we assumed that uncertainties coming from the curve fits are negligible as the R^2 values for both regression fits were above 0.95. Since the blood samples for calibration curve and the unknown samples were taken from the same individual on two separate occasions we used the average of COV in control and irradiated samples for *FDXR* gene obtained from 32 blood donors described in previous chapter as an approximation of

Table 16. Dose estimation for unknown samples using polynomial or linear fit

Unknown samples	Dose used	Dose estimation			
		polynomial	Difference (Gy)	linear	Difference (Gy)
1	0	0.07	0.1	-0.21	0.2
2	3	x	x	3.99	1.0
3	2.2	2.85	0.7	3.12	0.9
4	6.4	x	x	6.02	0.4
5	2	x	x	3.63	1.6
6	0.1	0.17	0.1	-0.03	0.1
7	1.4	1.35	0.1	1.72	0.3
8	0.7	0.72	0.0	0.85	0.1
9	4.2	x	x	3.80	0.4
10	2.6	2.86	0.3	3.13	0.5

Values in red represent dose estimation different for more than 0.5 Gy from a real dose

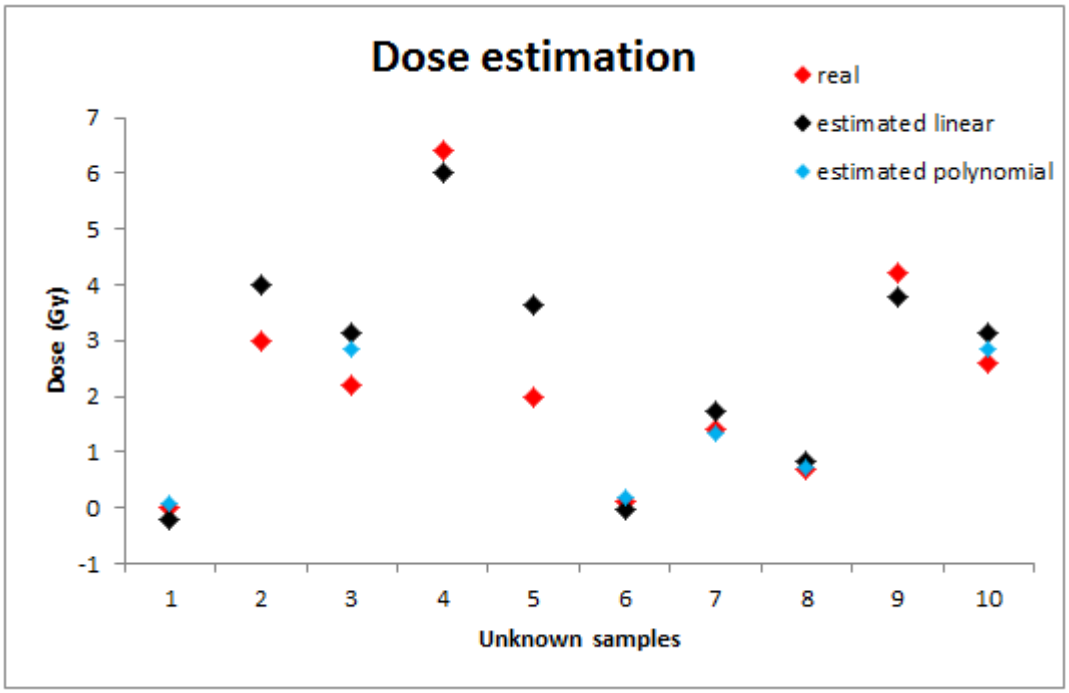

Figure 42. Graphical representation of dose estimates provided by polynomial and linear fits.

The doses delivered to unknown samples were estimated by linear (black) and polynomial (blue) fits. For seven out of ten samples the dose estimates were very close to the doses delivered (red). The three remaining samples had the doses overestimated by more than 0.5 Gy.

intra-individual variability. The estimated uncertainties associated with dose estimation are presented in **Table 17**.

3.4.5. *In vivo* dose estimation

To confirm usefulness of our candidate gene for biodosimetry purposes, we wanted to validate it *in vivo*. Unfortunately, we did not have an access to uniformly exposed donors, however Dr Ales Tichy from University of Defence in Czech Republic, kindly provided us with blood samples from two endometrium cancer patients undergoing radiotherapy. None of the patients had previous chemo- or radiotherapy; the blood samples were taken just before the first fraction of radiotherapy and then 24 h after the first fraction of 1.9 Gy of X-ray. We measured expression level of the *FDXR* gene in these samples and in the calibration curve from **chapter 3.4.4** in order to estimate the dose received by the white blood cells (**Figure 43**). We could clearly distinguish between blood samples taken before and after radiotherapy, also the *FDXR* expression level was very similar in both patients in control and exposed samples. We attempted to estimate the dose that both radiotherapy patients received to the blood cells by using the quadratic equation obtained from calibration curve (**Figure 44**), we also assessed uncertainty associated with dose estimation as in previous chapter, using data from blood samples obtained from 32 donors as approximation of inter-individual variability. The results are presented in **Table 18**. The dose estimates for blood samples taken 24 h after first fraction of radiotherapy were 0.64 (dose range 0.57 – 1.14 Gy) and 0.74 (dose range 0.66 – 1.25 Gy) for patient A and B respectively.

3.4.6. Discussion

In a large-scale radiological incident it will be important to quickly separate individuals requiring urgent medical attention from the “worried-well” who are not

Table 17. Dose estimation for unknown samples with associated uncertainty values

Unknown samples	Dose used	Measurement error	Intra-individual variability	Dose estimation uncertainty	Dose estimation			
					Polynomial	Dose range	linear	Dose range
1	0	39%	21%	44%	0.07	0.04 - 0.10	-0.21	-0.31 - (-0.12)
2	3	3%	21%	22%	-	-	3.99	3.12 - 4.85
3	2.2	19%	21%	29%	2.85	2.03 - 3.67	3.12	2.22 - 4.02
4	6.4	14%	21%	26%	-	-	6.02	4.47 - 7.58
5	2	11%	21%	24%	-	-	3.63	2.75 - 4.50
6	0.1	25%	21%	33%	0.17	0.12 - 0.23	-0.03	-0.04 - (-0.02)
7	1.4	8%	21%	23%	1.35	1.04 - 1.66	1.72	1.33 - 2.11
8	0.7	7%	21%	23%	0.72	0.55 - 0.88	0.85	0.66 - 1.04
9	4.2	5%	21%	22%	-	-	3.80	2.97 - 4.64
10	2.6	7%	21%	22%	2.86	2.21 - 3.50	3.13	2.42 - 3.83

Values in red represent doses which were not in a range of dose estimation uncertainty.

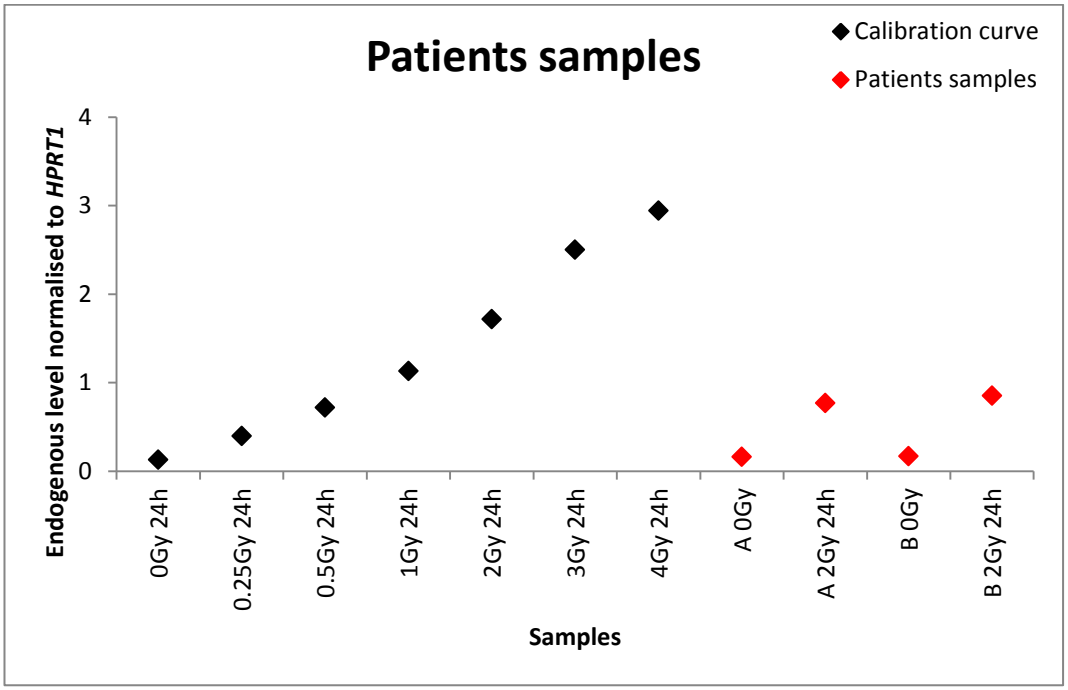

Figure 43. *FDXR* expression in radiotherapy patients samples.

FDXR expression level was measured in blood samples obtained from two endometrium cancer patients (A and B) undergoing radiotherapy (red diamonds) and in calibration curve samples from **chapter 3.4.4** (black diamonds)

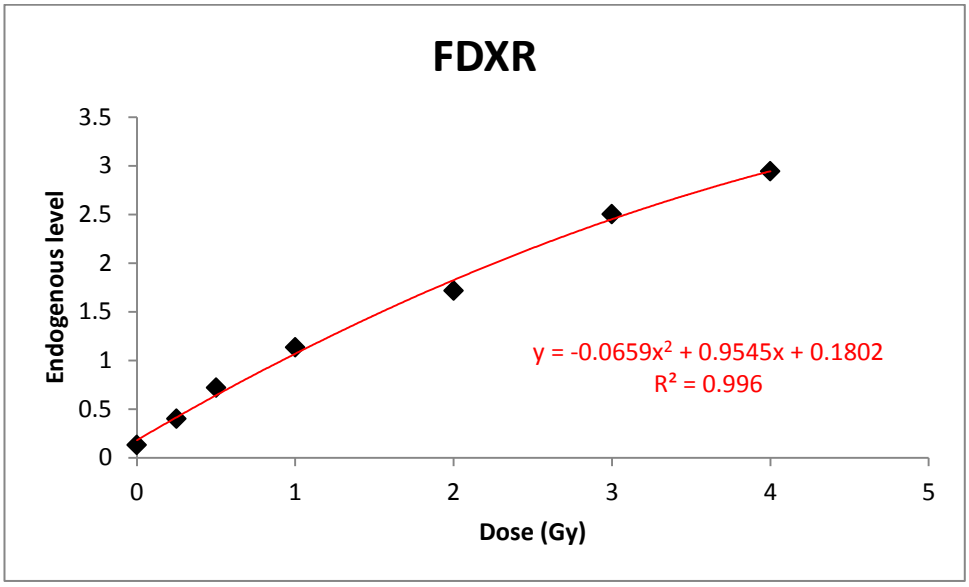

Figure 44. Endogenous level of *FDXR* obtained from blood calibration curve run together with radiotherapy patients samples.

Quadratic regression fit was employed in order to estimate the dose of radiotherapy patients samples.

Table 18. Dose estimation with associated uncertainty for radiotherapy patients samples using polynomial regression fit.

Unknown samples	Dose used	Measurement error	Inter-individual variability	Dose estimation uncertainty	Dose estimation	
					Polynomial	Dose range
A 0Gy	0	38%	27%	47%	0.170867	0.09 - 0.25
A 1.9Gy 24h	1.9	20%	27%	33%	0.855016	0.57 - 1.14
B 0Gy	0	44%	27%	52%	0.176686	0.09 - 0.27
B 1.9Gy 24h	1.9	15%	27%	31%	0.956233	0.66 - 1.25

expected to require early medical attention. Gene expression assays have the potential to screen large numbers of individuals and, as demonstrated here, dose estimation can be provided within 8 h from receiving the samples (Badie et al., 2013). The reporting time can potentially be decreased by using fast cDNA synthesis protocols and faster thermal cycling conditions, although these modifications would have to be validated.

Here we attempted to validate the candidate genes identified and characterised in **chapters 3.2** and **3.3** for use in radiological biodosimetry. In the *in vitro* part of the work, a calibration curve was constructed with blood sample taken from one individual and irradiated with doses ranging from 0 to 4 Gy. We measured expression of eight radiation responsive genes the expression of which was modified in blood 24 h post exposure selected from **chapter 3.2** and the literature (Manning et al., 2013) in calibration curve samples. All tested genes showed similar shaped dose-response curves and these fitted best quadratic functions (**Figure 38**) which is in agreement with published reports (Paul and Amundson, 2008, Manning et al., 2013). The quadratic function shape of the dose-response curve has two important implications for biodosimetry – first, it implies that there is a maximum dose of radiation to which the expression of the particular gene will increase but at higher doses due to various mechanisms as cell killing or pathway saturation, a relative decrease in the expression of the gene would be observed. In other words, two distinctive doses in theory can induce the expression of candidate gene to the same level, as observed for miRNAs (**Figure 36**), however it will have to be experimentally validated. Second, it cannot provide dose estimation for expression level higher than the maximum of the function. It is possible that the polynomial shape of the dose-response curve in blood irradiated *ex-vivo* is an artefact of the 24 h incubation at 37 °C,

however, Filliano *et al* measured expression of five genes in mice exposed *in vivo* to different doses of radiation 23 h post exposure and three genes showed quadratic dose response (Filiano et al., 2011). Interestingly, *Ccng1* expression increased linearly with dose of radiation (Filiano et al., 2011) indicating that there may be gene, organism or type of exposure differences in the shape of dose response curve.

In the second part of the *in vitro* experiment we received ten blood samples from the same individual which were exposed to unknown doses and we provided the dose estimates using the calibration curve prepared before. One of the aims of this exercise was to measure the time necessary to report the dose estimation, therefore we focused our interest on the *FDXR* gene only as it demonstrated the highest R^2 value for polynomial regression fit and the most linear response of all tested genes (**Figure 38**). *FDXR* expression in four unknown samples was higher than the maximum of the quadratic function and for those samples, we were unable to extrapolate the dose from the quadratic equation. For that reason, we also used linear regression fit to estimate the doses to which the unknown samples were exposed to. In six unknown samples, for which we obtained dose estimates using the quadratic function, the estimations were more accurate than those obtained with linear regression fit (**Table 16**). In order to obtain more accurate dose estimations it would be beneficial to have a calibration curve spanning wider range of doses. It would be also worth investigating possibility of using two or three genes for biodosimetry instead of one as it has been reported that using two genes produced better dose estimates than any single gene in blood exposed *in vitro* to IR (Manning et al., 2013).

We noticed that two 'unknown' samples exposed to doses 2 and 3 Gy had higher *FDXR* expression level than the calibration sample exposed to 4 Gy. This

unexpected result could be caused by technical error or high intra-individual variation in expression of *FDXR* gene, as high intra- or inter-individual variation would negatively impact dose estimation in real case scenario. In order to address this issue, *FDXR* expression was measured in blood samples taken on three independent occasions from 32 healthy individuals and irradiated *in vitro* with a sham dose or exposed to 2 Gy of X-ray. We also measured expression of *CDKN1A* and *CCNG1* which were reported to have respectively high and low inter-individual variation in response to IR exposure (Manning et al., 2013).

CCNG1 shoved very low intra- and inter-individual variability that would be very beneficial for biodosimetry purposes, however our data indicates that *CCNG1* expression reaches a plateau at doses of 3 Gy and above (**Figure 38**) in agreement with previous findings (Manning et al., 2013). Alternatively, *CDKN1A* expression showed high intra- and inter-individual variation both in control and in irradiated samples. The variability in *CDKN1A* expression may reflect individual sensitivity to radiation. We have shown previously that *CDKN1A* expression can identify individuals with acute skin reaction to radiotherapy (Badie C, 2008). We have also demonstrated that induction of *Cdkn1a* after IR exposure depends on Atm/Chk2/TP53 pathway activity and it is correlated with cancer incidence in mice (Kabacik et al., 2011b). These features make *CDKN1A* poor candidate for biodosimetry purposes but it would be informative to investigate further its potential as biomarker of radiation sensitivity or cancer susceptibility.

The observed intra-individual variation in *FDXR* expression in control samples was low, very similar to variation in *CCNG1* expression, however it increased in irradiated samples (**Table 14**). It is possible that some environmental factors can

influence *FDXR* induction upon IR exposure. For example, it has been reported that *FDXR* can also be induced by lipopolysaccharide (Budworth et al., 2012) and although it is unlikely that an infection caused the different response to IR exposure in our experiment as the control level showed good reproducibility between three independent repeats, we cannot exclude the possibility that there are other factors modifying response to IR which have not been identified yet. The inter-individual variation in *FDXR* expression was relatively low in control samples however it increased after irradiation, which could cause problems in dose estimation in a real scenario. This potential issue could be resolved by creating a calibration curve with several donors representing real inter-individual variability. We showed that, when a calibration curve was constructed with blood samples obtained from ten donors, we could predict a 2 Gy dose received by 25 donors with a mean estimate of 1.6 Gy (range 0.78 - 2.8 Gy) and 1 Gy dose with a mean estimate of 0.8 Gy (range 0.35 – 1.15 Gy) using expression of the *FDXR* gene (Manning et al., 2013). The dose estimations for some donors are outside the recommended 0.5 Gy threshold for accurate dosimetry, however it should be kept in mind that, whereas from a biodosimetry point of view, it is crucial to get the dose estimates as accurate as possible, from a clinical perspective the prospect of quick separation of individuals who received a dose in the range needing immediate medical attention from those who do not would be extremely beneficial.

Gene expression changes have been successfully used to predict dose in mice irradiated *in vivo* (Dressman et al., 2007, Meadows et al., 2008, Filiano et al., 2011). There are also two reports utilising gene expression (Paul et al., 2011) and miRNA expression (Templin et al., 2011b) changes for dose assessment in cancer patients undergoing total body irradiation prior bone marrow transplant, both of them

presenting impressive accuracy. However, in a real scenario, the majority of individuals will probably receive non-uniform exposures due to partial body shielding. Therefore we decided to investigate if gene expression changes could be detected in patients partially exposed to IR. We measured *FDXR* expression in two endometrium cancer patients undergoing radiotherapy. Unfortunately, we did not have access to patients treatment plans and we were not able to assess how accurate our dose estimates were. However, the standard treatment for endometrium cancer is a surgery, whereas inoperable or unsuitable cases are treated with aggressive radiotherapy which covers large volume of abdomen where a high concentration of lymph nodes is (www.nhs.gov.uk). It is estimated that only about 2 % of lymphocytes are circulating in the blood stream, the remaining 98 % are located in tissues and particularly high concentrations are found in lymph nodes, tonsils, thymus, spleen and bone marrow (IAEA, 2011). It is known that inflammation is associated with cancer and white blood cells infiltrate the tumour to various extents (Hanahan and Weinberg, 2011), meaning that the population of blood cells in the radiotherapy beam could be relatively high. Any particular lymphocyte cell is present in the peripheral blood for about 30 min, and then moves to the extravascular pools. When the radiation exposure is partial, it takes about 24 h to establish equilibrium between populations of irradiated and non-exposed lymphocytes in peripheral blood (IAEA, 2011) therefore sampling blood 24 h post exposure should provide a representative population of irradiated cells in the blood.

Taking all this into account, we were surprised to detect an up-regulation in *FDXR* expression in both patients with relatively high and similar dose estimation. To our knowledge there is only one report investigating gene expression changes in mice

partially exposed to IR; the microarray based approach generated multiple gene signatures however, these were specific to irradiated site and poorly discriminated the doses (Meadows et al., 2010). Meadows and colleagues also showed that gene expression signatures obtained from total body irradiated mice, failed to predict doses in partially irradiated mice (Meadows et al., 2010) which additionally complicates the use of gene expression for biodosimerty purposes.

Our *in vivo* experiment cannot answer the question how accurate the dose estimation using gene expression profiling is in this case but it demonstrates that partial exposure induces gene expression changes that are different from those in unexposed samples and these differences can be detected in peripheral human blood. This single gene protocol is much quicker than the microarray approach and does not require complicated and time consuming data analysis. Of course it would have to be validated with a larger number of patients but single gene analysis is clearly a promising complementary approach for traditional biodosimetry in the case of a mass casualty scenario.

Chapter 4. General discussion and future perspectives

In the event of a radiological accident or incident there is a need to quickly separate people exposed to high doses of radiation from others including the 'worried-well' in order to provide those exposed with necessary medical treatment. The dicentric chromosome assay is the "gold standard" in radiological dosimetry as it is specific to radiation and can provide accurate dose estimation even for partial body exposures (IAEA, 2011). However, it is not well suited for mass casualty incidents as it is time consuming, labour intense and requires highly trained staff to perform the scoring (Wojcik et al., 2010). Here we investigated the possibility of using gene expression as an alternative assay for radiation dosimetry. qPCR was selected the as a quick and sensitive method for assessing changes in expression of IR-responsive genes.

Extensive technique optimisation was performed, which resulted in creating a protocol allowing simultaneous measurement of the expression of six genes, which, by itself is an achievement. We believe the optimised qPCR protocol was the main reason why we performed so well in the NATO biodosimetry exercise as all participants received exactly the same samples and all the differences in dose estimations were due to methodology used (Badie et al., 2013).

Gene expression changes after IR-exposure are well documented and many genes show dose- and time-dependent changes in expression following exposure, which made them particularly promising candidates as radiation biomarkers (Amundson SA, 2004, Gruel et al., 2008, Kabacik et al., 2011a, Manning et al., 2013). First, a microarray experiment was performed to identify genes suitable for biodosimetry using resting blood leukocytes and stimulated T-lymphocytes from three healthy human donors. Some genes showed cell type specific expression but ten genes (*GADD45A, CDKN1A, SESN1, CCNG1, FAS, FBXW2, RBM15, PPM1D, RPS27L* and

BLOC1S2) were consistently up-regulated in all three donors for at least one dose in blood and lymphocytes, indicating that these genes may play a role in the general response to IR. Although in this part of the project, we focused on four genes (*GADD45A, CDKN1A, SESN1, CCNG1*), which showed the greatest modulation of expression flowing IR-exposure, and *FAS* is already well known radiation responsive gene (Manning et al., 2013), it would be valuable to further investigate the remaining five genes. To our knowledge, none of the remaining five genes was studied in details for biodosimetry purposes, although PPM1D and RPS27L were among a 74-gene signature published by Paul *et al* used for dose estimation (Paul and Amundson, 2008). *PPM1D* is a serine/threonine protein phosphatase involved in negative feedback control of DDR. It is a direct TP53 target and following DNA damage it takes part in silencing the DDR signal by targeting TP53 (Crescenzi et al., 2013) and ATM (Choi et al., 2013) proteins. *RPS27L* is another direct p53 target up-regulated following genotoxic stress and it positively regulates *CDKN1A* expression (Li et al., 2007, He and Sun, 2007). PPM1D and RPS27L are clearly involved in DDR, however the remaining three genes do not seem to have any obvious links with it: *FBXW2* is a subunit of ubiquitin protein ligase responsible for glial cell missing homolog 1 ubiquitination and degradation (Chiang et al., 2008), *BLOC1S2* is associated with centromeres, γ-tubulin, lysosome formation and it promotes proliferation (Wang et al., 2004) and *RBM15* is a repressor of myeloid differentiation in hematopoietic cells (Ma et al., 2007).

Next, the transcriptional responses to IR of ten genes identified by our microarray experiment or literature search as high responders in stimulated lymphocytes was characterised in more detail. Additionally, the expression of 19 miRNAs identified in the literature and three lncRNAs following IR exposure was

investigated. To our knowledge, this is the first time when expression of protein-coding genes, miRNAs and lncRNAs is investigated in the same samples following IR exposure. Temporal expression patterns and dose-responses were studied in stimulated human T-lymphocytes obtained from two healthy donors and one AT patient. For the majority of protein coding genes, their transcriptional response to IR at early time-points allowed the AT donor and healthy controls to be distinguished; however, the differences disappeared after 24 h.

Although AT is a rare recessive disease, it is estimated that AT carriers comprise 0.05 – 1 % of the population (Swift et al., 1991). It has been shown that some genes and miRNAs have different endogenous levels and respond differently to IR in AT carriers than in healthy donors (Watts et al., 2002, Smirnov and Cheung, 2008). Moreover, carriers of another recessive disorder, Nijmegen Breakage Syndrome which also manifests itself with hypersensitivity to IR, also have gene expression profiles distinct from both healthy donors and AT carriers (Cheung and Ewens, 2006). Additionally, we have shown that transcriptional response to IR of Tp53 downstream target genes depend on *Tp53* copy number in mice (Kabacik et al., 2011b). All these factors can influence gene expression and therefore negatively impact gene expression-based dosimetry. Our data suggests that it is important to perform gene expression-based dose estimation at least 24 h post exposure to avoid impaired DSB signalling pathway confounding the results as at this time-point the expression level of tested genes is the same in stimulated T-lymphocytes obtained from healthy donors and in AT patient even though the later one has severe defect in DSB signalling and repair. Of course, it still remains to be established if expression profile of IR-responsive genes in blood obtained from AT patients is similar as in stimulated T-lymphocytes.

This study also found for the first time that lncRNA *FAS-AS1* is IR-responsive in human stimulated T-lymphocytes and we presented it's time-course and dose-response to IR. *FAS-AS1* is transcribed from intron 1 of *FAS* gene but in the opposite direction and it was proposed that it might protect T-lymphocytes from FAS-mediated apoptosis and might regulate the alternative *FAS* splice forms through pre-mRNA processing (Yan et al., 2005). These results are very promising, as using lncRNA in biodosimetry is a new concept in radiation biology and very few lncRNAs have been investigated in terms of IR responsiveness. lncRNAs hold a great potential as the number of lncRNAs greatly exceeds number of protein coding genes in mammalian cells (Djebali et al., 2012) and they usually show tissue specific expression (Mercer et al., 2008). It would be extremely useful to perform a large scale screen for lncRNA biomarkers of radiation exposure and validate the potential candidates for use in radiation dosimetry.

In the last part of the thesis, the usefulness of gene expression assays for radiation dosimetry was assessed *in vitro* and *in vivo*. First, we investigated the dose-responses of eight protein coding genes in human blood exposed to IR *ex-vivo*. Dose responses in human blood follows linear quadratic function (Paul and Amundson, 2008) (Manning et al., 2013) and *FDXR* gene showed the highest R^2 value of all tested genes and the most linear response. As a part of a larger biodosimetry comparison study, we needed to report dose estimations in the shortest possible time, therefore expression of only two genes was measured: *FDXR* and a reference gene *HPRT1*. However, the protocol developed here allows the measurement of six genes simultaneously, it is possible to use a combination of two or more IR-responsive genes

which might provide more accurate dose estimation than only one gene (Manning et al., 2013).

Finally, the *FDXR* gene dose-response was used to estimate a dose of IR *in vivo*. Blood samples from two cancer patients undergoing radiotherapy were obtained before the first fraction and 24 h after a 1.9 Gy partial body irradiation (large volume of abdomen). Importantly, none of the cancer patients had previous chemo- or radiotherapy which could have confounded the gene expression results. To our knowledge, this is the first attempt to use gene expression for dose estimation of partial exposure in humans, as so far only one similar experiment was performed using animals (Meadows et al., 2010).

The *FDXR* level in patients control samples and the calibration curve unexposed sample were very similar justifying the validity of using an *in vitro* standard curve for *in vivo* dose estimation. Surprisingly, both patients also showed very similar *FDXR* expression levels after irradiation, suggesting that inter-individual variability in *FDXR* expression may not be as large *in vivo* as has been observed in *in vitro* experiments. It should be noted that the blood samples for inter- and intra-individual variability experiments were prepared differently than the samples for dose estimation, and this could explain some of the differences in the results. Conversely, as we used blood samples from only two donors, the similar expression level between the samples could be just a coincidence. Undoubtedly, more samples are needed to address this issue.

Also, a larger experiment would be needed to assess the influence of other possible confounding factors like infection or smoking, which potentially could affect the accuracy of gene expression-based dosimetry. It has been reported that expression of three genes often quoted as suitable for IR biodosimetry: *CDKN1A*, *FDXR* and *PUMA*

was also modified by lipopolysaccharide (LPS) and their transcriptional response to IR was altered by inflammation, which can compromise the usefulness of these genes as biomarkers of radiation exposure (Budworth et al., 2012). Additionally, Paul *et al* identified eight genes for which radiation-response was modified by smoking status and 14 genes for which radiation response was different depending on gender (Paul and Amundson, 2011).

Moreover, it would be very interesting to investigate lncRNA and miRNA expression in cancer patients samples, as it has been shown that miRNAs can be also useful for dose estimation (Templin et al., 2011b) (Jacob et al., 2013) and there is no data on lncRNAs so far.

Ideal biomarker of IR exposure should be specific to IR, sensitive and accurate. Unfortunately, so far no IR-specific transcript or miRNA have been identified. Gene expression is very complex and influenced by many factors, what makes gene expression based dosimetry challenging. Our experiments show, that *FDXR* expression was up-regulated in blood following an *in vitro* dose of 0.1 Gy. Moreover, in human stimulated T-lymphocytes three genes (*MDM2*, *CDKN1A* and *SESN1*) showed linear response to IR in doses ranging from 5 to 100 mGy, suggesting that gene expression changes are sensitive enough to detect very low doses of radiation. The accuracy of dose estimations for ten samples exposed to IR *in vitro* was encouraging, as only one out of six and three out of ten estimates were more than 0.5 Gy from the real dose when respectively quadratic and linear functions were used. However, time of reporting the dose estimates, which is significantly shorter than for dicentric assay is the biggest advantage of using the gene expression assay for biodosimetry purposes.

In summary, we have developed a sensitive, robust and quick protocol for measuring expression of six genes simultaneously. We have identified IR-responsive genes, miRNAs and lncRNAs which could be potentially used as biomarkers of IR exposure and we characterised their temporal and dose-response. Finally, we validated *FDXR* gene as promising biomarker for dose estimation *in vitro* and *in vivo*. Our experiments serve as a proof of principle that gene expression can be used in radiation biodosimetry to aid classical cytogenetics tools in an event of mass causality.

Bibliography

ABOU-EL-ARDAT, K., MONSIEURS, P., ANASTASOV, N., ATKINSON, M., DERRADJI, H., DE MEYER, T., BEKAERT, S., VAN CRIEKINGE, W. & BAATOUT, S. 2012. Low dose irradiation of thyroid cells reveals a unique transcriptomic and epigenetic signature in RET/PTC-positive cells. *Mutat Res,* 731**,** 27-40.

ABRUZZO, L. V., LEE, K. Y., FULLER, A., SILVERMAN, A., KEATING, M. J., MEDEIROS, L. J. & COOMBES, K. R. 2005. Validation of oligonucleotide microarray data using microfluidic low-density arrays: a new statistical method to normalize real-time RT-PCR data. *Biotechniques,* 38**,** 785-92.

AKANE, A., MATSUBARA, K., NAKAMURA, H., TAKAHASHI, S. & KIMURA, K. 1994. Identification of the heme compound copurified with deoxyribonucleic acid (DNA) from bloodstains, a major inhibitor of polymerase chain reaction (PCR) amplification. *J Forensic Sci,* 39**,** 362-72.

ALBANESE, J., MARTENS, K., KARANITSA, L. V., SCHREYER, S. K. & DAINIAK, N. 2007. Multivariate analysis of low-dose radiation-associated changes in cytokine gene expression profiles using microarray technology. *Exp Hematol,* 35**,** 47-54.

ALBRECHT, H., DURBIN-JOHNSON, B., YUNIS, R., KALANETRA, K. M., WU, S., CHEN, R., STEVENSON, T. R. & ROCKE, D. M. 2012. Transcriptional response of ex vivo human skin to ionizing radiation: comparison between low- and high-dose effects. *Radiat Res,* 177**,** 69-83.

AMUNDSON, S. A., BITTNER, M., CHEN, Y., TRENT, J., MELTZER, P. & FORNACE, A. J., JR. 1999a. Fluorescent cDNA microarray hybridization reveals complexity and heterogeneity of cellular genotoxic stress responses. *Oncogene,* 18**,** 3666-72.

AMUNDSON, S. A., DO, K. T. & FORNACE, A. J., JR. 1999b. Induction of stress genes by low doses of gamma rays. *Radiat Res,* 152**,** 225-31.

AMUNDSON, S. A., DO, K. T., SHAHAB, S., BITTNER, M., MELTZER, P., TRENT, J. & FORNACE, A. J., JR. 2000. Identification of potential mRNA biomarkers in peripheral blood lymphocytes for human exposure to ionizing radiation. *Radiat Res,* 154**,** 342-6.

AMUNDSON, S. A., DO, K. T., VINIKOOR, L., KOCH-PAIZ, C. A., BITTNER, M. L., TRENT, J. M., MELTZER, P. & FORNACE, A. J., JR. 2005. Stress-specific signatures: expression profiling of p53 wild-type and -null human cells. *Oncogene,* 24**,** 4572-9.

AMUNDSON SA, G. M., MCLELAND CB, EPPERLY MW, YEAGER A, ZHAN Q, GREENBERGER JS, FORNACE AJ JR 2004. Human in vivo radiation-induced biomarkers: gene expression changes in radiotherapy patients. *Cancer Research,* 64**,** 6368-6371.

AMUNDSON, S. A., GRACE, M. B., MCLELAND, C. B., EPPERLY, M. W., YEAGER, A., ZHAN, Q., GREENBERGER, J. S. & FORNACE, A. J., JR. 2004. Human in vivo radiation-induced biomarkers: gene expression changes in radiotherapy patients. *Cancer Res,* 64**,** 6368-71.

AMUNDSON SA, L. R., KOCH-PAIZ CA, BITTNER ML, MELTZER P, TRENT JM, FORNACE AJ JR. 2003. Differential responses of stress genes to low dose-rate gamma irradiation. *Molecular Cancer Research,* 1**,** 445-52.

ANDERSEN CL, J. J., ØRNTOFT TF. 2004. Normalization of real-time quantitative reverse transcription-PCR data: a model-based variance estimation approach to identify

genes suited for normalization, applied to bladder and colon cancer data sets. *Cancer Research,* 64**,** 5245-50.

ARIAS-LOPEZ, C., LAZARO-TRUEBA, I., KERR, P., LORD, C. J., DEXTER, T., IRAVANI, M., ASHWORTH, A. & SILVA, A. 2006. p53 modulates homologous recombination by transcriptional regulation of the RAD51 gene. *EMBO Rep,* 7**,** 219-24.

BADIE C, D. S., RAFFY C, TSIGANI T, ALSBEIH G, MOODY J, FINNON P, LEVINE E, SCOTT D, BOUFFLER S. 2008. Aberrant CDKN1A transcriptional response associates with abnormal sensitivity to radiation treatment. *British Journal of Cancer,* 98**,** 1845-51.

BADIE, C., DZIWURA, S., RAFFY, C., TSIGANI, T., ALSBEIH, G., MOODY, J., FINNON, P., LEVINE, E., SCOTT, D. & BOUFFLER, S. 2008. Aberrant CDKN1A transcriptional response associates with abnormal sensitivity to radiation treatment. *Br J Cancer,* 98**,** 1845-51.

BADIE, C., KABACIK, S., BALAGURUNATHAN, Y., BERNARD, N., BRENGUES, M., FAGGIONI, G., GREITHER, R., LISTA, F., PEINNEQUIN, A., POYOT, T., HERODIN, F., MISSEL, A., TERBRUEGGEN, B., ZENHAUSERN, F., ROTHKAMM, K., MEINEKE, V., BRASELMANN, H., BEINKE, C. & ABEND, M. 2013. Laboratory intercomparison of gene expression assays. *Radiat Res,* 180**,** 138-48.

BAKKENIST, C. J. & KASTAN, M. B. 2003. DNA damage activates ATM through intermolecular autophosphorylation and dimer dissociation. *Nature,* 421**,** 499-506.

BANIN, S., MOYAL, L., SHIEH, S., TAYA, Y., ANDERSON, C. W., CHESSA, L., SMORODINSKY, N. I., PRIVES, C., REISS, Y., SHILOH, Y. & ZIV, Y. 1998. Enhanced phosphorylation of p53 by ATM in response to DNA damage. *Science,* 281**,** 1674-7.

BARBER, J. B., WEST, C. M., KILTIE, A. E., ROBERTS, S. A. & SCOTT, D. 2000. Detection of individual differences in radiation-induced apoptosis of peripheral blood lymphocytes in normal individuals, ataxia telangiectasia homozygotes and heterozygotes, and breast cancer patients after radiotherapy. *Radiat Res,* 153**,** 570-8.

BARBER, R., PLUMB, M. A., BOULTON, E., ROUX, I. & DUBROVA, Y. E. 2002. Elevated mutation rates in the germ line of first- and second-generation offspring of irradiated male mice. *Proc Natl Acad Sci U S A,* 99**,** 6877-82.

BARBER, R. C., HICKENBOTHAM, P., HATCH, T., KELLY, D., TOPCHIY, N., ALMEIDA, G. M., JONES, G. D., JOHNSON, G. E., PARRY, J. M., ROTHKAMM, K. & DUBROVA, Y. E. 2006. Radiation-induced transgenerational alterations in genome stability and DNA damage. *Oncogene,* 25**,** 7336-42.

BARNETT, G. C., WEST, C. M., DUNNING, A. M., ELLIOTT, R. M., COLES, C. E., PHAROAH, P. D. & BURNET, N. G. 2009. Normal tissue reactions to radiotherapy: towards tailoring treatment dose by genotype. *Nat Rev Cancer,* 9**,** 134-42.

BENGTSSON, M., STAHLBERG, A., RORSMAN, P. & KUBISTA, M. 2005. Gene expression profiling in single cells from the pancreatic islets of Langerhans reveals lognormal distribution of mRNA levels. *Genome Res,* 15**,** 1388-92.

BIOMARKERS DEFINITIONS WORKING, G. 2001. Biomarkers and surrogate endpoints: preferred definitions and conceptual framework. *Clin Pharmacol Ther,* 69**,** 89-95.

BOUVARD, V., ZAITCHOUK, T., VACHER, M., DUTHU, A., CANIVET, M., CHOISY-ROSSI, C., NIERUCHALSKI, M. & MAY, E. 2000. Tissue and cell-specific expression of the

p53-target genes: bax, fas, mdm2 and waf1/p21, before and following ionising irradiation in mice. *Oncogene,* 19**,** 649-60.

BRANNAN, C. I., DEES, E. C., INGRAM, R. S. & TILGHMAN, S. M. 1990. The product of the H19 gene may function as an RNA. *Mol Cell Biol,* 10**,** 28-36.

BRENGUES, M., PAAP, B., BITTNER, M., AMUNDSON, S., SELIGMANN, B., KORN, R., LENIGK, R. & ZENHAUSERN, F. 2010. Biodosimetry on small blood volume using gene expression assay. *Health Phys,* 98**,** 179-85.

BRENNER, D. J. 2014. What we know and what we don't know about cancer risks associated with radiation doses from radiological imaging. *Br J Radiol,* 87**,** 20130629.

BROCKDORFF, N., ASHWORTH, A., KAY, G. F., COOPER, P., SMITH, S., MCCABE, V. M., NORRIS, D. P., PENNY, G. D., PATEL, D. & RASTAN, S. 1991. Conservation of position and exclusive expression of mouse Xist from the inactive X chromosome. *Nature,* 351**,** 329-31.

BUDWORTH, H., SNIJDERS, A. M., MARCHETTI, F., MANNION, B., BHATNAGAR, S., KWOH, E., TAN, Y., WANG, S. X., BLAKELY, W. F., COLEMAN, M., PETERSON, L. & WYROBEK, A. J. 2012. DNA repair and cell cycle biomarkers of radiation exposure and inflammation stress in human blood. *PLoS One,* 7**,** e48619.

BURMA, S., CHEN, B. P., MURPHY, M., KURIMASA, A. & CHEN, D. J. 2001. ATM phosphorylates histone H2AX in response to DNA double-strand breaks. *J Biol Chem,* 276**,** 42462-7.

BURNS, T. F. & EL-DEIRY, W. S. 2003. Microarray analysis of p53 target gene expression patterns in the spleen and thymus in response to ionizing radiation. *Cancer Biol Ther,* 2**,** 431-43.

BUSTIN, S. A. 2002. Quantification of mRNA using real-time reverse transcription PCR (RT-PCR): trends and problems. *J Mol Endocrinol,* 29**,** 23-39.

BUSTIN, S. A. 2004. *A-Z of Quantitative PCR*, International University Line.

BUSTIN, S. A., BENES, V., GARSON, J. A., HELLEMANS, J., HUGGETT, J., KUBISTA, M., MUELLER, R., NOLAN, T., PFAFFL, M. W., SHIPLEY, G. L., VANDESOMPELE, J. & WITTWER, C. T. 2009. The MIQE guidelines: minimum information for publication of quantitative real-time PCR experiments. *Clin Chem,* 55**,** 611-22.

CALDECOTT, K. W. 2001. Mammalian DNA single-strand break repair: an X-ra(y)ted affair. *Bioessays,* 23**,** 447-55.

CAMPBELL, C., MITUI, M., ENG, L., COUTINHO, G., THORSTENSON, Y. & GATTI, R. A. 2003. ATM mutations on distinct SNP and STR haplotypes in ataxia-telangiectasia patients of differing ethnicities reveal ancestral founder effects. *Hum Mutat,* 21**,** 80-5.

CANMAN, C. E., LIM, D. S., CIMPRICH, K. A., TAYA, Y., TAMAI, K., SAKAGUCHI, K., APPELLA, E., KASTAN, M. B. & SILICIANO, J. D. 1998. Activation of the ATM kinase by ionizing radiation and phosphorylation of p53. *Science,* 281**,** 1677-9.

CANMAN, C. E., WOLFF, A. C., CHEN, C. Y., FORNACE, A. J., JR. & KASTAN, M. B. 1994. The p53-dependent G1 cell cycle checkpoint pathway and ataxia-telangiectasia. *Cancer Res,* 54**,** 5054-8.

CARNEY, J. P., MASER, R. S., OLIVARES, H., DAVIS, E. M., LE BEAU, M., YATES, J. R., 3RD, HAYS, L., MORGAN, W. F. & PETRINI, J. H. 1998. The hMre11/hRad50 protein complex and Nijmegen breakage syndrome: linkage of double-strand break repair to the cellular DNA damage response. *Cell,* 93**,** 477-86.

CARNINCI, P., KASUKAWA, T., KATAYAMA, S., GOUGH, J., FRITH, M. C., MAEDA, N., OYAMA, R., RAVASI, T., LENHARD, B., WELLS, C., KODZIUS, R., SHIMOKAWA, K.,

BAJIC, V. B., BRENNER, S. E., BATALOV, S., FORREST, A. R., ZAVOLAN, M., DAVIS, M. J., WILMING, L. G., AIDINIS, V., ALLEN, J. E., AMBESI-IMPIOMBATO, A., APWEILER, R., ATURALIYA, R. N., BAILEY, T. L., BANSAL, M., BAXTER, L., BEISEL, K. W., BERSANO, T., BONO, H., CHALK, A. M., CHIU, K. P., CHOUDHARY, V., CHRISTOFFELS, A., CLUTTERBUCK, D. R., CROWE, M. L., DALLA, E., DALRYMPLE, B. P., DE BONO, B., DELLA GATTA, G., DI BERNARDO, D., DOWN, T., ENGSTROM, P., FAGIOLINI, M., FAULKNER, G., FLETCHER, C. F., FUKUSHIMA, T., FURUNO, M., FUTAKI, S., GARIBOLDI, M., GEORGII-HEMMING, P., GINGERAS, T. R., GOJOBORI, T., GREEN, R. E., GUSTINCICH, S., HARBERS, M., HAYASHI, Y., HENSCH, T. K., HIROKAWA, N., HILL, D., HUMINIECKI, L., IACONO, M., IKEO, K., IWAMA, A., ISHIKAWA, T., JAKT, M., KANAPIN, A., KATOH, M., KAWASAWA, Y., KELSO, J., KITAMURA, H., KITANO, H., KOLLIAS, G., KRISHNAN, S. P., KRUGER, A., KUMMERFELD, S. K., KUROCHKIN, I. V., LAREAU, L. F., LAZAREVIC, D., LIPOVICH, L., LIU, J., LIUNI, S., MCWILLIAM, S., MADAN BABU, M., MADERA, M., MARCHIONNI, L., MATSUDA, H., MATSUZAWA, S., MIKI, H., MIGNONE, F., MIYAKE, S., MORRIS, K., MOTTAGUI-TABAR, S., MULDER, N., NAKANO, N., NAKAUCHI, H., NG, P., NILSSON, R., NISHIGUCHI, S., NISHIKAWA, S., et al. 2005. The transcriptional landscape of the mammalian genome. *Science,* 309**,** 1559-63.

CARTER, S. L., EKLUND, A. C., KOHANE, I. S., HARRIS, L. N. & SZALLASI, Z. 2006. A signature of chromosomal instability inferred from gene expression profiles predicts clinical outcome in multiple human cancers. *Nat Genet,* 38**,** 1043-8.

CESANA, M., CACCHIARELLI, D., LEGNINI, I., SANTINI, T., STHANDIER, O., CHINAPPI, M., TRAMONTANO, A. & BOZZONI, I. 2011. A long noncoding RNA controls muscle differentiation by functioning as a competing endogenous RNA. *Cell,* 147**,** 358-69.

CHA, H. J., SEONG, K. M., BAE, S., JUNG, J. H., KIM, C. S., YANG, K. H., JIN, Y. W. & AN, S. 2009. Identification of specific microRNAs responding to low and high dose gamma-irradiation in the human lymphoblast line IM9. *Oncol Rep,* 22**,** 863-8.

CHAUDHRY, M. A. 2013. Expression Pattern of Small Nucleolar RNA Host Genes and Long Non-Coding RNA in X-rays-Treated Lymphoblastoid Cells. *Int J Mol Sci,* 14**,** 9099-110.

CHAUDHRY, M. A., KREGER, B. & OMARUDDIN, R. A. 2010a. Transcriptional modulation of micro-RNA in human cells differing in radiation sensitivity. *Int J Radiat Biol,* 86**,** 569-83.

CHAUDHRY, M. A., OMARUDDIN, R. A., KREGER, B., DE TOLEDO, S. M. & AZZAM, E. I. 2012. Micro RNA responses to chronic or acute exposures to low dose ionizing radiation. *Mol Biol Rep,* 39**,** 7549-58.

CHAUDHRY, M. A., SACHDEVA, H. & OMARUDDIN, R. A. 2010b. Radiation-induced micro-RNA modulation in glioblastoma cells differing in DNA-repair pathways. *DNA Cell Biol,* 29**,** 553-61.

CHEN, C. Y., OLINER, J. D., ZHAN, Q., FORNACE, A. J., JR., VOGELSTEIN, B. & KASTAN, M. B. 1994. Interactions between p53 and MDM2 in a mammalian cell cycle checkpoint pathway. *Proc Natl Acad Sci U S A,* 91**,** 2684-8.

CHEN, G., ZHU, W., SHI, D., LV, L., ZHANG, C., LIU, P. & HU, W. 2010. MicroRNA-181a sensitizes human malignant glioma U87MG cells to radiation by targeting Bcl-2. *Oncol Rep,* 23**,** 997-1003.

CHEUNG, V. G. & EWENS, W. J. 2006. Heterozygous carriers of Nijmegen Breakage Syndrome have a distinct gene expression phenotype. *Genome Res,* 16**,** 973-9.

CHI, S. W., ZANG, J. B., MELE, A. & DARNELL, R. B. 2009. Argonaute HITS-CLIP decodes microRNA-mRNA interaction maps. *Nature,* 460**,** 479-86.

CHIANG, M. H., CHEN, L. F. & CHEN, H. 2008. Ubiquitin-conjugating enzyme UBE2D2 is responsible for FBXW2 (F-box and WD repeat domain containing 2)-mediated human GCM1 (glial cell missing homolog 1) ubiquitination and degradation. *Biol Reprod,* 79**,** 914-20.

CHOI, D. W., NA, W., KABIR, M. H., YI, E., KWON, S., YEOM, J., AHN, J. W., CHOI, H. H., LEE, Y., SEO, K. W., SHIN, M. K., PARK, S. H., YOO, H. Y., ISONO, K., KOSEKI, H., KIM, S. T., LEE, C., KWON, Y. K. & CHOI, C. Y. 2013. WIP1, a homeostatic regulator of the DNA damage response, is targeted by HIPK2 for phosphorylation and degradation. *Mol Cell,* 51**,** 374-85.

CICCIA, A. & ELLEDGE, S. J. 2010. The DNA damage response: making it safe to play with knives. *Mol Cell,* 40**,** 179-204.

COLLADO, M., BLASCO, M. A. & SERRANO, M. 2007. Cellular senescence in cancer and aging. *Cell,* 130**,** 223-33.

CONSORTIUM, M., SHI, L., REID, L. H., JONES, W. D., SHIPPY, R., WARRINGTON, J. A., BAKER, S. C., COLLINS, P. J., DE LONGUEVILLE, F., KAWASAKI, E. S., LEE, K. Y., LUO, Y., SUN, Y. A., WILLEY, J. C., SETTERQUIST, R. A., FISCHER, G. M., TONG, W., DRAGAN, Y. P., DIX, D. J., FRUEH, F. W., GOODSAID, F. M., HERMAN, D., JENSEN, R. V., JOHNSON, C. D., LOBENHOFER, E. K., PURI, R. K., SCHRF, U., THIERRY-MIEG, J., WANG, C., WILSON, M., WOLBER, P. K., ZHANG, L., AMUR, S., BAO, W., BARBACIORU, C. C., LUCAS, A. B., BERTHOLET, V., BOYSEN, C., BROMLEY, B., BROWN, D., BRUNNER, A., CANALES, R., CAO, X. M., CEBULA, T. A., CHEN, J. J., CHENG, J., CHU, T. M., CHUDIN, E., CORSON, J., CORTON, J. C., CRONER, L. J., DAVIES, C., DAVISON, T. S., DELENSTARR, G., DENG, X., DORRIS, D., EKLUND, A. C., FAN, X. H., FANG, H., FULMER-SMENTEK, S., FUSCOE, J. C., GALLAGHER, K., GE, W., GUO, L., GUO, X., HAGER, J., HAJE, P. K., HAN, J., HAN, T., HARBOTTLE, H. C., HARRIS, S. C., HATCHWELL, E., HAUSER, C. A., HESTER, S., HONG, H., HURBAN, P., JACKSON, S. A., JI, H., KNIGHT, C. R., KUO, W. P., LECLERC, J. E., LEVY, S., LI, Q. Z., LIU, C., LIU, Y., LOMBARDI, M. J., MA, Y., MAGNUSON, S. R., MAQSODI, B., MCDANIEL, T., MEI, N., MYKLEBOST, O., NING, B., NOVORADOVSKAYA, N., ORR, M. S., OSBORN, T. W., PAPALLO, A., PATTERSON, T. A., PERKINS, R. G., PETERS, E. H., et al. 2006. The MicroArray Quality Control (MAQC) project shows inter- and intraplatform reproducibility of gene expression measurements. *Nat Biotechnol,* 24**,** 1151-61.

CRESCENZI, E., RAIA, Z., PACIFICO, F., MELLONE, S., MOSCATO, F., PALUMBO, G. & LEONARDI, A. 2013. Down-regulation of wild-type p53-induced phosphatase 1 (Wip1) plays a critical role in regulating several p53-dependent functions in premature senescent tumor cells. *J Biol Chem,* 288**,** 16212-24.

DAUER, L. T., BROOKS, A. L., HOEL, D. G., MORGAN, W. F., STRAM, D. & TRAN, P. 2010. Review and evaluation of updated research on the health effects associated with low-dose ionising radiation. *Radiat Prot Dosimetry,* 140**,** 103-36.

DEGTEREV, A. & YUAN, J. 2008. Expansion and evolution of cell death programmes. *Nat Rev Mol Cell Biol,* 9**,** 378-90.

DENLI, A. M., TOPS, B. B., PLASTERK, R. H., KETTING, R. F. & HANNON, G. J. 2004. Processing of primary microRNAs by the Microprocessor complex. *Nature,* 432**,** 231-5.

DERVEAUX, S., VANDESOMPELE, J. & HELLEMANS, J. 2010. How to do successful gene expression analysis using real-time PCR. *Methods,* 50**,** 227-30.

DI LEONARDO, A., LINKE, S. P., CLARKIN, K. & WAHL, G. M. 1994. DNA damage triggers a prolonged p53-dependent G1 arrest and long-term induction of Cip1 in normal human fibroblasts. *Genes Dev,* 8**,** 2540-51.

DING, L. H., SHINGYOJI, M., CHEN, F., HWANG, J. J., BURMA, S., LEE, C., CHENG, J. F. & CHEN, D. J. 2005. Gene expression profiles of normal human fibroblasts after exposure to ionizing radiation: a comparative study of low and high doses. *Radiat Res,* 164**,** 17-26.

DJEBALI, S., DAVIS, C. A., MERKEL, A., DOBIN, A., LASSMANN, T., MORTAZAVI, A., TANZER, A., LAGARDE, J., LIN, W., SCHLESINGER, F., XUE, C., MARINOV, G. K., KHATUN, J., WILLIAMS, B. A., ZALESKI, C., ROZOWSKY, J., RODER, M., KOKOCINSKI, F., ABDELHAMID, R. F., ALIOTO, T., ANTOSHECHKIN, I., BAER, M. T., BAR, N. S., BATUT, P., BELL, K., BELL, I., CHAKRABORTTY, S., CHEN, X., CHRAST, J., CURADO, J., DERRIEN, T., DRENKOW, J., DUMAIS, E., DUMAIS, J., DUTTAGUPTA, R., FALCONNET, E., FASTUCA, M., FEJES-TOTH, K., FERREIRA, P., FOISSAC, S., FULLWOOD, M. J., GAO, H., GONZALEZ, D., GORDON, A., GUNAWARDENA, H., HOWALD, C., JHA, S., JOHNSON, R., KAPRANOV, P., KING, B., KINGSWOOD, C., LUO, O. J., PARK, E., PERSAUD, K., PREALL, J. B., RIBECA, P., RISK, B., ROBYR, D., SAMMETH, M., SCHAFFER, L., SEE, L. H., SHAHAB, A., SKANCKE, J., SUZUKI, A. M., TAKAHASHI, H., TILGNER, H., TROUT, D., WALTERS, N., WANG, H., WROBEL, J., YU, Y., RUAN, X., HAYASHIZAKI, Y., HARROW, J., GERSTEIN, M., HUBBARD, T., REYMOND, A., ANTONARAKIS, S. E., HANNON, G., GIDDINGS, M. C., RUAN, Y., WOLD, B., CARNINCI, P., GUIGO, R. & GINGERAS, T. R. 2012. Landscape of transcription in human cells. *Nature,* 489**,** 101-8.

DRESSMAN, H. K., MURAMOTO, G. G., CHAO, N. J., MEADOWS, S., MARSHALL, D., GINSBURG, G. S., NEVINS, J. R. & CHUTE, J. P. 2007. Gene expression signatures that predict radiation exposure in mice and humans. *PLoS Med,* 4**,** e106.

DUBROVA, Y. E., PLUMB, M., GUTIERREZ, B., BOULTON, E. & JEFFREYS, A. J. 2000. Transgenerational mutation by radiation. *Nature,* 405**,** 37.

DUCHAUD, E., RIDET, A., STOPPA-LYONNET, D., JANIN, N., MOUSTACCHI, E. & ROSSELLI, F. 1996. Deregulated apoptosis in ataxia telangiectasia: association with clinical stigmata and radiosensitivity. *Cancer Res,* 56**,** 1400-4.

EBISUYA, M., YAMAMOTO, T., NAKAJIMA, M. & NISHIDA, E. 2008. Ripples from neighbouring transcription. *Nat Cell Biol,* 10**,** 1106-13.

EDWARDS, A. A., LINDHOLM, C., DARROUDI, F., STEPHAN, G., ROMM, H., BARQUINERO, J., BARRIOS, L., CABALLIN, M. R., ROY, L., WHITEHOUSE, C. A., TAWN, E. J., MOQUET, J., LLOYD, D. C. & VOISIN, P. 2005. Review of translocations detected by FISH for retrospective biological dosimetry applications. *Radiat Prot Dosimetry,* 113**,** 396-402.

FACHIN, A. L., MELLO, S. S., SANDRIN-GARCIA, P., JUNTA, C. M., GHILARDI-NETTO, T., DONADI, E. A., PASSOS, G. A. & SAKAMOTO-HOJO, E. T. 2009. Gene expression profiles in radiation workers occupationally exposed to ionizing radiation. *J Radiat Res,* 50**,** 61-71.

FADOK, V. A., VOELKER, D. R., CAMPBELL, P. A., COHEN, J. J., BRATTON, D. L. & HENSON, P. M. 1992. Exposure of phosphatidylserine on the surface of apoptotic lymphocytes triggers specific recognition and removal by macrophages. *J Immunol,* 148**,** 2207-16.

FALT, S., HOLMBERG, K., LAMBERT, B. & WENNBORG, A. 2003. Long-term global gene expression patterns in irradiated human lymphocytes. *Carcinogenesis,* 24**,** 1837-45.

FEI, P., BERNHARD, E. J. & EL-DEIRY, W. S. 2002. Tissue-specific induction of p53 targets in vivo. *Cancer Res,* 62**,** 7316-27.

FELDSTEIN, O., NIZRI, T., DONIGER, T., JACOB, J., RECHAVI, G. & GINSBERG, D. 2013. The long non-coding RNA ERIC is regulated by E2F and modulates the cellular response to DNA damage. *Mol Cancer,* 12**,** 131.

FENECH, M. 1993. The cytokinesis-block micronucleus technique: a detailed description of the method and its application to genotoxicity studies in human populations. *Mutat Res,* 285**,** 35-44.

FILIANO, A. N., FATHALLAH-SHAYKH, H. M., FIVEASH, J., GAGE, J., CANTOR, A., KHARBANDA, S. & JOHNSON, M. R. 2011. Gene expression analysis in radiotherapy patients and C57BL/6 mice as a measure of exposure to ionizing radiation. *Radiat Res,* 176**,** 49-61.

FILIPOWICZ, W., BHATTACHARYYA, S. N. & SONENBERG, N. 2008. Mechanisms of post-transcriptional regulation by microRNAs: are the answers in sight? *Nat Rev Genet,* 9**,** 102-14.

FINNON, P., KABACIK, S., MACKAY, A., RAFFY, C., A'HERN, R., OWEN, R., BADIE, C., YARNOLD, J. & BOUFFLER, S. 2012. Correlation of in vitro lymphocyte radiosensitivity and gene expression with late normal tissue reactions following curative radiotherapy for breast cancer. *Radiother Oncol,* 105**,** 329-36.

FINNON, P., ROBERTSON, N., DZIWURA, S., RAFFY, C., ZHANG, W., AINSBURY, L., KAPRIO, J., BADIE, C. & BOUFFLER, S. 2008. Evidence for significant heritability of apoptotic and cell cycle responses to ionising radiation. *Hum Genet,* 123**,** 485-93.

FLEIGE, S., WALF, V., HUCH, S., PRGOMET, C., SEHM, J. & PFAFFL, M. W. 2006. Comparison of relative mRNA quantification models and the impact of RNA integrity in quantitative real-time RT-PCR. *Biotechnol Lett,* 28**,** 1601-13.

FRANCO, N., LAMARTINE, J., FROUIN, V., LE MINTER, P., PETAT, C., LEPLAT, J. J., LIBERT, F., GIDROL, X. & MARTIN, M. T. 2005. Low-dose exposure to gamma rays induces specific gene regulations in normal human keratinocytes. *Radiat Res,* 163**,** 623-35.

GEISS, G. K., BUMGARNER, R. E., BIRDITT, B., DAHL, T., DOWIDAR, N., DUNAWAY, D. L., FELL, H. P., FERREE, S., GEORGE, R. D., GROGAN, T., JAMES, J. J., MAYSURIA, M., MITTON, J. D., OLIVERI, P., OSBORN, J. L., PENG, T., RATCLIFFE, A. L., WEBSTER, P. J., DAVIDSON, E. H., HOOD, L. & DIMITROV, K. 2008. Direct multiplexed measurement of gene expression with color-coded probe pairs. *Nat Biotechnol,* 26**,** 317-25.

GIRARDI, C., DE PITTA, C., CASARA, S., SALES, G., LANFRANCHI, G., CELOTTI, L. & MOGNATO, M. 2012. Analysis of miRNA and mRNA expression profiles highlights alterations in ionizing radiation response of human lymphocytes under modeled microgravity. *PLoS One,* 7**,** e31293.

GOTTLIEB, E., HAFFNER, R., KING, A., ASHER, G., GRUSS, P., LONAI, P. & OREN, M. 1997. Transgenic mouse model for studying the transcriptional activity of the p53 protein: age- and tissue-dependent changes in radiation-induced activation during embryogenesis. *EMBO J,* 16**,** 1381-90.

GOULTER, A. B., HARMER, D. W. & CLARK, K. L. 2006. Evaluation of low density array technology for quantitative parallel measurement of multiple genes in human tissue. *BMC Genomics,* 7**,** 34.

GREGORY, R. I., YAN, K. P., AMUTHAN, G., CHENDRIMADA, T., DORATOTAJ, B., COOCH, N. & SHIEKHATTAR, R. 2004. The Microprocessor complex mediates the genesis of microRNAs. *Nature,* 432**,** 235-40.

GRUEL, G., LUCCHESI, C., PAWLIK, A., FROUIN, V., ALIBERT, O., KORTULEWSKI, T., ZAROUR, A., JACQUELIN, B., GIDROL, X. & TRONIK-LE ROUX, D. 2006. Novel microarray-based method for estimating exposure to ionizing radiation. *Radiat Res,* 166**,** 746-56.

GRUEL, G., VOISIN, P., VAURIJOUX, A., ROCH-LEFEVRE, S., GREGOIRE, E., MALTERE, P., PETAT, C., GIDROL, X., VOISIN, P. & ROY, L. 2008. Broad modulation of gene expression in CD4+ lymphocyte subpopulations in response to low doses of ionizing radiation. *Radiat Res,* 170**,** 335-44.

GUTTMAN, M., AMIT, I., GARBER, M., FRENCH, C., LIN, M. F., FELDSER, D., HUARTE, M., ZUK, O., CAREY, B. W., CASSADY, J. P., CABILI, M. N., JAENISCH, R., MIKKELSEN, T. S., JACKS, T., HACOHEN, N., BERNSTEIN, B. E., KELLIS, M., REGEV, A., RINN, J. L. & LANDER, E. S. 2009. Chromatin signature reveals over a thousand highly conserved large non-coding RNAs in mammals. *Nature,* 458**,** 223-7.

GUTTMAN, M., DONAGHEY, J., CAREY, B. W., GARBER, M., GRENIER, J. K., MUNSON, G., YOUNG, G., LUCAS, A. B., ACH, R., BRUHN, L., YANG, X., AMIT, I., MEISSNER, A., REGEV, A., RINN, J. L., ROOT, D. E. & LANDER, E. S. 2011. lincRNAs act in the circuitry controlling pluripotency and differentiation. *Nature,* 477**,** 295-300.

HALL, E. J. & GIACCIA, A. J. 2011. *Radiobiology for radiologist*, Lippincott Williams & Wilkins.

HALLAHAN, D. E., SPRIGGS, D. R., BECKETT, M. A., KUFE, D. W. & WEICHSELBAUM, R. R. 1989. Increased tumor necrosis factor alpha mRNA after cellular exposure to ionizing radiation. *Proc Natl Acad Sci U S A,* 86**,** 10104-7.

HANAHAN, D. & WEINBERG, R. A. 2011. Hallmarks of cancer: the next generation. *Cell,* 144**,** 646-74.

HATZI, V. I., TERZOUDI, G. I., PARASKEVOPOULOU, C., MAKROPOULOS, V., MATTHOPOULOS, D. P. & PANTELIAS, G. E. 2006. The use of premature chromosome condensation to study in interphase cells the influence of environmental factors on human genetic material. *ScientificWorldJournal,* 6**,** 1174-90.

HAUPT, Y., MAYA, R., KAZAZ, A. & OREN, M. 1997. Mdm2 promotes the rapid degradation of p53. *Nature,* 387**,** 296-9.

HE, H. & SUN, Y. 2007. Ribosomal protein S27L is a direct p53 target that regulates apoptosis. *Oncogene,* 26**,** 2707-16.

HE, L., HE, X., LIM, L. P., DE STANCHINA, E., XUAN, Z., LIANG, Y., XUE, W., ZENDER, L., MAGNUS, J., RIDZON, D., JACKSON, A. L., LINSLEY, P. S., CHEN, C., LOWE, S. W., CLEARY, M. A. & HANNON, G. J. 2007. A microRNA component of the p53 tumour suppressor network. *Nature,* 447**,** 1130-4.

HENKE, J. I., GOERGEN, D., ZHENG, J., SONG, Y., SCHUTTLER, C. G., FEHR, C., JUNEMANN, C. & NIEPMANN, M. 2008. microRNA-122 stimulates translation of hepatitis C virus RNA. *EMBO J,* 27**,** 3300-10.

HINDSON, C. M., CHEVILLET, J. R., BRIGGS, H. A., GALLICHOTTE, E. N., RUF, I. K., HINDSON, B. J., VESSELLA, R. L. & TEWARI, M. 2013. Absolute quantification by droplet digital PCR versus analog real-time PCR. *Nat Methods,* 10**,** 1003-5.

HIRAO, A., KONG, Y. Y., MATSUOKA, S., WAKEHAM, A., RULAND, J., YOSHIDA, H., LIU, D., ELLEDGE, S. J. & MAK, T. W. 2000. DNA damage-induced activation of p53 by the checkpoint kinase Chk2. *Science,* 287**,** 1824-7.

HOFFMAN, Y., BUBLIK, D. R., PILPEL, Y. & OREN, M. 2014. miR-661 downregulates both Mdm2 and Mdm4 to activate p53. *Cell Death Differ,* 21**,** 302-9.

HOLODNIY, M., KIM, S., KATZENSTEIN, D., KONRAD, M., GROVES, E. & MERIGAN, T. C. 1991. Inhibition of human immunodeficiency virus gene amplification by heparin. *J Clin Microbiol,* 29**,** 676-9.

HRUZ, T., WYSS, M., DOCQUIER, M., PFAFFL, M. W., MASANETZ, S., BORGHI, L., VERBRUGGHE, P., KALAYDJIEVA, L., BLEULER, S., LAULE, O., DESCOMBES, P., GRUISSEM, W. & ZIMMERMANN, P. 2011. RefGenes: identification of reliable and condition specific reference genes for RT-qPCR data normalization. *BMC Genomics,* 12**,** 156.

HU, H., DU, L., NAGABAYASHI, G., SEEGER, R. C. & GATTI, R. A. 2010a. ATM is down-regulated by N-Myc-regulated microRNA-421. *Proc Natl Acad Sci U S A,* 107**,** 1506-11.

HU, W., CHAN, C. S., WU, R., ZHANG, C., SUN, Y., SONG, J. S., TANG, L. H., LEVINE, A. J. & FENG, Z. 2010b. Negative regulation of tumor suppressor p53 by microRNA miR-504. *Mol Cell,* 38**,** 689-99.

HUANG, J., ZHOU, N., WATABE, K., LU, Z., WU, F., XU, M. & MO, Y. Y. 2014. Long non-coding RNA UCA1 promotes breast tumor growth by suppression of p27 (Kip1). *Cell Death Dis,* 5**,** e1008.

HUARTE, M., GUTTMAN, M., FELDSER, D., GARBER, M., KOZIOL, M. J., KENZELMANN-BROZ, D., KHALIL, A. M., ZUK, O., AMIT, I., RABANI, M., ATTARDI, L. D., REGEV, A., LANDER, E. S., JACKS, T. & RINN, J. L. 2010. A large intergenic noncoding RNA induced by p53 mediates global gene repression in the p53 response. *Cell,* 142**,** 409-19.

HUBE, F., VELASCO, G., ROLLIN, J., FURLING, D. & FRANCASTEL, C. 2011. Steroid receptor RNA activator protein binds to and counteracts SRA RNA-mediated activation of MyoD and muscle differentiation. *Nucleic Acids Res,* 39**,** 513-25.

HUNG, T., WANG, Y., LIN, M. F., KOEGEL, A. K., KOTAKE, Y., GRANT, G. D., HORLINGS, H. M., SHAH, N., UMBRICHT, C., WANG, P., WANG, Y., KONG, B., LANGEROD, A., BORRESEN-DALE, A. L., KIM, S. K., VAN DE VIJVER, M., SUKUMAR, S., WHITFIELD, M. L., KELLIS, M., XIONG, Y., WONG, D. J. & CHANG, H. Y. 2011. Extensive and coordinated transcription of noncoding RNAs within cell-cycle promoters. *Nat Genet,* 43**,** 621-9.

HUTVAGNER, G., MCLACHLAN, J., PASQUINELLI, A. E., BALINT, E., TUSCHL, T. & ZAMORE, P. D. 2001. A cellular function for the RNA-interference enzyme Dicer in the maturation of the let-7 small temporal RNA. *Science,* 293**,** 834-8.

HWANG, B. J., FORD, J. M., HANAWALT, P. C. & CHU, G. 1999. Expression of the p48 xeroderma pigmentosum gene is p53-dependent and is involved in global genomic repair. *Proc Natl Acad Sci U S A,* 96**,** 424-8.

IAEA 2010. *Radiation Biology: a handbook for teachers and students,* Vienna, International Atomic Energy Agency.

IAEA 2011. *Cytogenetic dosimetry: applications in preparedness for and response to radiation emergencies,* Vienna, International Atomic Energy Agency.

ICRP 2007. The 2007 Recommendations of the International Commission on Radiological Protection. *Ann. ICRP,* 37**,** 2-4.

ILNYTSKYY, Y., ZEMP, F. J., KOTURBASH, I. & KOVALCHUK, O. 2008. Altered microRNA expression patterns in irradiated hematopoietic tissues suggest a sex-specific protective mechanism. *Biochem Biophys Res Commun,* 377**,** 41-5.

IMAMURA, T., YAMAMOTO, S., OHGANE, J., HATTORI, N., TANAKA, S. & SHIOTA, K. 2004. Non-coding RNA directed DNA demethylation of Sphk1 CpG island. *Biochem Biophys Res Commun,* 322**,** 593-600.

INNOCENTE, S. A., ABRAHAMSON, J. L., COGSWELL, J. P. & LEE, J. M. 1999. p53 regulates a G2 checkpoint through cyclin B1. *Proc Natl Acad Sci U S A,* 96**,** 2147-52.

IRIZARRY, R. A., WARREN, D., SPENCER, F., KIM, I. F., BISWAL, S., FRANK, B. C., GABRIELSON, E., GARCIA, J. G., GEOGHEGAN, J., GERMINO, G., GRIFFIN, C., HILMER, S. C., HOFFMAN, E., JEDLICKA, A. E., KAWASAKI, E., MARTINEZ-MURILLO, F., MORSBERGER, L., LEE, H., PETERSEN, D., QUACKENBUSH, J., SCOTT, A., WILSON, M., YANG, Y., YE, S. Q. & YU, W. 2005. Multiple-laboratory comparison of microarray platforms. *Nat Methods,* 2**,** 345-50.

JACKSON, S. P. & BARTEK, J. 2009. The DNA-damage response in human biology and disease. *Nature,* 461**,** 1071-8.

JACOB, N. K., COOLEY, J. V., YEE, T. N., JACOB, J., ALDER, H., WICKRAMASINGHE, P., MACLEAN, K. H. & CHAKRAVARTI, A. 2013. Identification of sensitive serum microRNA biomarkers for radiation biodosimetry. *PLoS One,* 8**,** e57603.

JAZAYERI, A., FALCK, J., LUKAS, C., BARTEK, J., SMITH, G. C., LUKAS, J. & JACKSON, S. P. 2006. ATM- and cell cycle-dependent regulation of ATR in response to DNA double-strand breaks. *Nat Cell Biol,* 8**,** 37-45.

JEN, K. Y. & CHEUNG, V. G. 2003. Transcriptional response of lymphoblastoid cells to ionizing radiation. *Genome Res,* 13**,** 2092-100.

JEN, K. Y. & CHEUNG, V. G. 2005. Identification of novel p53 target genes in ionizing radiation response. *Cancer Res,* 65**,** 7666-73.

JOHNSON, C. D., ESQUELA-KERSCHER, A., STEFANI, G., BYROM, M., KELNAR, K., OVCHARENKO, D., WILSON, M., WANG, X., SHELTON, J., SHINGARA, J., CHIN, L., BROWN, D. & SLACK, F. J. 2007. The let-7 microRNA represses cell proliferation pathways in human cells. *Cancer Res,* 67**,** 7713-22.

JOSSON, S., SUNG, S. Y., LAO, K., CHUNG, L. W. & JOHNSTONE, P. A. 2008. Radiation modulation of microRNA in prostate cancer cell lines. *Prostate,* 68**,** 1599-606.

KABACIK, S., MACKAY, A., TAMBER, N., MANNING, G., FINNON, P., PAILLIER, F., ASHWORTH, A., BOUFFLER, S. & BADIE, C. 2011a. Gene expression following ionising radiation: identification of biomarkers for dose estimation and prediction of individual response. *Int J Radiat Biol,* 87**,** 115-29.

KABACIK, S., MANNING, G., RAFFY, C., BOUFFLER, S. & BADIE, C. 2015. Time, Dose and Ataxia Telangiectasia Mutated (ATM) Status Dependency of Coding and Noncoding RNA Expression after Ionizing Radiation Exposure. *Radiat Res,* 183**,** 325-37.

KABACIK, S., ORTEGA-MOLINA, A., EFEYAN, A., FINNON, P., BOUFFLER, S., SERRANO, M. & BADIE, C. 2011b. A minimally invasive assay for individual assessment of the ATM/CHEK2/p53 pathway activity. *Cell Cycle,* 10**,** 1152-61.

KAKAROUGKAS, A. & JEGGO, P. A. 2014. DNA DSB repair pathway choice: an orchestrated handover mechanism. *Br J Radiol,* 87**,** 20130685.

KASTAN, M. B., ZHAN, Q., EL-DEIRY, W. S., CARRIER, F., JACKS, T., WALSH, W. V., PLUNKETT, B. S., VOGELSTEIN, B. & FORNACE, A. J., JR. 1992. A mammalian cell cycle checkpoint pathway utilizing p53 and GADD45 is defective in ataxia-telangiectasia. *Cell,* 71**,** 587-97.

KATAYAMA, S., TOMARU, Y., KASUKAWA, T., WAKI, K., NAKANISHI, M., NAKAMURA, M., NISHIDA, H., YAP, C. C., SUZUKI, M., KAWAI, J., SUZUKI, H., CARNINCI, P.,

HAYASHIZAKI, Y., WELLS, C., FRITH, M., RAVASI, T., PANG, K. C., HALLINAN, J., MATTICK, J., HUME, D. A., LIPOVICH, L., BATALOV, S., ENGSTROM, P. G., MIZUNO, Y., FAGHIHI, M. A., SANDELIN, A., CHALK, A. M., MOTTAGUI-TABAR, S., LIANG, Z., LENHARD, B., WAHLESTEDT, C., GROUP, R. G. E. R., GENOME SCIENCE, G. & CONSORTIUM, F. 2005. Antisense transcription in the mammalian transcriptome. *Science,* 309**,** 1564-6.

KAWAI, J., SHINAGAWA, A., SHIBATA, K., YOSHINO, M., ITOH, M., ISHII, Y., ARAKAWA, T., HARA, A., FUKUNISHI, Y., KONNO, H., ADACHI, J., FUKUDA, S., AIZAWA, K., IZAWA, M., NISHI, K., KIYOSAWA, H., KONDO, S., YAMANAKA, I., SAITO, T., OKAZAKI, Y., GOJOBORI, T., BONO, H., KASUKAWA, T., SAITO, R., KADOTA, K., MATSUDA, H., ASHBURNER, M., BATALOV, S., CASAVANT, T., FLEISCHMANN, W., GAASTERLAND, T., GISSI, C., KING, B., KOCHIWA, H., KUEHL, P., LEWIS, S., MATSUO, Y., NIKAIDO, I., PESOLE, G., QUACKENBUSH, J., SCHRIML, L. M., STAUBLI, F., SUZUKI, R., TOMITA, M., WAGNER, L., WASHIO, T., SAKAI, K., OKIDO, T., FURUNO, M., AONO, H., BALDARELLI, R., BARSH, G., BLAKE, J., BOFFELLI, D., BOJUNGA, N., CARNINCI, P., DE BONALDO, M. F., BROWNSTEIN, M. J., BULT, C., FLETCHER, C., FUJITA, M., GARIBOLDI, M., GUSTINCICH, S., HILL, D., HOFMANN, M., HUME, D. A., KAMIYA, M., LEE, N. H., LYONS, P., MARCHIONNI, L., MASHIMA, J., MAZZARELLI, J., MOMBAERTS, P., NORDONE, P., RING, B., RINGWALD, M., RODRIGUEZ, I., SAKAMOTO, N., SASAKI, H., SATO, K., SCHONBACH, C., SEYA, T., SHIBATA, Y., STORCH, K. F., SUZUKI, H., TOYO-OKA, K., WANG, K. H., WEITZ, C., WHITTAKER, C., WILMING, L., WYNSHAW-BORIS, A., YOSHIDA, K., HASEGAWA, Y., KAWAJI, H., KOHTSUKI, S., HAYASHIZAKI, Y., TEAM, R. G. E. R. G. P. I. & THE, F. C. 2001. Functional annotation of a full-length mouse cDNA collection. *Nature,* 409**,** 685-90.

KENDALL, G. M., LITTLE, M. P., WAKEFORD, R., BUNCH, K. J., MILES, J. C., VINCENT, T. J., MEARA, J. R. & MURPHY, M. F. 2013. A record-based case-control study of natural background radiation and the incidence of childhood leukaemia and other cancers in Great Britain during 1980-2006. *Leukemia,* 27**,** 3-9.

KLASE, Z., KALE, P., WINOGRAD, R., GUPTA, M. V., HEYDARIAN, M., BERRO, R., MCCAFFREY, T. & KASHANCHI, F. 2007. HIV-1 TAR element is processed by Dicer to yield a viral micro-RNA involved in chromatin remodeling of the viral LTR. *BMC Mol Biol,* 8**,** 63.

KLATTENHOFF, C. A., SCHEUERMANN, J. C., SURFACE, L. E., BRADLEY, R. K., FIELDS, P. A., STEINHAUSER, M. L., DING, H., BUTTY, V. L., TORREY, L., HAAS, S., ABO, R., TABEBORDBAR, M., LEE, R. T., BURGE, C. B. & BOYER, L. A. 2013. Braveheart, a long noncoding RNA required for cardiovascular lineage commitment. *Cell,* 152**,** 570-83.

KNOPS, K., BOLDT, S., WOLKENHAUER, O. & KRIEHUBER, R. 2012. Gene expression in low- and high-dose-irradiated human peripheral blood lymphocytes: possible applications for biodosimetry. *Radiat Res,* 178**,** 304-12.

KOMAROVA, E. A., CHERNOV, M. V., FRANKS, R., WANG, K., ARMIN, G., ZELNICK, C. R., CHIN, D. M., BACUS, S. S., STARK, G. R. & GUDKOV, A. V. 1997. Transgenic mice with p53-responsive lacZ: p53 activity varies dramatically during normal development and determines radiation and drug sensitivity in vivo. *EMBO J,* 16**,** 1391-400.

KOOPMAN, G., REUTELINGSPERGER, C. P., KUIJTEN, G. A., KEEHNEN, R. M., PALS, S. T. & VAN OERS, M. H. 1994. Annexin V for flow cytometric detection of

phosphatidylserine expression on B cells undergoing apoptosis. *Blood,* 84**,** 1415-20.

KOTURBASH, I., ZEMP, F., KOLB, B. & KOVALCHUK, O. 2011. Sex-specific radiation-induced microRNAome responses in the hippocampus, cerebellum and frontal cortex in a mouse model. *Mutat Res,* 722**,** 114-8.

KOTURBASH, I., ZEMP, F. J., KUTANZI, K., LUZHNA, L., LOREE, J., KOLB, B. & KOVALCHUK, O. 2008. Sex-specific microRNAome deregulation in the shielded bystander spleen of cranially exposed mice. *Cell Cycle,* 7**,** 1658-67.

KRAEMER, A., ANASTASOV, N., ANGERMEIER, M., WINKLER, K., ATKINSON, M. J. & MOERTL, S. 2011. MicroRNA-mediated processes are essential for the cellular radiation response. *Radiat Res,* 176**,** 575-86.

KRAUSE, K., WASNER, M., REINHARD, W., HAUGWITZ, U., DOHNA, C. L., MOSSNER, J. & ENGELAND, K. 2000. The tumour suppressor protein p53 can repress transcription of cyclin B. *Nucleic Acids Res,* 28**,** 4410-8.

KRISHNAN, J. & MISHRA, R. K. 2014. Emerging trends of long non-coding RNAs in gene activation. *FEBS J,* 281**,** 34-45.

KRISHNAN, K., STEPTOE, A. L., MARTIN, H. C., WANI, S., NONES, K., WADDELL, N., MARIASEGARAM, M., SIMPSON, P. T., LAKHANI, S. R., GABRIELLI, B., VLASSOV, A., CLOONAN, N. & GRIMMOND, S. M. 2013. MicroRNA-182-5p targets a network of genes involved in DNA repair. *RNA,* 19**,** 230-42.

KUBBUTAT, M. H., JONES, S. N. & VOUSDEN, K. H. 1997. Regulation of p53 stability by Mdm2. *Nature,* 387**,** 299-303.

LAKIN, N. D., HANN, B. C. & JACKSON, S. P. 1999. The ataxia-telangiectasia related protein ATR mediates DNA-dependent phosphorylation of p53. *Oncogene,* 18**,** 3989-95.

LANDMARK, H., NAHAS, S. A., AAROE, J., GATTI, R., BORRESEN-DALE, A. L. & RODNINGEN, O. K. 2007. Transcriptional response to ionizing radiation in human radiation sensitive cell lines. *Radiother Oncol,* 83**,** 256-60.

LAVIN, M. F. 2008. Ataxia-telangiectasia: from a rare disorder to a paradigm for cell signalling and cancer. *Nat Rev Mol Cell Biol,* 9**,** 759-69.

LE, M. T., TEH, C., SHYH-CHANG, N., XIE, H., ZHOU, B., KORZH, V., LODISH, H. F. & LIM, B. 2009. MicroRNA-125b is a novel negative regulator of p53. *Genes Dev,* 23**,** 862-76.

LEE, R. C., FEINBAUM, R. L. & AMBROS, V. 1993. The C. elegans heterochronic gene lin-4 encodes small RNAs with antisense complementarity to lin-14. *Cell,* 75**,** 843-54.

LEE, Y., KIM, M., HAN, J., YEOM, K. H., LEE, S., BAEK, S. H. & KIM, V. N. 2004. MicroRNA genes are transcribed by RNA polymerase II. *EMBO J,* 23**,** 4051-60.

LI, B., SHI, X. B., NORI, D., CHAO, C. K., CHEN, A. M., VALICENTI, R. & WHITE RDE, V. 2011. Down-regulation of microRNA 106b is involved in p21-mediated cell cycle arrest in response to radiation in prostate cancer cells. *Prostate,* 71**,** 567-74.

LI, J., TAN, J., ZHUANG, L., BANERJEE, B., YANG, X., CHAU, J. F., LEE, P. L., HANDE, M. P., LI, B. & YU, Q. 2007. Ribosomal protein S27-like, a p53-inducible modulator of cell fate in response to genotoxic stress. *Cancer Res,* 67**,** 11317-26.

LINDHOLM, C., STRICKLIN, D., JAWORSKA, A., KOIVISTOINEN, A., PAILE, W., ARVIDSSON, E., DEPERAS-STANDYLO, J. & WOJCIK, A. 2010. Premature chromosome condensation (PCC) assay for dose assessment in mass casualty accidents. *Radiat Res,* 173**,** 71-8.

LU, J., GETZ, G., MISKA, E. A., ALVAREZ-SAAVEDRA, E., LAMB, J., PECK, D., SWEET-CORDERO, A., EBERT, B. L., MAK, R. H., FERRANDO, A. A., DOWNING, J. R., JACKS, T., HORVITZ, H. R. & GOLUB, T. R. 2005. MicroRNA expression profiles classify human cancers. *Nature,* 435**,** 834-8.

LUND, E., GUTTINGER, S., CALADO, A., DAHLBERG, J. E. & KUTAY, U. 2004. Nuclear export of microRNA precursors. *Science,* 303**,** 95-8.

MA, X., RENDA, M. J., WANG, L., CHENG, E. C., NIU, C., MORRIS, S. W., CHI, A. S. & KRAUSE, D. S. 2007. Rbm15 modulates Notch-induced transcriptional activation and affects myeloid differentiation. *Mol Cell Biol,* 27**,** 3056-64.

MAES, O. C., AN, J., SAROJINI, H., WU, H. & WANG, E. 2008. Changes in MicroRNA expression patterns in human fibroblasts after low-LET radiation. *J Cell Biochem,* 105**,** 824-34.

MALONE, J. H. & OLIVER, B. 2011. Microarrays, deep sequencing and the true measure of the transcriptome. *BMC Biol,* 9**,** 34.

MANNING, G., KABACIK, S., FINNON, P., BOUFFLER, S. & BADIE, C. 2013. High and low dose responses of transcriptional biomarkers in ex vivo X-irradiated human blood. *Int J Radiat Biol,* 89**,** 512-22.

MANNING, G., KABACIK, S., FINNON, P., PAILLIER, F., BOUFFLER, S. & BADIE, S. 2011. Assessing a new gene expression analysis technique for radiation biodosimetry. *Radiation Measurements,* 46**,** 1014–18.

MARSIT, C. J., EDDY, K. & KELSEY, K. T. 2006. MicroRNA responses to cellular stress. *Cancer Res,* 66**,** 10843-8.

MATHEWS, J. D., FORSYTHE, A. V., BRADY, Z., BUTLER, M. W., GOERGEN, S. K., BYRNES, G. B., GILES, G. G., WALLACE, A. B., ANDERSON, P. R., GUIVER, T. A., MCGALE, P., CAIN, T. M., DOWTY, J. G., BICKERSTAFFE, A. C. & DARBY, S. C. 2013. Cancer risk in 680,000 people exposed to computed tomography scans in childhood or adolescence: data linkage study of 11 million Australians. *BMJ,* 346**,** f2360.

MATHONNET, G., FABIAN, M. R., SVITKIN, Y. V., PARSYAN, A., HUCK, L., MURATA, T., BIFFO, S., MERRICK, W. C., DARZYNKIEWICZ, E., PILLAI, R. S., FILIPOWICZ, W., DUCHAINE, T. F. & SONENBERG, N. 2007. MicroRNA inhibition of translation initiation in vitro by targeting the cap-binding complex eIF4F. *Science,* 317**,** 1764-7.

MATSUOKA, S., BALLIF, B. A., SMOGORZEWSKA, A., MCDONALD, E. R., 3RD, HUROV, K. E., LUO, J., BAKALARSKI, C. E., ZHAO, Z., SOLIMINI, N., LERENTHAL, Y., SHILOH, Y., GYGI, S. P. & ELLEDGE, S. J. 2007. ATM and ATR substrate analysis reveals extensive protein networks responsive to DNA damage. *Science,* 316**,** 1160-6.

MATSUOKA, S., ROTMAN, G., OGAWA, A., SHILOH, Y., TAMAI, K. & ELLEDGE, S. J. 2000. Ataxia telangiectasia-mutated phosphorylates Chk2 in vivo and in vitro. *Proc Natl Acad Sci U S A,* 97**,** 10389-94.

MAYA, R., BALASS, M., KIM, S. T., SHKEDY, D., LEAL, J. F., SHIFMAN, O., MOAS, M., BUSCHMANN, T., RONAI, Z., SHILOH, Y., KASTAN, M. B., KATZIR, E. & OREN, M. 2001. ATM-dependent phosphorylation of Mdm2 on serine 395: role in p53 activation by DNA damage. *Genes Dev,* 15**,** 1067-77.

MEADOWS, S. K., DRESSMAN, H. K., DAHER, P., HIMBURG, H., RUSSELL, J. L., DOAN, P., CHAO, N. J., LUCAS, J., NEVINS, J. R. & CHUTE, J. P. 2010. Diagnosis of partial body radiation exposure in mice using peripheral blood gene expression profiles. *PLoS One,* 5**,** e11535.

MEADOWS, S. K., DRESSMAN, H. K., MURAMOTO, G. G., HIMBURG, H., SALTER, A., WEI, Z., GINSBURG, G. S., CHAO, N. J., NEVINS, J. R. & CHUTE, J. P. 2008. Gene

expression signatures of radiation response are specific, durable and accurate in mice and humans. *PLoS One,* 3**,** e1912.

MEIJER, H. A., KONG, Y. W., LU, W. T., WILCZYNSKA, A., SPRIGGS, R. V., ROBINSON, S. W., GODFREY, J. D., WILLIS, A. E. & BUSHELL, M. 2013. Translational repression and eIF4A2 activity are critical for microRNA-mediated gene regulation. *Science,* 340**,** 82-5.

MELANSON, B. D., BOSE, R., HAMILL, J. D., MARCELLUS, K. A., PAN, E. F. & MCKAY, B. C. 2011. The role of mRNA decay in p53-induced gene expression. *RNA,* 17**,** 2222-34.

MERCER, T. R., DINGER, M. E., SUNKIN, S. M., MEHLER, M. F. & MATTICK, J. S. 2008. Specific expression of long noncoding RNAs in the mouse brain. *Proc Natl Acad Sci U S A,* 105**,** 716-21.

MERCER, T. R. & MATTICK, J. S. 2013. Structure and function of long noncoding RNAs in epigenetic regulation. *Nat Struct Mol Biol,* 20**,** 300-7.

METHEETRAIRUT, C. & SLACK, F. J. 2013. MicroRNAs in the ionizing radiation response and in radiotherapy. *Curr Opin Genet Dev,* 23**,** 12-9.

METTLER, F. A., JR., HUDA, W., YOSHIZUMI, T. T. & MAHESH, M. 2008. Effective doses in radiology and diagnostic nuclear medicine: a catalog. *Radiology,* 248**,** 254-63.

MI, S., LU, J., SUN, M., LI, Z., ZHANG, H., NEILLY, M. B., WANG, Y., QIAN, Z., JIN, J., ZHANG, Y., BOHLANDER, S. K., LE BEAU, M. M., LARSON, R. A., GOLUB, T. R., ROWLEY, J. D. & CHEN, J. 2007. MicroRNA expression signatures accurately discriminate acute lymphoblastic leukemia from acute myeloid leukemia. *Proc Natl Acad Sci U S A,* 104**,** 19971-6.

MIYASHITA, T. & REED, J. C. 1995. Tumor suppressor p53 is a direct transcriptional activator of the human bax gene. *Cell,* 80**,** 293-9.

MIZUTANI, R., WAKAMATSU, A., TANAKA, N., YOSHIDA, H., TOCHIGI, N., SUZUKI, Y., OONISHI, T., TANI, H., TANO, K., IJIRI, K., ISOGAI, T. & AKIMITSU, N. 2012. Identification and characterization of novel genotoxic stress-inducible nuclear long noncoding RNAs in mammalian cells. *PLoS One,* 7**,** e34949.

MLADENOV, E. & ILIAKIS, G. 2011. Induction and repair of DNA double strand breaks: the increasing spectrum of non-homologous end joining pathways. *Mutat Res,* 711**,** 61-72.

MORANDI, E., SEVERINI, C., QUERCIOLI, D., PERDICHIZZI, S., MASCOLO, M. G., HORN, W., VACCARI, M., NUCCI, M. C., LODI, V., VIOLANTE, F. S., BOLOGNESI, C., GRILLI, S., SILINGARDI, P. & COLACCI, A. 2009. Gene expression changes in medical workers exposed to radiation. *Radiat Res,* 172**,** 500-8.

MORGAN, W. F. & BAIR, W. J. 2013. Issues in low dose radiation biology: the controversy continues. A perspective. *Radiat Res,* 179**,** 501-10.

MORI, M., BENOTMANE, M. A., TIRONE, I., HOOGHE-PETERS, E. L. & DESAINTES, C. 2005. Transcriptional response to ionizing radiation in lymphocyte subsets. *Cell Mol Life Sci,* 62**,** 1489-501.

MORONI, M. C., HICKMAN, E. S., LAZZERINI DENCHI, E., CAPRARA, G., COLLI, E., CECCONI, F., MULLER, H. & HELIN, K. 2001. Apaf-1 is a transcriptional target for E2F and p53. *Nat Cell Biol,* 3**,** 552-8.

MOURTADA-MAARABOUNI, M., HEDGE, V. L., KIRKHAM, L., FARZANEH, F. & WILLIAMS, G. T. 2008. Growth arrest in human T-cells is controlled by the non-coding RNA growth-arrest-specific transcript 5 (GAS5). *J Cell Sci,* 121**,** 939-46.

MUELLER, A. C., SUN, D. & DUTTA, A. 2013. The miR-99 family regulates the DNA damage response through its target SNF2H. *Oncogene,* 32**,** 1164-72.

MULLENDERS, L., ATKINSON, M., PARETZKE, H., SABATIER, L. & BOUFFLER, S. 2009. Assessing cancer risks of low-dose radiation. *Nat Rev Cancer,* 9**,** 596-604.

MUNSON, G. P. & WOLOSCHAK, G. E. 1990. Differential effect of ionizing radiation on transcription in repair-deficient and repair-proficient mice. *Cancer Res,* 50**,** 5045-8.

MYERS, J. S. & CORTEZ, D. 2006. Rapid activation of ATR by ionizing radiation requires ATM and Mre11. *J Biol Chem,* 281**,** 9346-50.

NAKANO, K. & VOUSDEN, K. H. 2001. PUMA, a novel proapoptotic gene, is induced by p53. *Mol Cell,* 7**,** 683-94.

NG, W. L., YAN, D., ZHANG, X., MO, Y. Y. & WANG, Y. 2010. Over-expression of miR-100 is responsible for the low-expression of ATM in the human glioma cell line: M059J. *DNA Repair (Amst),* 9**,** 1170-5.

NIKIFOROVA, M. N., GANDHI, M., KELLY, L. & NIKIFOROV, Y. E. 2011. MicroRNA dysregulation in human thyroid cells following exposure to ionizing radiation. *Thyroid,* 21**,** 261-6.

NOLAN, T., HANDS, R. E. & BUSTIN, S. A. 2006. Quantification of mRNA using real-time RT-PCR. *Nat Protoc,* 1**,** 1559-82.

NOSEL, I., VAURIJOUX, A., BARQUINERO, J. F. & GRUEL, G. 2013. Characterization of gene expression profiles at low and very low doses of ionizing radiation. *DNA Repair (Amst),* 12**,** 508-17.

O'CARROLL, D. & SCHAEFER, A. 2013. General principals of miRNA biogenesis and regulation in the brain. *Neuropsychopharmacology,* 38**,** 39-54.

O'DRISCOLL, M., CEROSALETTI, K. M., GIRARD, P. M., DAI, Y., STUMM, M., KYSELA, B., HIRSCH, B., GENNERY, A., PALMER, S. E., SEIDEL, J., GATTI, R. A., VARON, R., OETTINGER, M. A., NEITZEL, H., JEGGO, P. A. & CONCANNON, P. 2001. DNA ligase IV mutations identified in patients exhibiting developmental delay and immunodeficiency. *Mol Cell,* 8**,** 1175-85.

ODA, E., OHKI, R., MURASAWA, H., NEMOTO, J., SHIBUE, T., YAMASHITA, T., TOKINO, T., TANIGUCHI, T. & TANAKA, N. 2000. Noxa, a BH3-only member of the Bcl-2 family and candidate mediator of p53-induced apoptosis. *Science,* 288**,** 1053-8.

OKAMOTO, K. & BEACH, D. 1994. Cyclin G is a transcriptional target of the p53 tumor suppressor protein. *EMBO J,* 13**,** 4816-22.

OKAMURA K, P. M., TYLER DM, DUAN H, CHOU YT, LAI EC. 2008. The regulatory activity of microRNA* species has substantial influence on microRNA and 3' UTR evolution. *Nat Struct Mol Biol,* 15**,** 354-63.

OKAZAKI, Y., FURUNO, M., KASUKAWA, T., ADACHI, J., BONO, H., KONDO, S., NIKAIDO, I., OSATO, N., SAITO, R., SUZUKI, H., YAMANAKA, I., KIYOSAWA, H., YAGI, K., TOMARU, Y., HASEGAWA, Y., NOGAMI, A., SCHONBACH, C., GOJOBORI, T., BALDARELLI, R., HILL, D. P., BULT, C., HUME, D. A., QUACKENBUSH, J., SCHRIML, L. M., KANAPIN, A., MATSUDA, H., BATALOV, S., BEISEL, K. W., BLAKE, J. A., BRADT, D., BRUSIC, V., CHOTHIA, C., CORBANI, L. E., COUSINS, S., DALLA, E., DRAGANI, T. A., FLETCHER, C. F., FORREST, A., FRAZER, K. S., GAASTERLAND, T., GARIBOLDI, M., GISSI, C., GODZIK, A., GOUGH, J., GRIMMOND, S., GUSTINCICH, S., HIROKAWA, N., JACKSON, I. J., JARVIS, E. D., KANAI, A., KAWAJI, H., KAWASAWA, Y., KEDZIERSKI, R. M., KING, B. L., KONAGAYA, A., KUROCHKIN, I. V., LEE, Y., LENHARD, B., LYONS, P. A., MAGLOTT, D. R., MALTAIS, L., MARCHIONNI, L., MCKENZIE, L., MIKI, H., NAGASHIMA, T., NUMATA, K., OKIDO, T., PAVAN, W. J., PERTEA, G., PESOLE, G., PETROVSKY, N., PILLAI, R., PONTIUS, J. U., QI, D., RAMACHANDRAN, S., RAVASI, T., REED, J. C., REED, D. J., REID, J.,

RING, B. Z., RINGWALD, M., SANDELIN, A., SCHNEIDER, C., SEMPLE, C. A., SETOU, M., SHIMADA, K., SULTANA, R., TAKENAKA, Y., TAYLOR, M. S., TEASDALE, R. D., TOMITA, M., VERARDO, R., WAGNER, L., WAHLESTEDT, C., WANG, Y., WATANABE, Y., WELLS, C., WILMING, L. G., WYNSHAW-BORIS, A., YANAGISAWA, M., et al. 2002. Analysis of the mouse transcriptome based on functional annotation of 60,770 full-length cDNAs. *Nature,* 420**,** 563-73.

OZGUR, E., MERT, U., ISIN, M., OKUTAN, M., DALAY, N. & GEZER, U. 2013. Differential expression of long non-coding RNAs during genotoxic stress-induced apoptosis in HeLa and MCF-7 cells. *Clin Exp Med,* 13**,** 119-26.

PANG, K. C., FRITH, M. C. & MATTICK, J. S. 2006. Rapid evolution of noncoding RNAs: lack of conservation does not mean lack of function. *Trends Genet,* 22**,** 1-5.

PAPATHANASIOU, M. A., KERR, N. C., ROBBINS, J. H., MCBRIDE, O. W., ALAMO, I., JR., BARRETT, S. F., HICKSON, I. D. & FORNACE, A. J., JR. 1991. Induction by ionizing radiation of the gadd45 gene in cultured human cells: lack of mediation by protein kinase C. *Mol Cell Biol,* 11**,** 1009-16.

PARK, W. Y., HWANG, C. I., IM, C. N., KANG, M. J., WOO, J. H., KIM, J. H., KIM, Y. S., KIM, J. H., KIM, H., KIM, K. A., YU, H. J., LEE, S. J., LEE, Y. S. & SEO, J. S. 2002. Identification of radiation-specific responses from gene expression profile. *Oncogene,* 21**,** 8521-8.

PAUL, S. & AMUNDSON, S. A. 2008. Development of gene expression signatures for practical radiation biodosimetry. *Int J Radiat Oncol Biol Phys,* 71**,** 1236-1244.

PAUL, S. & AMUNDSON, S. A. 2011. Gene expression signatures of radiation exposure in peripheral white blood cells of smokers and non-smokers. *Int J Radiat Biol,* 87**,** 791-801.

PAUL, S., BARKER, C. A., TURNER, H. C., MCLANE, A., WOLDEN, S. L. & AMUNDSON, S. A. 2011. Prediction of in vivo radiation dose status in radiotherapy patients using ex vivo and in vivo gene expression signatures. *Radiat Res,* 175**,** 257-65.

PAUL, S., SMILENOV, L. B. & AMUNDSON, S. A. 2013. Widespread decreased expression of immune function genes in human peripheral blood following radiation exposure. *Radiat Res,* 180**,** 575-83.

PAWLIK, A., DELMAR, P., BOSSE, S., SAINZ, L., PETAT, C., PIETU, G., THIERRY, D. & TRONIK-LE ROUX, D. 2009. Changes in transcriptome after in vivo exposure to ionising radiation reveal a highly specialised liver response. *Int J Radiat Biol,* 85**,** 656-71.

PEARCE, M. S., SALOTTI, J. A., LITTLE, M. P., MCHUGH, K., LEE, C., KIM, K. P., HOWE, N. L., RONCKERS, C. M., RAJARAMAN, P., SIR CRAFT, A. W., PARKER, L. & BERRINGTON DE GONZALEZ, A. 2012. Radiation exposure from CT scans in childhood and subsequent risk of leukaemia and brain tumours: a retrospective cohort study. *Lancet,* 380**,** 499-505.

PENNY, G. D., KAY, G. F., SHEARDOWN, S. A., RASTAN, S. & BROCKDORFF, N. 1996. Requirement for Xist in X chromosome inactivation. *Nature,* 379**,** 131-7.

PEREZ-NOVO, C. A., CLAEYS, C., SPELEMAN, F., VAN CAUWENBERGE, P., BACHERT, C. & VANDESOMPELE, J. 2005. Impact of RNA quality on reference gene expression stability. *Biotechniques,* 39**,** 52, 54, 56.

PESCADOR, N., PEREZ-BARBA, M., IBARRA, J. M., CORBATON, A., MARTINEZ-LARRAD, M. T. & SERRANO-RIOS, M. 2013. Serum circulating microRNA profiling for identification of potential type 2 diabetes and obesity biomarkers. *PLoS One,* 8**,** e77251.

PFEFFER, S., ZAVOLAN, M., GRASSER, F. A., CHIEN, M., RUSSO, J. J., JU, J., JOHN, B., ENRIGHT, A. J., MARKS, D., SANDER, C. & TUSCHL, T. 2004. Identification of virus-encoded microRNAs. *Science,* 304**,** 734-6.

POLISENO, L., SALMENA, L., ZHANG, J., CARVER, B., HAVEMAN, W. J. & PANDOLFI, P. P. 2010. A coding-independent function of gene and pseudogene mRNAs regulates tumour biology. *Nature,* 465**,** 1033-8.

PRESTON, D. L., SHIMIZU, Y., PIERCE, D. A., SUYAMA, A. & MABUCHI, K. 2003. Studies of mortality of atomic bomb survivors. Report 13: Solid cancer and noncancer disease mortality: 1950-1997. *Radiat Res,* 160**,** 381-407.

RASHI-ELKELES, S., ELKON, R., SHAVIT, S., LERENTHAL, Y., LINHART, C., KUPERSHTEIN, A., AMARIGLIO, N., RECHAVI, G., SHAMIR, R. & SHILOH, Y. 2011. Transcriptional modulation induced by ionizing radiation: p53 remains a central player. *Mol Oncol,* 5**,** 336-48.

RAVASI, T., SUZUKI, H., PANG, K. C., KATAYAMA, S., FURUNO, M., OKUNISHI, R., FUKUDA, S., RU, K., FRITH, M. C., GONGORA, M. M., GRIMMOND, S. M., HUME, D. A., HAYASHIZAKI, Y. & MATTICK, J. S. 2006. Experimental validation of the regulated expression of large numbers of non-coding RNAs from the mouse genome. *Genome Res,* 16**,** 11-9.

REIMAN, A., SRINIVASAN, V., BARONE, G., LAST, J. I., WOOTTON, L. L., DAVIES, E. G., VERHAGEN, M. M., WILLEMSEN, M. A., WEEMAES, C. M., BYRD, P. J., IZATT, L., EASTON, D. F., THOMPSON, D. J. & TAYLOR, A. M. 2011. Lymphoid tumours and breast cancer in ataxia telangiectasia; substantial protective effect of residual ATM kinase activity against childhood tumours. *Br J Cancer,* 105**,** 586-91.

RENWICK, A., THOMPSON, D., SEAL, S., KELLY, P., CHAGTAI, T., AHMED, M., NORTH, B., JAYATILAKE, H., BARFOOT, R., SPANOVA, K., MCGUFFOG, L., EVANS, D. G., ECCLES, D., BREAST CANCER SUSCEPTIBILITY, C., EASTON, D. F., STRATTON, M. R. & RAHMAN, N. 2006. ATM mutations that cause ataxia-telangiectasia are breast cancer susceptibility alleles. *Nat Genet,* 38**,** 873-5.

RIECKE, A., RUFA, C. G., CORDES, M., HARTMANN, J., MEINEKE, V. & ABEND, M. 2012. Gene expression comparisons performed for biodosimetry purposes on in vitro peripheral blood cellular subsets and irradiated individuals. *Radiat Res,* 178**,** 234-43.

RILEY, T., SONTAG, E., CHEN, P. & LEVINE, A. 2008. Transcriptional control of human p53-regulated genes. *Nat Rev Mol Cell Biol,* 9**,** 402-12.

RINN, J. L., KERTESZ, M., WANG, J. K., SQUAZZO, S. L., XU, X., BRUGMANN, S. A., GOODNOUGH, L. H., HELMS, J. A., FARNHAM, P. J., SEGAL, E. & CHANG, H. Y. 2007. Functional demarcation of active and silent chromatin domains in human HOX loci by noncoding RNAs. *Cell,* 129**,** 1311-23.

ROMM, H., OESTREICHER, U. & KULKA, U. 2009. Cytogenetic damage analysed by the dicentric assay. *Ann Ist Super Sanita,* 45**,** 251-9.

ROTHKAMM, K., BALROOP, S., SHEKHDAR, J., FERNIE, P. & GOH, V. 2007. Leukocyte DNA damage after multi-detector row CT: a quantitative biomarker of low-level radiation exposure. *Radiology,* 242**,** 244-51.

ROTHKAMM, K., BEINKE, C., ROMM, H., BADIE, C., BALAGURUNATHAN, Y., BARNARD, S., BERNARD, N., BOULAY-GREENE, H., BRENGUES, M., DE AMICIS, A., DE SANCTIS, S., GREITHER, R., HERODIN, F., JONES, A., KABACIK, S., KNIE, T., KULKA, U., LISTA, F., MARTIGNE, P., MISSEL, A., MOQUET, J., OESTREICHER, U., PEINNEQUIN, A., POYOT, T., ROESSLER, U., SCHERTHAN, H., TERBRUEGGEN, B., THIERENS, H., VALENTE, M., VRAL, A., ZENHAUSERN, F., MEINEKE, V.,

BRASELMANN, H. & ABEND, M. 2013. Comparison of established and emerging biodosimetry assays. *Radiat Res,* 180**,** 111-9.

ROTHKAMM, K. & HORN, S. 2009. gamma-H2AX as protein biomarker for radiation exposure. *Ann Ist Super Sanita,* 45**,** 265-71.

ROTHKAMM, K. & LOBRICH, M. 2003. Evidence for a lack of DNA double-strand break repair in human cells exposed to very low x-ray doses. *Proc Natl Acad Sci U S A,* 100**,** 5057-62.

RUBY, J. G., JAN, C. H. & BARTEL, D. P. 2007. Intronic microRNA precursors that bypass Drosha processing. *Nature,* 448**,** 83-6.

SAK, A., GREHL, S., ERICHSEN, P., ENGELHARD, M., GRANNASS, A., LEVEGRUN, S., POTTGEN, C., GRONEBERG, M. & STUSCHKE, M. 2007. gamma-H2AX foci formation in peripheral blood lymphocytes of tumor patients after local radiotherapy to different sites of the body: dependence on the dose-distribution, irradiated site and time from start of treatment. *Int J Radiat Biol,* 83**,** 639-52.

SALEH, A. D., SAVAGE, J. E., CAO, L., SOULE, B. P., LY, D., DEGRAFF, W., HARRIS, C. C., MITCHELL, J. B. & SIMONE, N. L. 2011. Cellular stress induced alterations in microRNA let-7a and let-7b expression are dependent on p53. *PLoS One,* 6**,** e24429.

SAVIOZZI, S., SALUTO, A., TAYLOR, A. M., LAST, J. I., TREBINI, F., PARADISO, M. C., GROSSO, E., FUNARO, A., PONZIO, G., MIGONE, N. & BRUSCO, A. 2002. A late onset variant of ataxia-telangiectasia with a compound heterozygous genotype, A8030G/7481insA. *J Med Genet,* 39**,** 57-61.

SAVITSKY, K., BAR-SHIRA, A., GILAD, S., ROTMAN, G., ZIV, Y., VANAGAITE, L., TAGLE, D. A., SMITH, S., UZIEL, T., SFEZ, S., ASHKENAZI, M., PECKER, I., FRYDMAN, M., HARNIK, R., PATANJALI, S. R., SIMMONS, A., CLINES, G. A., SARTIEL, A., GATTI, R. A., CHESSA, L., SANAL, O., LAVIN, M. F., JASPERS, N. G., TAYLOR, A. M., ARLETT, C. F., MIKI, T., WEISSMAN, S. M., LOVETT, M., COLLINS, F. S. & SHILOH, Y. 1995. A single ataxia telangiectasia gene with a product similar to PI-3 kinase. *Science,* 268**,** 1749-53.

SCHENA, M., SHALON, D., DAVIS, R. W. & BROWN, P. O. 1995. Quantitative monitoring of gene expression patterns with a complementary DNA microarray. *Science,* 270**,** 467-70.

SCHMITZ, A., BAYER, J., DECHAMPS, N., GOLDIN, L. & THOMAS, G. 2007. Heritability of susceptibility to ionizing radiation-induced apoptosis of human lymphocyte subpopulations. *Int J Radiat Oncol Biol Phys,* 68**,** 1169-77.

SENGUPTA, S. & HARRIS, C. C. 2005. p53: traffic cop at the crossroads of DNA repair and recombination. *Nat Rev Mol Cell Biol,* 6**,** 44-55.

SHARMA, S., FINDLAY, G. M., BANDUKWALA, H. S., OBERDOERFFER, S., BAUST, B., LI, Z., SCHMIDT, V., HOGAN, P. G., SACKS, D. B. & RAO, A. 2011. Dephosphorylation of the nuclear factor of activated T cells (NFAT) transcription factor is regulated by an RNA-protein scaffold complex. *Proc Natl Acad Sci U S A,* 108**,** 11381-6.

SHERMAN, M. L., DATTA, R., HALLAHAN, D. E., WEICHSELBAUM, R. R. & KUFE, D. W. 1990. Ionizing radiation regulates expression of the c-jun protooncogene. *Proc Natl Acad Sci U S A,* 87**,** 5663-6.

SHI, Y., ZHANG, X., TANG, X., WANG, P., WANG, H. & WANG, Y. 2012. MiR-21 is continually elevated long-term in the brain after exposure to ionizing radiation. *Radiat Res,* 177**,** 124-8.

SHIBATA, A., CONRAD, S., BIRRAUX, J., GEUTING, V., BARTON, O., ISMAIL, A., KAKAROUGKAS, A., MEEK, K., TAUCHER-SCHOLZ, G., LOBRICH, M. & JEGGO, P. A. 2011. Factors determining DNA double-strand break repair pathway choice in G2 phase. *EMBO J,* 30**,** 1079-92.

SHIBATA, A. & JEGGO, P. A. 2014. DNA double-strand break repair in a cellular context. *Clin Oncol (R Coll Radiol),* 26**,** 243-9.

SHIN, S., CHA, H. J., LEE, E. M., JUNG, J. H., LEE, S. J., PARK, I. C., JIN, Y. W. & AN, S. 2009. MicroRNAs are significantly influenced by p53 and radiation in HCT116 human colon carcinoma cells. *Int J Oncol,* 34**,** 1645-52.

SIGURDSON, A. J., HA, M., HAUPTMANN, M., BHATTI, P., SRAM, R. J., BESKID, O., TAWN, E. J., WHITEHOUSE, C. A., LINDHOLM, C., NAKANO, M., KODAMA, Y., NAKAMURA, N., VOROBTSOVA, I., OESTREICHER, U., STEPHAN, G., YONG, L. C., BAUCHINGER, M., SCHMID, E., CHUNG, H. W., DARROUDI, F., ROY, L., VOISIN, P., BARQUINERO, J. F., LIVINGSTON, G., BLAKEY, D., HAYATA, I., ZHANG, W., WANG, C., BENNETT, L. M., LITTLEFIELD, L. G., EDWARDS, A. A., KLEINERMAN, R. A. & TUCKER, J. D. 2008. International study of factors affecting human chromosome translocations. *Mutat Res,* 652**,** 112-21.

SIMONE, N. L., SOULE, B. P., LY, D., SALEH, A. D., SAVAGE, J. E., DEGRAFF, W., COOK, J., HARRIS, C. C., GIUS, D. & MITCHELL, J. B. 2009. Ionizing radiation-induced oxidative stress alters miRNA expression. *PLoS One,* 4**,** e6377.

SKOWRONSKA, A., AUSTEN, B., POWELL, J. E., WESTON, V., OSCIER, D. G., DYER, M. J., MATUTES, E., PRATT, G., FEGAN, C., MOSS, P., TAYLOR, M. A. & STANKOVIC, T. 2012. ATM germline heterozygosity does not play a role in chronic lymphocytic leukemia initiation but influences rapid disease progression through loss of the remaining ATM allele. *Haematologica,* 97**,** 142-6.

SLEUTELS, F., ZWART, R. & BARLOW, D. P. 2002. The non-coding Air RNA is required for silencing autosomal imprinted genes. *Nature,* 415**,** 810-3.

SMIRNOV, D. A. & CHEUNG, V. G. 2008. ATM gene mutations result in both recessive and dominant expression phenotypes of genes and microRNAs. *Am J Hum Genet,* 83**,** 243-53.

SMITS, K., GOOSSENS, K., VAN SOOM, A., GOVAERE, J., HOOGEWIJS, M., VANHAESEBROUCK, E., GALLI, C., COLLEONI, S., VANDESOMPELE, J. & PEELMAN, L. 2009. Selection of reference genes for quantitative real-time PCR in equine in vivo and fresh and frozen-thawed in vitro blastocysts. *BMC Res Notes,* 2**,** 246.

SOKOLOV, M. V., PANYUTIN, I. V. & NEUMANN, R. D. 2012. Unraveling the global microRNAome responses to ionizing radiation in human embryonic stem cells. *PLoS One,* 7**,** e31028.

SORENSEN, K. P., THOMASSEN, M., TAN, Q., BAK, M., COLD, S., BURTON, M., LARSEN, M. J. & KRUSE, T. A. 2013. Long non-coding RNA HOTAIR is an independent prognostic marker of metastasis in estrogen receptor-positive primary breast cancer. *Breast Cancer Res Treat,* 142**,** 529-36.

ST CLAIR, S., GIONO, L., VARMEH-ZIAIE, S., RESNICK-SILVERMAN, L., LIU, W. J., PADI, A., DASTIDAR, J., DACOSTA, A., MATTIA, M. & MANFREDI, J. J. 2004. DNA damage-induced downregulation of Cdc25C is mediated by p53 via two independent mechanisms: one involves direct binding to the cdc25C promoter. *Mol Cell,* 16**,** 725-36.

STAHLBERG, A., HAKANSSON, J., XIAN, X., SEMB, H. & KUBISTA, M. 2004. Properties of the reverse transcription reaction in mRNA quantification. *Clin Chem,* 50**,** 509-15.

STOIMENOV, I. & HELLEDAY, T. 2009. PCNA on the crossroad of cancer. *Biochem Soc Trans,* 37**,** 605-13.

STRUHL, K. 2007. Transcriptional noise and the fidelity of initiation by RNA polymerase II. *Nat Struct Mol Biol,* 14**,** 103-5.

SU, Y. & SWIFT, M. 2000. Mortality rates among carriers of ataxia-telangiectasia mutant alleles. *Ann Intern Med,* 133**,** 770-8.

SUZUKI, H. I., YAMAGATA, K., SUGIMOTO, K., IWAMOTO, T., KATO, S. & MIYAZONO, K. 2009. Modulation of microRNA processing by p53. *Nature,* 460**,** 529-33.

SWIFT, M., MORRELL, D., MASSEY, R. B. & CHASE, C. L. 1991. Incidence of cancer in 161 families affected by ataxia-telangiectasia. *N Engl J Med,* 325**,** 1831-6.

TAFT, R. J., PHEASANT, M. & MATTICK, J. S. 2007. The relationship between non-protein-coding DNA and eukaryotic complexity. *Bioessays,* 29**,** 288-99.

TAKEI, Y., ISHIKAWA, S., TOKINO, T., MUTO, T. & NAKAMURA, Y. 1998. Isolation of a novel TP53 target gene from a colon cancer cell line carrying a highly regulated wild-type TP53 expression system. *Genes Chromosomes Cancer,* 23**,** 1-9.

TAKETANI, K., KAWAUCHI, J., TANAKA-OKAMOTO, M., ISHIZAKI, H., TANAKA, Y., SAKAI, T., MIYOSHI, J., MAEHARA, Y. & KITAJIMA, S. 2012. Key role of ATF3 in p53-dependent DR5 induction upon DNA damage of human colon cancer cells. *Oncogene,* 31**,** 2210-21.

TAWN, E. J. & WHITEHOUSE, C. A. 2003. Persistence of translocation frequencies in blood lymphocytes following radiotherapy: implications for retrospective radiation biodosimetry. *J Radiol Prot,* 23**,** 423-30.

TAYLOR, A. M. & BYRD, P. J. 2005. Molecular pathology of ataxia telangiectasia. *J Clin Pathol,* 58**,** 1009-15.

TAYLOR, A. M., HARNDEN, D. G., ARLETT, C. F., HARCOURT, S. A., LEHMANN, A. R., STEVENS, S. & BRIDGES, B. A. 1975. Ataxia telangiectasia: a human mutation with abnormal radiation sensitivity. *Nature,* 258**,** 427-9.

TEMPLIN, T., AMUNDSON, S. A., BRENNER, D. J. & SMILENOV, L. B. 2011a. Whole mouse blood microRNA as biomarkers for exposure to gamma-rays and (56)Fe ion. *Int J Radiat Biol,* 87**,** 653-62.

TEMPLIN, T., PAUL, S., AMUNDSON, S. A., YOUNG, E. F., BARKER, C. A., WOLDEN, S. L. & SMILENOV, L. B. 2011b. Radiation-induced micro-RNA expression changes in peripheral blood cells of radiotherapy patients. *Int J Radiat Oncol Biol Phys,* 80**,** 549-57.

TEMPLIN, T., YOUNG, E. F. & SMILENOV, L. B. 2012. Proton radiation-induced miRNA signatures in mouse blood: characterization and comparison with 56Fe-ion and gamma radiation. *Int J Radiat Biol,* 88**,** 531-9.

TIBBETTS, R. S., BRUMBAUGH, K. M., WILLIAMS, J. M., SARKARIA, J. N., CLIBY, W. A., SHIEH, S. Y., TAYA, Y., PRIVES, C. & ABRAHAM, R. T. 1999. A role for ATR in the DNA damage-induced phosphorylation of p53. *Genes Dev,* 13**,** 152-7.

TOMIMATSU, N., MUKHERJEE, B. & BURMA, S. 2009. Distinct roles of ATR and DNA-PKcs in triggering DNA damage responses in ATM-deficient cells. *EMBO Rep,* 10**,** 629-35.

TSUBOI, K., MORITAKE, T., TSUCHIDA, Y., TOKUUYE, K., MATSUMURA, A. & ANDO, K. 2007. Cell cycle checkpoint and apoptosis induction in glioblastoma cells and fibroblasts irradiated with carbon beam. *J Radiat Res,* 48**,** 317-25.

TUCKER, J. D., DIVINE, G. W., GREVER, W. E., THOMAS, R. A., JOINER, M. C., SMOLINSKI, J. M. & AUNER, G. W. 2013. Gene expression-based dosimetry by dose and time in mice following acute radiation exposure. *PLoS One,* 8**,** e83390.

TUCKER, J. D., GREVER, W. E., JOINER, M. C., KONSKI, A. A., THOMAS, R. A., SMOLINSKI, J. M., DIVINE, G. W. & AUNER, G. W. 2012. Gene expression-based detection of radiation exposure in mice after treatment with granulocyte colony-stimulating factor and lipopolysaccharide. *Radiat Res,* 177**,** 209-19.

TUCKER, J. D., JOINER, M. C., THOMAS, R. A., GREVER, W. E., BAKHMUTSKY, M. V., CHINKHOTA, C. N., SMOLINSKI, J. M., DIVINE, G. W. & AUNER, G. W. 2014. Accurate gene expression-based biodosimetry using a minimal set of human gene transcripts. *Int J Radiat Oncol Biol Phys,* 88**,** 933-9.

TURTOI, A., BROWN, I., OSKAMP, D. & SCHNEEWEISS, F. H. 2008. Early gene expression in human lymphocytes after gamma-irradiation-a genetic pattern with potential for biodosimetry. *Int J Radiat Biol,* 84**,** 375-87.

TURTOI, A., SHARAN, R. N., SRIVASTAVA, A. & SCHNEEWEISS, F. H. 2010. Proteomic and genomic modulations induced by γ-irradiation of human blood lymphocytes. *Int J Radiat Biol,* 86**,** 888-904.

UEHARA, Y., ITO, Y., TAKI, K., NENOI, M., ICHINOHE, K., NAKAMURA, S., TANAKA, S., OGHISO, Y., TANAKA, K., MATSUMOTO, T., PAUNESKU, T., WOLOSCHAK, G. E. & ONO, T. 2010. Gene expression profiles in mouse liver after long-term low-dose-rate irradiation with gamma rays. *Radiat Res,* 174**,** 611-7.

UNSCEAR 2008. Sources and effects of ionising radiation. New York: United nations Publications.

UNSCEAR 2013. Sources, effects and risks of ionizing radiation UNSCEAR 2013 report. New York: United Nations Publication.

UZIEL, T., LERENTHAL, Y., MOYAL, L., ANDEGEKO, Y., MITTELMAN, L. & SHILOH, Y. 2003. Requirement of the MRN complex for ATM activation by DNA damage. *EMBO J,* 22**,** 5612-21.

VARON, R., VISSINGA, C., PLATZER, M., CEROSALETTI, K. M., CHRZANOWSKA, K. H., SAAR, K., BECKMANN, G., SEEMANOVA, E., COOPER, P. R., NOWAK, N. J., STUMM, M., WEEMAES, C. M., GATTI, R. A., WILSON, R. K., DIGWEED, M., ROSENTHAL, A., SPERLING, K., CONCANNON, P. & REIS, A. 1998. Nibrin, a novel DNA double-strand break repair protein, is mutated in Nijmegen breakage syndrome. *Cell,* 93**,** 467-76.

VASUDEVAN, S., TONG, Y. & STEITZ, J. A. 2007. Switching from repression to activation: microRNAs can up-regulate translation. *Science,* 318**,** 1931-4.

VERMEULEN, J., DE PRETER, K., LEFEVER, S., NUYTENS, J., DE VLOED, F., DERVEAUX, S., HELLEMANS, J., SPELEMAN, F. & VANDESOMPELE, J. 2011. Measurable impact of RNA quality on gene expression results from quantitative PCR. *Nucleic Acids Res,* 39**,** e63.

VILLUNGER, A., MICHALAK, E. M., COULTAS, L., MULLAUER, F., BOCK, G., AUSSERLECHNER, M. J., ADAMS, J. M. & STRASSER, A. 2003. p53- and drug-induced apoptotic responses mediated by BH3-only proteins puma and noxa. *Science,* 302**,** 1036-8.

VINCENTI, S., BRILLANTE, N., LANZA, V., BOZZONI, I., PRESUTTI, C., CHIANI, F., ETNA, M. P. & NEGRI, R. 2011. HUVEC respond to radiation by inducing the expression of pro-angiogenic microRNAs. *Radiat Res,* 175**,** 535-46.

VOUSDEN, K. H. & LANE, D. P. 2007. p53 in health and disease. *Nat Rev Mol Cell Biol,* 8**,** 275-83.

VRAL, A., THIERENS, H. & DE RIDDER, L. 1997. In vitro micronucleus-centromere assay to detect radiation-damage induced by low doses in human lymphocytes. *Int J Radiat Biol,* 71**,** 61-8.

WAGNER-ECKER, M., SCHWAGER, C., WIRKNER, U., ABDOLLAHI, A. & HUBER, P. E. 2010. MicroRNA expression after ionizing radiation in human endothelial cells. *Radiat Oncol,* 5**,** 25.

WAN, G., HU, X., LIU, Y., HAN, C., SOOD, A. K., CALIN, G. A., ZHANG, X. & LU, X. 2013a. A novel non-coding RNA lncRNA-JADE connects DNA damage signalling to histone H4 acetylation. *EMBO J,* 32**,** 2833-47.

WAN, G., MATHUR, R., HU, X., LIU, Y., ZHANG, X., PENG, G. & LU, X. 2013b. Long non-coding RNA ANRIL (CDKN2B-AS) is induced by the ATM-E2F1 signaling pathway. *Cell Signal,* 25**,** 1086-95.

WANG, X., ARAI, S., SONG, X., REICHART, D., DU, K., PASCUAL, G., TEMPST, P., ROSENFELD, M. G., GLASS, C. K. & KUROKAWA, R. 2008. Induced ncRNAs allosterically modify RNA-binding proteins in cis to inhibit transcription. *Nature,* 454**,** 126-30.

WANG, X. W., ZHAN, Q., COURSEN, J. D., KHAN, M. A., KONTNY, H. U., YU, L., HOLLANDER, M. C., O'CONNOR, P. M., FORNACE, A. J., JR. & HARRIS, C. C. 1999. GADD45 induction of a G2/M cell cycle checkpoint. *Proc Natl Acad Sci U S A,* 96**,** 3706-11.

WANG, Z., WEI, H., YU, Y., SUN, J., YANG, Y., XING, G., WU, S., ZHOU, Y., ZHU, Y., ZHANG, C., ZHOU, T., ZHAO, X., SUN, Q. & HE, F. 2004. Characterization of Ceap-11 and Ceap-16, two novel splicing-variant-proteins, associated with centrosome, microtubule aggregation and cell proliferation. *J Mol Biol,* 343**,** 71-82.

WATTS, J. A., MORLEY, M., BURDICK, J. T., FIORI, J. L., EWENS, W. J., SPIELMAN, R. S. & CHEUNG, V. G. 2002. Gene expression phenotype in heterozygous carriers of ataxia telangiectasia. *Am J Hum Genet,* 71**,** 791-800.

WEIDHAAS, J. B., BABAR, I., NALLUR, S. M., TRANG, P., ROUSH, S., BOEHM, M., GILLESPIE, E. & SLACK, F. J. 2007. MicroRNAs as potential agents to alter resistance to cytotoxic anticancer therapy. *Cancer Res,* 67**,** 11111-6.

WIEBUSCH, L. & HAGEMEIER, C. 2010. p53- and p21-dependent premature APC/C-Cdh1 activation in G2 is part of the long-term response to genotoxic stress. *Oncogene,* 29**,** 3477-89.

WIGHTMAN, B., HA, I. & RUVKUN, G. 1993. Posttranscriptional regulation of the heterochronic gene lin-14 by lin-4 mediates temporal pattern formation in C. elegans. *Cell,* 75**,** 855-62.

WOJCIK, A., LLOYD, D., ROMM, H. & ROY, L. 2010. Biological dosimetry for triage of casualties in a large-scale radiological emergency:capacity of the EU member states. *Radiat Prot Dosimetry,* 138**,** 397-401.

WOLOSCHAK, G. E. & CHANG-LIU, C. M. 1990. Differential modulation of specific gene expression following high- and low-LET radiations. *Radiat Res,* 124**,** 183-7.

WOLOSCHAK, G. E., CHANG-LIU, C. M., JONES, P. S. & JONES, C. A. 1990. Modulation of gene expression in Syrian hamster embryo cells following ionizing radiation. *Cancer Res,* 50**,** 339-44.

XIAO, J., LIN, H., LUO, X., LUO, X. & WANG, Z. 2011. miR-605 joins p53 network to form a p53:miR-605:Mdm2 positive feedback loop in response to stress. *EMBO J,* 30**,** 524-32.

XU, J. & MORRIS, G. F. 1999. p53-mediated regulation of proliferating cell nuclear antigen expression in cells exposed to ionizing radiation. *Mol Cell Biol,* 19**,** 12-20.

YAJIMA, H., FUJISAWA, H., NAKAJIMA, N. I., HIRAKAWA, H., JEGGO, P. A., OKAYASU, R. & FUJIMORI, A. 2013. The complexity of DNA double strand breaks is a critical factor enhancing end-resection. *DNA Repair (Amst),* 12**,** 936-46.

YAN, D., NG, W. L., ZHANG, X., WANG, P., ZHANG, Z., MO, Y. Y., MAO, H., HAO, C., OLSON, J. J., CURRAN, W. J. & WANG, Y. 2010. Targeting DNA-PKcs and ATM with miR-101 sensitizes tumors to radiation. *PLoS One,* 5**,** e11397.

YAN, M. D., HONG, C. C., LAI, G. M., CHENG, A. L., LIN, Y. W. & CHUANG, S. E. 2005. Identification and characterization of a novel gene Saf transcribed from the opposite strand of Fas. *Hum Mol Genet,* 14**,** 1465-74.

YOON, H., HE, H., NAGY, R., DAVULURI, R., SUSTER, S., SCHOENBERG, D., PELLEGATA, N. & CHAPELLE ADE, L. 2007. Identification of a novel noncoding RNA gene, NAMA, that is downregulated in papillary thyroid carcinoma with BRAF mutation and associated with growth arrest. *Int J Cancer,* 121**,** 767-75.

YOON, J. H., ABDELMOHSEN, K., KIM, J., YANG, X., MARTINDALE, J. L., TOMINAGA-YAMANAKA, K., WHITE, E. J., ORJALO, A. V., RINN, J. L., KREFT, S. G., WILSON, G. M. & GOROSPE, M. 2013. Scaffold function of long non-coding RNA HOTAIR in protein ubiquitination. *Nat Commun,* 4**,** 2939.

YU, J. & ZHANG, L. 2008. PUMA, a potent killer with or without p53. *Oncogene,* 27 Suppl 1**,** S71-83.

YU, J., ZHANG, L., HWANG, P. M., KINZLER, K. W. & VOGELSTEIN, B. 2001. PUMA induces the rapid apoptosis of colorectal cancer cells. *Mol Cell,* 7**,** 673-82.

YU, M., ZHAN, Q. & FINN, O. J. 2002. Immune recognition of cyclin B1 as a tumor antigen is a result of its overexpression in human tumors that is caused by non-functional p53. *Mol Immunol,* 38**,** 981-7.

ZHAN, Q., FAN, S., BAE, I., GUILLOUF, C., LIEBERMANN, D. A., O'CONNOR, P. M. & FORNACE, A. J., JR. 1994. Induction of bax by genotoxic stress in human cells correlates with normal p53 status and apoptosis. *Oncogene,* 9**,** 3743-51.

ZHANG, A., ZHOU, N., HUANG, J., LIU, Q., FUKUDA, K., MA, D., LU, Z., BAI, C., WATABE, K. & MO, Y. Y. 2013. The human long non-coding RNA-RoR is a p53 repressor in response to DNA damage. *Cell Res,* 23**,** 340-50.

ZHANG, H. G. & GRIZZLE, W. E. 2014. Exosomes: a novel pathway of local and distant intercellular communication that facilitates the growth and metastasis of neoplastic lesions. *Am J Pathol,* 184**,** 28-41.

ZHANG, J. & BYRNE, C. D. 1999. Differential priming of RNA templates during cDNA synthesis markedly affects both accuracy and reproducibility of quantitative competitive reverse-transcriptase PCR. *Biochem J,* 337 (Pt 2)**,** 231-41.

ZHANG, X., WAN, G., BERGER, F. G., HE, X. & LU, X. 2011. The ATM kinase induces microRNA biogenesis in the DNA damage response. *Mol Cell,* 41**,** 371-83.

ZHAO, J., SUN, B. K., ERWIN, J. A., SONG, J. J. & LEE, J. T. 2008. Polycomb proteins targeted by a short repeat RNA to the mouse X chromosome. *Science,* 322**,** 750-6.

ZHAO, T., LI, G., MI, S., LI, S., HANNON, G. J., WANG, X. J. & QI, Y. 2007. A complex system of small RNAs in the unicellular green alga Chlamydomonas reinhardtii. *Genes Dev,* 21**,** 1190-203.

ZHOU, Y., ZHONG, Y., WANG, Y., ZHANG, X., BATISTA, D. L., GEJMAN, R., ANSELL, P. J., ZHAO, J., WENG, C. & KLIBANSKI, A. 2007. Activation of p53 by MEG3 non-coding RNA. *J Biol Chem,* 282**,** 24731-42.

ZSCHENKER, O., BORGMANN, K., STREICHERT, T., MEIER, I., WRONA, A. & DIKOMEY, E. 2006. Lymphoblastoid cell lines differing in p53 status show clear differences in basal gene expression with minor changes after irradiation. *Radiother Oncol,* 80**,** 236-49.

Appendices

Appendix A

Primers and probes sequences for human and mouse genes

Gene	Name	Sequence 5'=>3'
ATF3	**primer F**	AGGTTTGCCATCCAGAACAA
	primer R	CTGACAGTGACTGATTCC
	covering primer F	the same as primer F
	covering primer R	CTTCTTGTTTCGGCACTTTGC
	probe	CCTCTGCCACCGGATGTCCTCT
BBC3	**primer F**	CGGAGACAAGAGGAGCAG
	primer R	GGAGTCCCATGATGAGATTG
	covering primer F	the same as primer F
	covering primer R	the same as primer R
	probe	CCCTCACCCTGGAGGGTCCTGT
CCNB1	**primer F**	ATAAGGCGAAGATCAACATGGC
	primer R	TTTGTTACCAATGTCCCCAAGAG
	covering primer F	GAGTCACCAGGAACTCGAAAA
	covering primer R	CACTGGCACCAGCATAGGTA
	probe	CGCAAAGCGCGTTCCTACGGCC
CCNG1	**primer F**	GGAGCTGCAGTCTCTGTCAAG
	primer R	TGACATCTAGACTCCTGTTCCAA
	covering primer F	the same as primer F
	covering primer R	the same as primer R
	probe	AACTGCTACACCAGCTGAATGCCC
CDKN1A	**primer F**	GCAGACCAGCATGACAG
	primer R	TAGGGCTTCCTCTTGGA
	covering primer F	GGAAGACCATGTGGACCTGT
	covering primer R	AAGATGTAGAGCGGGCCTTT
	probe	TTTCTACCACTCCAAACGCCGGCT
DDB2	**primer F**	GTCACTTCCAGCACCTCACA
	primer R	ACGTCGATCGTCCTCAATTC
	covering primer F	CAGAAGAGCGAGATCCGAGT
	covering primer R	CATTAAGCGAACTGATGCCA
	probe	AGCCTGGCATCCTCGCTACAACC
FAS-AS1	**primer F**	CCTCATTTCGCCATCTGTA
	primer R	GCATAGCGAGAGAAGTGTT
	covering primer F	AGCTCTCTGAACCTCATTTC
	covering primer R	GGAGGCTCATTTGAGTACC
	probe	ACTACATGGCTCTCGTGAGAATCC
FDXR	**primer F**	GTACAACGGGCTTCCTGAGA
	primer R	CTCAGGTGGGGTCAGTAGGA
	covering primer F	TGGAAATTCCTGGTGAGGAG
	covering primer R	TGGAAATTCCTGGTGAGGAG
	probe	CGGGCCACGTCCAGAGCCA
GADD45A	**primer F**	CTGCGAGAACGACATCAAC

	primer R	AGCGTCGGTCTCCAAGAG
	covering primer F	ACGAGGACGACGACAGAGAT
	covering primer R	TCCCGGCAAAAACAAATAAG
	probe	ATCCTGCGCGTCAGCAACCCG
HPRT1	**primer F**	TCAGGCAGTATAATCCAAAGATGGT
	primer R	AGTCTGGCTTATATCCAACACTTCG
	covering primer F	GACCAGTCAACAGGGGACAT
	covering primer R	CCTACAACAAACTTGTCTGGAATTT
	probe	CGCAAGCTTGCTGGTGAAAAGGACCC
MDM2	**primer F**	CCATGATCTACAGGAACTTGGTAGTA
	primer R	ACACCTGTTCTCACTCACAGATG
	covering primer F	TGCCAAGCTTCTCTGTGAAA
	covering primer R	GTGGCGTTTTCTTTGTCGT
	probe	CAATCAGCAGGAATCATCGGACTCAG
PANDAR	**primer F**	GTCCTGATGCAGACCATAAA
	primer R	GATAGCTGGAAAGCTGAGAG
	covering primer F	GAGGCCAACTAGCACCA
	covering primer R	CACAAGTGCAGGAGAGAATC
	probe	CCTTCAGAGGTGGTCCAGATATGT
PHPT1	**primer F**	TCGCTCTCATTCCTGATGTG
	primer R	TCGTAGATGTCCGCATGGTA
	covering primer F	TCGCTCTCATTCCTGATGTG
	covering primer R	GCCATGGAATAGCCGTACAC
	probe	CTTGTAGCCGCGCACGATCTCCTT
PLK3	**primer F**	ATCAGCGCGAGAAGATCCTA
	primer R	GATGTTGTCAGCGTCCTCAA
	covering primer F	CTGACACAGAGACTGGCAGC
	covering primer R	GATCTGCCGCAGGTAGTAGC
	probe	CGAGACCTGCAGCACCGCC
PCR1	**primer F**	AATCTGATGCTACTTCTGGAATC
	primer R	AGCCACAGCTGGTTGACTGA
	covering primer F	CCACCTGTTCAGGGAAGAAA
	covering primer R	AAGGTTTCAAGCACGCCTAA
	probe	CAATTCAACCAACATCCAGTCCTGAGAA
SESN1	**primer F**	GCTGTCTTGTGCATTACTTGTG
	primer R	CTGCGCAGCAGTCTACAG
	covering primer F	GCTCAGCAACAACCATTTTG
	covering primer R	AGGCAGAGGCAGAGAGACTG
	probe	ACATGTCCCACAACTTTGGTGCTGG
TP53TG1	**primer F**	CCAAATGAGCTGTCCTAACT
	primer R	AGAGTGCCTTCTAGATCCT
	covering primer F	GGTGCCAAATGAGCTGT
	covering primer R	GAGGAGCGTGTGGTAAG
	probe	CAGCTTCCTGCATGATGCTGG
Atf3	**primer F**	ACAGACCCCTGGAGATGT
	primer R	CGCCTCCTTTTCCTCTCA
	covering primer F	ATAAACACCTCTGCCATCGG
	covering primer R	GCAGGCACTCTGTCTTCTCC
	probe	GCCGCCTCAGACTTGGTGACTG

Bbc3	**primer F**	CGGCGGAGACAAGAAGAG
	primer R	AGGAGTCCCATGAAGAGATTG
	covering primer F	CCCAGCAGCACTTAGAGTC
	covering primer R	CCTAGTTGGGCTCCATTTCT
	probe	CATCGACACCGACCCTCACCCTGG
Ccnb1	**primer F**	GTGCATTTTGCTCCTTCTCA
	primer R	CCATTCACCGTTGTCAAGAA
	covering primer F	TAAAGTCGGAGAGGTTGACG
	covering primer R	AGGGAGTCTTCACTGTAGGA
	probe	CAGCGCTAAGCAGAAAGCCCCAGC
Cdkn1a	**primer F**	GCAAGAGAAAACCCTGAAGTG
	primer R	CACACAGAGTGAGGGCTAAG
	covering primer F	TATCACTCCAAGCGCAGATT
	covering primer R	CAGGCAGCGTATATACAGGA
	probe	ACGGGAGCCCCGCCCTCTT
Cenpe	**primer F**	AAAGCTTCTGACTGCAAACC
	primer R	CTCGCAATGGAGCTTAACAC
	covering primer F	GAACAAAGCTCTCACTTCCG
	covering primer R	CTCCTGGCTCAGTTTGATCT
	probe	TGTTCCCTGGAGTTCCACAGAGCCC
Fdxr	**primer F**	AGCTTCGGGAGATGATTCAG
	primer R	ACGGGGGACATCCTTAATTC
	covering primer F	AAACAGACATCACAGAGGCT
	covering primer R	CTTCCACTCCTGGCTTCTC
	probe	AACCCGGCCCATTTTGGATCCTTCG
Hprt	**primer F**	GGACAGGACTGAAAGACTTG
	primer R	TAATCCAGCAGGTCAGCAAA
	covering primer F	AGTGTTTATTCCTCATGGACTGA
	covering primer R	CCAATAACTTTTATGTCCCCCG
	probe	CCCTTGAGCACACAGAGGGCCACA
Phpt1	**primer F**	AAGTCAGGTCTCTGCTCTTG
	primer R	CAGATTGGTCTGGCCTCTAA
	covering primer F	GGCTACTCTATGGGTTACGG
	covering primer R	GGCATATCAATGCTTTTAATTCCT
	probe	AGCACAGGGCCAGCCCCTCA
Sesn1	**primer F**	CATTATCGGCACTACATTGGAA
	primer R	TGCAGATTCACCAGGTAGGA
	covering primer F	GCTTTGGGTCGTCTGGATAA
	covering primer R	TCTGCAGTTTTTGAGGAGCA
	probe	ACTGATGCCTCGCTGCCGCC
Sesn2	**primer F**	CGTTTTGAGCTGGAGAAGTCA
	primer R	GTGGAGAAGGCTCCAGGATA
	covering primer F	ACCCACTGAACAACTCAGGG
	covering primer R	TATAATCCTGGGCACGGAAG
	probe	AGCCTGCTGGTGACCCCCTCAGC